Microglial migration and adhesion molecules during embryonic brain development

Sophie Smolders

Université Pierre et Marie Curie

Universiteit Hasselt

CERVEAU - COGNITION - COMPORTEMENT

Neurosciences Paris Seine, UPMC INSERM S 1130, CNRS UMR 8246

Development of Spinal Cord Organization

La migration des microglies et les molécules adhésives au cours du développement embryonnaire du cerveau

Par Sophie Smolders

Thèse de doctorat de Neurosciences

Dirigée par Pascal Legendre et Bert Brône

Présentée et soutenue publiquement le 30 octobre 2017

Devant un jury composé de :

Prof. dr Marcel Ameloot, Universiteit Hasselt, Diepenbeek, Belgium, *Maître de conférences*
Prof. dr. Bert Brône, Universiteit Hasselt, Diepenbeek, Belgium, *promotor*
Dr. Pascal Legendre, Université Pierre et Marie Curie, Paris, France, *promotor*
Prof. dr. Niels Hellings, Universiteit Hasselt, Diepenbeek, Belgium
Dr. Isabelle Dusart, Université Pierre et Marie Curie, Paris, France
Dr. Michel Mallat, Université Pierre et Marie Curie, Paris, France
Dr. Etienne Audinat, Université Paris Descartes, Paris, France, *rappoteur*
Prof. Dr. Charles ffrench-Constant, University of Edinburgh, Edinburgh, UK, *rapporteur*

"What we observe is not nature itself,
but nature exposed to our method of questioning"

Werner Heisenberg

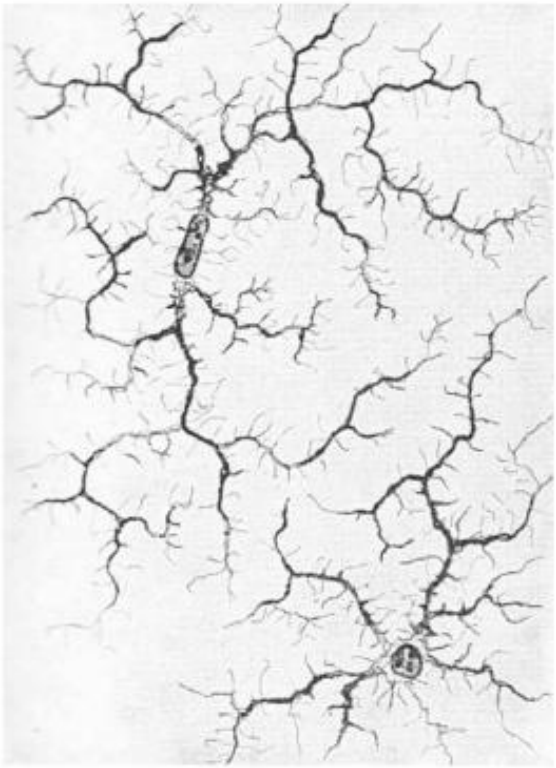

Microglia. Río-Hortega, 1919 & 1921

Table of contents

Table of contents **I**

List of Abbreviations **V**

CHAPTER 1: **1**

General introduction and aims

1.1 Basics of embryonic brain development 3

1.1.1 Progenitor amplification: E9-E12 3

1.1.2 Neurogenesis and cortical layering: E11-E18 4

1.1.3 Angiogenesis: from E8.0 4

1.1.4 Gliogenesis: E16-P20 5

1.2 The microglial cell: versatile outsider and one of a kind 6

1.2.1 Origin of microglia 7

1.2.2 Migration into the CNS 9

1.2.3 Microglial maturation inside the CNS 15

1.2.4 Homeostasis of microglia in the adult CNS 16

1.2.5 Undersigned, I, the microglial cell 17

1.2.6 Parenchymal and non-parenchymal CNS macrophages 18

1.2.7 Physiological functions of microglia 22

1.2.8 Functions of microglia in pathology 26

1.2.9 Gender differences 30

1.3 Cell Migration 31

1.3.1 ECM 32

1.3.2 Integrins 35

1.3.3 ECM/integrin signaling in microglia and their mobility 39

1.4 Study aims 42

CHAPTER 2: **45**

Complex invasion pattern of the cerebral cortex by microglial cells during development of the mouse embryo

2.1 Abstract 46

2.2 Introduction 46

2.3 Materials and methods 47

2.4 Results 50

2.5 Discussion 62

CHAPTER 3: **65**

Age-specific function of α5β1 integrin in microglial migration during early colonization of the developing mouse cortex

3.1 Abstract 66

3.2 Introduction 66

3.3 Materials and Methods 67

3.4 Results 72

3.5 Discussion 87

CHAPTER 4: **95**

The CXCL12/CXCR4/integrinß1 signaling axis in microglial migration: an exploratory study

4.1 Abstract 96

4.2 Introduction 96

4.3 Materials and Methods 98

4.4 Results 102

4.5 Discussion 114

4.6 Conclusion 119

4.7 Supplemental data description 119

CHAPTER 5: **129**

Maternal immune activation evoked by polyinosinic:polycytidylic acid does not evoke microglial cell activation in the embryo

5.1 Abstract 130

5.2 Introduction 130

5.3 Materials and Methods 132

5.4 Results 134

5.5 Discussion 145

CHAPTER 6: **149**

General discussion and perspectives

6.1 Properties of microglia during colonization of the embryonic brain 150

6.1.1 Morphology and protein markers 151

6.1.2 Maturation and the microenvironment 152

6.2 The microglial migration behaviour in the embryonic brain 152

6.2.1 Microglial settlement during embryogenesis 153

6.2.2 Regulation of microglial migration speed 154

6.3 Complex regulation of integrin function in microglial migration during development 155

6.4 Candidate cues for steering parenchymal microglial migration during development 156

6.4.1 Chemoattractants and chemorepellants 156
6.4.2 Cell death and synaptogenesis 157
6.5 Microglial interactions with blood vessels 158
6.5.1 Mechanisms of interaction 158
6.5.2 Attraction towards blood vessels 158
6.5.3 Mechanisms of influencing blood vessel branching 159
6.6 Does microglial activation by maternal immune activation lead to neurodevelopmental disorders? 160
6.6.1 Priming of microglia 160
6.6.2 Reported alterations in microglia upon MIA 161
6.6.3 Controversies in microglial activation following MIA 161
6.7 Limitations of this work 162
6.8 Outstanding questions 164
List of references **165**
Résumé **189**
Nederlandse samenvatting **191**
English summary **193**
Curriculum Vitae **195**
Dankwoord - Acknowledgments **199**

List of Abbreviations

Akt	Serine/threonine kinase
ASD	Autism spectrum disorder
ATP	Adenosin triphosphate
BBB	Blood-brain barrier
BDNF	Brain derived neurotrophic factor
BP	Bandpass
BSA	Bovine serum albumin
C	Complement
CCL	C-C motif chemokine
CCR	C-C motif chemokine receptor
CD	Cluster of differentiation
CNS	Central nervous system
CNS	Central nervous system
CNTF	Cilliary neurotrophic factor
CR	Complement receptor
CSF (R)	Colony stimulating factor (receptor)
CSPGs	Chondroitin sulphate proteoglycans
CT-1	Cardiotrophin-1
CX3CR1	Chemokine (C-X3-C motif) receptor 1
CXCL	C-X-C motif chemokine
CXCR	C-X-C motif chemokine receptor
DAP12	DNAX activation protein of 12kDa
DAPI	4',6-diamidino-2-phenylindole
DMEM	Dulbecco's Modified Eagle's Medium
E	Embryonic day
ECM	Extracellular matrix
eGFP	Enhanced green fluorescent protein
ERK	Extracellular signal–regulated kinases
FAK	Focal adhesion kinase
FBS	Fetal bovine serum
FN	Fibronectin
GABA	γ-aminobutyric acid
GDNF	Glial derived neurtrophic factor
GE	Ganglionic eminences
GFAP	Glial fibrillary acidic protein
GLAST	Glutamate aspartate transporter
(G)M-CSF(R)	(Granulocyt) macrophage coloniy-stimulating factor
GTP	Guanine triphosphate
HBSS	Hank's Balanced Salt Solution
HEPES	4-(2-hydroxyethyl)-1-piperazineethanesulfonic acid
HIV-1	Human type 1 immunodeficiency virus
HS	Horse serum
HSC	Hematopoietic stem cell
Iba-1	Ionized calcium-binding adapter molecule 1
ICAM-1	Intercellular Adhesion Molecule 1
IFN	Interferon
IGF	Insulin-like growth factor
IL	Interleukin
iNOS	Inducible nitric oxide synthase
iPLA2	Calcium-independent phospholipase A2
KO	Knockout
LFA	Lymphocyte function-associated antigen
LGE	Lateral ganglionic eminence

LIF	Leukemia inhibitory factor
LPS	Lipopolysaccharide
Mac-2	Macrophage-2 antigen
MAPK	Mitogen-activated protein kinases
MCP-1	Monocyte chemotactic protein 1
MECP2	Methyl-CpG-binding protein 2
MEK	Mitogen-activated protein kinase kinase
MFI	Median fluorescence intensity
MGE	Medial ganglionic eminences
MIA	Maternal immune activation
MIP	Macrophage inflammatory protein
MMP	Matrix metalloproteinase
MP	Myeloid progenitors
mRNA	Messenger ribonucleic Acid
NF-κB	Nuclear factor kappa-light-chain-enhancer of activated B cells
NGF	Nerve growth factor
NO	Nitric oxide
NOS	Nitric oxide synthase
NOX	NADPH oxidase
NT	Neurotrophin
P	Postnatal day
P/S	Penicillin Streptomycin
PBS	Phosphate-buffered saline
PCD	Programmed cell death
PFA	Paraformaldehyde
PKA	Protein kinase A
PI3K	Phosphatidylinositol 3-kinase
PLC	Phospholipase C
PM	Primary microglia
Poly (I:C)	Polyinosinic:polycytidylic acid
RANTES	Regulated on Activation, Normal T Cell Expressed and Secreted
RGD	Arginine-Glycine-Aspartate sequence
Rpm	Revolutions per minute
RT	Room temperature
SDF-1	Stromal cell-derived factor 1
SFK	Src family kinases
SVZ	Subventricular zone
TGF-β	Transforming growth factor-β
TLR	Toll like receptor
TNF	Tumour necrosis factor
TTX	Tetrodotoxin
VEGF	Vascular endothelial growth factor
VEGFR-1	Vascular endothelial growth factor receptor 1
VZ	Ventricular zone
Wnt	Wingless-type MMTV integration site family member

CHAPTER 1:

General introduction and aims

Why study microglia during brain development? The brain and spinal cord make up the central nervous system (CNS). These organs process all motor and sensory information and form the control center for all our daily activities. In the human CNS, approximately 100 billion neurons send electrochemical signals in dense networks and establish in total more than 600 trillion connections, called synapses that are necessary for us to breath, feel, move, and think [1, 2]. The CNS consists of neurons and glia, with the latter defined by Virchow in the 19th century as the cells that support the neurons by acting as a "glue" [3]. Depending on the brain region and age, roughly 50% of the cells in the brain are glia in humans, primates and rodents [4]. The largest and most important information-processing network in the mammalian brain is the neocortex, which consists of 20-25 billion neurons [5]. This is the outer layer of the cerebral hemispheres and it processes sensory information, controls motor output and mediates higher cognitive functions [1, 6]. This structure has a glia to neuron ratio of 3.76 and its cellular composition is highly conserved between humans, primates and rodents [4]. Glial cells can be subdivided into macroglia (astrocytes and oligodendrocytes) and microglia. The latter cell type constitutes 5-15% of all cells in the adult human brain and 6-18% of all neocortical cells [4, 7].

During development, one layer of germ cells called the neurectoderm, will generate these billions of neurons that eventually establish these trillions of connections by following highly conserved developmental programs. These processes are highly complex, dynamic, under strict genetic control and require a smooth operation [1]. Microglia are the first glial cells to be present in the brain and they populate the brain alongside the developing neurons. The timing of their appearance with regard to the onset of important developmental processes has led to many speculations about special functions of microglia in CNS development. Studies of the last decade have indeed established **critical tasks for microglia in guiding brain development**. However, **many aspects of their physiology and mechanisms underpinning their behaviour are still unresolved** [4, 8].

This dissertation focuses on migration of microglial cells during embryonic cortical development and explores whether adverse conditions during pregnancy can affect these cells. More in particular, this work addresses the following questions: when and where can we find microglial cells and how can we characterize them **(Chapter 2)**? How do microglia move once inside the brain tissue and are there any molecules or structures involved in their movement **(Chapter 3&4)**? Finally, the question whether maternal immune activation during pregnancy, which is associated with an increased risk for neurodevelopmental disorders in the offspring, can change the microglial activation status in the embryo is briefly evaluated **(Chapter 5)**.

The necessary context to understand the data and thoughts presented in this manuscript is provided in the current chapter (**Chapter 1**: General introduction and aims). First (Section 1.1), the basics of brain development and the time windows for the key events during corticogenesis are explained. Next (Section 1.2), the microglial cell and its functions in adult brain homeostasis and pathology are briefly examined. Subsequently, the origin of microglia, their maturation and functions during development are described, which will clarify the importance of studying microglial cells during embryonic corticogenesis. Then, the introduction is narrowed down to the mechanisms of microglial CNS invasion and colonization. The chapter proceeds (Section 1.3) with addressing the hallmarks of cell migration and it further focuses on the functions of the extracellular matrix and their major receptors, namely integrins, during brain development. Next,

an overview is given of the current knowledge with regard to integrin expression and function during microglial migration. The introduction closes with the development of the study aims (Section 1.4) accompanied by a scheme summarizing these aims with the most important study highlights and the chapters in which the different subaims are addressed **(Figure 1.11)**.

1.1 Basics of embryonic brain development

Brain development follows a strict stepwise program: neuroepithelial cells first generate neurons, then astrocytes and subsequently oligodendrocytes **(Fig. 1.1)**. The sequence of appearance of the different brain cells is similar in humans and rodents but the duration and the timing with regard to birth is species dependent [9]. Throughout this work, embryonic and postnatal ages (E and P, respectively, followed by a number indicating the amount of embryonic/postnatal days) always refer to those in mice, unless stated otherwise.

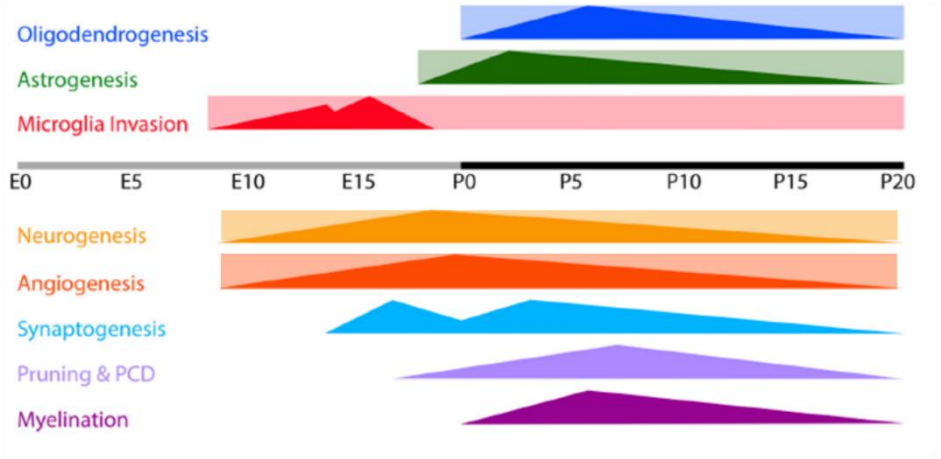

Fig. 1.1. **Timeline of developmental processes in the developing mouse brain.** Rectangles indicate the estimated periods during/from which different cell types are present in the brain. Triangles indicate the onset and peaks of the developmental processes. Neurogenesis refers to the continuum of processes from progenitor amplification to cortical layering and maturation. This is a general scheme, timing can slightly vary according to the region. Modified from Reemst *et al.* (2016) [4]. E, embryonic day; P, Postnatal day; PCD, programmed cell death.

1.1.1 Progenitor amplification: E9-E12

From E9 to E12 **(Fig. 1.1)**, the neuroepithelial cells first form a single cell layer called the neural plate. Then they divide symmetrically, which means that they generate a sister neuroepithelial cell to increase the size of the progenitor pool. Symmetrical division first occurs in the ventricular zone (VZ), which is the innermost apical zone lining the ventricular lumen, and then starts in the zone basal to it, the subventricular zone (SVZ) [10, 11]. Around E9 to E10 the neuroepithelial cells start to acquire a bipolar phenotype with astrocytic features, such as astrocyte-specific glutamate transporter (GLAST), brain lipid binding protein and calcium-binding protein S100β [10]. Until E12, they thus transform into radial glia that act as precursors for neurons, astrocytes and oligodendrocytes [10, 12]. A radial glial cell traverses the thickness of the neocortex with one long radial process extending from the ventricular zone (VZ), where its soma is located, right up dorsally to the pial surface.

1.1.2 Neurogenesis and cortical layering: E11-E18

From E11 onwards **(Fig. 1.1)**, radial glial cells start to divide asymmetrically to give rise to neurons or intermediate progenitors, in order to steadily increase the progenitor pool before any further cell differentiation [10, 11, 13]. Newborn neurons migrate away from the VZ/SVZ towards the pial surface, using the processes of the radial glia. This timely orchestrated mobilization results in the six layers of the cortex [10]. The generation of each of the neuronal layers depends on a combination of transcription factor signaling to specify its fate and on an intrinsic genetic program that involves a number of divisions before the progenitor enters an asymmetrical division to generate a neuron [11]. Around E11.0, the first postmitotic neurons constitute the preplate. At E12 the first neuronal layer forming one of the future cortical layers starts migrating and splits the preplate into the marginal zone, containing Cajal-Retzius cells, and the subplate [11, 14]. Subplate neurons form a transient population of neurons that resides just underneath (apically) the cortical plate. The subplate is the first layer to form cortical projections and acts as a scaffold for the generation of afferent thalamocortical connections, but it progressively disappears near birth by programmed cell death (PCD) [11, 15, 16].

When new neurons are born, they migrate outwards to a more superficial layer in the cortical plate where they reach the Cajal-Retzius cells and stop. This results in the inside-out arrangement of the six layers (layer VI containing the oldest and layer II/III the youngest neurons) of the adult neocortex [17]. This radial migration process holds true for projection neurons of the cortex [11]. The inhibitory interneurons (approximately 25% of all cortical neurons in the adult) are born from E11.5 until birth in the ventral forebrain, more specifically in the medial and caudal ganglionic eminences (MGE and CGE, respectively), and migrate tangentially, in other words parallel to the CNS surface to reach the cortical plate between E12.5 and birth [18]. Tangential migration of interneurons is followed by radial migration in order to fully populate the different layers of the cortex. Both types of migration are the basis for the cellular complexity of forebrain circuits and for the general cytoarchitecture of the cortex [1, 19]. Differentiation of neurons into layer-specific subtypes can be influenced by neutrophins, such as brain derived neutrophic factor (BDNF), nerve growth factor (NGF), neurotrophin-3 (NT-3) and neurotrophin-4 (NT-4) [11]. Migration of projection and interneurons is under control of many chemoattractants and chemorepulsive signals such as reelin, stromal derived factor 1 (SDF-1), ephrins, slit proteins, semaphorins and neuregulins [11].

1.1.3 Angiogenesis: from E8.0

Blood vessels in the brain develop only from pre-existing vessels through a process called angiogenesis [4]. Upon the start of progenitor amplification at E9.0, vascular plexi form **(Fig. 1.1)** [11, 20]. The first capillary sprouts invading the nervous parenchyma are visible at E9.5-E10. These new capillaries consist of tip cells at the vascular front and of proliferative stalk cells further down. Tip cells are attracted by vascular endothelial growth factor-A (VEGF-A), which induces a negative feedback loop in the adjacent cells to suppress the angiogenic and promote the stalk cell phenotype [21]. Then, neighboring tip cells anastomose to create vascular loops. These processes are repeated constantly in order to establish vascular plexi inside the ventricular zone,

subventricular zone and cortical plate, that are connected by tangential blood vessels at E14 **(Fig. 1.2)** [11, 21]. By E15, a few tangential blood vessels start to appear in the intermediate zone, but this region remains less vascularized in comparison to the others. At E18, towards the end of neurogenesis, the ventricular plexus is not well distinguishable anymore. By P8, a more homogeneous structure with many small parenchymal arteries is present **(Fig. 1.2)** [4, 11]. Outgrowth and alignment of blood vessels is controlled by pericytes and by chemoattractive and repulsive signals involved in neurogenesis such as VEGF, semaphorins and netrins [11, 22]. Development of the blood-brain barrier (BBB), which consists of endothelial cells coupled with tight junctions, a basement membrane, pericytes and astroglial endfeet, starts at E13.5 and is fully functional at E16.5 in the cerebral cortex [22]. This means that already during embryonic development, the BBB separates the fetal environment from the exterior together with the choroid plexus epithelial barrier and arachnoid barrier [11, 23].

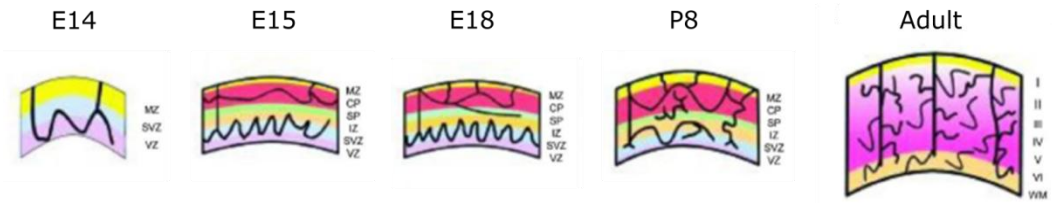

Fig. 1.2. Schematics of cortical vasculature development. The first blood vessels sprout into the parenchyma around E10 and at E14 two dense plexi in the ventricular zone (VZ), subventricular zone (SVZ) and cortical plate (CP) are visbible, connected by tangential blood vessels. The vascular network increases in complexity through angiogenesis and evolves to a homogenous structure supplying blood in all layers of the cortex. Modified from Stolp *et al.* (2012) [11]. E, embryonic day; IZ, intermediate zone; MZ, marginal zone; P, postnatal day; SP, subplate; WM, white matter; I-VI, cortical layers I-IV.

1.1.4 Gliogenesis: E16-P20

Around E16 gliogenesis starts and lasts until the end of the first postnatal month **(Fig. 1.1)**. Around this age, radial glia cease the production of neurons and the developmental program largely switches to astrocytogenesis and later oligodendrogenesis [10, 24]. This switch is under control of epigenetic regulation, such as DNA (de)methylation and/or acetylation that as long as neurogenesis is ongoing, represses the activity of the astrocytic promoters Glial fibrillary acidic protein (GFAP) and S100β, as well as the sensitivity of the progenitor cell to pro-astrocyte lineage directing cues present in the environment, such as Leukemia inhibitory factor (LIF), Ciliary neutrophic factor (CNTF) and Cardiotophin (CT)-1 [11]. Newly generated astrocytes migrate first tangentially and then radially to their final positions where they mature and induce synapse maturation during the first two to three postnatal weeks [11]. Similar to astrocytes, oligodendrocytes arise from radial glia **(Fig. 1.1)** but in this case through a pro-oligodendrocytic epigenetic switch that involves Wingless-related integration site (Wnt) signaling. Oligodendrocyte precursors arise in three waves and from different progenitors. The VZ of the ganglionic eminences gives rise to the majority of precursors in two prenatal waves. After neurogenesis completes postnatally, a third production wave arises in the cortical VZ [11]. Oligodendrocyte precursors first migrate to the cortex, where they appear by E16 [25]. Subsequently they mature and initiate myelination postnatally.

1.1.5 Synaptogenesis, Pruning and Programmed Cell Death: mainly postnatally

Maturation of the cortex proceeds postnatally and involves not only cell differentiation, connecting and strengthening of synaptic networks, but also the elimination of superfluous neurons produced during neurogenesis, which is called PCD. The majority of these processes occur during the first three postnatal weeks in mice **(Fig. 1.1)** [26]. Nevertheless, the first wave of synaptogenesis already occurs from E14.5 to E18.5 in the subplate **(Fig. 1.1)** [27, 28] and is regulated by thrombospondins, BDNF and anti-inflammatory cytokines [4, 29]. Synaptogenesis further peaks during the first postnatal week, followed by elimination (pruning) of excessive synapses, which allows further maturation of the remaining ones **(Fig. 1.1)** [16]. Similar to synapses, neurons are also produced in excessive numbers. Approximately 50% of neurons formed during development are cleared from the brain starting prenatally and peaking between P4 and P7 for projection neurons and between P7 and P11 for interneurons **(Fig. 1.1)** [4, 30]. Generally, PCD follows the inside-out gradient of neuronal migration during cortical layer formation [15].

Altogether, the time windows and major processes during brain development were described in the sections above. Another major event during brain development is the colonization by microglial cells. The physiology and functions of this cell type is put into the spotlight in the next sections.

1.2 The microglial cell: versatile outsider and one of a kind

A giant leap for neuroscience occurred in 1873 when Camillo Golgi developed his famous "Black reaction" staining technique. This discovery allowed neurohistologists to obtain images of neural cells in their entity and morphologically characterize the cells of the nervous system [31]. In 1898, Franz Nissl was the first to visualize "Stäbchenzellen" (rod cells) which he suggested to have a capacity for migration and phagocytosis [23]. In the 1910's, Pio Del Rio Hortega, a student of the Santiago Ramón y Cajal School and pupil of Nicolás Achùcarro, developed the famous silver-carbonate method [3]. Using this technique and light microscopy, Del Rio Hortega was finally allowed in 1924 to baptize the cells visualized by Nissl as "microglia" after a long-standing conflict between himself and Cajal [3, 31]. Although almost a century old, Del Rio Hortega's postulations about the mesodermal origin of microglia, their capacity for migration and phagocytosis still hold true today [32]. Microglia are often referred to as the CNS resident macrophage population.

In the healthy adult mouse CNS, microglia adopt a ramified morphology characterized by a small cellular body (± 4 to 7 µm in diameter *in vivo*) and multiple long and thin branched processes that can extend up to 50 µm from the soma [33-35]. Ramified microglia were classically defined as 'resting' cells, but this view was challenged by groundbreaking research of Axel Nimmerjahn and Dimitri Davalos in 2005 [34, 36]. Through cranial windows (thinned skull) in the adult mouse they observed highly motile microglial processes constantly protruding and retracting. Using this active scanning behaviour microglia survey the entire brain in just a couple of hours [34, 36]. In contrast, the amoeboid-like morphology is characterized by a large rounded soma (± 10 to 12 µm in diameter *in vivo*) with fewer, thicker and shorter processes. This morphology appears primarily during embryonic development and upon encountering activating stimuli, such as cytokines, products of invading organisms and intracellular contents [16, 33, 37]. It should be noted that a

large continuum of microglial morphologies exists in between these two extremes. Also, function and morphology are not necessarily linked and both can be influenced by the brain region in which they reside [35, 38-43].

1.2.1 Origin of microglia

Until the 1990's, researchers heavily debated whether microglia are ectodermally or mesodermally derived cells [23]. Later in 2006, it turned out Del Rio Hortega had been right all these years: it was demonstrated that mice lacking the transcription factor Pu.1, were also devoid of microglia [44, 45]. At that point the hematopoietic nature of microglia was established, but until 2010 it remained unclear whether the adult microglial population consisted of cells descending from embryonic progenitors or from circulating blood monocytes [23].

Embryonic hematopoiesis

Human and mouse hematopoiesis share a similar course and occur in three sequential but overlapping waves [46-48] **(Fig. 1.3)**. During the first wave, named primitive hematopoiesis, primitive myeloid progenitors (MP) are generated from E7.0 until E9.0 depending on the transcription factors Pu.1 and Scl-Tal-1 [46, 47]. These cells arise from hematopoietic progenitors inside the blood islands of the extra-embryonic yolk sac. Slightly later around E8.25-E8.5, but in overlap with MP generation, a transient wave of definitive hematopoiesis is initiated in the hemogenic endothelium of the yolk sac, in the endothelial cells lining the blood islands [49]. This wave lasts until E10.5-E11.5 and gives rise to erythromyeloid progenitors (EMPs), depending on the transcription factors Pu.1, stem cell leukemia/T-cell acute lymphoblastic leukemia 1 (Scl/Tal1), core-binding factor subunit beta (CBfb) and runt-related transcription factor 1 (Runx1) [47]. Starting from E9.0-E9.5 but in overlap with EMP generation, a second wave of definitive hematopoiesis is initiated and lasts until E12.5 in the aorta-gonads-mesonephros region and in the umbilical and vitelline arteries [46, 47]. This wave generates hematopoietic stem cells (HSCs) from the arterial hemogenic endothelium, depending on c-Myb, Scl-Tal-1, CBfb, Runx1 and Notch1, but no longer on Pu.1 (though macrophage differentiation is compromised upon Pu.1 absence) [46, 47]. Of note, the terminology "primitive" and "definitive" has been a source of confusion and in particular EMP generation is often mistakenly referred to as being part of the primitive wave [46, 49]. Since EMPs have the potential to generate erythrocytes and PMs not, the PM wave is strictly primitive while the EMP wave is not [46, 49]. Both EMPs and HSCs colonize the fetal liver around E10-E10.5 [48]. From E11.0-E11.5 on, the fetal liver is the major site for hematopoiesis and generates all hematopoietic lineages. From here, HSCs will colonize other hematopoietic organs such as the bone marrow at E15 to activate hematopoiesis in this site from E17 [47, 48].

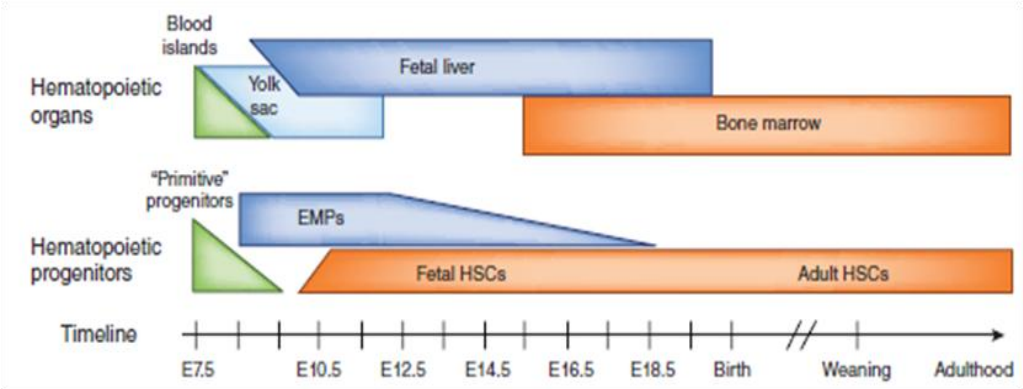

Fig. 1.3. Time scale for the development of hematopoietic progenitor cells in the mouse embryo. There are three successive but overlapping waves of hematopoietic progenitor cells during development, each of which has the potential to give rise to fetal macrophages. While primitive progenitor cells have been found only in a small time window (middle), definitive progenitor cells (including EMPs and HSCs) co-exist during most fetal development in the fetal liver. Only HSC-derived hematopoiesis then shifts to the bone marrow niche. The three waves of progenitor cells can also be distinguished by their differentiation potential *in vivo* (bottom). Primitive progenitor cells are restricted to the erythroid or myeloid lineage, while EMPs have both erythroid and myeloid potential. EMP-derived hematopoiesis gives rise to erythrocytes, macrophages, monocytes, granulocytes and mast cells. Modified from Perdiguero *et al.* (2016) with permission [47]. E, embryonic day; EMPs, erythromyeloid precursors; HSC, hematopoietic stem cells.

Microglia arise from hematopoietic progenitors in the yolk sac

Macrophages are generated in two phases: primitive and definitive hematopoiesis [47]. MP- and EMP-derived macrophages colonize the entire embryo starting from E9-E10. However, HSC-derived macrophages will colonize the tissues around E13.5-E14.5 and largely replace the yolk sac macrophages, but not microglia [48]. The developing BBB might shield the brain from these HSC-derived macrophages [48]. In fact, though still significant amount of controversy remains about the exact precursors, it is genuinely acknowledged that microglia emerge from c-kit^{+} (alternatively Mast/stem cell growth factor receptor or CD117) embryonic yolk sac progenitors before E8.5 in mice [20, 50-52]. These precursors develop into CD45^{+} c-kit^{lo} Chemokine (C-X3-C motif) receptor 1 (CX3CR1)$^{-}$ immature (A1) cells and mature into CD45^{+} c-kit^{-} CX3CR1^{+} (A2) cells that downregulate CD31 and upregulate F4/80 and Macrophage-colony stimulating factor receptor (M-CSFR) [52]. Microglial development is independent of Myb [52, 53], but dependent on Pu.1 [52], interferon regulatory factor 8 (Irf8) [52] and colony stimulating factor 1 receptor (Csf1R) [20, 54] (summarized in **Table 1.1** and **Fig. 1.6)**. Deletion of these genes resulted in embryos either devoid of microglia (Pu.1 knockout (KO)) [52], a ~1.6 fold (Irf8 KO) [52] or a ~4.3 fold to complete reduction (Csf1r KO) in microglial cells [20, 54]. More in particular, Irf8 seemed to be involved in the maturation of microglia from A1 to A2 precursors, while lack of Pu.1 clearly affected the size of the A1 population. So Irf8 is a factor implicated in the early microgliogenesis [52]. The maturation processes occur in the blood islands and cephalic mesenchyme before these cells invade the neuroepithelium [55]. The proliferating A2 population gives rise to microglia that travel to the brain rudiment between E8.5 and E9.5 using a functional blood circulation [20, 50-52]. Microglia are detectable in the cephalic mesenchyme already by E9.0 and from then express

CX3CR1, CD45 and F4/80 [20, 52]. By E9.5-E10.5 they are found in the neuroepithelium in the brain [20, 52] and by E11.5 they invade the spinal cord parenchyma [37] (Timeline of microglia development see **Fig. 1.5**). In humans, microglia invade the forebrain around 4.5 to 5.5 gestational weeks [56, 57].

The yolk sac origin of microglia is conserved across vertebrate species such as humans, rodents and avians [10, 23]. However, high temporal-spatial resolution fate mapping in zebrafish showed that microglia in the developing vs. the adult zebrafish CNS derive from different sources and show differential transcription factor dependencies [51]. Embryonic microglia develop from the rostral blood island which is the zebrafish equivalent of the yolk sac, while adult microglia arise from the ventral wall of the dorsal aortoa, which is the equivalent of the aorta-gonads-mesonephros, giving rise to HSCs. It remains to be shown whether this zebrafish-mouse discrepancy is due to species differences or to the lack of high temporal-spatial resolution of the current fate mapping strategies in rodents [51]. Therefore, at this moment a small contribution from non-yolk sac progenitors recruited later during development cannot be excluded.

1.2.2 Migration into the CNS

Attracting molecules

The mechanisms underlying microglial recruitment into the CNS have been partly assessed. Signaling of interleukin-34 (IL-34) and colony stimulating factor-1 (CSF-1) through their receptor CSF-1R on microglia, is essential for microglial survival and precursor entry into the CNS [20, 58]. Whether these attractants are required for microglia production in the yolk sac, to travel from the yolk sac to the brain or to infiltrate the CNS is unclear [59]. IL-34 mRNA is detectable at E11.5 in the embryonic mouse brain and preceeds the expression of Csf-1 mRNA [60]. Interestingly, during development both IL-34 and Csf1 transcripts are expressed in the cortex, but in complementary regions [61]. At E15.5 IL-34 is restricted to the marginal zone while Csf-1 is present in the subventricular and the ventricular zone. From P0-P20, IL-34 is found in cortical layers V to II, while Csf-1 expression is restricted to layer VI. This complementary expression patterns suggests different functions of these CSF-1R ligands during embryonic CNS invasion by microglia.

Additional studies have shed light on the attractive cues for microglia inside the cortex by using multiple gene KO and inhibitor approaches [62, 63]. Arno *et al.* demonstrated that microglia in the embryonic cortex accumulate in the VZ/SVZ, regions where C-X-C motif chemokine 12 (CXCL12, alternatively SDF-1) is highly expressed by basal progenitors located within these zones [62]. CXCL12 signals through binding on microglial CXCR4 and CXCR7 [62]. They found that ablation of basal progenitors as well as impairing their production of CXCL12 through genetic depletion or pharmacologically interfering with its signaling axis, resulted in local 20-40% decreases in microglial density in the embryonic cortex depending on the method [62]. So the CXCL12/CXCR4 signaling axis is involved in microglial recruitment to the VZ/SVZ. The role of this signaling axis in microglial migration inside the parenchyma is further investigated in **Chapter 4**. In addition, Lelli *et al.* showed that microglial density in the SVZ of nicotinamide adenine dinucleotide phosphate (NADPH) oxidase 2 (NOX2) deficient P3 mice, had decreased ~2.7 fold [63]. This effect was not

due to a defect in microglial proliferation and it was not observed in embryos, only in pups [63]. They further found that Nox2 acts downstream of vascular endothelial growth factor receptor 1 (VEGFR1) and CSF-1R signaling in primary microglia. Accordingly, microglial precursors inside the ventricle of newborn mice that lack the VEGFR1-tyrosin kinase domain necessary for signaling of this receptor, did not show Nox2 activation and consequently microglial infiltration into the SVZ was decreased by ~3.3-fold at P3. Presumably, hydrogen peroxide generated by Nox2 at the front edge of microglial extensions, controls remodeling of the actin cytoskeleton and promotes microglial migration [63]. However, the effect of Nox2 absence was transient since at P10 the abnormal microglial distribution had restored, possibly by a combination of proliferation and migration of nearby microglial cells [63]. Together, during early postnatal (P0-P3), but not embryonic development, microglia depend on VEGFR1-mediated Nox2 activation to escape from the lateral ventricles and infiltrate into the SVZ of the cortex [63]. Kierdorf *et al.* have investigated the contribution of other chemokines in microglial recruitment to the CNS [52]. They found that yolk sac progenitors express high mRNA levels of the following chemokine and chemokine receptor pairs: Cxcl4 and Cxcr3, Cx3cl1 and Cx3cr1, Ccl2 and Ccr2, Ccl9 and Ccr1. However none of these genes influenced microglial numbers and morphology at E14.0 in single KO strains [52]. Microglial density in CX3CR1 KO mice was transiently decreased by on average ~1.4 fold in the postnatal hippocampus between P8 and P28 [64] and by ~3 fold in the somatosensory barrel cortex at P6-P7, but was not changed at embryonic ages [65]. On the contrary, in 5 day old CX3CR1 KO animals, the density of microglia increased ~1.4 fold in the subcortical white matter [66]. Additionally, mRNA for matrix metalloproteinases (MMPs) 8 and 9, enzymes involved in remodeling of the extracellular matrix, was highly expressed in microglial progenitors that still needed to invade the mouse CNS parenchyma [52]. Upon maternal administration of MMP inhibitors at E13.0, microglial presence in the E14.0 brain had diminished roughly by half, suggesting that MMPs play a role in microglial migration/invasion into the brain [52]. Further, progranulin-a, a soluble growth factor expressed inside the early developing brain possibly attracts microglia into neuroepithelial tissues of the *in vivo* developing zebrafish [67]. In this case, decreased proliferation of microglial precursors outside the brain cannot be excluded as the cause for decreased numbers of retinal microglia in progranulin-a absence since besides cell migration, this molecule stimulates cell proliferation [67].

Next to chemokines and growth factors, a role for apoptotic neurons resulting from the naturally occurring PCD during development, in microglial attraction inside the brain has been hypothesized [16]. Microglia have been found in close association with apoptotic cells in different CNS regions during development [16]. Factors released by these dying neurons, such as CXCL1, lysophosphatidylcholine, sphingosine 1 phosphate and Adenosin triphosphate (ATP) and Uridine triphosphate, might attract microglial cells [16]. Xu *et al.* indeed found that apoptotic neurons and lysophosphatidylcholine promoted microglial colonization in the zebrafish optic tectum [68]. Also in quails, microglial entry and dispersion into retinal explants, mimicking the *in situ* developing retina, relies on purinergic signaling by extracellular ATP and Uridine diphosphate and coincides with an increase in retinal cell detah, suggesting microglial cells are attracted towards those dying cells [69]. However, live imaging studies in the excised developing mouse hippocampus have shown that microglial mobilization is not dependent on developmental cell death [70]. Whether apoptotic

cues are important for microglia recruitment towards the mammalian brain has not been investigated yet [4]. Other molecules such as semaphorins, netrins, Monocyte chemotactic protein 1 (MCP1 or alternatively CCL2), Macrophage inflammatory protein (MIP) 1-α and the purinergic receptors P2X4R and P2Y12R, might be involved in the recruitment process as well, but will not be discussed here because of lack of *in vivo* evidence (for review see [16]).

Together, these studies indicate that CXCR4, VEGFR-1, CX3CR1 signaling and MMP expression are involved in the attraction and invasion of microglial cells to the CNS during either embryonic, for CXCR4 and MMP8 and 9, or postnatal development, for VEGFR-1 and CX3CR1. After initial recruitment to the CNS, microglia intensively migrate (depending on the region in combination with proliferation) throughout the parenchyma in order to reach their final positions and to exert their manifold tasks [71-73]. It is however not known which molecules microglia use to migrate inside the parenchyma. This is further investigated in **Chapters 3 and 4**.

Colonization pattern

Microglia colonize the CNS through two waves of invasion, characterized by a steep increase in microglial cell number. The first wave starts in the early embryo and the second one start around birth. These waves have been documented in different CNS regions in humans, rabbits, rodents and quails [37, 55, 74-81]. Although microglia are already detectable in the embryonic human brain around 4.5-5.5 gestational weeks, the major influx and distribution begins around 16 weeks, around 22 weeks microglia with increased ramifications are widely distributed in the intermediate zone and by 35 weeks the microglial population is highly ramified [56, 82, 83]. Microglial proliferation and colonization during embryonic spinal cord development is dependent on P2X7 signaling [84]. Microglial numbers in different brain regions increase significantly to reach a peak during the first two postnatal weeks, when about 95% of microglial population has been established [26, 35, 64, 85-88]. Alliot *et al.* concludes that the postnatal increase in microglial numbers is due to *in situ* proliferation of microglial cells, though this percentage decreased steadily from 45% at P0 to 4% at P14 [85]. However in the rat developing brain, proliferation percentages were much higher, peaking at 99% at P9 [77]. Despite variations across regions, species and proliferation marker used, microglial proliferation seems to decrease steadily during the second postnatal week in rodents [16, 77, 89, 90]. Active proliferation is thus a key underlying mechanism of the colonization of the spinal cord, retina, corpus callosum, hippocampus and cortex by microglia during development and can be regulated by Granulocyte-macrophage colony-stimulating factor (GM-CSF), CSF-1, NT-3, IL-4 and 5, Migration inhibitory factor 1-α [16, 62, 91]. In addition to proliferation, attraction of microglia from outside the CNS seems a plausible explanation for the increase in cell number. Accordingly, Askew *et al.* reported an infiltrating monocyte wave into the parenchyma proper that peaked at P3 in mice but found that this population quickly underwent apoptosis between P3 and P6 and did not contribute to the adult microglial population [86]. The function of this monocyte-derived wave is unknown, though the authors speculate about a role in inducing cell death in a subpopulation of yolk sac-derived microglia [86]. Because this monocyte wave rapidly disappears, it cannot account for the peak in microglial density at P14. This suggest that microglia might be recruited from microglial precursors already formed and waiting outside the nervous parenchyma, for example in the ventricle, to infiltrate the CNS at the appropriate time

points, as reported by Lelli *et al.* [63]. Nevertheless, multiple lines of evidence in rodents indicate that the adult microglial density is acquired after a rapid decrease of 50% in cell number between the third and the sixth postnatal week resulting from decreased proliferation and increased apoptosis, to remain steady during adulthood [26, 55, 64, 86]. These major events in microglial development during embryogenesis are summarized in **Fig. 1.5**.

After invading the CNS, microglia distribute into the parenchyma according to specific spatiotemporal patterns that are well studied throughout development in different species, such as humans, rodents, avians and zebrafish [92]. Live imaging in the developing zebrafish brain shows that microglia have a high capacity to patrol throughout the parenchyma, which allows them to explore the dense neuroepithelium efficiently and possibly deliver signaling molecules [93]. The exact infiltration route into the CNS is not yet fully known, but histological studies mainly from birds and humans suggest that microglia might enter the brain from the meninges, the ventricles and through blood vessels [16, 55, 92] **(Fig. 1.4)**. These proposed entry routes are based on the presence of microglia inside the ventricles [57], on the high microglial density in the meninges [57, 94] and their near association with blood vessels [92]. When the brain is vascularized but the BBB is not yet fully established (in the cortex the BBB becomes fully functional at E16.5 [22]), it has been suggested that microglial progenitors may enter the parenchyma by crossing the blood vessel wall [37, 94]. Once inside the neuroepithelium, microglial colonization occurs dorsally to ventrally and rostrally to caudally [92]. Studies in the developing quail retina, optic tectum and cerebellum have suggested that microglia in regions of laminar organization use definite routes to migrate to their final destinations, namely tangential and radial routes [95-97]. First, microglia spread in a full single layer throughout each CNS region and this seems to occur along long tangential oriented axonal fascicles, which pass near the microglial entry "hot spots". Tangential migration of microglia in the retina occurs using the end-feet of Müller cells, the local radial glia [78]. Doing so, microglia adopt a flat morphology, probably because of the laminar environment, with extensive lamellipodia. Some microglia were clearly polarized in the movement direction, others were non-polarized with projections radiating in all directions. This could indicate that microglial cells explore their microenvironment in order to orient their movement. In other CNS regions made of axonal fascicles, microglia appear more rounded but show similar morphological characteristics as described above. Additionally, they are in close contact with their substrate [78, 91]. Then, the cells change direction, to migrate perpendicularly to the surface of the CNS to populate the different layers of the nervous parenchyma [57, 91]. This radial migration towards the pial surface has been described in the retina, optic tectum and cerebellum of the quail embryo [91]. In the developing human cortex, microglia migrate towards the cortical plate and accumulate at its ventral border, at the junction with the subplate [57]. This layer contains mature neurons that receive afferent input from thalamic neurons.

In the developing brain, microglia are not homogenously distributed. Instead they are found in specific locations, such as in areas of cell death, in association with the developing vasculature and radial glia, in regions containing developing axon fascicles and acellular spaces (reviewed in [92]). These associations are mainly related to locally exerted functions of microglia as later discussed in **Point 1.2.7**. Nevertheless, structures such as blood vessels and radial glia might aid microglia in

their turn to spread throughout the nervous parenchyma **(Fig. 1.4)**. In different CNS regions and species, including human, microglia interact with blood vessels during development [35, 92]. Adhesion molecules present on blood vessels, such as intercellular adhesion molecule (ICAM)-1 and its receptor lymphocyte function-associated antigen (LFA)-1 (alternatively CD11a or integrin αLβ2) on microglia could mediate migration along blood vessels [98]. Effectively, microglia can use blood vessels to migrate along in a model of acute brain damage [99]. In this way, it is clear that blood vessels can function as substrates for migration, so obviously a reciprocal interaction exists between blood vessels and microglia [21]. The molecular basis for this contact is further explored upon in **Chapter 3**. Contact between microglia and radial glia was also observed in several CNS regions and species and extracellular matrix (ECM) deposition along radial glia could serve as a mechanical substrate mediating migration (see **Point 1.3.1**) [92]. In the E13.5 ventral part of the developing mouse spinal cord, 50% of microglial cells were found to interact with radial glial fibers, which suggest that radial glia may guide radial migration of microglial cells into the spinal cord parenchyma [37]. In the retina, microglia adhered to the processes of Müller cells, proposing these cells as a mechanical substrate for radial migration [91]. Indeed, a subsequent study indicated that radially migrating microglia in the developing quail retina use the processes of laminin (an extracellular matrix glycoprotein)-expressing Müller cells as a substratum and that they ramify while migrating [81]. Of note, the studies mentioned above are all based on immunohistochemical analysis and lack live approaches to follow microglial migration along these structures in real time during embryonic development.

Microglial colonization of the CNS seems to be a highly conserved process among species and this pattern is likely related to the functions that these cells exert during development. Whether the same microglial migration phases and substrates occur in a more complex structure of the mammalian CNS, such as the neocortex, and whether *in situ* findings can be extrapolated to the *in vivo* setting, remain open questions. The microglial colonization pattern of the cortex together with the cell's characteristics are investigated in **Chapter 2**.

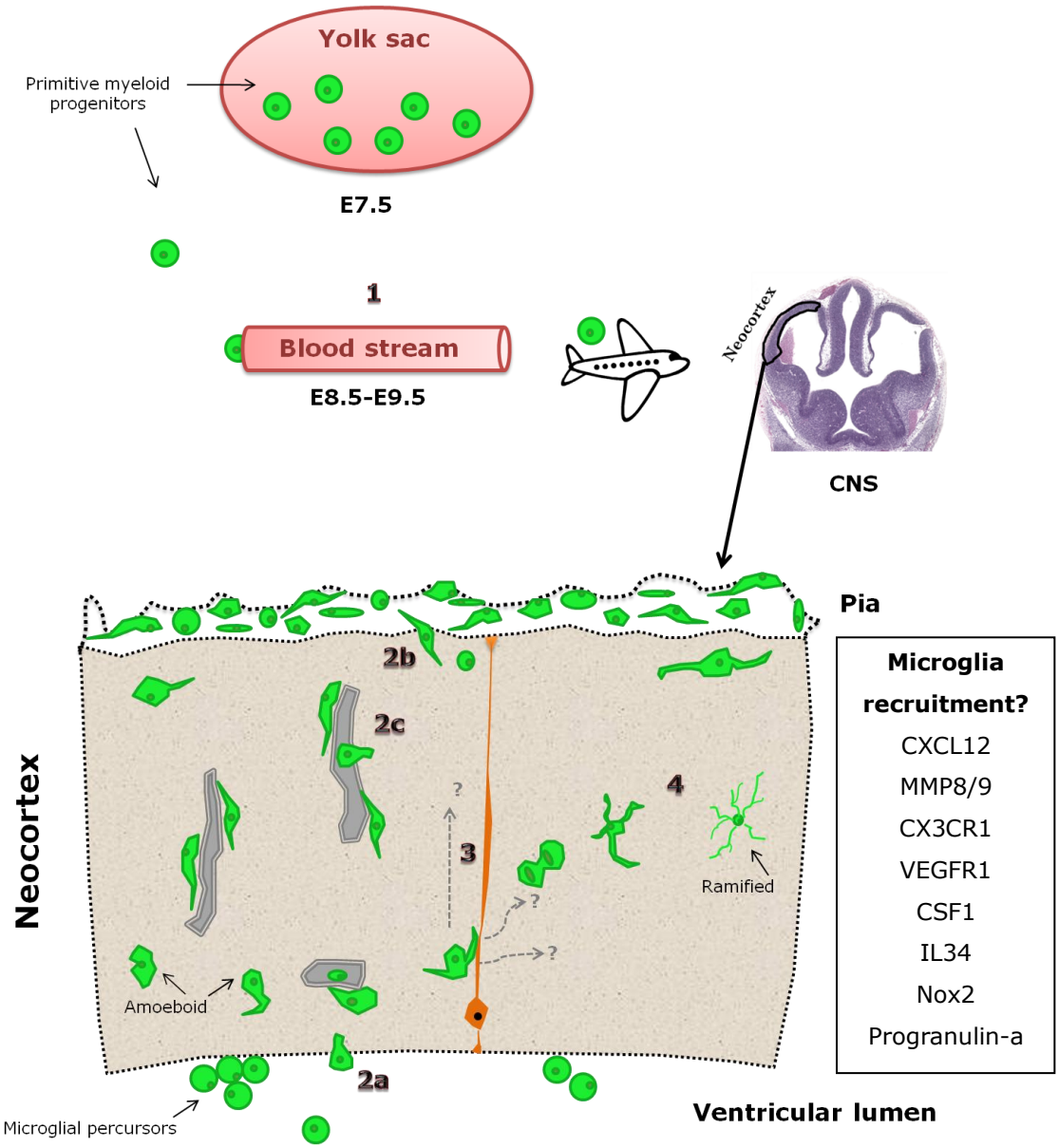

Fig. 1.4. Hypothetical scheme of microglial colonization of the neocortex. 1. Primitive myeloid progenitors arise in the yolk sac around E7.5 and travel to the CNS between E8.5 and E9.5 via the developing circulation. **2.** Once arrived in the CNS, microglial precursors are thought to invade the brain parenchyma in amoeboid forms by crossing the ventricular lining **(2a)**, the pia **(2b)** or in a later phase by penetrating the blood vessel wall (grey filled structures) **(2c)**. **3.** Next, microglia actively proliferate and migrate throughout the tissue to reach their final destinations. Migration can be guided through interaction with radial glia (orange) and/or blood vessels. **4.** In a last phase, these cells differentiate into fully ramified microglia, characterized by multiple thin processes, constantly scanning the microenvironment for changes. Drawings are not to scale. Adapted from Master thesis Smolders SMT (2011). E, embryonic day; CNS, central nervous system.

1.2.3 Microglial maturation inside the CNS

Once inside the CNS, microglia gradually mature. Research in zebrafish larvae shows that at these early time points these so called immature cells already move their processes, suggesting an active contribution to brain development [93]. However, the mechanisms underpinning this event *in vivo* are poorly understood up to date, though transcriptional profiling studies bring valuable information to the field. Maturation can be considered from different angles: morphology, function and transcriptional profile (reviewed in [16]).

In culture, astrocyte-derived soluble factors including cytokines (transforming growth factor-β (TGF-β), M-CSF and GM-CSF and purines (ATP and adenosine) induce microglial ramification even in the absence of physical contact with astrocytes [16]. Another *in vitro* study however shows that the physical contact (even in fixed conditions) is essential to influence the ramification process [100]. Recently, it was confirmed *in vivo* that the level of microglial process ramification in the adult brain is under control of purinergic signaling [101]. *In vivo*, the actual transformation of microglia from "amoeboid" to "ramified" was reported to start around P10, when transcription factor Runx1 is lost [102, 103]. By P28 the ramification process is complete [102, 104] **(overview in Fig. 1.5)**. Several studies in human fetuses describe a general "pattern of microglial differentiation", which is associated with displacement of microglia from the deeper layers of the cerebral hemispheres towards the cortical plate, with increasing ramification and with a gradual loss of expression of several markers such as CD68, CD45, CD11b and Human leukocyte antigen-antigen D related (HLA-DR, or Major histocompatibility complex class II molecule, MHCII in mice) (reviewed in [82]). It is not clear yet whether the same pattern of differentiation is observed in rodents as well.

Functional (electrophysiological) maturation coincides in general with increasing ramification, although high heterogeneity remains in the microglial electrophysiological phenotypes at the same age [16, 35]. Amoeboid, embryonic microglia show an inward K^+ current while this current declines during postnatal maturation and transiently switches for a outward K^+ current. In contrast, adult microglia are almost devoid of voltage-dependent currents, which are usually observed only in activated microglia under pathological circumstances [35]. Astrocyte-derived diffusible factors such as TGF-β control the upregulation of outward K^+ currents [16]. The function of these voltage-dependent K+ currents mediated through Kv1.3 channels in embryonic microglia has not yet been elucidated, but might encompass a deactivation process [105] or alternatively, Kv1.3 might be related to integrin-mediated adhesion and migration **(see Point 1.3)** of microglia during postnatal development [35, 106-108]. In addition, microRNA-124 downregulates motility and phagocytic capacity and thus impairs the functional maturation of microglia in *in vivo* zebrafish larva [109]. microRNA-101a might also be involved in regulating the microglial morphology and immune response in the adult brain [110]. Further, CX3CR1 signaling is necessary for morphological maturation (ramification) and functional maturation such as the acquirement of an outward rectifying K^+ current and the ability to send out protrusions in response to ATP [111].

Matcovitch-Natan *et al.* demonstrated that microglia develop following discrete transcriptional phases: "early microglia" (E10.5 to E14), "pre-microglia" (E14 to P9), and "adult microglia" (4

weeks postnatal and onwards) [112] **(overview in Fig. 1.5)**. The emergence of an adult transcriptional profile remarkably coincides with a drop in microglial density after 4 weeks postnatal and the establishment of the mature ramified morphology at P28 [16, 102, 112]. The study of Butovsky *et al.* corroborates these findings and shows that microglia gain their mature transcriptional signature possibly a bit earlier than P21, but for sure after P4 in mice [113]. At that point, their transcriptional profile is already distinct from macrophages recruited to the CNS in disease settings, from primary microglial cultures (from P1-2), from embryonic stem cell derived microglia and from the most common used microglia cell lines (BV2 and N9). Interestingly, they found that the transcriptional signature from freshly sorted newborn (P1) and cultured primary microglia mimicked the *in vivo* adult microglial signature the best [113]. Together, both studies found marked differences between the embryonic and the adult microglia transcriptome, which stresses that the series of maturation events are possibly regulated by the rapidly changing local environment [112, 113]. In addition, the different tasks microglia fulfill depending on the developmental needs might be reflected in their transcriptional signature.

Recently, expression of Sall1 and other genes important for microglial development and function, was shown to be under control of NRROS, a myeloid expressed transmembrane protein in the cell's endoplasmatic reticulum [114]. In addition, MafB, one of the principal transcription factors highly elevated upon the shift from pre-to adult microglia, turns out to be a key regulatory gene in microglial homeostasis as well [112]. MafB critically influences the ability of microglia to acquire an adult transcriptional signature and is an important "off" signal that regulates the anti-viral response [112]. Furthermore, recent evidence demonstrates a role for the gut microbiota, i.e the microflora that colonizes the gut, in regulating microglial maturation as well [112, 115]. In the absence of the microbiota, microglia display morphological characteristics and a gene expression profile that correlates to an immature status, which is maintained throughout adulthood [112, 115]. In addition, developmental maturation of the microglial transcriptional signature appears to be delayed in males compared to females [116].

In summary, microglia constitute the only macrophage population that in the adult steady state is derived mainly or maybe entirely from yolk sac-derived progenitors. After initial maturation from precursors at the places where they originate, they mature further in the brain in specific transcriptional phases. From postnatal week 4 they have acquired an adult and matured morphologic and transcriptional phenotype.

1.2.4 Homeostasis of microglia in the adult CNS

In the rodent adult brain in steady state conditions, microglia are dispersed ubiquitously throughout both white and gray matter while each cell occupies its own (variable) micro territory [29, 34, 86]. Microglial cell bodies are dispersed at 50 to 60 µm distance from each other [34] and are seeded in densities of about 240 cells/mm² in the adult rodent cortex, which remains stable over the animal's lifetime [86, 113]. Askew *et al.* recently discovered that microglia have a surprisingly fast turnover rate of 0.79% per day in mice [86]. They calculated that the whole microglial population renews itself in 95 days by coupled proliferation and apoptosis **(Fig. 1.5)**. Further investigation on microglial proliferation rates in the homeostatic mouse brain revealed high

differences in proliferation rates between brain regions [117]. The microglial proliferation rate corresponds to the overall level of proliferation in their local environment and results in a long-lived population of cortical microglia while olfactory bulb microglia are replaced in 8 weeks [117]. Of note, ^{14}C analyses demonstrate that also the human cortical microglial population shows a slow and nearly complete turnover over the life span of an individual with some cells possibly being decades old [118]. While some studies using depletion approaches suggested that microglia proliferate from local nestin-positive progenitors, this was not true in the normal undisturbed brain [58, 86, 117, 119].

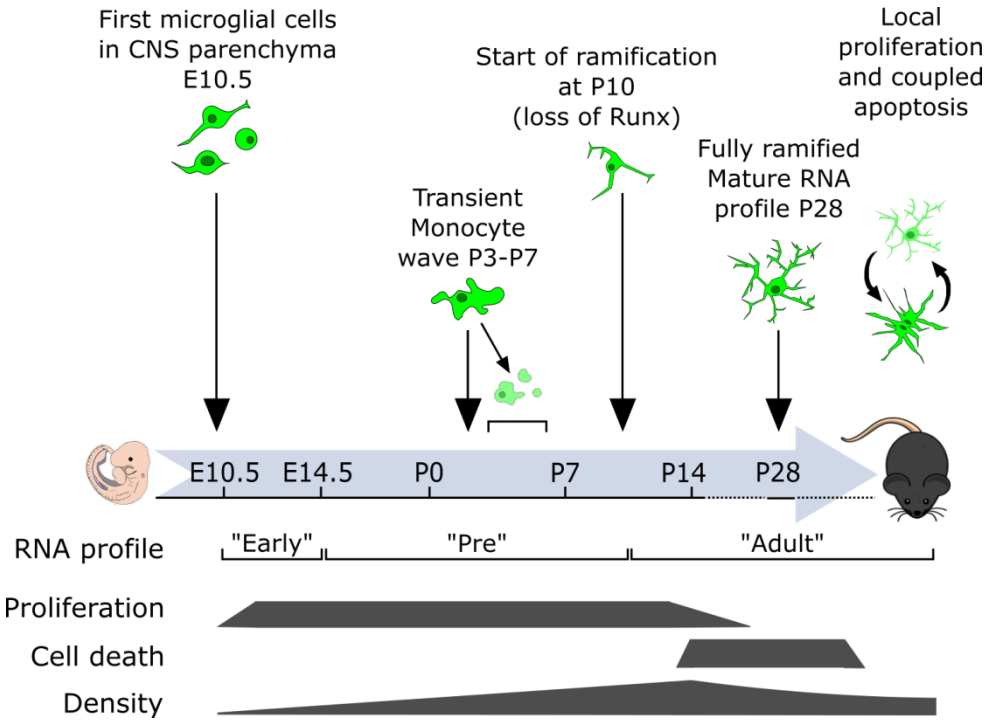

Fig 1.5. Regulation of the microglial population. Scheme is not to scale. Timing of events is approximately and can vary across CNS regions. CNS, Central nervous system; E, Embryonic day; P, Postnatal day.

1.2.5 Undersigned, I, the microglial cell

Cell-fate mapping and transcriptional profiling studies have revealed that tissue macrophages possess a highly specialized gene expression signature, depending on their local environment [120-125]. This holds true equally well for microglia: both the location where they reside inside the CNS and the age of the organism contribute to differences in gene expression and function [40, 43, 112, 113, 116, 124, 126-130]. For example microglia from cortex, spinal cord, hippocampus and olfactory bulb show subtle differences in gene expression levels, while microglia from cerebellum and eyes seem to be less comparable to microglia from the previously mentioned regions [113] and spinal cord microglia react more intense to traumatic injury than their counterparts in the brain [128].

Over the past 4 years a plethora of studies have established a microglia (CNS resident) vs. macrophage (non-CNS resident) specific transcriptional signature **(Table 1.1 and Fig. 1.6)**, which is also established in zebrafish and humans (for review see [31]). This unique genetic signature clearly distinguishes microglia from any other brain or (infiltrating) immune cell. Microglia and recruited monocytes during neuroinflammation maintain their own molecular signature, as was validated in experimental autoimmune enchepahlomyelitis chimeric mice [113]. However, a study on the human brain showed that the homeostatic microglial signature is lost in multiple sclerosis lesions (for example P2Y12R expression), which indicates that the microglial signature might not be entirely stable under all circumstances [131].

1.2.6 Parenchymal and non-parenchymal CNS macrophages

Two recent studies established important discrepancies with regard to origin, gene and protein expression between CNS parenchymal macrophages, i.e. microglia, and CNS non-parenchymal macrophages such as meningeal macrophages, perivascular macrophages and choroid plexus macrophages [123, 126] **(Table 1.1 and Fig. 1.6)**, all of which have been mostly grouped under the numerator of "microglia". Importantly, Goldmann *et al.* found that all but one CNS resident macrophage populations originate from progenitors in the yolk sac and have no contribution from HSCs in the bone-marrow [126] **(see Point 1.2.1)**. Choroid plexus macrophages form the exception: they are partially derived from HSCs and turn over more rapidly **(Table 1.1)** [126]. These studies established that adult parenchymal microglia have a unique transcriptional profile that is characterized by high expression of the genes *P2ry12, Hexb* and *Sall1* and *Tmem119* [123, 126, 132].

From the multiple transcriptional profiling studies and microglia-specific gene depletion models, Sall1 and TGF-β1 emerged as the guards of the adult microglial cell identity and function [113, 123]. Sall1 is exclusively expressed by the parenchymal microglia population and by no other CNS resident or non-resident macrophage and is therefore the preferred gene to perform microglia specific manipulations *in vivo* [123]. However, it must be noted that neuronal and glial progenitors during embryogenesis highly express *Sall1*, which unfortunately precludes this gene for microglia-specific approaches during development [133]. In the steady state, microglia specific depletion of Sall1 or TGF-β1 resulted in a shift from a resting microglia to an inflammatory macrophage phenotype [123]. Thus, Sall1 and TGF-β1 are key genes that keep microglia in a homeostatic phenotype. For an extensive and recent review on how microglial phenotypes are transcriptionally controlled in healthy and pathological circumstances, see Holtman *et al*. (2017) [134].

In summary, CNS parenchymal macrophages, i.e. microglia, have a unique gene expression signature depending on the CNS environment that enables differentiation from other CNS and peripheral macrophages.

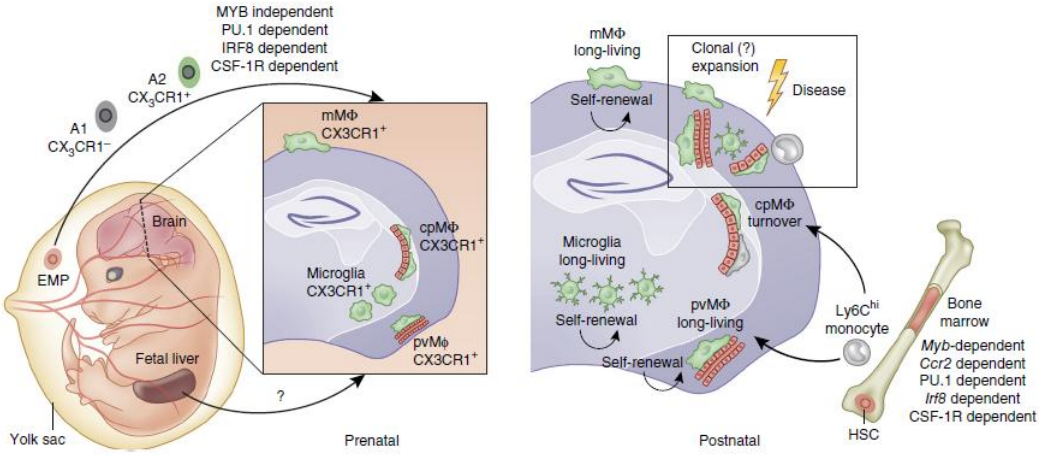

Fig. 1.6. Origin and tunrover of CNS resident tissue macrophages. CNS macrophages are derived from prenatal sources (left) and have no exchange with blood cells in the healthy adult brain (right). A transient early wave of myeloid cell development (left) takes place at E7.0–E8.0. At this time, EMP cells develop in blood islands of the yolk sac. Their progeny further proliferate, differentiate and populate several tissues, including the brain (left). CX3CR1^{+} A2 progenitor cells derive from c-Kit^{+}CX3CR1^{-} A1 cells and differentiate within the brain into microglia, perivascular macrophages (pvMΦ), meningeal macrophages (mMΦ) and choroid-plexus macrophages (cpMΦ). Factors important for proper CNS macrophage development are PU.1, IRF8 and CSF-1R, whereas all these cells develop independently of MYB. During further development, myelopoiesis is taken over by progenitor cells found from E12.5 in the fetal liver. Maturing myeloid cells continue to engraft in all tissues beyond E14.5–E15.5; however, due to the BBB, the microglia and largely non-parenchymal CNS macrophages are thought to be excluded from a fetal contribution. Starting around birth (right), myelopoiesis is thought to be restricted to bone marrow. Whereas choroid-plexus macrophages are the only cells with a substantial contribution from bone-marrow progenitors, meningeal macrophages and perivascular macrophages exhibit extreme longevity and self-renewal potential. Bone-marrow cells can enter CNS compartments only under disease conditions or following irradiation. From Prinz *et al.* (2017) with permission [135]. BBB, Blood-brain barrier; CNS, central nervous system; EMP, erythromyeloid precursor; HSC, hematopoietic stem cell.

Table 1.1.Origin and markers for macrophages at central nervous system interfaces in the mouse.

Myeloid Cell Type	Location	Origin	Turnover rate	Transcriptional signature	Protein markers	TFs for develop-ment	TFs for survival	*in vivo* behaviour
CNS resident Mononuclear phagocytes								
Microglia	CNS Parenchyma	Yolk sac (E7.25 - E8.0) [20, 52, 53, 85, 126]	After 46 weeks still steady [126] 95 days for whole population self-renewal [86] Region dependent [117]	P2ry12 ^{hi} [113, 126] Hexb ^{hi} [113, 126] Sall1 ^{hi} [113, 123] Lyve1 ^{int} [123] Tgfbr1 [113] Gpr34 [113] Tmem119 [113, 132, 136] Fcrls [113] Olfml3 [113]	P2RY12 [113] Ly6C ^{lo} [123] CD45 ^{lo} [123] MHCII ^{lo} [123] TMEM 119 [132]	Pu.1[52] Csf1r [20] Irf8 [52]	Csf1r [58, 86, 123]	Stationary, scanning [34, 36, 126]
Perivascular macrophages	Sandwiched between endothelial and glial basement membranes [126]	Yolk sac [126]	After 46 weeks still steady [126]	Mrc1 [126] Lyve1 ^{hi} [123] Sall1 ^{lo}[123] Cd163 [135] Hpgd [135] Slc40a1 [135] F13a1 [135]	CD206 [126] Ly6C ^{lo} [123] CD36 [126] CD45 ^{hi} [123] MHCII ^{lo} [123]	Pu.1 Csf1r Irf8 NA [126]	Csf1r [58, 86, 123]	Stationary, scanning along blood vessel wall [126]
Meningeal macrophages	Subdural meninges Close vicinity to ER-TR7^{+} fibroblast like cells [126]	Yolk sac [126]	After 46 weeks still steady [126]	Sall1 NA [123]	CD206 [135] MHCII ^{hi} [135]	Pu.1 Csf1r Irf8 [126]	Csf1r [58, 86, 123]	Tendency to migrate, more amoeboid morphology [126]
Choroid plexus macrophages	Stroma and epithelial layer of choroid plexus [126]	Yolk sac [126] Bone marrow [126]	35 weeks to half in [126]	Lyve1 ^{int} [123]	CD206 [123] CD45 ^{hi} [123] Ly6C ^{lo} [123] MHCII ^{hi} [123]	Pu.1 Csf1r Flt3 [126] Irf8 indep. [126]	Csf1r [58, 86, 123]	NA

Non-CNS resident Mononuclear Phagocytes

Patrolling monocytes [48]	Blood	HSCs after E11.5 [48, 137]	5-7 days [138]	Sall1 ^{neg} [123] P2ry12 ^{neg} [113]	Ly6C $^{lo\ or\ neg}$ CCR2 ^{lo} [48, 137] CX3CR1 ^{hi} [137] CD45 ^{hi} [123] Lyve1 ^{int} [123] MHCII ^{lo} [123]	Csf1r dep [48] Myb NUR77 [48, 137] CX3CR1 [48]	Csf1r [48] NUR77 [48]	Dependent on activation status
Inflammatory monocytes [48]	Pathogenic site	HSCs [48]	8 -20 hours [48, 138]		Ly6C ^{hi} CCR2 ^{hi} [137] CX3CR1 ^{lo} [137] CD45 ^{hi} [123] Dependent on activation status	Myb GM-CSF [137]		
Other tissue-resident macrophages*	Tissue-specific	E8.5-E9.0 yolk sac but later re-placed °		P2ry12 ^{lo} [113]	Dependent on activation status	Csf1r [20] Myb indep and dep Pu.1 [48]		

Involved genes and markers are considered only under homeostatic conditions.
All cells in this table express CX3CR1, Iba-1, CD11b, MERTK [135, 139]. Development of all macrophages is Batf3 indepenbent, besides monocytes [126]. Ly6C is the rodent equivalent of human CD14, KIT (CD117), FLT3 (CD135). Protein markers to differentiate CNS resident macrophages from non-resident infiltrated macrophages are CCR2 and Ly6C (both not in CNS resident Mφ), TMEM119 (only in resident Mφ from P14 onwards [132]), CD45 $^{hi/lo}$ (Parenchymal microglia CD45 ^{lo}), Sall1 and P2RY12 (both ony in parenchymal microglia), MHCII (not in parenchymal microglia) [135].
Not all microglia contacting blood vessels are pvMφ (Fig. 1 in [126]). pvMφ are not yet fully developed by E16.
** Other tissue-resident macrophages include macrophages from spleen red-pulp, lung alveoli, epidermis (Langerhans) cells), liver (Kupffer cells), peritoneum, pancreas (F4/80 bright cells), kidney and the heart.*
dep., dependent; Hi, high; HSCs, hematopoietic setm cells; indep., independent; Lo, low; NA, Not assessed in general or in the study reffered to; TF, transcription factor.
Not searched for in literature.
For review publications on this topic see [31, 47, 135, 140].

1.2.7 Physiological functions of microglia

in the developing CNS

Microglia exert a plethora of functions during CNS development **(Fig. 1.7)**. One of microglia's most evident tasks comprises clearing enormous amounts of dead cells resulting from PCD. A recurrent question is whether microglia merely serve as housekeeping cells to clean up the debris, or whether they actually trigger cell death themselves. Factors secreted by microglia *in vitro,* such as TNF-α and NGF, promote cell death [16]. Further *in vivo* evidence shows that microglia bear cerebellar Purkinje cell derived inclusions and that elimination of microglia resulted in a reduced Purkinje cell apoptosis, which is otherwise promoted by the microglial respiratory burst [141]. Further, microglial CD11b and the immunoreceptor DNAX activation protein of 12kDa (DAP12) act in convergent pathways to control microglial superoxide ion release which results in neuronal cell death [142]. *In vitro* as well as *in vivo* evidence shows that microglia can both decrease and increase the number of neural precursor cells within proliferative zones in the primate and rodent neocortex [10, 62, 143, 144]. With respect to decreasing the neuronal precursor population, this regulation occurs through phagocytosis of viable neurons, a process named phagoptosis, and does not depend on the typical eat-me signals [145]. Notably, the microglial phenotype (pro- or anti-inflammatory) influences whether progenitors are phagocytosed or not [145].

Next to killing and cleaning up neurons, microglia can provide trophic support to promote neuronal survival and proliferation. This support occurs through secretion of factors known to promote neuronal survival such as BDNF, NT-3 and glial-derived neurotrophic factor (GDNF) [16, 146, 147]. *In vitro*, microglial derived soluble factors increase the proliferation of cerebellar granule cells and neural precursors [16]. Notably, two recent *in vivo* studies established a clear trophic action of microglia on developing neurons. Neuronal survival was stimulated in layer V of the cortex at early postnatal stages through neurotrophic insulin-like growth factor 1 (IGF-1) and CX3CL1 signals [66]. Comparable neurotrophic (and also oligotrophic) support was reported in the underlying cortical SVZ at the same ages, while here not IGF-1 but microglial release of IL-1β, IL-6, tumour necrosis factor-α (TNF-α) and interferon (IFN)-γ were involved [54, 148]. Interestingly, a certain state of microglia activity was needed for proper neurogenesis as well as for oligodendrogenesis [54, 148]. In its turn, the microglial cytokine production, phagocytosis and migration can be regulated by neural progenitors that release VEGF and CXCL12 (alternatively SDF-1) [62, 149]. Together, these studies indicate that like in the adult, there is a bi-directional communication between developing neurons and microglia with regard to proliferation/survival and attraction [59, 62].

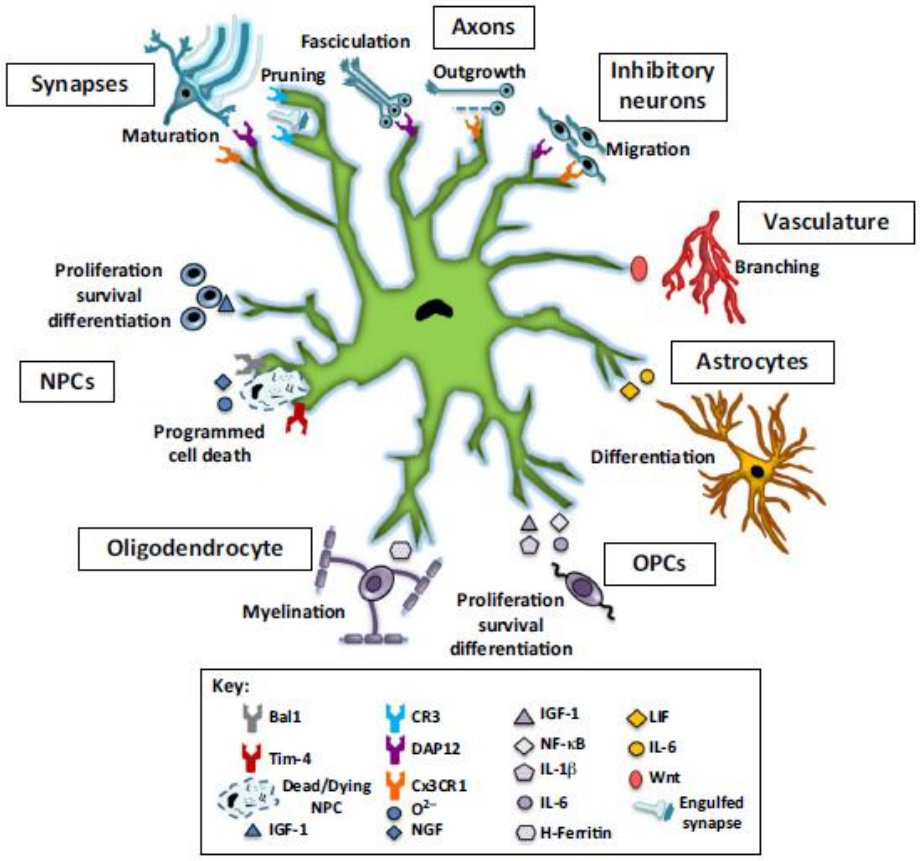

Fig. 1.7. Microglial functions during CNS embryonic development. From Frost *et al.* (2016) with permission [8]. CR3, complement receptor 3; DAP12, DNAX-activation protein 12; IGF, insulin-like growth factor 1; IL, interleukin; LIF, leukaemia inhibitory factor; NF-kB, nuclear factor-kappaB; NGF, nerve growth factor; NPC, neural precursor cell; OPC, oligodendrocyte precursor cell.

In vitro and *in vivo* studies indicate a role for microglia in regulating radial glia differentiation, possibly through nitric oxide production by nitric oxide synthase 2 (NOS2) or iNOS, known to be expressed by microglia during embryonic development [92, 150]. Of note, NOS1 and NOS3 are expressed by neurons and endothelial cells respectively. Further, the spatiotemporal distribution pattern of microglia in the intermediate zone and subplate (predominant zones where astrocyt differentiation takes place) preceeding the differentiation of astrocytes has led to speculations on a role in astrocyte differentiation [4, 92]. *In vitro,* microglia secrete factors, such as IL-1β, IL-6 and LIF that are known to stimulate astrocyte proliferation and differentiation [92]. Further, microglial-derived soluble factors indeed promote astrocyte differentiation *in vitro* [143]. In contrast, another study found increased numbers of astrocytes after microglia depletion, which points to a inhibiting role for microglia in astrocytogenesis [54]. In addition, microglia also phagocytose radial glial processes postnatally, which indicates these cells might regulate the transformation into astrocytes [89]. Microglia were recently found to regulate oligodendrogenesis and myelination as well [43]. Subpopulations of amoeboid and highly metabolically active microglia residing in myelintaing regions of the mouse brain during the first postnatal weeks were found to be crucial for

oligodendrocyte progenitor maintenance - also in the adult brain - and maturation and the following myelination process [43].

During embryonic development, Squarzoni *et al.* spotted microglia accumulating at the crossroads of important highways for neuronal migration and along axonal fiber tracts [151]. In particular, microglia were found in association with progenitor zones, the corpus callosum and the external capsule. They also make contacts with incoming dopaminergic axons in the ventral telencephalon. At these hotspots, microglia regulate outgrowth of dopaminergic axons, they contribute to corpus callosum fasciculation [152] and impact on the laminar positioning of Lhx6 expressing interneurons, through CX3CR1 and DAP12 signaling [151].

In addition to the contribution of microglial BDNF to synaptogenesis (explained on **p25**), *in vitro* work showed a role for thrombospondin, an extracellular matrix protein that is produced by microglia during development, in neurite outgrowth [153, 154]. During brain development excess synaptic connections are formed and in order to establish properly functioning neuronal networks, many of these immature synapses are removed by "synaptic pruning". How microglia molecularly sculpt these structures is addressed on **p25**. The recognition process most likely occurs through find-me (for example neuronal secretion of CX3CL1) and eat-me (C1q and C3 expression by neurons) signals [155]. In addition, CX3CR1 KO mice show transient synaptic pruning defects leading to an immature connectivity and behavioural deficits [64, 156]. Also, in the developing somatosensory cortex, a delay of microglia recruitment in the in CX3CR1 KO mice resulted in immature thalamocortical synapses [65].

Microglia invade the brain before blood vessels start to sprout inside the neuroepithelium and are often found in close contact with blood vessels *in vivo* during development and in the adult [34, 35, 92]. Thus, these CNS resident macrophages are ideally positioned to influence the development and remodeling of the CNS vasculature. Indeed, microglial depletion studies pinpointed that these cells are necessary for augmenting the vascular density/branching in the developing retina and hindbrain by facilitating anastomosis but not tip cell extension [157-159]. However, microglia do neither seem to be essential for maintaining the adult CNS vascular system [158], nor for BBB integrity [58]. In contrast, branching inhibiting effects have been demonstrated for microglia in the deep retinal plexus *in vivo*, mediated by Wnt-Flt signaling [160] and in a retina culture model *ex vivo* [161]. Concerning the underlying mechanisms of promoting vessel branching, microglia do not contribute significantly to the VEGF pool, which attract tip cells (described on **p4**), and VEGF does neither affect microglial survival nor attraction [159]. Additionally, VEGF-A and soluble Flt1 are not amongst the microglial-derived major soluble factors that mediate branching [162]. These findings suggest a different mechanism for microglia-mediated branching than the VEGF-based vascular sprouting [21]. In this respect, it was found that microglia-blood vessel contact enhances but is not essential to promote branching [162]. Further, Notch signaling in microglia is involved in mediating microglia-endothelial cell interactions in the retina [163]. It is further not known how microglial contact with blood vessels is mediated on the molecular level in other parts of the brain. This issue is further explored upon in **Chapter 3**. So, microglia clearly affect vascular branching, though the outcome depends on the local environment, but the underlying molecular mechanisms remain to be elucidated.

In summary, microglia are involved in neuro- and gliogenesis, in developmental cell death and clearing of debris, in outgrowth of axons, in positioning of interneurons, in synapse formation and maturation, and in blood vessel branching during CNS development and homeostasis.

in the adult CNS

Research into the non-immunological functions of microglia has been booming since the findings of Nimmerjahn and Davalos in 2005 [34, 36, 164]. These researchers concluded that the energy the brain invests in the constantly moving microglial processes should serve a purpose, a hypothesis that triggered the clockwork in many researchers' minds [165]. Although microglia also interact with neurons in the aging and pathological brain (see **Point 1.2.8**) [73, 166], the next paragraphs address the function of their interactions with neurons in the healthy adult CNS.

In the *in vivo* adult somatosensory and visual cortex microglial processes make direct contact with synaptic terminals during four to five minutes at a frequency of once per hour [167]. This contact is dependent on neuronal activity: the frequency of these contacts decreases with decreasing neuronal activity and the duration of contact increases in pathological circumstances. Research in zebrafish larvae confirmed these findings and revealed that neuronal activity itself is regulated by microglial contact [168]. The mechanism underlying the microglial scanning activity and contact formation was found to depend on extracellular ATP, released through neuronal and astrocytic Pannexin-1 hemichannels, that binds to purinergic P2 receptors on microglia [36, 168, 169].

The dynamic contact of microglia with synapses implies they exert local tasks. Microglia indeed remodel these structures dependent on activity and age through inducing the formation of dendritic spines and eliminating synaptic elements, a process called synaptic pruning [167, 170]. The underlying signaling mechanisms have mainly emerged from research during postnatal development *in vivo*. Research between P8 and P11 determined that formation of new spines involves microglial BDNF [171, 172] and direct contact with the dendrite, which leads to Ca^{2+} currents, actin accumulation and filopodia formation in the latter [104]. Synapse elimination is based on TGF-β-induced expression of complement (C)1q followed by C3 tagging of the synapses to be pruned [173-175]. In general, tagged synapses harbor less active pre-synaptic inputs, as shown at P5 and P15 [64, 174] and microglia recognize and sculpt away these synapses through their complement receptor 3 (CR3, alternatively CD11b/CD18). Flagging of C1q and C3 likely happens in an activity-dependent way as well. Accordingly, *in vitro* findings indicate that neurons secrete exosomes based on their activity and these exosomes stimulate synaptic pruning by microglia [176]. Of note, microglial CR3 expression does not necessarily promote clearance of material, as shown by the CR3-limiting influence on Aβ clearance in a mouse model of Alzheimer's disease [177].

Microglia also mediate functional synaptic plasticity, which encompasses strengthening or weakening of the synapse based on its activity. These immune cells regulate long-term potentiation, which is an increase in synaptic strength involved in learning and memory, through CX3CL1/CX3CR1 signaling [178], and modulate γ-aminobutyric acid (GABA)-ergic transmission through BDNF and ATP *in vivo* [179, 180]. In addition, P2Y12R, DAP12 and CD200R function in

microglia are vital for synaptic plasticity [55, 64, 155, 181]. Cell and tissue culture studies support the role of microglia in the regulation of synaptic strength during adulthood and provide additional mechanistic details, such as the involvement of TNF-α, NOX, glycine, glutamate and GABA (reviewed in [155, 182]). In addition, a recent study revealed that microglia instantly control inhibitory neurotransmission [183]. Lipopolysacharide (LPS) stimulation of microglia in spinal cord explants induced lateral diffusion of glycine receptors, but not $GABA_A$ receptors, away from the synaptic site and resulted in decreased glycinergic postsynaptic currents. The underlying mechanism encompasses microglial secretion of Prostaglandin E2, eliciting protein kinase A (PKA) signaling in neurons, possibily phosphorylating glycine receptors [183].

In the adult neurogenic zones, namely the subgranular zone of the hippocampal dendate gyrus and the subventricular zone of the cortex, microglia regulate proliferation and differentiation of neuronal precursors [55, 123, 184-186]. TNF-α signaling via TNF receptors 1 and 2, IGF-1, IL-1β and CX3CL1 signaling are involved in regulating neurogenesis [184]. Microglia also control the number of newborn neurons in the hippocampus through phagocytosis. Apoptotic cells, expressing phosphatidylserine, may be recognized by microglia through their phosphatidylserine receptors [55, 123, 184-186].

In summary, microglia contribute actively to adult CNS homeostasis by responding to (aberrant) neuronal activity, by regulating synaptic plasticity important for learning and behavioural adaptation and by influencing adult neurogenesis to the environment.

1.2.8 Functions of microglia in pathology

Microglia constitute the first line defense in the CNS and are involved in both the innate and adaptive immune system. They are in the front seat of regulating the inflammatory response by producing cytokines, chemokines and free radicals, such as TNF-α, IL-1β and nitric oxide (NO) [187]. Immune activated microglia are capable of proliferation, migration, antigen presentation, inducing cell death and phagocytosis and upregulate surface markers such as CD11b, MHCII, CD68 and Mac-2 [187, 188]. The roles of microglia in neuroinflammation and degeneration have been widely studied. Microglia adopt a customized phenotype that can be both neuroprotective and neurotoxic, depending on the stimulus and their microenvironment [189, 190]. The M1/M2 nomenclature used to categorize macrophages into "classically" activated (M1, driven by production of pro-inflammatory cytokines), or alternatively activated (M2, related to an anti-inflammatory reaction and tissue repair) was initially used for microglia as well. However, these extreme classifications oversimplify the plethora of *in vivo* phenotypes [191]. To accommodate the inconsistencies with regard to ontogeny-, stimulus- and tissue-specific responses of macrophages, Ginhoux and co-workers recently proposed the "Multidimensional model of macrophage activation" [192]. The authors stress that future research should encompass high-resolution, single-cell and deep phenotyping techniques in order to develop therapeutic approaches that target specific subsets of macrophages.

Injury and regeneration

Despite the limitations of the M1/M2 classifications, research on this respect has yielded valuable insights into the divergent functions of microglia/macrophages during CNS injury and repair. For example after spinal cord injury trauma, microglia/macrophages migrate towards the lesion at different time points and have distinct roles [193]. M1 macrophages arrive first after injury while the M2 repsonse is mostly delayed [194]. M1 microglia/macrophages secrete IFN-γ, TNF-α, IL-6, IL-23 and reactive oxygen species which together are crucial for host defense but unfortunately damage the healthy tissue as well. The M1 phenotype contributes to axonal retraction and the formation of a growth-inhibitory glial scar - through excessive production of chondroitin sulphate proteoglycans (CSPGs) - that impairs axon regeneration [195-197]. M2 microglia/macrophages produce IL-10, IL-4, TGF-β, BDNF and GDNF so as to promote neuronal/axonal survival and regeneration and to degrade the inhibitory glial scar components [197-199]. M2's also produce matrix metalloproteinase-13 (MMP-13) and hereby degrade CSPGs [200] as well as internalize and degrade collagen [199, 201], all leading to improvement of scar resolution. Unfortunately, from day 7 post-injury, M1 microglia/macrophages outnumber M2's and stay present much longer at the lesion site [202]. In multiple sclerosis and related animal models, both detrimental and beneficial roles have been described for microglia as well that are mainly linked to oligodendrocyte survival, differentiation and clearance of myelin debris [203]. Here as well the phenotype of activated microglia/macrophages influences their function in myelin repair. At the start of remyelination microglia changed from an M1 to an predominant M2 phenotype that was indispensable for oligodendrocyt differentiation both *in vitro* and *in vivo* and this effect was mediated by activin-A [204].

Because of these M1/M2 dual roles, influencing microglia polarization has gained large interest in the search for therapeutic approaches to improve recovery. Hopeful approaches include transplantation of M2 microglia/macrophages, administration of protective factors secreted by M2 cells and inducing the switch from M1 to M2 through for example siRNA packed into nanoparticles that cross the BBB, lentiviral delivery of M2 inducers such as IL-10 or liposomal delivery of microRNAs or their inhibitors (for example targeted to microRNA-155) into macrophages [73, 205, 206].

The scapegoat in neurodevelopmental disorders?

Many of the developmental processes discussed in **Point 1.2.7**, which involve proper microglia functioning, are often found to be disturbed in neurodevelopmental disorders such as schizophrenia and autism spectrum disorders (ASDs), and in corresponding animal models [28, 207-211]. ASDs is the general name for a group of developmental disorders that includes a wide spectrum of symptoms, skills and levels of disability (National Institutes of Health definition) and is characterized by impairments in social, behavioural, intellectual, communicative and sometimes cognitive functions. ASDs affects 12-15% of the population worldwide [212]. Strong sex differences exist with respect to this prevalence: males are about four times more likely to be diagnosed with ASDs than females [213]. Schizophrenia and ASDs arise from complex interactions between both genes, which is well documented, and environment. Concerning the latter, cumulating

epidemiological and animal studies have now established a strong association between an activated immune system in the mother during pregnancy and the risk for the offspring to develop one of both disorders (reviewed in [208, 214]).

Maternal immune activation (MIA) can be caused for example by a bacterial or a viral infection, such as rubella and influenza virus, during pregnancy. In animal models, immune stimulations are mostly induced through LPS, an endotoxin from the outer membrane of gram-negative bacteria, or through polyinosinic:polycytidylic acid (Poly (I:C)) injections. Poly (I:C) is synthetic double stranded RNA and mimics the immune response following a viral infection through activating Toll-like receptor (TLR)-3 and raising systemic IFN-1, IFN-β TNF-α, IL-6, IL1-β and IL-17a [215-217]. The offspring from Poly (I:C) injected (and also LPS-injected [218]) pregnant mice and primates displayed core abnormalities associated with ASDs, such as deficits in social, communication and repetitive behaviours, which were also present in the offspring of pregnant mice that suffered from a viral infection [216, 217, 219-223]. MIA in rodents creates an inflammatory environment in the fetal brain by elevating levels of pro-inflammatory mediators, such as IL-6 and IL-17a [208, 216, 217]. Maternal systemic IL-6 and more in particular its downstream signaling cytokine IL-17a are key mediators of altered brain development and behavioural abnormalities in the offspring of Poly (I:C) induced MIA mice [216, 217].

Because (i) microglia are the immune cells of the CNS and possess the necessary receptors to sense changes in cytokine levels and react upon them [32] and (ii) they guide brain development [8] **(Point 1.2.7)**, it is tempting to suspect these cells to be in the driver's seat of the fetal inflammatory response and to be the executioners that disturb brain development and performance. Indeed several studies in patients with schizophrenia or ASDs report increased cytokine levels in the cerebrospinal fluid or in the fetal environment along with microglial alterations (recently reviewed in [224]). Several *post mortem* studies in patients with schizophrenia found increased serum levels of pro-inflammatory cytokines, including IL-6, neuropathological changes in microglial morphology and increased CD68 and HLA-DR expression, suggesting microglial activation [225-228]. Likewise, microglial activation and increased density was reported in cortical tissue from ASD patients alongside elevated levels of cytokines, including IL-6, in their cerebrospinal fluid [229-231]. Moreover, *in vivo* Positron emission tomography (PET) studies in patients with neurodevelopmental disorders show increased radioligand binding to translocator protein (TSPO), which suggests microglial activation (reviewed in [228, 231]). In contrast, one recent study using a novel second-generation TSPO radioligand did not find evidence for microglial activation in patients at high risk for psychosis [232]. Although several studies do indicate that microglia/macrophages are the main source of TSPO in CNS pathology [73], TSPO PET data should be interpreted with caution. TSPO is also expressed by macrophages, astrocytes and endothelial cells and is thus rather a marker for general glial and endothelial cell activation [233-235]. Moreover, the increase in TSPO expression after pro-inflammatory activation in microglia might only be the case in rodents and not in humans [236]. Nevertheless, transcriptional profiling indicates an association between ASDs and the elevation of genes involved in microglial immune activation [237]. In addition, MIA models show structural and functional abnormalities in the offspring, such as a smaller thickness of the neocortex and hippocampus, expression of reelin in

the forebrain and increased GFAP immunoreaction, cell death, macrophage infiltration, presynaptic hippocampal deficits, impaired learning and memory in the adult offspring [217, 222, 238-247], which could be mediated by aberrant microglia-neuroglial crosstalk. Accordingly, LPS-induced MIA evoked microglial immune activation and augmented phagocytosis of neural precursors prenatally in rats [144]. Whether Poly (I:C)-induced MIA during embryogenesis activates embryonic microglia in terms of immune marker expression, is investigated in **Chapter 5**. Lastly, fetal brain cytokine production increased following MIA during late gestation at E17 while it did not after mid gestation MIA at E9 [248], at which microglia do not reside yet in the embryonic CNS parenchyma. These studies point to the involvement of microglia in mediating MIA induced deficits in the offspring [248].

Despite the suggested involvement of microglial cells in the neurodevelopmental disorders (reviewed in [73, 249]), the chicken-or-the-egg problem remains. Microglia could be the first cells to sense the maternally induced fetal pro-inflammatory cytokines. This sensibilization might lead to abnormal task exertion during CNS development, which could ultimately result in behavioural disturbances. Or, the cytokine storm could directly alter neuro- and gliogenesis and network formation [250-252], to which microglia subsequently react. Although today no conclusive answer exists for this question, some animal studies point to a causative role for microglia dysfunction in the development of behavioural deficits reminiscent of neurodevelopmental disorders [151]. They also show that MIA can have comparable effects on connectivity and brain wiring as can microglial dysfunction, as discussed next [151].

Upon genetically or pharmacologically disturbing microglial function, cognitive or behavioural abnormalities arise in adolescent and adult mice. For example, CX3CR1 KO led to impaired connectivity (increased dendritic spines and immature synapses), impaired social interactions and increased repetitive behaviour [64, 156]. However, it is not clear yet whether the behavioural deficits are caused by a lack of CX3CR1 or by increased IL-1β signaling in CX3CR1 KO mice [178]. Deficits in microglial mediated synaptic pruning might impair the brain's excitatory versus inhibitory balance, which is frequently suggested as a common mechanism in a variety of neurodevelopmental disorders [253]. Mutation of DAP12 (only expressed in immune cells) in mice elicits a transient increase in microglial density at P0 along with the exhibition of a pro-inflammatory profile and impaired long-term potentiation [254]. Another study showed that DAP12 mutation as well as MIA resulted in microglia with a down regulation in genes involved in neurite formation together with subsequent malformations in the corpus callosum [152]. In parallel, DAP12 mutation in humans results in the development of an early form of dementia (Nasu-Hakola disease) [255]. Interestingly, LPS-induced MIA in wild type mice generated synaptic alterations reminiscent of the phenotype caused by DAP12 mutation [152, 256]. Additionally, another study showed that DAP12 KO as well as CX3CR1 KO partially mimicked the effect by LPS injection in pregnant mice which resulted in a laminar positioning impairment of a subtype of inhibitory interneurons (Lhx6 subtype) that integrates into the cortical plate [151]. Notably, genetic and pharmacologic microglial depletion established the same phenotype [151]. Ultimately, DAP12 KO results in behavioural alterations, such as reduced startle response and lowered prepulse inhibition which are associated with schizophrenia [257]. Next, microglia depletion as well as microglia-

specific KO of BDNF resulted in reduced motor learning and decreased fear response [171] and microglia were responsible for anxiety development after stress through recruiting of IL1β producing monocytes to the brain endothelium [258]. Knockout of homeobox protein b8 (Hoxb8), a *Hox* gene normally involved in establishing body plans, resulted in compulsive grooming behaviour, causing hair loss and skin lesions together with deficits in synaptic pruning [259]. Hoxb8 is specifically expressed by roughly 40% of microglia from P14 onwards and is also involved in maintenance and differentiation of myeloid progenitor cells. Symptoms caused by Hoxb8 deficiency are similar to the obstructive compulsive disorder "trichotillomania" in humans [259]. Progranulin deleted specifically in microglia resulted in excessive grooming as well and this could be prevented by inhibiting nuclear factor κB (NF-κB) in microglia [260]. Knockout of methyl-CpG-binding protein 2 (MECP2) in mice causes a Rett Syndrome-like phenotype, characterized by retarded growth, apneas, tremor, impaired gait and locomotor function and a short life expectancy [261]. In two studies this phenotype could be rescued by bone-marrow transplantation from wild type mice [261, 262], while another study could not reproduce the rescue [263]. A fourth and most recent study in the visual system determined that the excessive synaptic pruning in MECP2 KO mice mediated by microglia was independent on MECP2 expression in microglia themselves [264]. Further, mutations and allelic polymorphisms in microglial-related genes, such as Csf1r, Triggering receptor expressed on myeloid cells 2 (Trem2), CD33, Irf8, P2x7r and NRROS are associated with an increased likelihood to develop a plethora of neurological diseases, ranging from Alzheimer's disease to schizophrenia [8, 114, 265]. Most interestingly, the presence of microglia during the first two weeks of postnatal development is crucial for brain development and behaviour [266]. Transient reduction of the microglial population with 50% through depletion during the first postnatal week already resulted in enlarged ventricles and a thinned cortex by P10. Notably, this transient depletion caused sustained alterations in neonatal, juvenile and adult behaviours ranging from deficient prosocial behaviours to working memory deficits to male-specific impairments in sex behaviours [266].

Although some findings are still controversial, most studies described above point to a central role for microglia in neurodevelopmental disorders. It is however not clear yet if microglial dysfunction might initiate disease.

1.2.9 Gender differences

During the last years, important differences between males and females with regard to microglial density, morphology and function have been revealed [267, 268]. Microglial density varies notably between males and females in the parietal cortex, amygdala, hippocampus and preoptic area (POA) at different stages throughout life [267, 269]. The POA is the brain region essential for male sexual behaviour and shows clear anatomical differences between both sexes. Estradiol, the aromatized form of testosterone, has emerged as the dominant masculinising hormone in the rodent brain [269]. By P4, the male POA shows higher numbers of amoeboid microglia characterized by an enlarged soma, fewer ramifications and shorter process length compared to female POA. Treatment of female pups with estradiol at P0 and P1 leads to the masculinisation of microglial numbers and an increase in the number of ameboid microglia [270]. The microglial reactivity in males is also necessary to induce the masculine pattern of dendritic spines in the POA, which contributes to the

adult sexual behaviour in males [269, 270]. Further, the microglial immune reactivity and response to neuropathic pain and chronic stress also varies amongst genders [55, 116]. Masculinisation of the rodent brain occurs in a critical period between the last days of gestation and the end of the first postnatal week and coincides with key programs during development known to be influenced by both sexual differentiation and microglia, such as neural progenitor proliferation, cell survival, PCD, synaptogenesis and synaptic pruning [268, 269]. It has to be noted that sex differences in microglial function only can occur from late gestation, when the critical period starts [268]. Recently, one study found that the presence of microglial cells during this period is essential for development of juvenile and adult sex behaviour [266]. This central role of microglia in sex differentiation of the brain and behaviour has implications for the incidence of neurodevelopmental disorders in both sexes, as described in **Point 1.2.8** [267].

In conlusion of this section on microglial physiology, it is important to remember that microglia are yolk sac derived immune cells and constitute a well-established fraction of the total brain cell population. They maintain themselves through regular proliferation and apoptosis. These CNS macrophages actively survey and shape the nervous parenchyma and exhibit customized gene expression profiles and responses based on the trigger, the local environment and the gender. Microglia's ability to migrate is an important aspect of their physiology, but the cellular and molecular mechanisms underpinning this process, especially during development, are largely unknown.

1.3 Cell Migration

Cell migration is crucial for an organism to exist. It is most obviously critical for the organism to develop, as discussed for the establishment of the cortical layers and the colonization of the CNS by microglial cells in the previous sections. Cell migration is also indispensable for tissue maintenance and during pathology. Therefore, this field is extremely broad and evolves quickly with many dazzling discoveries over the past ten years.

A cell senses its environment and then polarizes towards a cue in a certain direction. In order to move forward the cell needs to transduce its contractile forces to the substratum, mediated through the connections it has established with its surroundings. *In vivo* and often *in vitro* as well, the cell is embedded within or located on top of ECM. Connections with adhesive glycoproteins inside the ECM, such as laminins, tenascins, collagens and fibronectin are typically mediated through receptors on the cell surface, such as integrins [271, 272].

Upon migration, the whole molecular and cytoskeletal machinery in the cell sets in motion which is crucial for the polarization of the cell into one direction, the coordinated outgrowth of protrusions and adhesion formation, the translocation of the cell body by contraction, the disassembly of adhesions and finally retraction of the rear [272]. This series of events are the major steps in cell migration and require well-coordinated molecular signaling in space and time. Focal adhesion kinase (FAK) binds to the cytoplasmic part of the integrin and promotes cell migration together with its downstream targets paxillin and p130Cas by signaling to Rho family guanosin triphosphate (GTP)-ases Rac, Rho and Cdc42 [272]. This molecular machinery regulating protrusion formation

and migration largely depends on the type of environment, e.g. 2D vs. 3D, which stresses the need for *in vivo*-approaching settings to extrapolate molecular data on migration to the *in vivo* situation [273].

In this section, the two major structures that are instructive for cell migration, the ECM and integrins, are explained, followed by a description of the current state of knowledge concerning ECM/integrin signaling in microglial physiology and migration.

1.3.1 ECM

ECM can be subdivided into the gel-like material distributed in between cells, called the interstitial matrix, and the one in close contact with the cells, such as basement membranes, called the pericellular matrix [274]. It is present throughout the whole body but its composition and viscoelastic properties can vary greatly between tissues and between specific regions or specialized microenvironments inside tissues [275, 276]. ECM is multifunctional as it not merely structurally supports the resident cells by providing points of anchorage. ECM also regulates a myriad of cellular processes such as proliferation, differentiation, migration, cell behaviour, cell-fate decisions, cell activation/metabolism (production of cytokines) and apoptosis. All these processes are mainly initiated through integrin signaling [271]. The regulation and outcome of these responses is highly complex and is influenced by all the facets associated with ECM, such as its composition [271], the conformation of ECM proteins [277-279], its biophysical properties such as rigidity and porosity [276, 280], its topography (structured vs. disorganized) and geometry (including 2D vs. 3D environments) [275, 281-283]. The matrix further controls the stability, movement, presentation and signaling of growth factors [271, 275, 276, 279]. ECM is not static and can be remodeled by the resident cells through the secretion of new ECM proteins, degradation and incorporation of newly formed matrix molecules, and exertion of traction forces [271, 275]. Finally, ECM is of uttermost importance for the organism, since fibronectin, collagen and laminin KO mice die at embryonic ages [271].

Types of ECM molecules

ECM molecules are typically classified as glycoaminoglycans, proteoglycans and glycoproteins. Glycoaminoglycans, such as hyaluronan, chondrotin sulfate and heparin sulfate are linear unbranched polysaccharides that are negatively charged and thus regulate water flux causing the interstitial space to swell. All glycoaminoglycans but hyaluronan covalently attach to core proteins to form proteoglycans, which are then termed for example chondrotin sulfate proteoglycans and heparin sulfate proteoglycans. Hyaluronan non-covalently assembles with aggregating proteoglycans, such as versican and aggrecan, for the constitution of pericellular matrices, such as the perineuronal nets in the brain which are discussed below [271, 284, 285].

The family of glycoproteins consists of collagens, which are well described in literature [286] but not further elaborated upon in this work because of low presence in the brain, and non-collagenous proteins such as laminins, tenascins and fibronectin. These proteins are encoded by multiple genes, in case of laminins, or by a single gene, in case of fibronectin and tenascins [271, 287]. Alternative splicing of tenascins and fibronectin increases complexity of molecular composition and the cellular

responses evoked [279, 287, 288]. Laminins are heterotrimeric proteins with a high molecular weight between 400 and 800 kDa, built up of three chains (α, β, γ) [289]. Tenascins are oligomers with subunits that range between 190 and 300 kDa each and fibronectin associates in dimers of each 220 to 250 kDa [279, 287]. All these glycoproteins can interact with other matrix components and have both adhesive and signaling properties through cell-surface receptor binding, which are primarily integrins [274].

ECM organization in the brain

The major components of adult brain ECM, which constitutes 10-20% of the brain volume, are hyaluronan, proteoglycans and tenascins [284, 285]. Fibronectin, laminin and collagens in the adult brain mainly localize to basement membranes while only low amounts can be detected in the interstitial matrix in some parts of the brain [290]. The adult's brain ECM localizes into three compartments, namely the basement membrane, the perineuronal nets and the neural interstitial matrix (ECM molecules dispersed into the parenchyma) **(Fig. 1.8)**. The basement membrane forms the boundary between endothelial cells and the nervous tissue and is highly present in the pial membrane, surrounding the CNS. It is one of the three components of the BBB and consists of type IV collagen, laminins, fibronectin and proteoglycans [276, 284]. Perineuronal nets are dense mesh-like structures made up from proteoglycans (mainly of the chrondroitin sulphate type), hyaluronan, tenascin-R and link proteins. They start forming at P14 (or before, but at least not at P7) in the cerebral cortex and are fully established by P40 [291]. The perineuronal nets compactly wrap around neuronal cell bodies and proximal dendrites and leave openings at synapses [284, 292]. Perineuronal nets protect neurons from oxidative stress and excitotoxicity through buffering ions, they control synaptic stabilization and plasticity, and hinder the deposition of aggregates proteins [284, 285, 293]. The neural interstitial matrix forms a dense network of proteoglycans, hyaluronan, tenascins, link proteins, small amounts of fibrous proteins (collagens and elastin) and adhesive glycoproteins, such as laminin and fibronectin [284].

The changing ECM landscape during brain development

The ECM's main function during development is to support cell proliferation, differentiation, migration, axonal outgrowth and synaptogenesis, while during adulthood its focus is on cell survival, synaptic plasticity and the response to damage [285]. Considering this shift in function, it is not surprising that the ECM landscape is significantly modified between development and adulthood. Of note, ECM composition changes drastically as well in pathology [276, 279, 284, 285, 294]. A few studies have assessed the developmental changes in mammalian brain cortical ECM composition [295-298]. In the rodent embryonic brain, the glycosaminoglycane molecule hyaluronic acid is widely distributed throughout the cortex and other brain regions [299, 300]. During brain development 90% of hyaluronic acid is associated with water and therefore creates a permeable and easily remodelable environment to promote cell migration [298]. Between P7 and P10 in rats hyaluronic acid levels decrease with 50% and reach stable levels of 28% of their peak concentration by P18 [298].

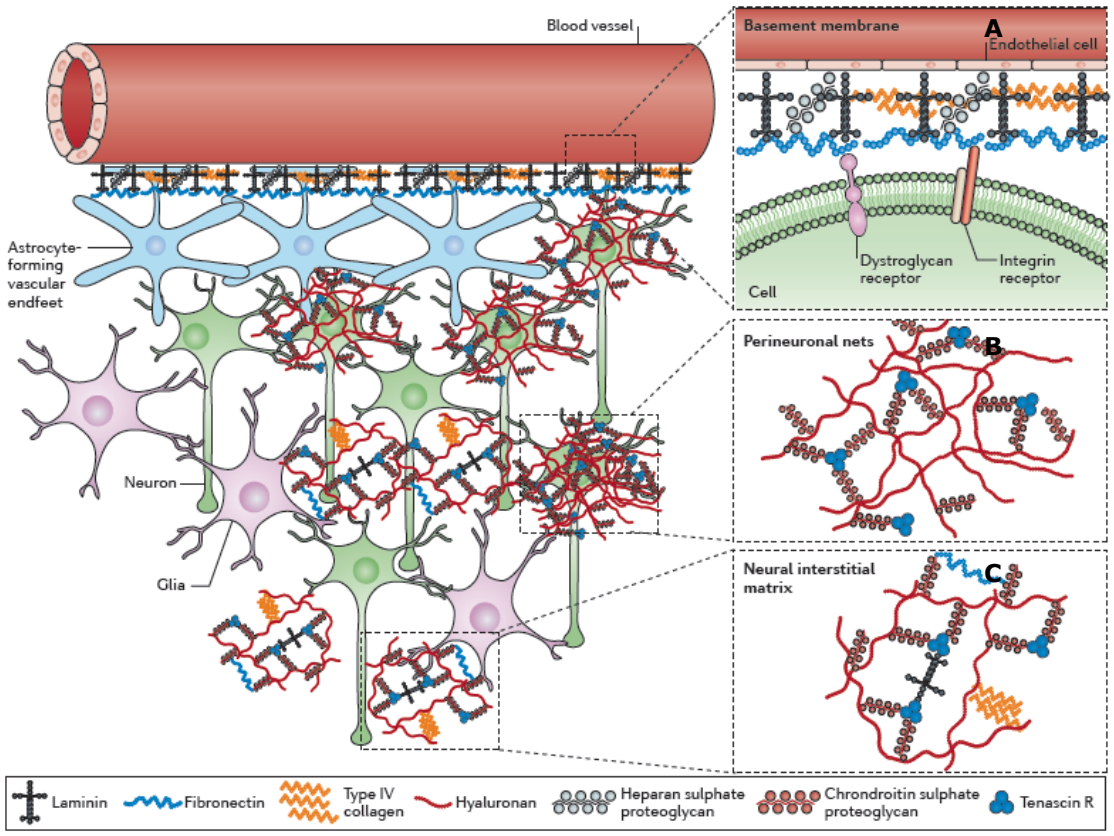

Fig. 1.8. ECM in the brain. Extracellular matrix (ECM) is arranged into three major compartments. **(A)** basement membranes that lie outside cerebral blood vessels, **(B)** condensed as perineuronal nets around the cell bodies and dendrites of neurons or **(C)** diffusely distributed as the neural interstitial matrix between cells of the CNS parenchyma. Pink cells depict astrocytes, oligodendrocytes and microglia. Cells are not drawn truthfully. From Lau *et al.* (2013) with permission [284].

Other studies on embryonic mouse brains describe that during development, chondroitin sulphate proteoglycans and the glycoproteins laminin, fibronectin and tenascin are present in specific spatiotemporal patterns. The laminin and fibronectin deposition pattern changes from a diffuse deposition around E10 in rodents to a marginal zone and subplate layer restricted presence upon cortical layer formation at E12-E13 and subsequently fades away [296, 297]. Radial glia produce the early fibronectin, while migrating neurons produce and align the late fibronectin along radial fibers [301]. The fading of the punctuate laminin staining is in conflict with the results of Lathia *et al.* in which the authors report on immunoreactivity for α2 and α4 laminin chains in the mouse brain cortex from E10 to E15 [295]. Also here, fibronectin was only detected in basement membranes and not in the parenchyma from E12 onwards. Chondroitin sulphate proteoglycan deposition showed a similar profile as did fibronectin, while tenascin starts to be detected in the marginal zone and subplate at E16, the time point at which laminin, fibronectin and chondroitin sulphate proetoglycans almost or already have disappeared [296]. From E17 to P2, tenascin labeling becomes widespread throughout the cortex and then gradually declines [296]. Also in humans similar to rodents, fibronectin, laminins and tenascin are expressed in the human foetus

[302]. Here, a similar fibronectin expression pattern localizing to periventricular zones during early gestation changed to the outer zones in later gestation.

Over embryonic development, the SVZ also becomes stiffer and these biomechanical changes were found to be instrumental for correct axon growth and neuronal migration [303]. The roles of the specific spatiotemporal deposition of ECM proteins are linked to neural stem cell proliferation and differentiation, neuronal migration along radial glial cells and terminal translocation and gliogenesis [275, 296, 304-306].

In summary, the ECM mediates a plethora of functions and is actively shaped by the cells residing in it. The brain has a specific ECM composition that changes drastically during development. Whether the changing ECM environment might influence microglial migration is addressed in **Chapter 3**.

1.3.2 Integrins

Integrins are transmembrane heterodimeric cell adhesion receptors composed of a non-covalently linked α and β subunits. Twenty four different integrin heterodimers (18 α and 8 β subunits) are described in vertebrates with varying ligand binding properties (eg. collagen, fibronectin, laminin) and cell and tissue distributions. Integrin heterodimer binding specificity is mainly determined by the α subunit and can vary between one specific or multiple ECM molecules, while one ECM molecule can be recognized by one or multiple integrins [307, 308]. Integrins are however classified into four subclasses based on their specificity for a recognition sequence, ligand or cell type: (i) arginine-glycine-aspartic acid (RGD) sequence-binding integrins binding fibronectin and vitronectin, (ii) laminin-binding integrins, (iii) collagen-binding integrins and (iv) leukocyte-specific integrins, which mediate cell-cell interactions between leukocytes and endothelial cells **(Fig. 1.9)**. Classification into β1, β2 and αV-dimerizing integrins is also common [308]. The ß1 subunit is the most ubiquitous since it interacts with the majority of the α subunits and is present in three of the four integrin subclasses [307, 308]. Not surprisingly, loss of ß1 results in embryonic death already at E6.5 [308].

Outside-in vs. inside-out signaling and integrin activation

Integrins can adopt two extreme conformations: extended, often referred to as "active"; or bent, "inactive" [309, 310]. The stretched conformation shows the highest affinity for the ligand, while the bent form shows weak affinity for the ligand [309, 311, 312]. During outside-in signaling, a ligand (ECM) binds the extracellular heads of the integrin and recruits intracellular adhesion signaling proteins, such as talin and kindlin to the cytoplasmic tail of the β subunit. On the contrary, during inside-out signaling talin and kindlin are recruited upon a signal coming from inside the cell itself, rather than from outside. Binding of talin or kindlin separates the integrin's cytoplasmic α and β tails, induces the extended conformation and connects the integrin with the actin cytoskeleton of the cell. Multiple signaling proteins (further referred to as the adhesome) will subsequently associate with the preformed complex, such as paxillin, FAK and Src to strengthen the connection and induce signaling [272]. The β subunit with bound talin not only physically links the ECM with the actin cytoskeleton enabling the cell to transduce forces necessary for soma

displacement [272], but it also switches on intracellular signaling pathways involved in a broad array of cell responses, as discussed previously in **Point 1.3.1 (Fig. 1.9)** [271, 308, 313]. Whether the ligand first has to bind the extracellular domain of the integrin in order to cause conformational stretching is debated [314], yet the αVβ3 integrin was reported to bind its ligand fibronectin in a bent conformation [315]. Ligand affinity can be increased by binding of Mg^{2+} or Mn^{2+} to cation coordination (MIDAS) sites on the extracellular domain of the integrin, by chelating Ca^{2+} which inhibits integrin activation through binding to ADMIDAS sites, by traction forces or collision with other membrane proteins and as discussed above by binding of talin and kindlins to the β-integrin tail which can be mediated through inside-out activation [310, 316]. The latter process often involves binding of chemokines or growth factors to their cellular receptors, which elicits Rap1-RIAM signaling that in its turn controls talin binding as fast as within 1 second [310, 314, 317]. On the contrary, integrin activation can be suppressed through inhibiting talin binding to the β-tail [310] or by integrin inactivators such as SHANK-associated RH domain interacting protein and filamins [318].

Biological relevance of integrin activation

Integrin activation is important in many physiological situations, such as in circulating blood cells or during development when timely migration of cells, or parts of cells such as axons, is required. External cues, such as injury to the vasculature or inflammatory signaling also impact on integrin activation [314]. Non-active integrins have low affinity for ligands and thus (almost) not engage in binding to ECM neither in intracellular signaling. As described above growth factors and chemokines play major roles in this process, especially in immune and cancer cells the link between chemokine signaling, such as CXCL12, and β1 integrin activation is well described [317, 319-321]. Often immune cell homing, rolling and extravasation or cancer cell proliferation and metastasis is influenced by chemokine and growth factor/integrin crosstalk, through increased adhesion to ECM molecules such as ICAM-1 or fibronectin. In fact, all processes that involve cell adhesion, such as proliferation, cell survival and migration can be influenced through inside-out and outside-in activation. Common intracellular signaling pathways launched through integrin activation are FAK, ERK, MAPK and Rho family, calcium entry, NF-κB and PI3K [322].

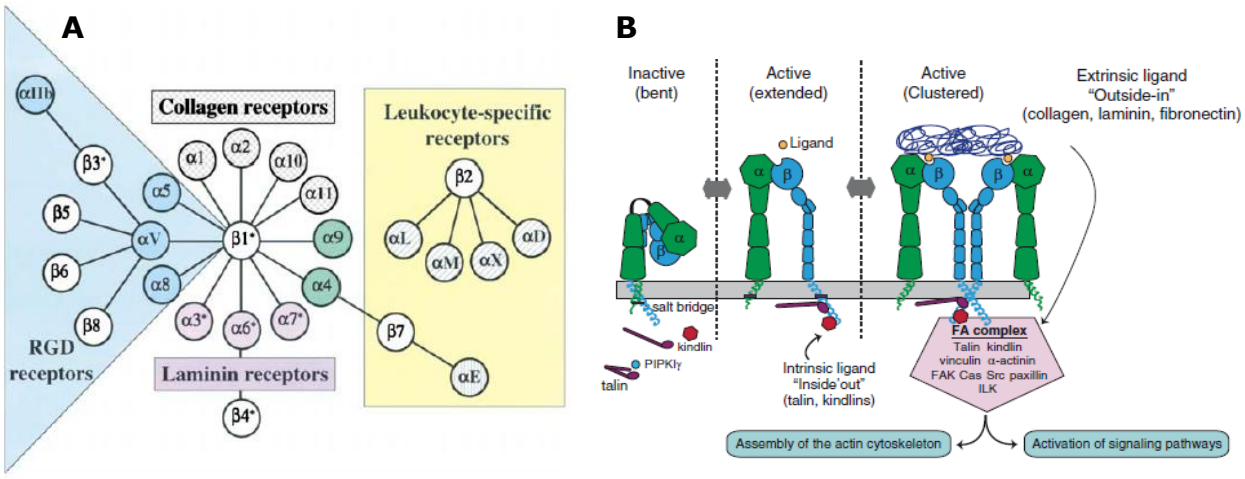

Fig. 1.9. Integrin heterodimer combinations, ligands and conformations. (A) Integrin subclasses based on their recognition sequences. **(B)** Integrin conformations. From Hynes (2002) and Zent *et al.*(2010) [308, 314].

Adhesion dynamics

How strong an integrin binds to its ligand is determined by affinity and avidity regulations. Affinity is regulated by the integrin's conformational status, while avidity depends on clustering of the integrins in the cell membrane. In practice, new and immature or "nascent" cell adhesions are formed through clustering of about 50 integrins per adhesion site [323] in the absence of acto-myosin-dependent force [324]. Despite most nascent adhesions turn over already after ~1 min, some stabilize and progress to "focal complexes", which can further mature into "focal adhesions". During this stabilization process the adhesion grows in size by attracting additional adhesion molecules such as α-actinin, non-muscle myosin II and RhoA, and changes in adhesion protein phosphorylation states occur [324-326]. Ultimately, α5β1-integrins can interact with tensin, an adaptor protein, to form long lasting and stable "fibrillar adhesions" on fibronectin [326]. During each maturation step the mechanical strength between the integrin and the actin cytoskeleton increases through association of more and more adhesion signaling proteins with the preformed adhesome at the integrin tails. Since adhesions mature centripetally from the lamellipodium towards the soma, nascent adhesions localize to the edges of the leading lamellipodium, focal contacts localize more proximal and focal adhesions appear at the ends of actin bundles. In order to form fibrillar, adhesions α5β1-integrins translocate further towards the cell body [327]. Over 2400 proteins have been identified in the adhesome, which underscores the complexity of adhesion regulation. In addition, the involvement of these molecules depends on multiple factors ranging from the integrin heterodimer to ECM rigidity and dimension [328-330].

In order for cells to migrate efficiently, adhesions must turn over (or disassemble) in a specific spatiotemporal manner. This process involves microtubule mediated endocytosis of the integrin, its targeting to an early endosome, followed by further modification or degradation; or by the recycling back to the plasma membrane [331]. Also, when the cell migrates further, integrins can be ripped off the membrane and left behind on the substrate [324-326].

Adhesion strength vs. migration speed

Migration speed is determined by the balance between cell-matrix adhesion strength and contractility of the cytoskeleton [332]. More in particular the strength of an adhesion is influenced at multiple levels: by the density of the ligand, by the density of the integrins engaged (defined as "valency"), by the ligand-binding affinity (discussed in the previous section on integrin activation), by the mechanical forces exerted on the adhesion, by the the size of the molecular adhesion complex (or maturation level) and by ECM stiffness [283, 330, 333-335]. Adhesion strength has a biphasic effect on migration speed [333, 336]. Migration speed increases between low and intermediate adhesion strength and slows down between intermediate and high adhesion strength. Importantly, molecular mechanisms of 3D migration are different from 2D migration [273, 330].

Integrin functions in the CNS

Integrins recognize ECM molecules, so they share most functions with ECM, such as roles in cell migration and intracellular signaling. The study of integrin function in the CNS, more specific with regard to neuronal development and migration, has received wide attention. Research over the past 30 years shows that integrins are implicated in (i) neuroepithelial cell division and fate (reviewed in [275]), (ii) neuronal migration and lamination (reviewed in [337, 338]), (iii) synapse formation, plasticity and behaviour (reviewed in [337, 339, 340]) and (iv) CNS angiogenesis and BBB integrity (reviewed in [337, 341, 342]).

β1 integrin appears to be a central player in all these processes. For example with regard to (i) neuroepithelial cell division and fate, β1 signaling regulates the attachment of neural stem cells to the inner surface of the ventricle and impacts on the amount and type of cell division of the neural stem cells in a non-cell autonomous way [343-345]. For (ii) neuronal migration and lamination, some controversy exists with regard to defects in neuronal migration which are possibly due to the use of conditional integrin KO models versus acute loss-of-function models using function blocking antibodies. Nevertheless, these studies point to important functions of β1 integrins in the maintenance of the radial glial scaffold and the migration of neurons establishing the cortical layers [343, 345-350]. More in particular, α6- and α5β1 integrins are implicated in the migration of neural precursors and their terminal translocation in the cortex, respectively [304, 350, 351]. With respect to (iii) synapse formation, plasticity and behaviour, β1 integrins influence dendritic arbor size and spine density, control actin remodeling and NMDA receptor trafficking, thereby regulating structural and functional plasticity [339, 340, 352, 353]. Loss of β1 results in behavioural alterations often associated with neurological disorders [339]. With regard to (iv) CNS angiogenesis and BBB integrity, endothelial cells show a developmental regulation in the expression of different β1 subtypes and a general increase in β1 expression [354]. In addition, β1 integrins anchor the endothelial cells to the basement membrane and regulate the permeability of the BBB [341, 354, 355].

Research has shed considerable light on integrin activation, its signaling pathways, functions, and their involvement in adhesion dynamics. Nevertheless, the specific integrin subtypes involved in the functions of integrins in the CNS remain largely unknown. At least, it is clear that β1 integrins

are indispensable molecules for CNS development and homeostasis. ECM/integrin signaling in microglia has received less attention and is discussed in the next section.

1.3.3 ECM/integrin signaling in microglia and their mobility

Most information available to date on microglial integrin expression and their functions originates from *in vitro* studies using primary rodent microglia or microglial cell lines. Cultured microglia derived from early postnatal mice express various integrins of the three main classes: β1, β2, and αV **(Fig. 1.10)** [356]. These immune cells specifically express the β1 integrins α4β1, α5β1, and α6β1, and the β2 integrins αLβ2 and αMβ2 (for alternative names see **Fig. 1.10**). αLβ2 and αMβ2 are also expressed by microglia in the normal developing and adult rodent CNS [37, 98, 357]. αMβ2 integrin is mostly known as Mac-1, CD11b or CR3 and plays a major function in microglial phagocytosis and synaptic remodelling [174]. From the αV heterodimer class, microglia express αVβ1, αVβ3, αVβ5 and αVβ8 [294, 356, 358, 359]. Like αMβ2, αVβ5 also plays a role in microglial phagocytosis [360]. Microglia do not express α1, α2, αX, β4, β3, β6, β7 and β8 [356]. Microglial activation and integrin expression are further influenced by exposure to cytokines, such as ILs, TNF, TGF-β and IFNs, as well as by the ECM [356]. Also, cultivation on fibronectin and vitronectin increases expression of the α4β1, α5β1 and αMβ2 integrins, while cultivation on laminin increases αV expression, most likely through outside-in signaling. All three ECM substrates increase expression of αLβ2 integrins. Additionally, fibronectin and vitronectin promote microglial pro-MMP9 expression through α5β1 and αvβ5 integrins respectively [294]. Microglia adhere strongly to plastic, fibronectin, and vitronectin, but only weakly to laminin, unless they are stimulated [361] **(Fig. 1.10)**. It is not known whether vitronectin is expressed in the embryonic brain, but it is deposited in the brain in pathological circumstances such as during Multiple sclerosis [294]. Adhesion to laminin and astrocyte ECM is regulated via PKC-dependent activation of α6β1 integrin [361]. Which integrins are expressed by embryonic microglia and their putative functions at those stages are explored in **Chapters 3 and 4**.

In addition to influencing microglial adhesion and MMP production, the ECM also influences microglial morphology through integrin signaling: fibronectin and vitronectin promote the amoeboid phenotype while laminin evokes a rounded-up phenotype which is weakly adherent [356]. These results are conform another study which shows that fibronectin promotes transformation of primary amoeboid microglia into the process-bearing morphology with a decreased phagocytosis capacity while laminin reversed this phenotype [362]. These results suggest that fibronectin and laminin play a role in the maturation of amoeboid, developing microglia towards the adult ramified phenotype.

Purinergic signaling, integrins and microglial mobility

In vitro as well as *in vivo,* purinergic signaling and the concurrent intracellular calcium increase seems to play central roles in promoting microglial mobility, which is used to refer to soma translocation (migration) and process remodeling (motility) together [71]. More in particular ATP, ADP and adenosine signaling through P2Y12R, P2X4R, $A2_AR$ are mostly implicated in regulating microglial process dynamics and chemotaxis [36, 363-371]. β1 integrin signaling occurs

downstream of purinergic receptor activation and plays pivotal roles in regulating microglial mobility. As such, ATP signaling through P2Y12R induces increased adhesion of microglia to collagen, which can be inhibited with RGD peptides, β1 integrin blocking antibodies and P2Y12R antagonists [372]. In particular, RGD and β1 integrin inhibitors inhibit process extension and lead to accumulations of β1 integrin in the protruding tip [372]. β1 integrin further regulates microglial migration towards α-synuclein [373] and towards human immunodeficiency virus-1 (HIV-1) Tat protein [374]. In primary rat microglia, the latter induces activation of non-muscle myosin light chain kinase (nmMYLK), followed by inside-out activation of microglial β1 integrin, outside-in signaling upon ligand binding and finally actin polymerization [374]. β3 integrin was not involved in microglial migration towards Tat [374]. ADP induces β1 integrin translocation to membrane ruffles (the motile areas on the cell surface that contain a meshwork of newly polymerized actin filaments) and in the presence of fibronectin substrate it induces β1-dependent chemotaxis through P2Y12/13R signaling [370]. Details of the signaling pathway(s) generated by β1 integrin translocation and the effect of this outside-in signaling on microglial chemotaxis are not known [370]. Regarding the role of β2 integrins, conflicting results are reported: αLβ2 integrin (alternatively CD11a or LFA-1) is necessary for normal migration of microglia to sites of excitotoxic injury [375] while microglial migration to injured neurons is unaffected in β2 deficient mice in cultured slices [376].

In addition to integrin signaling leading to adhesion and cytoskeleton remodeling, ion channels regulating sodium, chloride, potassium and calcium fluxes mediate protrusion formation and migration in microglia by inducing actin polymerization and regulation of local swellings and shrinking [368, 377-383]. Involvement of non-selective cation channels, such as Transient receptor potential (TRP) channels in microglial activation and migration has been extensively described as well [384].

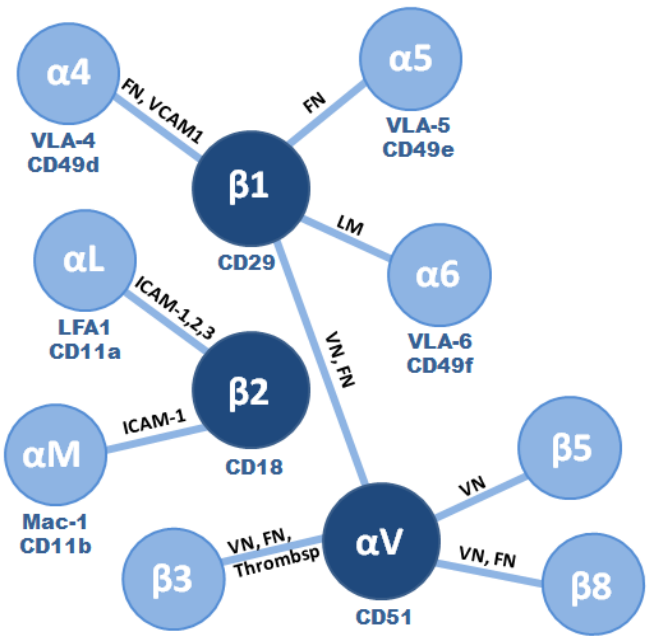

Fig. 1.10. Integrins reported in microglia *in vitro*. CD, cluster of differentiation; FN, fibronectin; ICAM, intercellular adhesion molecule; LFA, leukocyte function antigen; LM, laminin, VCAM, vascular cellular adhesion molecule; VLA, very late antigen; VN, vitronectin; Thrombsp, Thrombospondin [294, 356, 358, 359, 361].

Molecular signaling in microglial mobility

Though molecular signaling pathways underlying *in vivo* microglial migration remain largely unknown, *in vitro* studies proposed some mechanistic and signaling events underlying microglial chemotaxis/migration [385]. Primary microglia do not demonstrate classic types of adhesions during migration but instead form podosomes, 0.4-1μm multimolecular structures with an F-actin core surrounded by a ring of adhesion and structural proteins. Through calcium signaling in these podosomes, microglia were able to adhere to and degrade fibronectin substrates using matrix metalloproteinases [386, 387]. Podosome based migration seems a plausible mechanism for *in vivo* microglial migration, but this remains to be tested. The phosphatidylinositide 3-kinase (PI3K) signaling pathway appears to be one of the major signaling pathways in microglia chemotaxis. The activation of PI3K and its localization towards the leading edge membrane is instructive for microglial cell polarity through inducing F-actin polymerization at the cell front [385]. Activation of this pathway through purinergic receptors P2X4, P2Y12 is also involved in microglial migration and process outgrowth in response to ATP and ADP [372, 388-390]. Although ATP-stimulated chemotaxis in microglia requires PI3K activation, membrane ruffling (which can be considered as process motility) does not [388]. Of note, chemotaxis and chemokinesis occur through two distinct molecular pathways in microglia [391]. Chemotaxis is the directed migration towards a chemical source while chemokinesis in a non-directional increase of migration in response to a chemical stimulus. ATP stimulates a combination of both chemokinesis and chemotaxis, which are mediated by the ROCK signaling, while C5a stimulates only chemotaxis mediated by Rac1 signaling. Further, PI3K is only required for random basal microglial cell migration and not for directional migration [391]. P2Y12R signaling following TLR2 activation results in PI3K/Akt and Rac activation, which controls chemotaxis [392]. Next to inducing cytoskeletal remodeling, PI3K also induces MMP expression [393].

Intracellular Ca^{2+} -independent phospholipase A(2) ($iPLA_2$) was found to activate PI3K-Akt signaling in microglia through directing Src activation [390]. Active Src phosphorylates paxillin at Tyr^{31}, which is essential for focal adhesion assembly and microglial migration [394]. $iPLA_2$ also controls the recycling of α6 integrin vesicles and their delivery to focal adhesion during microglial chemotaxis [395]. Akt activation can also be regulated by a phosholipase C (PLC) mediated increase in intracellular calcium after P2Y12R signaling [389]. In addition, ERK1/2 (alternatively MAP kinase) signaling is directly involved in promoting chemotaxis by regulating phospohorylation states of adhesome proteins such as paxillin, required for adhesion dynamics [394].

While $iPLA_2$, PI3K-Akt and ERK1/2 signaling promote migration, PKA signaling inhibits it and this can occur also through ADP stimulation of P2Y12R [396]. In this case, P2Y12R signaling induced increased levels of cAMP, PKA activation which leads to phosphorylation of vasoldilator-stimulated phosphoprotein (VASP). However, prolonged phosphorylation of VASP by PKA disturbs focal adhesion formation/maturation and membrane ruffle formation resulting in a defective chemotaxis. A balanced regulation of phosphorylation and dephospohorylation of VASP is necessary for efficient chemotaxis [396]. On the contrary, ATP signaling through P2Y12R was found to decrease adenylyl cyclase levels, which normally lead to increased cAMP and PKA activation, and to induce increased microglial adhesion to collagen [372]. Also ADP stimulation through P2Y12R causes β1 to

translocate to membrane ruffles in order to promote migration and this is negatively regulated by PKA [370]. How PI3K-Akt and Ras-ERK1/2 pathways are involved in microglial migration in *ex vivo* embryonic brain slices, is explored in **Chapter 4.**

It is clear that microglia can detect changes in ECM composition through their expression of a wide range of integrins and changes in ECM reciprocally influence microglial metabolism. Upon purinergic stimulation microglia effectively use these integrins in regulating their mobility and β1 integrin, more than β2 and β3, plays a major role in this process. The underlying molecular signaling pathways are beginning to emerge as well. $iPLA_2$, Scr, PI3K-Akt and ERK1/2 signaling pathways converge on promoting adhesion formation, membrane ruffling, F-actin polymerization and thereby promoting microglial chemotaxis. In contrast, PKA can negatively regulate chemotaxis.

1.4 Study aims

Studies of the last decade have established pivotal roles for microglia in normal brain development. However, many aspects of the microglial physiology and how they colonize the embryonic mouse brain are still unresolved. After all, microglia must be present in the brain in order to coordinate brain development. The experiments conducted during this dissertation were designed **(1)** to unravel the microglial colonization mechanisms and **(2)** to assess the microglial population's sensitivity to external adverse conditions during development, such as maternal inflammation which is well known to increase the risk for neurodevelopmental disorders in the offspring **(Fig. 1.11)**. To this end, first **(1A)** the pattern of invasion, surface marker expression, proliferation rate and morphology of the microglial cells is mapped from the start of their appearance in the brain until late gestation **(Chapter 2)**. Second **(1B)**, the dynamic migration behavior of the microglial cells in the embryonic brain and the role of ECM-adhesion (fibronectin-integrin) mechanisms underpinning this migration are assessed **(Chapter 3)**. Third **(1C)**, the role of a candidate chemokine CXCL12 in steering microglial movement once inside the brain and its link with β1 integrin mediated migration is assessed **(Chapter 4)**. Last **(2)**, the effect of maternal immune activation during pregnancy on the microglial activation status in the embryonic offspring is determined **(Chapter 5).**

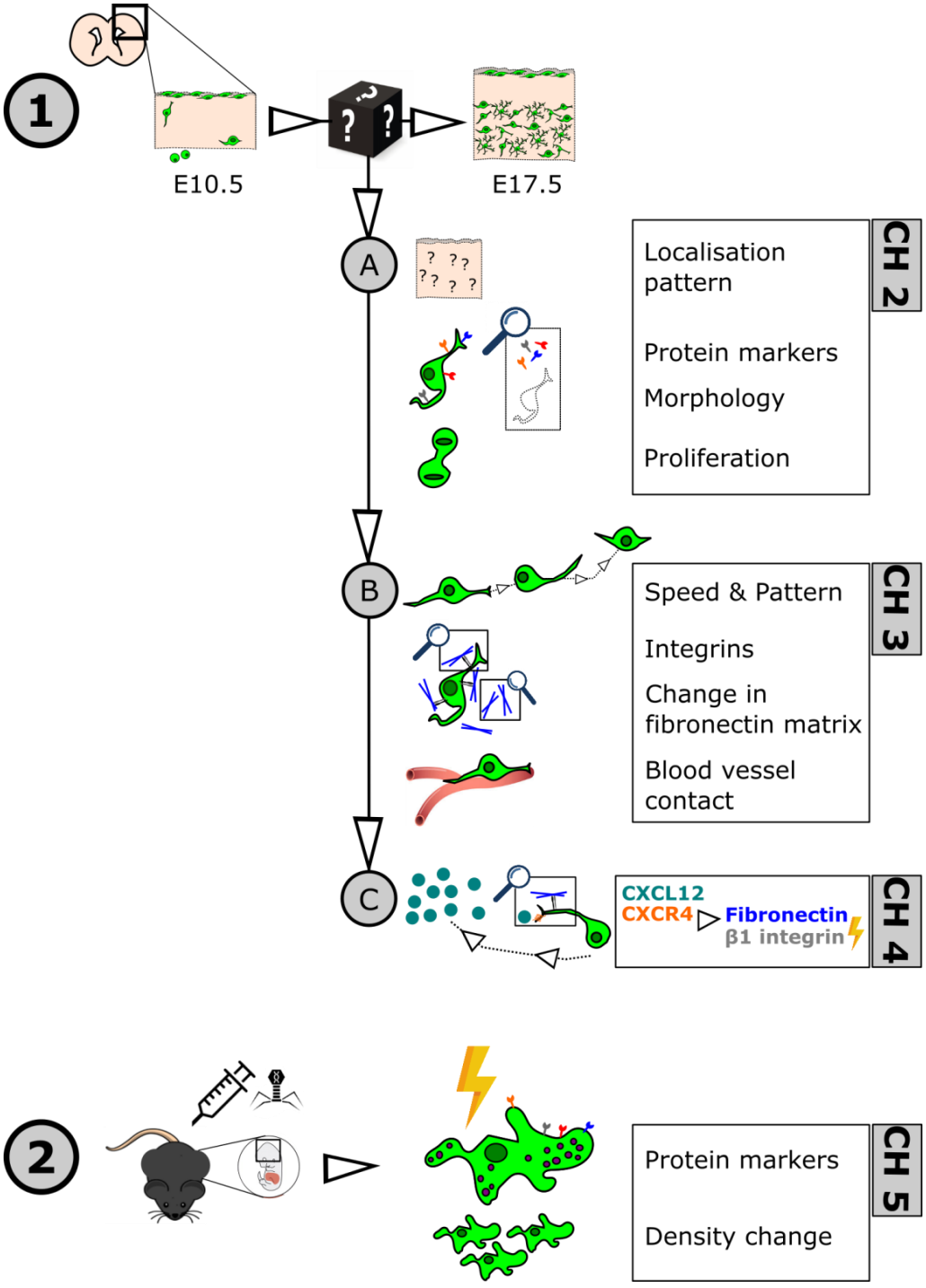

Fig. 1.11. Study aims. Green cells represent microglial cells. Arrowheads with dotted line indicate cell displacement. Drawings are not to scale. CH, Chapter; E, Embryonic day.

CHAPTER 2:

Complex invasion pattern of the cerebral cortex by microglial cells during development of the mouse embryo

Published as: Swinnen N, Smolders S, Avila A, Notelaers K, Paesen R, Ameloot M, Brone B, Legendre P and Rigo JM. Complex invasion pattern of the cerebral cortex by microglial cells during development of the mouse embryo. Glia, 2013. 61(2), 150-163.

Own contribution: Conduction and analysis of microglial distribution assessment inside the embryonic cortical wall. Conduction of the time-lapse experiments with 10min interval. Participation in writing the manuscript.

2.1 Abstract

Microglia are the immune cells of the central nervous system. They are suspected to play important roles in adult synaptogenesis and in the development of the neuronal network. Microglial cells originate from progenitors in the yolk sac. Although it was suggested that they invade the cortex at early developmental stages in the embryo, their invasion pattern remains largely unknown. To address this issue we analysed the pattern of cortical invasion by microglial cells in mouse embryos at the onset of neuronal cell migration using in vivo immunohistochemistry and *ex vivo* time-lapse analysis of microglial cells. Microglial cells begin to invade the cortex at 11.5 days of embryonic age (E11.5). They first accumulate at the pial surface and within the lateral ventricles, after which they spread throughout the cortical wall, avoiding the cortical plate region in later embryonic ages. The invasion of the cortical parenchyma occurs in different phases. First, there is a gradual increase of microglial cells between E10.5 and E14.5. From E14.5 to E15.5 there is a rapid phase with a massive increase in microglia, followed by a slow phase again from E15.5 until E17.5. At early stages, many peripheral microglia are actively proliferating before entering the parenchyma. Remarkably, activated microglia accumulate in the choroid plexus primordium, where they are in the proximity of dying cells. Time-lapse analysis shows that embryonic microglia are highly dynamic cells.

2.2 Introduction

Microglia are the resident immune cells of the central nervous system (CNS). In the healthy adult CNS, microglial cells have a ramified morphology, with a small cell soma and long, thin processes that constantly scan their environment [34, 36]. Microglia can play a beneficial role, through phagocytosis of cellular debris, trophic and anti-inflammatory factor release, but they can also have detrimental effects through reactive oxygen species production and inflammatory cytokine production [172, 397]. In addition, there is increasing evidence that they can also participate in the regulation of neuronal network and cell assembly in the adult [82, 141, 172, 254, 398-400].

Microglia derive from primitive myeloid progenitor cells that arise in the mouse before E8 in the yolk sac and can be detected in the brain at early developmental stages, by day E9.5 in mice embryos [20, 53]. This is also the case in human, rabbit, rat and quail embryos [74-78, 80, 81]. In the mouse embryonic spinal cord, microglial cells begin to invade the parenchyma at the end of neuronal migration (E11.5), during which local neuronal networks become functional [37]. Remarkably, microglia begin to invade the brain [20] and spinal cord [37] at similar ages in mouse embryos, but at this stage the cortex is less mature than the spinal cord and is characterized by the beginning of cortical neurogenesis [13, 24, 401, 402]. It is therefore unclear whether the embryonic microglia, although of similar origin, will have similar functions in both embryonic structures according to their developmental stages. This remains an open question, as the invasion pattern of the cortex by embryonic microglia with respect to the developmental stages of this structure is poorly documented and their functions during early brain development remain poorly understood. To address this issue, we investigated the colonization processes of the embryonic

cortex by microglia *in vivo* and *ex vivo*, with respect to the already known developmental pattern of the embryonic cortex.

Using the transgenic CX3CR1-eGFP mouse, immunohistochemical methods and time-lapse imaging, we show that the invasion process of the embryonic cortex occurs in three phases, an initial phase from E10.5 until E14.5, a second one occurring between E14.5 and E15.5, and a third one after E15.5. During this process, microglia are showing a highly dynamic behaviour. In the same period, microglial cells accumulate within the choroid plexus primordium, close to dying cells.

2.3 Materials and methods

2.3.1 Animals

Transgenic CX3CR1-eGFP knock-in mice [403] were used in order to visualize microglia in the embryonic cortex *in vivo*. In these animals, eGFP is expressed under the promoter of CX3CR1, also known as the fractalkine receptor, rendering all monocyte-derived cells, including microglia, green fluorescent [403]. All experiments were conducted in accordance with the European Community guiding principles on the care and use of animals and with the approval of the Ethical Committee on Animal Research of the Hasselt University. Mice were maintained in the animal facility of the Hasselt University in accordance with the guidelines of the Belgian Law and the European Council Directive. The heterozygous CX3CR1-eGFP +/- embryos that were used in this study were obtained by crossing homozygous CX3CR1-eGFP +/+ mice (mice were obtained from the European Mouse Mutant Archive – EMMA with the approval of Stephen Jung [403]) with wild type C57BL/6 mice. Females were checked for vaginal plugs each morning, the day of conception was designated as embryonic dag 0.5 (E0.5). Pregnant mice were sacrificed by means of cervical dislocation at the desired embryonic day and the embryos were removed.

2.3.2 Tissue Preparation and Immunostaining

The heads of E10.5 – E15.5 embryos were fixed in 4% paraformaldehyde for 3h at 4°C, 5h for E16.5 and E17.5 embryos. After fixation, the embryonic heads were cryoprotected overnight in phosphate-buffered saline (PBS) + 30% sucrose, frozen in optimal cutting temperature compound (Tissue-Tek) and stored at -80°C until sectioned. Ten and fifity-micrometer-thick coronal tissue sections were cut on a Leica CM1900 uv cryostat, mounted on Superfrost Plus glasses and stored at -20°C until staining.

Embryonic sections were washed three times in PBS, blocked with serum and permeabilized with Triton X-100 (Sigma-Aldrich). Subsequently they were incubated with the primary antibody (Table 2.1), this was performed overnight at 4°C, except for Ki-67 for which slices were incubated for 2h at room temperature. After washing, the sections were incubated with alexa-labeled secondary antibodies for 1h at room temperature and mounted with Vectashield (Vector laboratories) containing 4,6-diamidino-2-phenylindole (DAPI) to reveal cellular nuclei. All primary antibodies and working solutions are listed in Table 2.1. Staining controls for the secondary antibodies were performed by omitting the primary antibodies.

To determine if the CX3CR1 eGFP cells observed in the embryonic cortex were effectively microglial cells we used antibodies directed against ionized calcium binding adaptor molecule 1 (Iba-1) and cluster of differentiation (CD)68. Iba-1 is a marker for microglial cells, it is a small protein suggested to function as an adaptor molecule that mediates calcium signals in cells of the monocytic lineage, including microglia [404]. CD68, the murine homologue for macrosialin, is a transmembrane glycoprotein which is expressed in lysosomes and endosomes of monocytes, macrophages and microglia [405, 406].

In order to determine the activation state of the microglia present in the embryonic cortex, we used an antibody against Mac-2 (ATCC; Clone M3/38.1.2.8 HL.2). Mac-2, also known as galectin-3, is a member of the galectin family of β-galactoside binding lectins. It can be expressed by many cell types and is implicated in several processes. Expression of Mac-2 is a hallmark of microglial activation [407-412].

A Ki-67 antibody was used to identify active proliferating microglial cells The antigen is expressed during all active phases (the G1, S, G2 and M phases) of the cell cycle and cannot be detected in resting cells (G0 phase) [413].

Apoptotic cells were visualized using a cleaved caspase-3 antibody (Cell signaling; Asp175). This antibody detects endogenous levels of the large fragment (17/19 kDa) of activated caspase-3 and does not recognize the full length caspase-3 or other cleaved caspases [414].

Table 2.1. Overview of the primary antibodies

Primary Antibody	Company	Reference	Dilution
Anti-Iba-1	WAKO	019-19741	1:500
Anti-CD68	AbD Serotec	MCA1957GA	1:400
Anti-Mac-2	ATCC	TIB-166 Clone M3/38.1.2.8 HL.2	1:250
Anti-Ki-67	Abcam	ab15580	1:40 – 1:55
Anti-Cl. caspase-3	Cell Signaling	9661	1:500

2.3.3 Microscopy and Analysis of Immunostainings

Quantitative analysis of microglial cells was performed on images of 10-µm-thick coronal embryonic brain sections, except when quantifying microglial morphology then 50-µm-thick sections were used. Images were taken with a Nikon Eclipse 80i microscope and a Nikon digital sight camera DS-2MBWc. The objectives used were from Nikon; a 10x Nikon plan objective (numerical aperture (NA) of 0.25), a 20x Plan Fluor objective (NA of 0.5) and a 40x Plan Fluor objective (NA of 0.75). Ki-67 stainings were examined with an inverted Zeiss Axiovert 200M microscope attached to a Zeiss LSM 510 Meta Confocal laser scanning system, the different fluorophores were sequentially imaged through a 20x Plan-Apochromat objective (NA of 0.75). Images (1600 x 1200 or 512 x 512 pixels) were analysed with ImageJ 1.45e software (NIH, USA; http://rsb.info.nih.gov/ij/). Only eGFP-positive cell bodies were taken into account for the

measurements. Quantifications were made per cortical slice (supplemental table 1). Afterwards, an average of the quantifications of all the slices per embryo was made, so only one value for each embryo was included in the statistical analysis (number of embryos = n). For the quantification of cell morphology 50 µm sections were used, all protrusions with a length equal or more than 1/2 of the cell soma were considered as a ramification.All values are expressed as mean ± S.E.M. Statistical significance was assessed by nonparametric Kruskal-Wallis test, p-values smaller than 0.05 were considered significant.

In order to determine the location of a microglial cell in the cortex, pictures were loaded in the home-made analysis program "Angle", developed in the Matlab environment. The straight distance between the ventricular lining and the middle of the cell soma was measured together with the straight distance between the ventricular lining and the pia, running through the microglial soma in question and corresponding to the thickness of the cortex. The microglial location was expressed as the percentage of distance from the entire neocortex (measurements were performed on 3 embryos per age, E12.5 until E17.5, number of cells = n). Based on the resulting data, a probability distribution of this location was estimated for every age by applying the Kernel Smoothing Density procedure with a Gaussian kernel (Matlab).

2.3.4 Time-lapse imaging

Pregnant mothers were euthanized at E12.5, E14.5 and E17.5. Embryonic brains were isolated in ice-cold PBS-glucose (pH 7.4; 25mM), embedded in 3% low melting agarose (Fisher Scientific) and sliced coronally at a thickness of 300 µm using a Microm HM650V Vibrating Blade Microtome. Slices were mounted on MilliCell organotypic inserts (Millipore) and maintained in semi-hydrous conditions at 37°C and 5% CO2. The tissue was allowed to equilibrate for approximately 60 minutes before imaging. Migration media consisted of Neurobasal medium supplemented with 2mM L-glutamine, B27 supplement, N2 supplement and 0.5% penicillin-streptomycin (all from Invitrogen).

For live imaging, slices were transferred on their insert to a glass bottom microwell dish (MatTek) in semi-dry conditions. The microscope chamber was heated by constant air provision at 37°C. Humified air with 5% CO2 was continuously applied to the slice. The eGFP positive microglia were excited by a Mai Tai DeepSee Ti:Saphire pulsed laser (Spectra-Physics) with a central wavelength tuned at 900 nm and visualized using a KP 650 nm dichroic mirror. For the analysis of migration speed a z-stack, spanning 72 µm with serial optical sections (1024 x 1024; 8-bit) every 8 µm, was recorded every 10 minutes for a total duration of 5 – 7 hours. For the analysis of microglial behaviour a z-stack, spanning 32 µm with serial optical sections (1024 x 1024; 8-bit) every 8 µm, was recorded every 2 minutes for a total duration of 1 hour. Each time imaging started from a minimum depth of 50 µm under the cutting surface of the slice. A 20x EC plan-Neofluar objective (NA of 0.5 and 2 mm working distance) (Zeiss) was used, corresponding to a field of view measuring 450 x 450 µm. The ImageJ (NIH, USA; http://rsb.info.nih.gov/ij/) plug-in "MTrackJ" was used to manually track movement paths of microglia in 4D and to calculate migration speed [415]. The average distance the cells travel per step is plotted as a cumulative frequency. The migration

speed values are expressed as mean ± S.E.M. Statistical significance was assessed by nonparametric Kruskal-Wallis test, p-values smaller than 0.05 were considered significant.

2.4 Results

In mice, neurogenesis and neuron migration start on E11 in the cortex and last to E17, when initiation of synaptogenesis and neuron differentiation begin [401, 402]. We focused our analysis on the cerebral cortex area located dorsally to the lateral ganglionic eminences (LGE) and medial ganglionic eminences (MGE), obtained from CX3CR1-eGFP +/- mouse embryos aged from E10.5 to E17.5. This region of the cortex is well characterized on the functional and cellular level and the two GE structures are the major sources of cortical interneurons during embryonic neurogenesis [416-418].

First we determined to what extent the CX3CR1-eGFP cells observed in the embryonic brain were effectively microglial cells. Most of the eGFP cells in the embryonic brain were immunoreactive for Iba-1. At E10.5 91.7 ± 8.3% of the eGFP cells in the cortex were expressing Iba-1. This percentage remained stable between E10.5 and E17.5, ranging from 97.6 ± 1.6% at E11.5 to 99.8 ± 0.2% at E17.5 (n = 4 – 9 embryos) (E12.5, 99.1 ± 0.9%; E13.5, 99.1 ± 0.6%; E14.5, 99.2 ± 0.5%; E15.5, 99.6 ± 0.3%; E16.5, 100 ± 0%). The percentage of eGFP cells expressing Iba-1 between E10.5 and E17.5 was not significantly different ($p > 0.1$). Like for the Iba-1 immunoreactivity, most of the eGFP cells in the embryonic cortex were expressing CD68. At E10.5 ≈ 100% of the eGFP cells were CD68 positive and this percentage remained stable at all ages (E10.5, 100 ± 0%; E11.5, 86.1 ± 10.0%; E12.5, 85.8 ± 3.3%; E13.5, 93.9 ± 1.7%; E14.5, 88.2 ± 3.6%; E15.5, 95.4 ± 2.1%; E16.5, 98.2 ± 1.4%; E17.5, 97.1 ± 0.1% (n = 3 – 9 embryos). The percentage of eGFP cells expressing CD68 between E10.5 and E17.5 did not change significantly ($p > 0.1$). These results demonstrate that the eGFP cells present in the developing brain parenchyma are microglial cells or microglial precursors and will from now on be referred to as microglia.

2.4.1 Invasion of the embryonic cortex and ganglionic eminences by microglia between E10.5 and E17.5

The number of microglial cells present in the cortex significantly increased ($p < 0.001$; Kruskal-Wallis test) between E10.5 and E17.5 **(Fig. 2.2A)**. At the age of E10.5 **(Fig. 2.1A, 2.2A)** and E11.5 **(Fig. 2.1B, 2.2A)** almost no microglia could be observed in the cortex. At E10.5 and E11.5 we observed 0.5 ± 0.2 cells per slice (n = 4 embryos) and 2.6 ± 0.2 cells per slice (n = 6 embryos) respectively. Many faint eGFP positive cells were present at the pial surface of the cortex, their round morphology and prominent nucleus suggest that these cells were likely to be monocytes [37, 419]. At E12.5 (Fig 2.1C, 2.2A), microglial cells were still rarely observed in the cortical parenchyma, although their number (5.0 ± 0.4 cells per slice; n = 12 embryos) had doubled when compared to E11.5. The distribution of the microglial cells throughout the cortical wall was random. Between E12.5 and E14.5 the number of microglia remained stable (E14.5: 8.8 ± 0.6 cells per slice; n = 13 embryos; $p > 0.05$) **(Fig. 2.1D, 2.1E, 2.2A)**, to rise abruptly to 31 ± 2 cells per slice by the age of E15.5 (n = 8 embryos) **(Fig. 2.1F, 2.2A)**. After this sudden rise at E15.5, the cell number remained stable (E17.5: 40 ± 1 cells per slice; n = 6 embryos; $p > 0.05$)

(Fig. 2.1H, 2.2A). From E15.5 the cortical wall can be divided into three layers: the ventricular zone, intermediate zone and the cortical plate zone [420, 421]. Remarkably few microglia (5 ± 1% of the eGFP cells per slice) were present in the cortical plate region from E15.5 to E17.5.

During embryonic development, the surface of the cortex increases and its morphology becomes more complex **(Fig. 2.1A – H and Fig. 2.2B)**. The surface area of the cortex significantly increased 14-fold ($p < 0.001$; Kruskal-Wallis test) from E10.5 (3.3 x 104 ± 0.6 x 104 μm^2; n = 4 embryos) to E17.5 (47 x 104 ± 3.5 x 104 μm^2; n = 6 embryos).

To determine if the increase in microglial cell number with age **(Fig. 2.2A)** reflects a true colonization process or is related to the increase of cortex area only, we quantified the change in microglial cell density with embryonic age. The microglial density significantly increased ($p < 0.001$; Kruskal-Wallis test) 6-fold from E10.5 (1.5 x 10-5 ± 0.6 x 10-5 cells/μm^2; n = 4 embryos) to E17.5 (9.1 x 10-5 ± 0.7 x 10-5 cells/μm^2; n = 6 embryos) **(Fig. 2.2C)**. During this developmental period microglial cell density significantly increased from E10.5 to E11.5 ($p < 0.05$), remained stable between E11.5 and E14.5 and then significantly increased after E14.5 ($p < 0.05$).

Throughout development the general morphology of the cortical microglial cells significantly changed ($p < 0.05$; Kruskal-Wallis test) from an amoeboid form in the early stages, towards a more ramified one later in development. At E12.5 (n = 3 embryos) the majority of the microglial cells had an amoeboid form (61 ± 5 %) **(Fig. 2.2D)**. While at E16.5, 76 ± 1% of the microglial cells had 1 or more protrusions **(Fig. 2.2D)**.

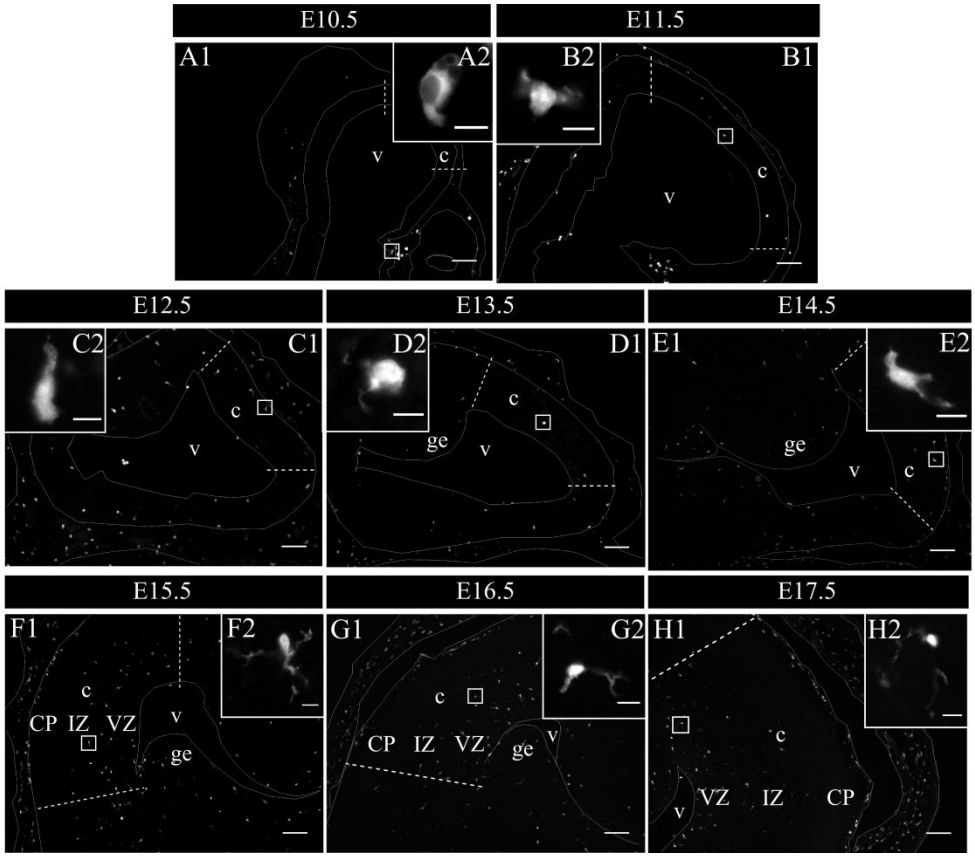

Fig. 2.1. Invasion and distribution of microglial cells in the developing cortex. (A – H) Coronal sections of mouse E10.5 – E17.5 embryonic brains, eGFP cells in white. The DAPI channel was not shown to preserve the clarity of the pictures, instead the structures are contoured by a white line. The dotted lines mark out the investigated cortical areas (see Supplemental fig. 1 for a schematic description of these areas). The number of microglial cells gradually increases with the development of the cortex. Their morphology changed from a predominantly amoeboid form towards a branched one (Fig. insets). Many faint eGFP cells, probably monocytes, could be observed at the pial surface of the cortex. At all developmental stages single and groups of eGFP cells were present in the lateral ventricle, as free floating or attached to the ventricular wall, and many eGFP cells were lining the pial surface of the brain. Number of embryonic brains tested in each group: E10.5 n = 4; E11.5 n = 6; E12.5 n = 12; E13.5 n = 11; E14.5 n = 13; E15.5 n = 8; E16.5 n = 5; E17.5 n = 6. c, cortex; CP, cortical plate; ge, ganglionic eminence; IZ, Intermediate zone; v, ventricle; VZ, Ventricular zone. Scale bars = 100µm, inset = 10µm.

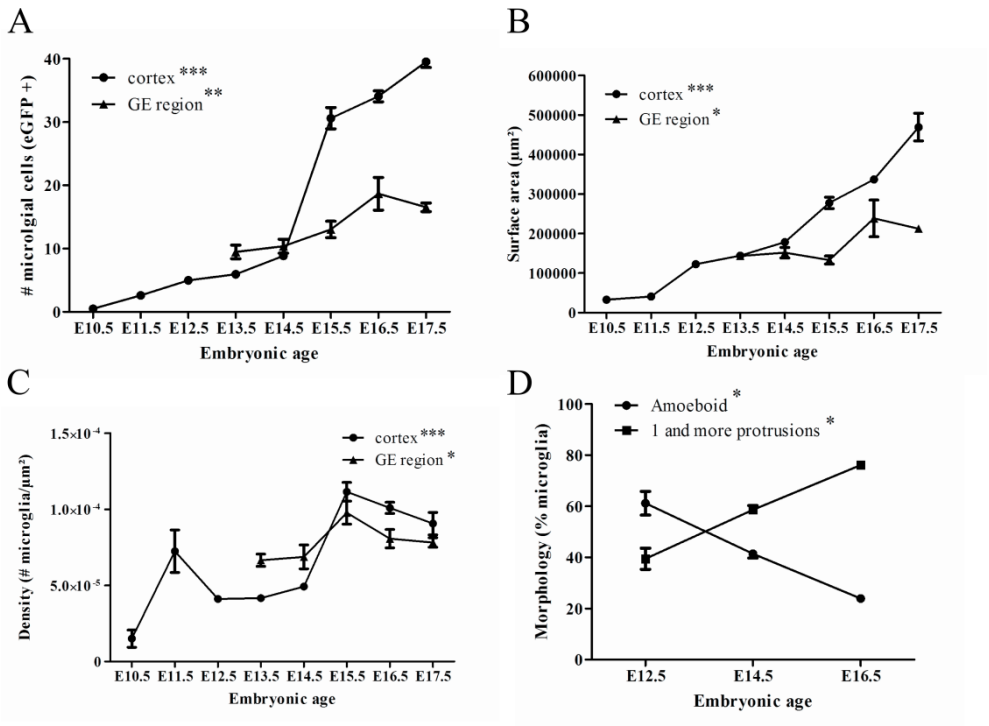

Fig. 2.2. Quantification of microglial cell invasion. (A) The microglial cell number significantly increased during development in both the cortical wall as the GE region. At E10.5 almost no eGFP cells were observed in the cortical parenchyma. From E11.5 until E14.5, eGFP cells slowly invaded the cortex, afterwards there was a drastic increase in their cell number. In the ganglionic eminences the cell number slowly increased from E13.5 until E17.5. **(B)** The cortex surface area significantly increases during development. From E10.5 to E11.5 the area stays constant and gradually started to increase from E11.5 on. The surface area of the GE region also significantly increases when the embryo ages. The area of the region stays constant between E13.5 and E15.5, after E15.5 it increases. **(C)** Cell density significantly increased during development in both the cortical wall as the GE region. In the cortex, two phases could be observed in eGFP cell density, a first small increase at E11.5 after which the density remained stable up until E14.5, at E15.5 there was a second rise. In the ganglionic eminences a peak at E15.5 in eGFP cell density was also observed. Number of embryonic brains tested in cortex group: E10.5 n = 4; E11.5 n = 6; E12.5 n = 12; E13.5 n = 11; E14.5 n = 13; E15.5 n = 8; E16.5 n = 5; E17.5 n = 6. Number of embryonic brains tested in ganglionic eminence group: E13.5 n = 9; E14.5 n = 8; E15.5 n = 7; E16.5 n = 3; E17.5 n = 3. **(D)** The morphology of the eGFP cells present in the cortical parenchyma gradually changed from predominantly amoeboid cells towards branched cells. Number of embryonic brains tested : n = 3. **(*** $p < 0.05$; ** $p < 0.01$; *** $p < 0.001$).

When looking at the microglial invasion of the region comprising the LGE and MGE, a similar pattern was observed as in the cortex from E13.5 to E17.5. The number of microglial cells significantly increased ($p < 0.01$; Kruskal-Wallis test) almost two-fold from E13.5 (10 ± 1 cells per slice; n = 9 embryos) to E17.5 (16.5 ± 0.7 cells per slice; n = 3 embryos) **(Fig. 2.2A)**.

During embryonic development, the surface area of the GE region significantly increased 1.5 times ($p < 0.05$; Kruskal-Wallis test) from E13.5 ($14 \times 10^4 \pm 0.9 \times 10^4$ µm²; n = 9 embryos) to E17.5 ($21 \times 10^4 \pm 0.2 \times 10^4$ µm²; n = 3 embryos) **(Fig. 2.2B)**.

Similarly as in the cortex, the microglial cell density was significantly different ($p < 0.05$; Kruskal-Wallis test) between E13.5 (6.7 x 10-5 ± 0.4 x 10-5 cells/µm²; n = 9 embryos) and E17.5 (7.8 x 10-5 ± 0.3 x 10-5 cells/µm²; n = 3 embryos) **(Fig. 2.2C)**.

In the mouse embryonic spinal cord, microglia proliferate before entering the parenchyma [37]. Hence, the percentage of microglia that was actively proliferating in the cerebral cortex was determined using a Ki-67 staining. As shown in Fig. 3, actively proliferating cells could be observed between E11.5 and E17.5 **(Fig. 2.3A3, B3, C3)**, with the majority located in the ventricular zone of the cortex where many precursors are located [401, 422, 423]. In addition, the embryonic brain was surrounded by proliferating cells during this time span in embryonic development **(Fig. 2.3A3, B3, C3)**, likely indicating the growth of blood vessels and the development of the meninges [424, 425]. From E11.5 until E17.5, the number of microglial cells in the cortex that was positive for Ki-67 remained constant **(Fig. 2.3D)** (E11.5: 0.7 ± 0.4 Ki-67 positive microglial cells per slice; n = 3 embryos). However, the percentage of microglia that were actively proliferating in the cortex parenchyma significantly decreased ($p < 0.01$; Kruskal-Wallis test) during this period. At E11.5 **(Fig. 2.3A2, A4, A6 and E)**, 40 ± 18% of the microglial cells (n = 3 embryos) were immunoreactive for the proliferation marker Ki-67. This percentage decreased to 28 ± 5% (n = 6 embryos) at E13.5 **(Fig. 2.3B2, B4, B6 and E)** and decreased even further to only 10 2% at E15.5 **(Fig. 2.3C2, C4, C6 and E)**. At E17.5 only 3 ± 1% (n = 3 embryos) of the eGFP cells were positive for Ki-67 **(Fig. 2.3E)**. We observed many eGFP cells in the meninges that were immunoreactive for Ki-67, likely corresponding to microglial progenitors and suggesting that the majority of these cells proliferate in the periphery, before they enter the cortical parenchyma. The number and percentage of eGFP cells proliferating in the pia followed the same tendency as that observed in the cortex. The absolute number of **(Fig. 2.3D)** proliferating microglia remained constant (E11.5: 1.6 ± 0.4 ki-67 positive microglial cells per slice; n = 5 embryos) while there was a significant decrease ($p < 0.001$; Kruskal-Wallis test) in the percentage **(Fig. 2.3E)** of proliferating microglial cells from E11.5 (71.5 ± 14.5% ; n = 5 embryos) to E17.5 (5.04 ± 1.47% ; n = 6 embryos).

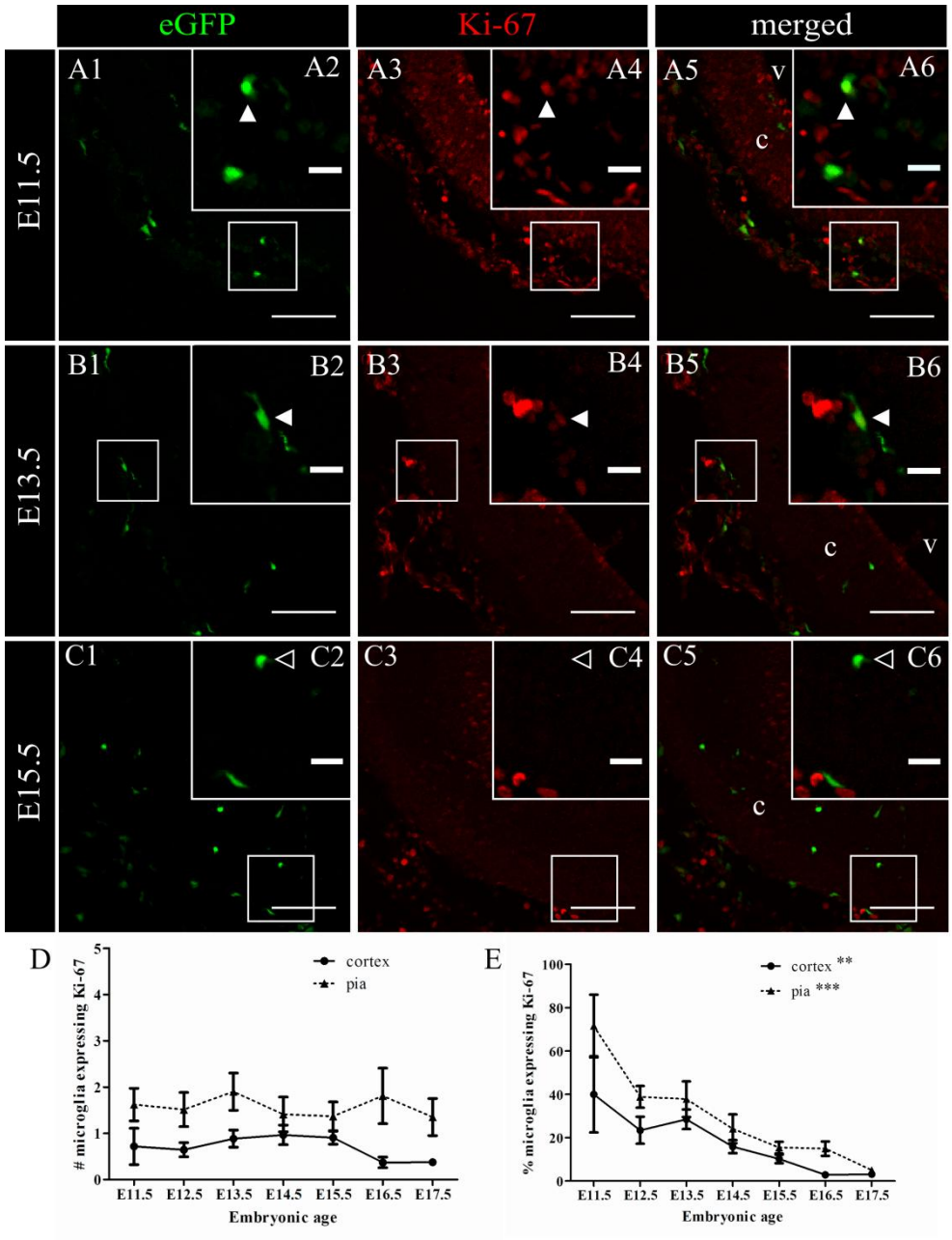

Fig. 2.3. Proliferation in the developing mouse embryonic cortex and pia. (A1, B1, C1) Microglial cells (green) in coronal sections of E11.5 – E15.5 brains. **(A3, B3, C4)** Actively proliferating cells were identified using the Ki-67 antibody (red). The DAPI channel was not shown to preserve the clarity of the merged pictures (A5, B5, C5). **(A2, A4, A6)** At E11.5 and (**B2, B4, B6)** E13.5, a rather high percentage of microglial cells were Ki-67 positive. White arrowheads indicate Ki-67 expressing microglial cells. **(C2, C4, C6)** At E15.5 only a small percentage of the microglial cells were showing immunoreactivity against Ki-67. Open arrowheads indicate non-proliferating microglia in the cortex. **(D)** The absolute number of microglial cells that were actively proliferating in the cortical parenchyma and at the pia remained constant throughout development. **(E)** The percentage of proliferating microglia significantly decreased as the embryo develops. Number of embryonic brains tested in each group for cortex: E11.5 and E17.5 n = 3; E12.5 – E15.5 n = 6. Number of embryonic brains tested in each group for pia: E11.5 n = 5; rest n = 6. c, cortex; v, ventricle. Scale bars = 100µm, insets = 20µm. (** $p < 0.01$; *** $p < 0.001$).

2.4.2 Microglia accumulate in the region of the choroid plexus primordium and associate with dying cells

The choroid plexus primordium can be recognized from E11 on in the mouse embryonic brain [426]. An increased accumulation of microglial cells was observed in the region of the choroid plexus primordium from E11.5 until E14.5 **(Fig. 2.4A1 and B1)**. The majority of microglial cells had an amoeboid morphology and endosomal-like compartments in their cell body **(Fig. 2.4A2 and B2)**. The number **(Fig. 2.4C)** and density **(Fig. 2.4D)** of the microglial cells in this accumulation remained stable between E11.5 and E15.5 (n = 13 – 15 embryos). By the age of E15.5, this accumulation became less apparent and was no longer visible at E16.5. Accordingly, the density of microglial in this structure significantly decreased ($p < 0.05$) from E15.5 ($8.2 \times 10^{-4} \pm 6.0 \times 10^{-5}$ cells/µm²; n = 15 embryos) to E16.5 ($4.6 \times 10^{-4} \pm 6.7 \times 10^{-5}$ cells/µm²; n = 14 embryos) **(Fig. 2.4D)**.In rodents, it was shown that the choroid plexus is already mature at an early stage of embryonic development (E15 in rats) [427] and that a significant amount of apoptosis takes place during embryonic development of this structure [428-430]. Indeed, the presence of apoptosis in this structure was identified by cleaved caspase-3 immunoreactivity **(Fig. 2.4A3-6)**. To the contrary, no immuno-reactivity for cleaved caspase-3 was found in the cortical parenchyma (data not shown).

Based on the presence of apoptosis and the morphology of the microglia that we observed in the choroid plexus, we hypothesized that the microglial cells in this structure acquired a phagocyte phenotype and cleared cellular debris from the apoptotic cells. To determine to what extent the microglial cells are activated, we performed an immunostaining for Mac-2/Galectin-3. Increased expression of Mac-2/Galectin-3 is related to the phagocyte phenotype in immune cells [407, 409, 410]. When looking at Mac-2 expression, almost no Mac-2 immunoreactive microglial cells were observed in the cortex: at all ages tested, less than 5% of the microglia were positive for Mac-2 (data not shown). At E11.5 only a few cells showed Mac-2 reactivity in the choroid plexus (7 ± 7%; n = 5 embryos). After E11.5 this percentage increased, to reach a peak at E14.5 (48 ± 6%; n = 4 embryos) **(Fig. 2.4B3-6)**. Subsequently this percentage decreased to 11 ± 2% (n = 6 embryos) at E16.5.

As observed in the cortex and its periphery, many proliferating cells could be observed in the choroid plexus primordium **(Fig. 2.5A3, B3, C3)**. Some microglial cells localized in the choroid plexus were also immunoreactive for Ki-67 **(Fig. 2.5A6, B6, C6 white arrowheads)**, indicating active proliferation. The absolute number of microglial cell positive for Ki-67 significantly decreased ($p < 0.001$; Kruskal-Wallis test) from 2.8 ± 0.8 Ki-67 positive microglial cells per slice at E11.5 (n = 5 embryos) to 0.1 ± 0.1 at E17.5 (n = 7 embryos) **(Fig. 2.5D)**. A same significant decrease ($p < 0.01$; Kruskal-Wallis test) was observed for the percentage of proliferating microglial cells in this area **(Fig. 2.5E)**, being 28 ± 9% at E11.5 (n = 5 embryos) **(Fig. 2.5A5, A6)** and 1 ± 1% at E17.5 (n = 7 embryos).

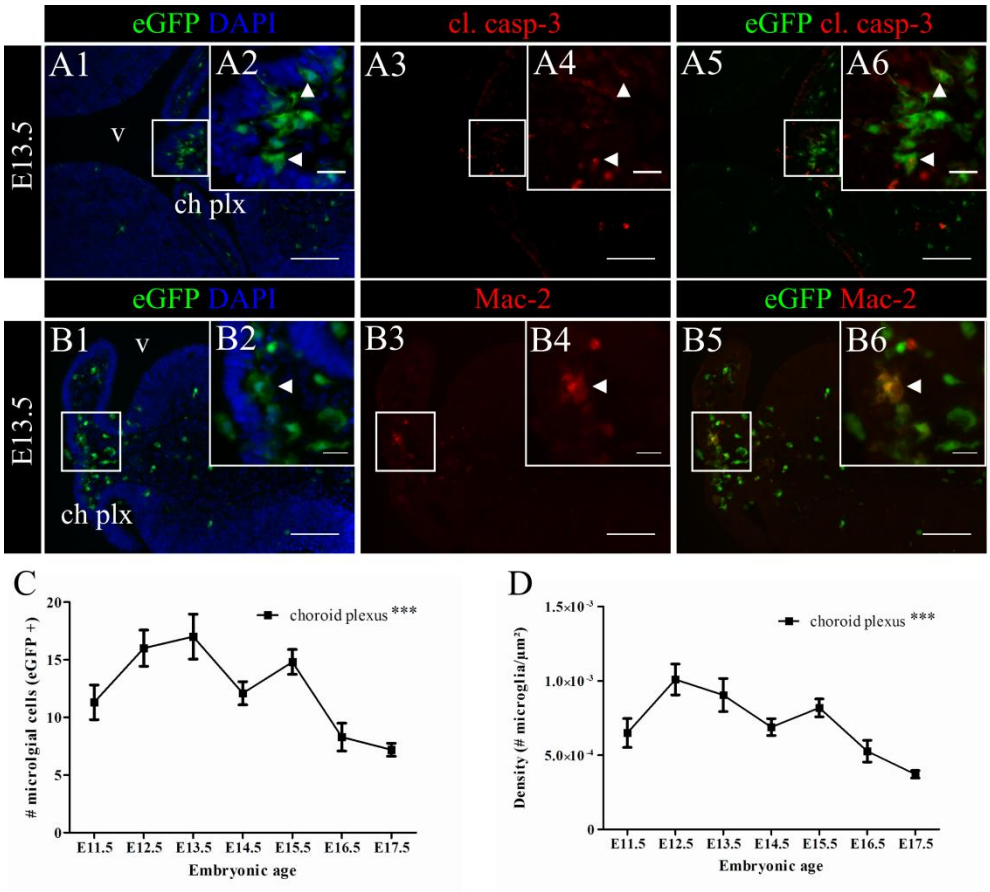

Fig. 2.4. Activated microglia accumulate in the choroid plexus region during developmental cellular death. (A1, B1) Coronal sections of mouse E13.5 embryonic brains with cell nucleus staining in blue (DAPI) and eGFP cells in green. From E11.5 until E14.5, an accumulation of eGFP cells in the choroid plexus primordium was observed. These eGFP cells had a predominantly amoeboid or unipolar morphology with endosomal-like compartments in their cell body (A2, B2). **(A3, A4)** Apoptotic cells were identified using the cleaved caspase-3 antibody (red). **(A5, A6)** At E13.5 apoptotic cells were found in the region comprising the choroid plexus (primordium), especially at the epithelial lining. Microglial cells present in the accumulation were in close proximity of these apoptotic cells (A2, A4, A6 white arrowheads). Several of them showed endosomal-like compartments and extended one or two processes through the epithelial lining of the plexus or around cleaved caspase-3 immunoreactive cells. **(B3, B4)** Immunohistochemical staining using a Mac-2 antibody (red) showed that the microglia present in this aggregate and close to the apoptotic cells are positive for the activation marker Mac-2 (B5, B6 white arrowhead). **(C – D)** In the choroid plexus primordium, the eGFP cell number (C) and density (D) significantly decreased throughout development. Number of embryonic brains tested in each group: E11.5 n = 5; E12.5 n = 6; E13.5 n = 6; E14.5 n = 9; E15.5 n = 6; E16.5 n = 3; E17.5 n = 3. ch plx, choroid plexus; v, ventricle. Scale bars = 100µm, inset = 20µm. (*** $p < 0.001$).

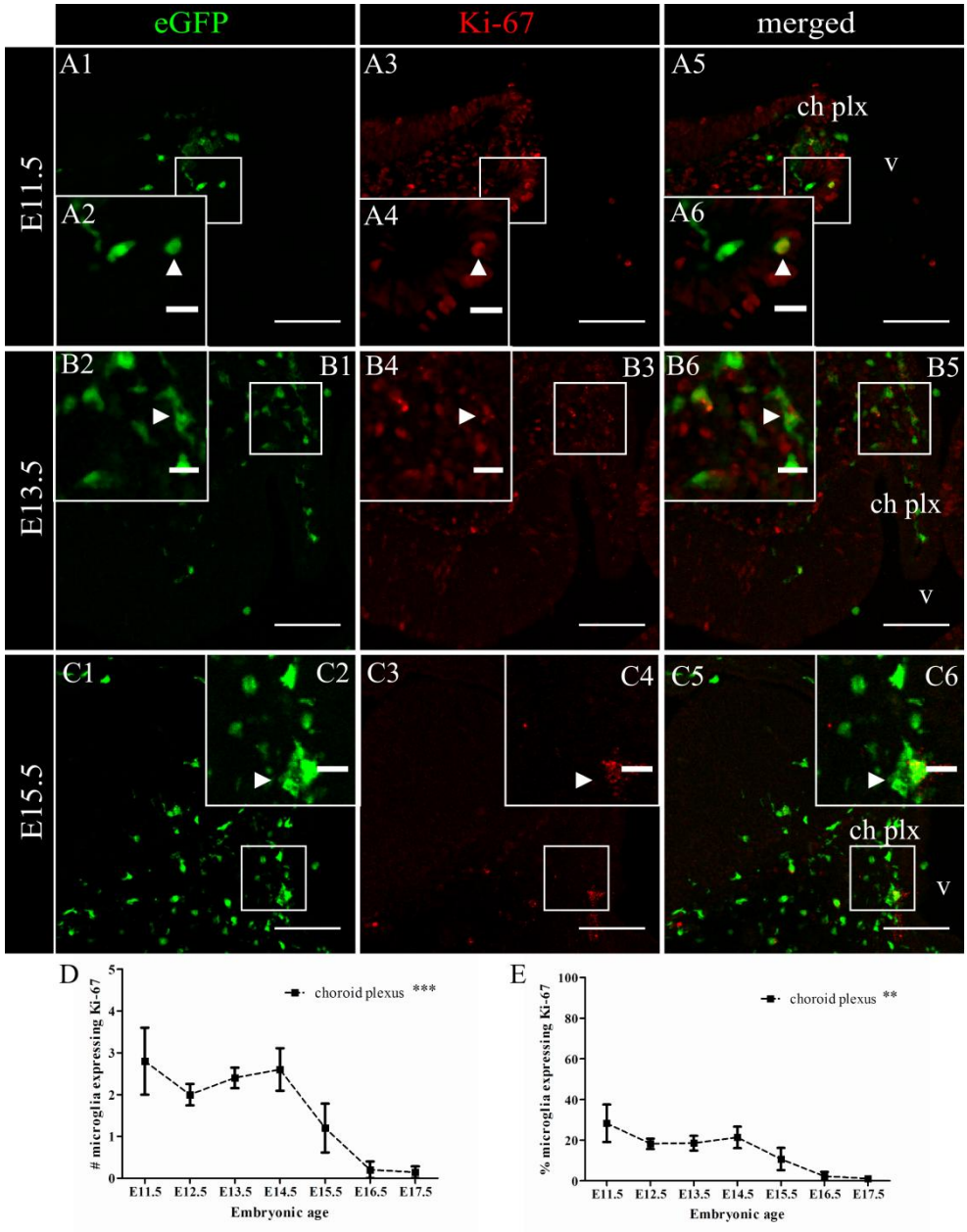

Fig. 2.5. Proliferation in the developing mouse embryonic choroid plexus primordium. (A1, B1, C1) Microglial cells (green) in coronal sections of E11.5 – E15.5 brains, the DAPI channel was not shown to preserve the clarity of the pictures. **(A3, B3, C3)** Actively proliferating cells were identified using the Ki-67 antibody (red). **(A2, A4, A6)** At E11.5 and **(B2, B4, B6)** E13.5 a relative high percentage of the microglial cells in the plexus primordium were positive for Ki-67, white arrowheads indicate Ki-67 expressing microglial cells. **(C2, C4, C6)** At E15.5 a smaller percentage of the microglial cells were showing immunoreactivity against Ki-67. However, Ki-67 positive microglia could still be detected in the plexus primordium, white arrowheads indicate proliferating microglia. **(D - E)** The number (D) and the percentage (E) of microglia that were actively proliferating in the choroid plexus primordium significantly decreased as the embryo matures. Number of embryonic brains tested in each group: E12.5 and E14.5 n = 4; rest n = 3. ch plx, choroid plexus; v, ventricle. Scale bars = 100µm, insets = 20µm. (** $p < 0.01$; *** $p < 0.001$).

2.4.3 Migration behaviour of microglial cells in the embryonic cortex

To study the dynamic behaviour of microglia in the neocortex at the onset of their colonization process, we first quantified their location within the cortex and then analysed their migration and behaviour in acutely prepared brain slices of embryos using two-photon excitation time-lapse microscopy. In order to look at the developmental change in the distribution of microglia in the embryonic cortex, we analysed the distribution of these eGFP cells within the parenchyma with respect to the ventricular lining as a position reference **(Fig. 2.6)**. At the onset of their invasion process (E12.5), the microglial cells accumulated at the ventricular wall (**Fig. 2.6**, dark bulb in E12.5 column at 0-20% region) and to the pial surface (**Fig. 2.6**, dark bulb in E12.5 column at 80-100% region). Afterwards, they became randomly distributed within the cortical wall. During the second phase of invasion (E14.5 to E15.5), characterized by an abrupt increase in cell density **(Fig. 2.2B)**, the relative density of microglia at the pial side of the cortex progressively decreased, while most microglia accumulated in the area close to the ventricle at E17.5 (**Fig. 2.6**, dark bulb in E17.5 column at 0-20% region). These observations suggest that microglia enter the cortex at early stages, both from the ventricular lining and pial surface. After E14.5 there was a reorganization of microglia distribution, which could be the result from changes in their dynamic behaviour during this developmental window.

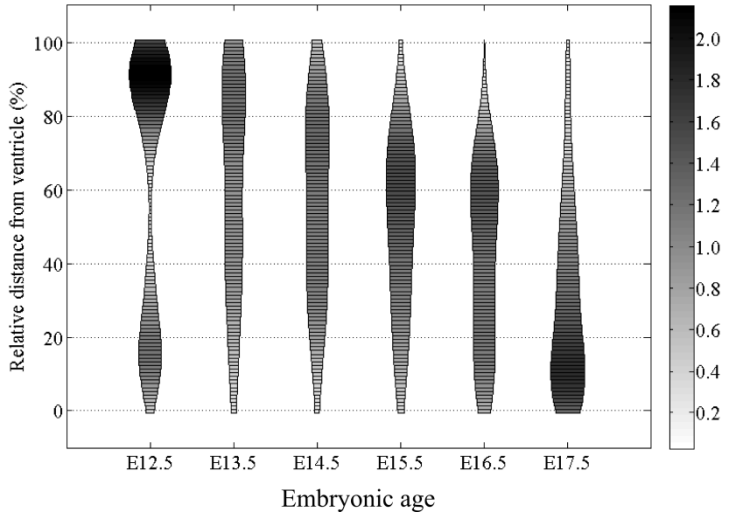

Fig. 2.6. Microglial distribution in the embryonic cortical wall. Absolute localization of the microglial cells in the cortical wall. The left axis represents the location of the microglia within the cortex relative to the entire thickness of the cortex (the distance between the ventricular lining and cell soma divided by the straight distance between ventricular lining and pia) shown in %, with 0% corresponding to the ventricular lining and 100% to the pia. The right grey scale axis indicates by its darkness the percentage of microglial cells that are located at a specific position in the cortical wall. The darker the color is and the wider the width of the column, the higher the percentage of cells at that position in the cortical wall. At E12.5, microglial cells are mostly located close to the ventricular lining and to the pial surface (indicated by the dark groups between 0-20% and 80-100%). From E13.5, these cells start to spread in order to populate the cortical layers in between. From E15.5 on the developing cortical plate is marked by an almost complete absence of microglial cells (indicated by the small, light groups between 80-100%). Measurements were performed on 3 embryos per age; number of cells in each age group: E12.5 n= 50; E13.5 n= 66; E14.5 n= 102; E15.5 n= 70; E16.5 n= 137 and E17.5 n= 142.

Time series analysis in live brain slices at E12.5, E14.5 and E17.5 revealed the heterogeneous and dynamic nature of the embryonic microglial cells. At E12.5, few microglial cells were present in the cortex and most of them had a predominant amoeboid morphology, however some cells displayed motile processes. The mean microglial migration speed was 26 ± 4 µm/h (11 cells) **(Fig. 2.7B and E)**. At E14.5, the migration speed was increased to 31 ± 2 µm/h (39 cells) **(Fig. 2.7C and E)**. Cells located close to the pial surface were seen to exit this structure and enter the cortical parenchyma. Conversely, microglial cells located in the parenchyma were seen to migrate into the pial surface, suggesting a complex behaviour that cannot reflect the colonization process leading to the invasion of the cortex only. The main migration direction of the cells was from the outside (being the region at the pial surface and the region next to the ventricle) to the middle of the wall (**Fig. 2.7C** white arrow). At E17.5 the migration speed (22 ± 1 µm/h; 37 cells) had significantly decreased ($p < 0.001$; Kruskal-Wallis test) compared to E14.5 **(Fig. 2.7D and E)**. Again the main migration direction of the cells was from the outside (being the region next to the ventricle) to the middle of the wall (**Fig. 2.7D** white arrow). Plotting for each age the cumulative frequency of the average distance the microglial cells travel per step **(Fig. 2.7F)** shows that this is significantly smaller at E17.5 compared to E14.5 ($p < 0.001$; Kruskal-Wallis test).

In these relatively long imaging experiments (5 to 7 hours, with 10 minutes interval) we observed that microglial movement did not occur continuously, but was characterized by phases of active migration interspersed with stationary phases, a pattern that can be described as saltatory locomotion and, at E14.5 and E17.5, the cells displayed highly motile processes. Imaging for one hour with a 2 minute interval at E14.5 **(Fig. 2.8)** confirmed that the embryonic microglia are very dynamic cells, constantly sending out (**Fig. 2.8** closed arrowheads) and retracting (**Fig. 2.8** open arrowheads) processes, which suggests they can already survey their local environment, as observed in the adult [34].

(next page) **Fig. 2.7. Microglial migration in the embryonic cortical wall. (A)** Representation of the different axes in the tissue slice for time-lapse imaging experiments. **(B)** Representation of microglial migration at E12.5 (length recording = 5 hours). The pial surface is located closest to the coordinate 0 on the y-axis. Many eGFP cells are present at this pial surface (yellow arrowheads). Asterisks indicate the start position of the microglial cells. **(C)** Representation of microglial migration at E14.5 (length recording = 7 hours). The orientation and marks are as described in panel B. There is some heterogeneity between microglia concerning their movement; some microglial cells migrate long distances whilst others remain approximately at their start position. White arrows indicate the main migration direction for cells located at the pial surface and cells located at the ventricular side. Dashed-dotted lines and dotted lines indicate respectively the beginning and ending positions in the y-direction. **(D)** Representation of microglial migration at E17.5 (length recording = 5 hours). The pial surface is located at the same side of the coordinate 0 on the y-axis however not visible due to the thickness of the wall at this age. Asterisks indicate the start position of the microglial cells. White arrow indicates the main migration direction for cells located at the ventricular side, dashed-dotted line and dotted line indicate respectively the begin and end position in the y-direction. **(E)** Migration speed of the microglial cells significantly changed during development with a peak at E14.5. **(F)** Plot showing the cumulative frequency of average distance the microglial cells migrate in between two steps during the whole recording session at E12.5 (red), E14.5 (green) and E17.5 (blue). The distance travelled by the cells significantly changed during development with a peak at E14.5. (E-F) Number of cells in each age group: E12.5 n= 6; E14.5 n= 39 and E17.5 n= 37. The imaging for the time-lapse experiments always started from a minimum depth of 50 µm under the cutting surface of the slice. (*** $p < 0.001$).

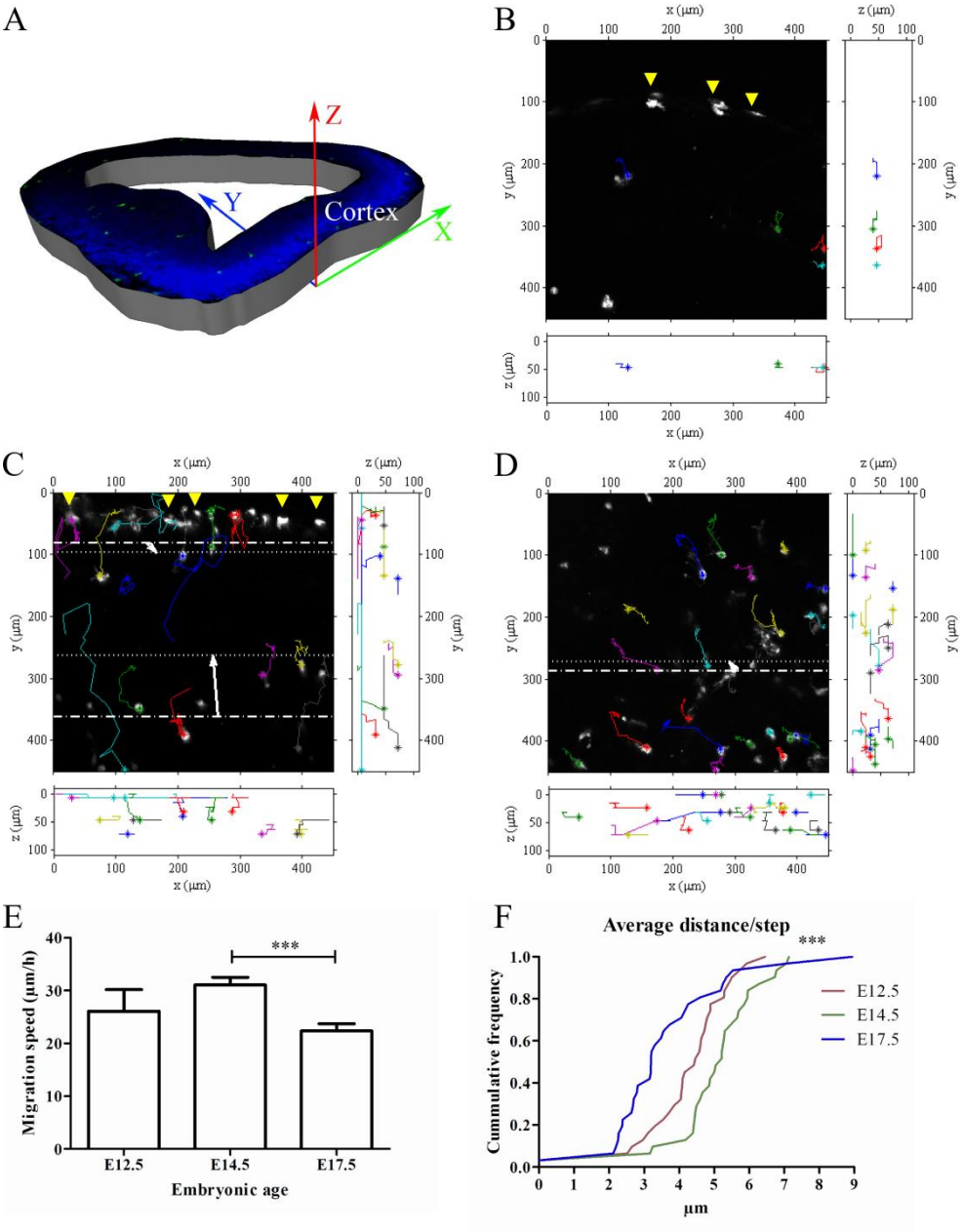
A
Z
Y
X
Cortex
B
C
D
x (µm)
y (µm)
z (µm)
E
Migration speed (µm/h)
***
E12.5
E14.5
E17.5
Embryonic age
F
Average distance/step
***
Cummulative frequency
E12.5
E14.5
E17.5
µm

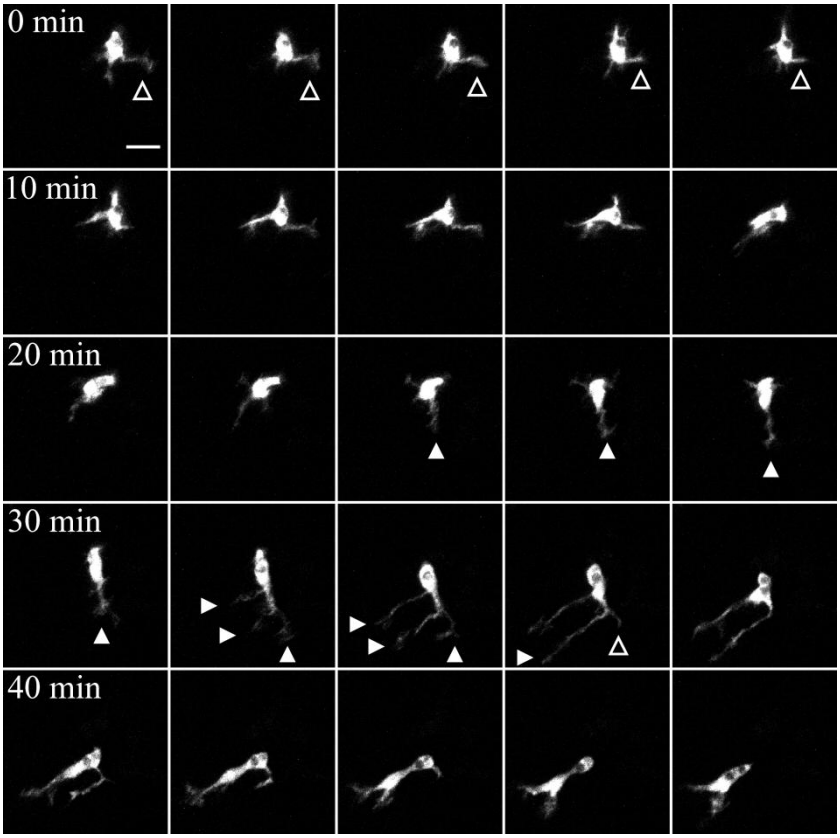

Fig. 2.8. Time-lapse confocal imaging demonstration of microglial cell behaviour at E14.5. A microglial cell showing highly dynamic behaviour. It seems to be scanning the environment by constantly sending out (closed arrowheads) and retracting (open arrowheads) protrusions. At 30 minutes the cell starts sending out more protrusions in the same direction after which it drags the cell soma in the same path resulting in a displacement of the cell. Images are cropped z-projections (5 optical slices with a z-step of 8µm and time interval of 2 minutes). Scale bar = 20µm.

2.5 Discussion

In this work, we show that cortical invasion by embryonic microglia is a complex process. We provide evidence that microglial cells and/or precursors accumulate at the pial surface of the cortex before they invade the parenchyma. Within the parenchyma they display a "resting" immunohistochemical phenotype but they are far from being static cells. An accumulation of microglial cells is also present in the choroid plexus primordium, which is related to the presence of cell death in this structure. Consequently, microglial cells in the proximity of the dying cells present a phagocytic phenotype.

2.5.1 Initial invasion of the embryonic cortex occurs in different phases

The colonization of the embryonic cortex by microglia occurs in three phases. The first one is characterized by a slow increase of microglial cells between E10.5 and E14.5. From E14.5 to E15.5 there is a rapid phase with a massive increase in microglia being followed by a second slow phase from E15.5 until E17.5. The increase in microglia cells during early development of the cortex could result from both microglia precursor cell invasion and microglial proliferation during invasion as suspected in the brain of the human fetus [57, 431]. Early in development (E11.5 – E13.5), more

than 20% of the microglial cells in the cortex are actively proliferating. After E14.5 there was a drastic increase in microglial cell number, which could not be explained by cell proliferation alone, since the percentage of proliferating microglia steeply decreased from E14.5 on. These observations suggest that proliferation of resident microglia plays an important role in the first invasion phase but lesser in the second one, which is probably the result of microglia entering the parenchyma from peripheral sources. These results are consistent with findings made by others in mouse embryos. In the embryonic mouse retina, the colonization occurs in two invasion waves, although at earlier developmental stages than in the cortex, with the first one occurring between E11.5 and E12.5, and the second one from E12.5 on [432]. In the embryonic mouse spinal cord the massive rise in cell number and cell density was observed earlier (around E12.5) than in the cortex [37].

At E12.5, most microglial cells in the cortex were located close to the pial surface and to the lateral ventricles.In addition, at all developmental stages single and groups of microglial cells were present in the lateral ventricle, as free floating or attached to the ventricular wall, and many eGFP cells were lining the pial surface of the brain. This suggests that microglia have entered the cortical parenchyma by crossing the pial membrane and ventricular wall, as suggested earlier by others [91]. Afterwards they spread throughout the entire cortical wall. From E15.5 on, when the third invasion phase takes place, the microglial cells are mainly located in the ventricular and intermediate zones of the cortical wall, avoiding the cortical plate region. This suggests that microglia could play a role in the proliferation and development of the progenitor cells located in the ventricular zone of the cortex. Indeed, studies on primary cultures indicate that microglial cells can influence progenitor proliferation, at least in vitro, as well as neurogenesis and astrogenesis [400, 433].

Since only a small number of microglial cells were present in the cortical plate region from E15.5 on we suggest that at these later ages the microglial cells use a different route to enter the cortical parenchyma than just the "simple" crossing of the pial surface. Based on our observations (data not shown) we hypothesize that, when the complexity of the cortical wall increases, the microglia travel along the pial surface towards the interhemispheric fissure and enter the cortex via the hippocampal primordium, whereupon they travel tangentially and radially to reach their final position in the cortical parenchyma.

2.5.2 Microglial cells accumulate in a region where developmental cell death occurs

At early developmental stages, an accumulation of activated microglial cells was observed in the choroid plexus primordium. In mice, the choroid plexus structure first appears at E11 and subsequently undergoes major morphological changes, which in turn results in an already well differentiated and quite extensive structure by the age of E14. [426, 428, 429]. The presence of this microglial aggregation and activation coincides with the occurrence of developmental cell death in this structure, as was visualized by cleaved caspase-3. The phagocytic morphology of the microglia in the choroid plexus primordium and their immunoreactivity for Mac-2 indicate that these cells have acquired a phagocytic phenotype in order to clear the apoptotic cells. An observation that has also been made in the brain of zebrafish embryos [434] and mouse embryonic

spinal cord [37]. It has been shown that microglial cells promote neuronal cell death in the developing mouse cerebellum [141] and hippocampus [142]. Accordingly, it is reasonable to hypothesize that the microglia observed in the choroid plexus primordium can also influence the developmental apoptosis in this structure.

2.5.3 Embryonic microglial cells are highly dynamic cells that scan their local environment during their migration process

Time-lapse imaging demonstrates that embryonic microglia have a highly dynamic nature with a high motility during their invasion process, a property that has also been described in the embryonic zebrafish [93, 435]. This is in contrast with microglia in the healthy, adult brain in which they are generally randomly localized and display no migration pattern. Surprisingly, besides the wandering of these cells throughout the parenchyma, live imaging showed that the embryonic microglial cells were constantly sending out and retracting processes during their migration process. This behaviour has already been described for microglia in the adult mammal CNS [34] but not in the embryonic brain. This scanning property of embryonic microglia processes was observed at E14.5 and E17.5 (and to a lesser extent also at E12.5) and probably reflects their capability to continuously scan their local environment, as described in the adult [34, 436]. During development, we saw an increase in the proportion of microglia with extensions; in addition to a simple change in their morphology and activation state this could also reflect a change in their dynamic nature. This suggests that classification of microglia according to their morphology highly reflects their momental shape, and thus not necessarily reflects their maturation. Accordingly, quantitative analysis of microglial morphology showed that at the age of E14.5, approximately 60% of the microglial cells had a branched morphology.

2.5.4 Conclusion

In conclusion, our results demonstrate that microglial cells invade the cortical parenchyma in three waves. During this colonization process the microglia display a dynamic behaviour. Our data indicate that although the embryonic microglial cells have the same origin, their invasion pattern and behaviour differ depending on the CNS structure they invade. Probably, the local environment plays an important role in determining their function during embryonic development.

CHAPTER 3:

Age-specific function of α5β1 integrin in microglial migration during early colonization of the developing mouse cortex

Based on: Smolders SMT, Swinnen N, Kessels S, Arnauts K, Smolders S, Le Bras B, Rigo JM, Legendre P*, Brône B*. Age-specific function of α5β1 integrin in microglial migration during early colonization of the developing mouse cortex. Glia, 2017; Jul;65(7):1072-1088 * equally contributing.

Added unpublished data (Fig 3.8 & 3.9): Transwell assays and zone specific time-lapse in slices

3.1 Abstract

Microglia, the immune cells of the central nervous system, take part in brain development and homeostasis. They derive from primitive myeloid progenitors that originate in the yolk sac and colonize the brain mainly through intensive migration. During development, microglial migration speed declines which suggests that their interaction with the microenvironment changes. However, the matrix-cell interactions allowing dispersion within the parenchyma are unknown. Therefore, we aimed to better characterize the migration behaviour and to assess the role of matrix-integrin interactions during microglial migration in the embryonic brain *ex vivo*. We focused on microglia-fibronectin interactions mediated through the fibronectin receptor α5β1 integrin because *in vitro* work indirectly suggested a role for this ligand-receptor pair. Using 2-photon time-lapse microscopy on acute *ex vivo* embryonic brain slices, we found that migration occurs in a saltatory pattern and is developmentally regulated. Most importantly, there is an age-specific function of the α5β1 integrin during microglial cortex colonization. At embryonic day (E)13.5, α5β1 facilitates migration while as from E15.5, it inhibits migration. These results indicate a developmentally regulated function of α5β1 integrin in microglial migration during colonization of the embryonic brain.

3.2 Introduction

Microglia, the immune cells of the central nervous system (CNS), are renowned as the first line defense during brain disease. The last decade researchers have been exploring the plentiful non-immunological tasks of these cells and found them to be involved in normal brain development and homeostasis, through influencing neurogenesis, axonal growth, synapse refinement, blood vessel branching and clearance of dying neurons [8, 437]. Microglial cells originate from primitive myeloid progenitor cells that arise from the yolk sac at embryonic day (E) 7.5 in mice. Primitive macrophages migrate to the CNS using the blood circulation and adopt a microglia phenotype when they invade the brain and spinal cord parenchyma around E10.5 and E11.5, respectively [20, 37, 72]. Several signaling pathways were recently proposed to be involved in microglia recruitment to the embryonic brain *in vivo*, including components such as colony stimulating factor-1 receptor (CSF1R), matrix metalloproteinases (MMPs), vascular endothelial growth factor receptor (VEGFR), Fractalkine receptor (CX3CR1) and stromal cell-derived factor 1 (SDF-1)/CXCR4 [59, 62]. Cortical colonization depends mainly on microglial invasion and migration since only a minority of these cells proliferates within the parenchyma during this developmental period [72]. Despite the fact that parenchymal migration of microglia is essential to brain colonization, the mechanisms allowing microglial dispersion have never been investigated *in vivo* [59, 71].

Cell migration relies on interactions with the extracellular matrix (ECM). Cell-ECM adherence is regulated through integrins, which are transmembrane heterodimeric cell adhesion receptors composed of a non-covalently linked α and β subunit. Upon activation, the β subunit physically links the ECM with the cytoskeleton and enables the cell to transduce forces necessary for soma displacement [272]. Twenty four different integrin heterodimers exist in vertebrates with varying ligand binding properties and cell and tissue distributions. They translate ligand binding signals to a broad array of cell responses, such as cytokine production, proliferation, differentiation and

migration [308]. Our research group previously showed that microglial migration speed changes during cortex colonization in the mouse embryo [72] which suggests the interaction of microglia with their local environment changes during the course of early development. Several *in vitro* findings point to a possible functional role of microglial interactions with fibronectin (an ECM protein) in migration during embryonic development. Fibronectin, a heterodimeric glycoprotein abundant in most tissues, is an important component of basement membranes. It is expressed in the developing mouse CNS [284, 290, 296] and is essential for normal embryonic development [438] where it regulates cell differentiation and migration in general [313, 438]. Microglia *in vitro* express the corresponding major fibronectin receptor, α5β1 integrin [356, 359] and it has been shown *in vitro* that these cells can migrate along fibronectin matrix [356, 370]. Moreover, they can interact with blood vessels that are known to express fibronectin during development [92, 99, 296, 313, 354, 439, 440].

Here, we explore the role of microglia-fibronectin interactions, mediated through α5β1 integrin, when the developing embryonic neocortex is colonized by microglia. We use e*x vivo* acute brain slice preparations in order to maintain the physiologic 3D brain environment, which is essential for studying normal migration behaviour [283, 441, 442]. We first extensively characterize microglial migration behaviour at E13.5, E15.5 and E17.5 using 2-photon time-lapse microscopy. We then analyse the presence of fibronectin in the developing cortex using immunofluorescence and western blotting and determine the expression level of α5β1 integrin receptor using flow cytometry on acutely isolated embryonic microglia. Finally, we assess the functional importance of fibronectin-α5β1 interactions during microglia contact with blood vessels and during parenchymal migration.

3.3 Materials and Methods

3.3.1 Animals

Wild type *mus musculus* C57BL/6 JOlaHsD females (Harlan, The Netherlands) were mated overnight with CX3CR1$^{eGFP/eGFP}$ knock-in males, obtained from the European Mouse Mutant Archive (EMMA) with the approval of Jung *et al.* [403]. The next morning, females were checked for the presence of a copulation plug and designated E0.5. Pregnant mothers were sacrificed at E13.5, E15.5, E17.5 by cervical dislocation. Resulting CX3CR1$^{+/eGFP}$ embryos harbor green fluorescent microglia, monocytes and subsets of natural killer cells and dendritic cells, without the disadvantages of a full CX3CR1 gene deletion [403]. All experiments were conducted in accordance with the European Community guiding principles on the care and use of animals and with the approval of the Ethical Committee on Animal Research of Hasselt University. Mice were maintained in the animal facility of Hasselt University in accordance with the guidelines of the Belgian Law and the European Council Directive.

3.3.2 Markers

The following primary antibodies were used: anti-fibronectin (1:100 for immunohistofluorescence, 1:1000 for western blotting, #Ab2413, Abcam), anti-β-actin antibody (1:10.000, #Sc47778, Santa Cruz), anti-α5-Phycoerythrin (clone 5H10-27 (MFR5), 1.5µg/ml, #557447, BD Biosciences). Isolectin GS-IB$_4$ from *Griffonia simplicifolia* conjugated to Alexa568 (5µg/ml for time-lapse imaging,

10µg/ml for immunohistofluorescence, #I21412, Life Technologies) was used to mark blood vessels. For blocking experiments, anti-α5β1 (clone BMC5, 10µl/ml, #NBP2-29788, Novus) or isotype control (clone RTK4174, 10µl/ml, #400710, Biolegend) were used. The following secondary antibodies were used for immunohistofluorescence: anti-rabbit-Alexa555 (1:500, #A31572, Life Technologies), anti-rabbit-Alexa647 (1:500, #A21245, Life Technologies); and for western blotting: anti-rabbit and anti-mouse-HRP (1:2000, #P0217 and 1:5000, #P0447, DAKO).

To label fibronectin, we used a polyclonal anti-fibronectin antibody [443]. Fibronectins are disulphide linked heterodimeric molecules of 235–270 kDa. Fibronectin molecular isoforms arise via alternative splicing of a single gene. Specificity was determined by the manufacturer by western blotting on different mouse tissue lysates and a single band was obtained around 250 kDa as predicted for the molecular weight of a single fibronectin subunit [313]. In time-lapse experiments related to microglia-blood vessel contact assessments, isolectin GS-IB_4-Alexa568 was added to the migration medium to visualize blood vessels [444]. It is widely used to label blood vessels and microglial cells in slice cultures and does not activate microglial cells [445]. To label α5β1 integrin on microglial cells dissociated from cortex homogenates for flow cytometry, we used a monoclonal anti-α5-Phycoerythrin conjugated antibody [446]. Because the α5 integrin subunit (alternatively named CD49e and VLA-5) exclusively associates with the β1 subunit, we consider its presence to be in heterodimeric form with β1 [337].

3.3.3 Time-lapse imaging

E13.5, E15.5 and E17.5 embryonic brains were isolated and sliced as described before [72]. Slices were transferred to MilliCell organotypic inserts (Merck Millipore) in a 24-well plate designed for confocal microscopy (IBIDI) and maintained in semidry conditions as described before [72]. Slicing quality was verified using the dissection microscope and slices that showed aberrant morphology (ruptures, insufficient flatness) were excluded from time-lapse measurements. In blocking experiments, migration medium was supplemented with either a function blocking antibody specifically targeting the α5ß1 integrin dimer [447] or with isotype control. Specificity of the α5ß1 antibody was verified by the manufacturer by the antibody's ability to immunoprecipitate α5ß1 heterodimers from (125)-I-surface labelled cells, by reciprocal depletion of α5ß1 antigen from cell lysate with antiserum against the cytoplasmatic domain of the α5 subunit, and by immunoprecipitation of α5ß1 integrin from cells known to express this integrin.

Image acquisition started after 1 h of tissue equilibration at 35°C with 5% CO2 and within 3.5 h after decapitation. During measurements humidified air with 5% CO_2 was continuously applied to the slice, kept at 35°C. Per experiment (1 mother animal), six slices were imaged sequentially and this was repeated every 10 min during 6 h using the '*multitime macro*' in the Zeiss LSM510 software (version 4.2 SP1, Zeiss) on an inverted Zeiss Axiovert 200M microscope with a Zeiss LSM 510 Meta confocal laser scanning system and a 20x EC plan-Neofluar objective (NA of 0.5 and 2 mm working distance). A Mai Tai DeepSee Ti:Saphire laser (Spectra-Physics) with a central wavelength tuned at 900 nm was used to visualize eGFP positive microglial cells and isolectin GS-IB_4-A568 labeled blood vessels. Z-stacks spanning 30 µm, with serial optical sections (voxel size

0.88 x 0.88 x 3.3 µm) were recorded starting from a minimal depth of 50 µm beneath the surface of the slice to avoid cells activated by slicing [448, 449].

3.3.4 Migration tracking and analysis

Image processing and migration tracking were performed using open source Fiji software (ImageJ 2.0.0-rc-643/1.50i). Time series were first corrected for 3D drift using the 3D drift correction plugin and microglial migration was manually tracked in 4D using the MTrackJ plugin designed by Erik Meijering [415]. Only cells remaining in the field of view for at least 100 min were included in the analysis. Per experiment, at least one control and/or isotype condition were performed.

Average migration speed (µm/h) was calculated as the total length of the travelled path divided by the duration of the track. The immobile fraction was calculated as the percentage of total microglia that did not migrate further than 45 µm over the total imaging time span. This threshold corresponds to 3 times the average cell diameter and was applied because of small errors due to residual tissue drift after 3D drift correction and manual tracking. Relative idling time was calculated using a custom made Excel macro developed by Gorelik et al [450] and is defined as the percentage of time the cell spent on pausing, further designated as idling, with regard to the total duration of the track. The threshold for idling was set at roughly half a cell diameter (8 µm) per 10 minutes and was verified by inspecting subsequent displacements of non-migratory cells in MTrackJ. Instantaneous speeds of the active migration events ($v_{inst.\ act.}$ = µm/min), i.e. events above the idling threshold of 0.8 µm/min, were calculated as the distance travelled between each time frame, divided by the frame interval (10 min). Migration parameters are grouped under treatment and age. At least 8 slices from embryos of 5 different mothers were quantified. For zone specific analysis of migration speed **(Fig. 3.8)**, the respective zones were cropped from the dataseries based on the transmission image and cells were tracked as described above.

3.3.5 Fixed tissue preparation and immunohistofluorescence

Pregnant mice were sacrificed and embryonic tissue was processed as described before [72]. 10-20 µm coronal sections were cut on a Leica CM3050S cryostat, mounted on Superfrost Plus slides (ThemoFisher) and stored at −20°C until staining. For fibronectin stainings, sections were washed and blocked during 1 h with PBS-20% NXS (Normal Goat or Donkey Serum, Chemicon). All steps occurred at room temperature (RT) unless stated otherwise. Primary antibody was diluted in PBS-1% NXS and incubated overnight at 4°C. For fibronectin-isolectin GS-IB_4 double labelling, the isolectin was incubated at 10µg/ml together with the primary antibody overnight at RT. Sections were washed 3 x 10 min in PBS and incubated 1 h with the secondary antibody diluted in PBS-1% NXS. Sections were washed 3 x 5 min in PBS, submerged in distilled water and mounted using vectashield including 4,6-diamidino-2-phenylindole (DAPI) (Vector, Burlingame). For negative controls, primary antibodies were omitted. Secondary antibodies were centrifuged 5 min at 5000 revolutions per minute prior to use.

3.3.6 Microscopy and mean grey value assessment

Images of fibronectin immunostainings were acquired using a Digital sight DS-2MBWc fluorescence camera adapted on a Nikon Eclipse 80i microscope. Fibronectin presence was quantified in the embryonic cerebral cortex area located dorsally to the lateral ganglionic eminences (LGE) and medial ganglionic eminences as previously described [72]. Background signal was determined using the line plot profile tool in Fiji for each image separately. Signal below 2.5 times the background was removed. In each slice a region of interest (ROI; white dotted lines **Fig. 3.4 A**) was determined including the entire cortex but excluding the meninges. The mean grey value, defined as the average grey value of all pixels inside the ROI, was assessed using the '*Measure*' function in Fiji. These measurements resulted in a mean grey value per pixel (0.16 µm²) automatically corrected for the surface of the ROI and therefore also for the size of the growing cortex. Slices were from 3 different embryos of at least 2 different mothers.

Images of fibronectin-isolectin GS-IB_4-A568 double immunostainings (20 µm tissue sections) were acquired using an inverted Zeiss Axiovert 200M microscope with a Zeiss LSM 510 Meta confocal laser scanning system. An Arg-ion laser at 488 nm, a HeNe laser at 543 and 633 nm and a Mai Tai DeepSee Ti:Saphire laser (Spectra-Physics) tuned at 710 nm were used for excitation of eGFP, Alexa568, Alexa647 and DAPI, respectively. Overview pictures (voxel size 0.44 x 0.44 x 1 µm; 10-15 µm Z-stacks) were acquired using a 40x LD C-Apochomat/1.1 W Korr UV-Vis-IR objective (NA=1.1) with the Zeiss Laser scanning microscope LSM510 software. A 4x confocal zoom was applied to cells of interest (voxel size 0.11 x 0.11 x 2 µm).

3.3.7 Western blotting

Embryonic brains were isolated as described before [72], the meninges were removed, cortices were excised and stored at -80°C. Cortices were lysed in cold RIPA buffer (50mM Tris pH 7.4; 150mM NaCl; 1mM EDTA; 1% NP-40; 0.25% Na-deoxycholate; protease inhibitor (#11873580000, Roche)). Protein concentrations of individual cortices were determined by the BCA protein assay kit (#23225, Thermo Fisher). Samples containing equal amount of proteins (10 µg) were separated on a 12% SDSPAGE gel, transferred to a polyvinylidene fluoride (PVDF) membrane and blocked for 1 h with Tris buffered saline-0.1% Tween 20 (TBS-T) containing 5% milk powder (Marvel) followed by incubation overnight at 4°C in the presence of anti-fibronectin antibody. Mouse anti-β-actin antibody was subsequently incubated for 2 h followed by horseradish peroxidase-conjugated secondary antibodies incubation for 1 h. All antibodies were diluted in blocking buffer and incubations were at RT unless stated otherwise. Enhanced chemiluminescence using the Pierce ECL Plus Western Blotting Substrate (#32132, Thermo Scientific) was used before imaging with the ImageQuant LAS4000 mini (GE Healthcare Life Sciences). Quantification was performed using ImageQuantTL.

3.3.8 Microglia isolation and flow cytometry

Cortical microglia from CX3CR1$^{+/eGFP}$ E13.5, E15.5 and E17.5 brains were isolated as described before [451] with modifications. The tissue was mechanically homogenized in neurobasal medium (Gibco, Thermo Fisher Scientific) supplemented with 2mM L-glutamine, N2 supplement, B27

supplement and 1% penicillin/streptomycin (all from Thermo Fisher Scientific). The homogenate was centrifugated 5 min at 700 g at 4°C, the pellet was resuspended in cold PBS and stained with Fixable Viability stain 620 (FVS620) (BD Biosciences) during 10 min at RT. Cell suspensions were fixed in 4% PFA during 10 min, washed and dissolved in PBS. Cells were incubated for 15 min on RT with an α5- Phycoerythrin conjugated antibody in PBS. After washes, cells were acquired in a FACS Fortessa (BD Biosciences) and analysed with FACS Diva 8.0.1 software (BD Biosciences). Within the living cell population (FVS620 low) the eGFP positive microglia (110-4799 cells per tube) were gated. Within the microglial population, the percentage of α5 positive microglia and its median fluorescence intensity (MFI) were analysed. Because α5 measurements were part of a panel not further described here, Fluorescence-minus-one (FMO) controls (for justification see [452]) were used to gate the positive cell population. At E13.5, embryos were pooled per 2 or 3 (N=8). At E15.5 (N=16) and E17.5 (N=20), embryos were analysed separately. Data were obtained from 3 different mothers (M=3).

3.3.9 Microglia-blood vessel contact analysis

To quantify microglia-blood vessel interactions, we added isolectin GS-IB_4-A568 (see section 'Time-lapse imaging') in the imaging medium 1 h prior to imaging onset to visualize blood vessels. Quantification occurred on the 30 µm Z-stacks acquired from 3 h after onset of imaging, in order for the GS-IB4 labeling to sufficiently penetrate the tissue, until 6 h. Only cells located in the parenchyma and that were visible during at least 9 subsequent time points were included in the analysis. For each cell throughout the Z-stack at each time point, the type of contact was noted as full soma, touching with a process or no contact (free). Microglia that made contact with a blood vessel (soma or process) during 1 or more frames, were considered to be in contact with blood vessels for the analysis in **Fig. 3.5C** and a percentage was calculated per slice. The percentage of time each cell spent on a particular contact **(Fig. 3.5D)** was calculated and data from cells were pooled per treatment and age. At least 7 different embryonic brain slices (N=7) of 3 different mothers (M=3) were quantified per treatment. All blood vessel contact analyses were performed blinded.

3.3.10 BV-2 Transwell assay

The immortalized mouse microglial BV-2 cell line was cultured in Dulbecco's Modified Eagle's medium (DMEM (D5796), Sigma) supplemented with 10% fetal bovine serum (FBS, Gibco) and 1% penicillin-streptomycin (P/S, Invitrogen). For transwell assays, cells were serum starved overnight. Confluent cell cultures were detached by trypsin-EDTA treatment (T3924, Sigma) after rinsing with PBS. BV-2 cell basal migration assays were performed using Corning transwell membrane filters (8 µm pore size, Corning Costar). Inserts were precoated with fibronectin (0.1; 1 and 10 µg/ml; Sigma) for 1 h at 37°C, washed twice in PBS and placed in a 24 well plate containing serumfree medium. Cells ($1x10^5$/100µl) were preincubated during 30 min in the top well in serum free medium. Serumfree medium in the bottom well was then changed for serumfree medium containing the integrin α5β1 function blocking antibody (5µg/ml) or isotype control (5µg/ml) (see "3.3.2 Markers"). After 6 h, cells were fixed in 4% PFA and stained with 0,05% crystal violet for 2 min. Remaining cells were removed from the upper side of the membrane using cotton swabs.

Three non-overlapping regions (1141µm x 856µm, 10x objective) were photographed per insert using a Zeiss Primovert microscope coupled to an Axiocam camera. Median grey values of whole images were determined, averaged per insert and considered as a measure for migration, further referred to as "migration index". Treatment conditions were normalized to control (serumfree bottom well). Data are from 4 independent experiments (N). Each insert represents n=1.

3.3.11 Statistical analysis

The number of analysed cells, steps or inserts is indicated as "n", the number of embryos or slices as "N" and the number of mothers or independent experiments as "M". The #cells/#embryos or slices/#mothers is thus designated in the text as n/N/M unless stated otherwise. The reader is referred to the figure legends for details about the sample size used for statistical analysis. Data are described in the text as "median [interquartile range (IQR)]" according to standards for describing nonparametric data [453]. Statistical analyses and graphs were produced using SAS JMP® Pro 12.1.0. Data are represented as box plots with whiskers to 1.5x the IQR (Tukey representation). Data distributions were assessed for normality (Shapiro-Wilk) and equality of variance (Brown-Forsythe). In case these assumptions were met for all groups, a Student *t*-test in case of 2 groups or ANOVA was performed in case of three groups followed by Tukey HSD post-hoc, correcting for multiple comparisons. In **Fig. 3.4D, 4H and 9C** data were transformed on a log10 scale to meet the equality of variance assumption, though the original scales were used for data presentation for ease of interpretation. When data distribution of least one group was non-gaussian, nonparametric tests such as Mann-Whitney in case of two groups or Kruskal-Wallis with Dunn's multiple comparison post-hoc in case of three groups were performed. *P*-values smaller than 0.05 were considered significant with * $P<0.05$, ** $P<0.01$ and *** $P<0.001$. *P*-values smaller than 0.1 were considered as a trend (~).

3.4 Results

3.4.1 Microglial migration speed decreases with development

Microglial colonization of the embryonic mouse brain cortex occurs in three phases based on microglial density: an initial phase of fast increasing cell density from E10.5 until E14.5, followed by a plateau phase between E14.5 and E15.5, and a third invasion phase after E15.5 [72]. During mammalian development these cells are already highly mobile, with the capacity to phagocytose dying cells and scan the microenvironment as observed in the adult brain [34, 71, 72, 454]. Two-photon time-lapse microscopy was used in this study to investigate developmental changes in microglial migration within the time frame of ongoing neuronal migration [72, 455]. To this end, acute brain slices obtained from E13.5, E15.5 and E17.5 $CX3CR1^{+/eGFP}$ embryos were used, representing the 3 aforementioned phases in microglial development. Migration was analysed starting from E13.5, because on E12.5 very few cells reside yet in the cortical parenchyma and mobility is low [72]. We focused our analysis on the cerebral cortex area located dorsally to the lateral ganglionic eminences (LGE) and medial ganglionic eminences (MGE) (see also **Fig. 3.4A a1, b1 and c1)** [72]. Representative Z-projections of time-lapse experiments with overlaid migration tracks are shown for each age in **Fig. 1A**.

The cell average migration speed within one brain slice was highly variable **(Fig. 3.1B)**. The median average speed at E13.5 (33.4 µm/h [IQR: 22.5-44.4]) did not differ significantly from the speed at E15.5 (33.63 µm/h [IQR: 21.2-47.4]) **(Fig. 3.1B and C)**. At E17.5 average migration speed significantly decreased (24.2 µm/h [IQR: 15.7-34.3]) compared to E13.5 and E15.5 **(Fig. 3.1B and C)**. The decrease in speed suggests that with development, microglia start to acquire their final locations. To evaluate this presumption, we analysed the percentage of immobile cells per slice from E13.5 to E17.5 and found that the immobile fraction rose significantly from 0.0% [IQR: 0.0-2.1] at E13.5 to 9.1% [IQR: 3.1-15.1] at E17.5 **(Fig. 3.1D)**. To rule out that the decrease in migration speed was solely due to an increase in immobile fraction, we reassessed the average migration speed of the mobile fraction. We also found a significant decrease in speed with development (E13.5 vs. E17.5 or E15.5: $P<0.001$, Kruskal-Wallis with Dunn's post test) (data not shown).

The parallel decrease in migration speed and increase in immobile fraction suggest that microglial migration speed is developmentally regulated during early colonization of the embryonic cortex.

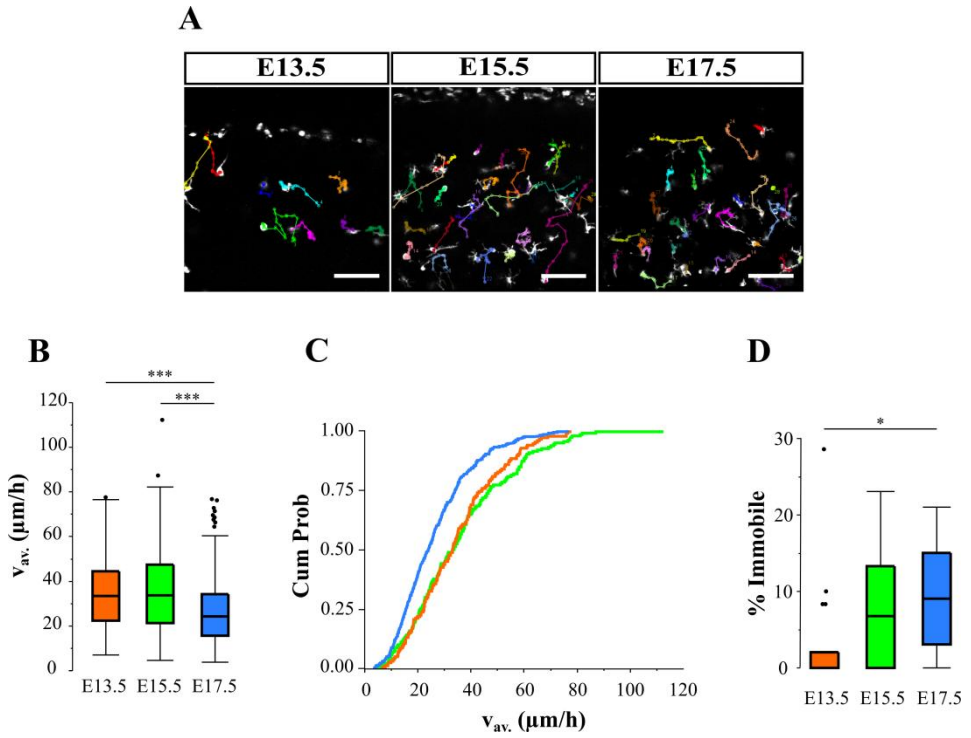

Fig. 3.1. Microglial migration is developmentally regulated. Microglia movement was recorded in acute brain slices during 6 h using 2-photon time-lapse imaging and cell somas were manually tracked. **(A)** Representative microglial migration tracks in different colors at E13.5 (left panel), E15.5 (middle panel) and E17.5 (right panel) (eGFP/microglia, green). The meninges is located at the top of the image and the ventricle at the bottom (not visible at E15.5 and E17.5). **(B)** Microglial average migration speed $v_{av.}$ (µm/h) decreased significantly over development (Kruskal-Wallis with Dunn's, E17.5 vs E13.5 and E15.5, $P<0.001$). **(C)** Cumulative probability plots of migration speed with matching colors for the ages in (B). E17.5 migration speed distribution shows a shift to lower average speeds. **(D)** The percentage of immobile microglia significantly rose from E13.5 to E17.5 (Kruskal-Wallis with Dunn's, $P=0.014$). Sample size (A-C) as n=cells /N=slices/M=mothers at E13.5: 160/18/12; E15.5: 170/10/8; E17.5: 341/14/9. n (cells) was used as sample size in statistical tests. Sample size (D) as N=slices/M=mothers at E13.5: 18/12; E15.5: 10/8; E17.5: 14/9. N (slices) was used as sample size in statistical tests. Scale bar=100 µm.

3.4.2 Microglia adopt a saltatory migration pattern over development

In their migration process microglia first scan their environment, send out one or multiple processes, and displace their soma in the direction of one of the protrusions while retracting the others. Subsequently the cell idles, i.e. the migration of the cell body pauses, explores the environment again and the cycle is repeated **(Fig. 3.2A; zoom-ins Fig. 3.3)**. This locomotion pattern can be described as saltatory and was observed at each age tested. To visualize this saltatory behaviour, the speed between two subsequent time points, defined as instantaneous speed, was plotted in function of time for three microglial cells that are representative for cells with high, intermediate and low average speeds **(Fig. 3.2B)**. To better characterize the saltatory behaviour over development and to find the underlying mechanism of changes in average speed, the median relative idling time and the median instantaneous speed of the migration events above the idling threshold were determined [450]. For example, average speed can be decreased because the cells spend more time idling, and/or because when migrating, distances between subsequent time points become shorter. The relative idling time was calculated as the percentage of the time the cell spends on idling with regard to the total track duration [450] and was significantly increased over development (E13.5: 77.0% [IQR: 64.3-88.6], E15.5: 74.3% [IQR: 63.2-86.1], E17.5: 82.8% [IQR: 72.8-91.7]) **(Fig. 3.2C)**. Instantaneous speed (μm/min) was calculated as the travelled distance between subsequent time points, divided by the frame interval and was found to be significantly decreased only between E15.5 (1.4 μm/min [IQR: 1.1-2.0]) and E17.5 (1.3 μm/min [1.0-1.8]) **(Fig. 3.2D and E)**.

Our results thus show that microglia during early colonization of the embryonic cortex migrate with jumps and that the developmental decrease in microglial average migration speed is due to the cells spending more time pausing and additionally migrating in smaller steps.

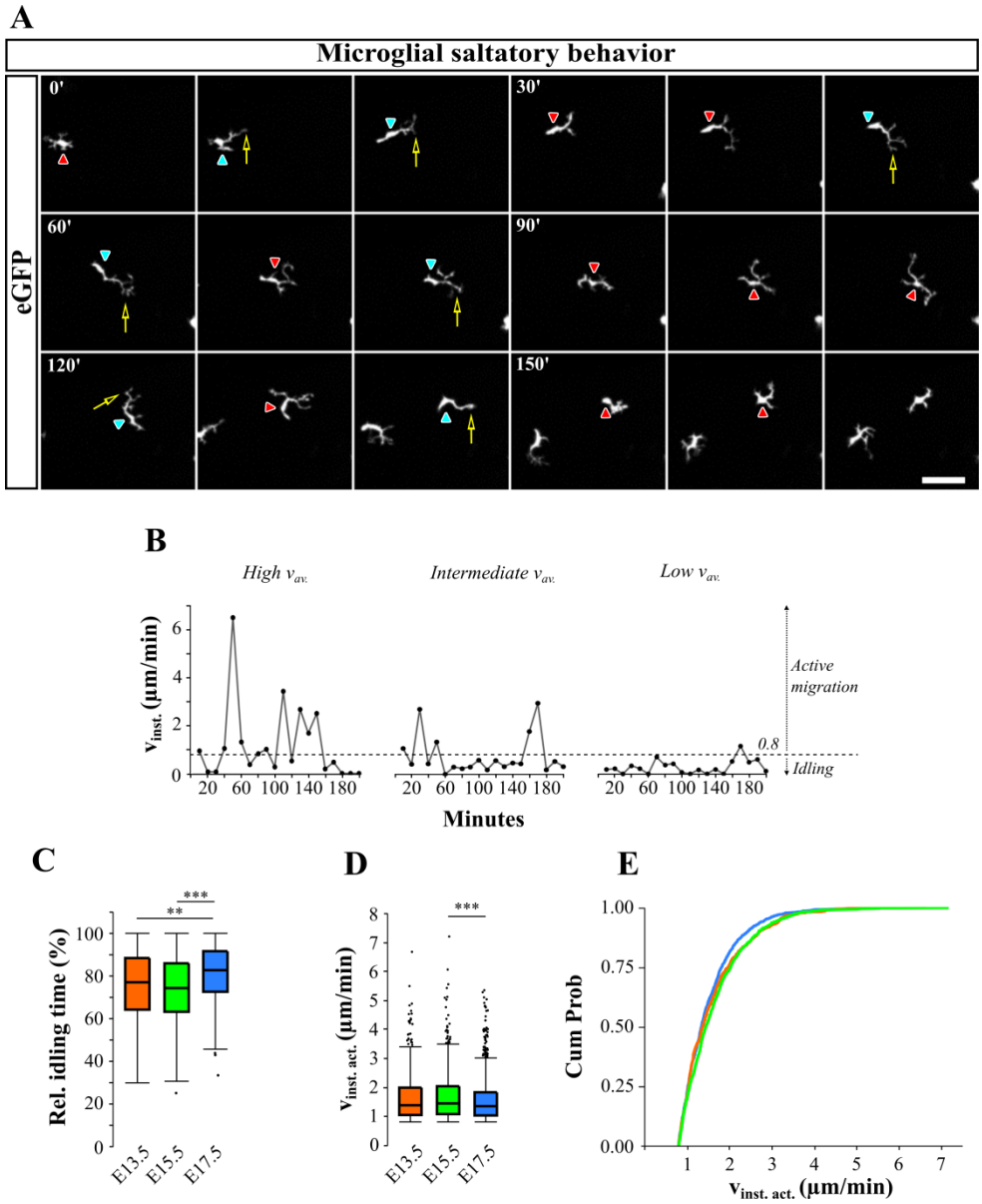

Fig. 3.2. Microglial migration behaviour. Experimental set-up see Fig. 3.1. **(A)** Z-projections (30 µm) of representative time-lapse sequences showing characteristic microglial jumping behaviour during migration at E13.5. The microglial soma (arrowheads) translocates in jumps. They first scan their environment (=idling, frames with red arrowheads) by sending out and retracting multiple processes and then migrate in the direction of one process (indicated by yellow arrows). The cell soma then displaces in the direction of that process (=active migration, frames with blue arrowheads) followed by a stationary phase during which the cells explores its environment again (=idling, frames with red arrowheads). The action of the cell towards the next time frame (interval=10min) determines the color of the arrowhead. Zoom-ins see Fig. 3.3. **(B)** Representative instantaneous velocity in function of time plots of a cell migrating at high (left panel), intermediate (middle panel) and low (right panel) speed. Plots show phases of active migration interspersed with idling, defined as an instantaneous speed lower than the threshold of 0.8 µm/min (dotted line). **(C)** Relative idling time increased significantly over development (Kruskal-Wallis, E17.5 vs E13.5 and E15.5, P=0.004 and P<0.001). **(D)** Instantaneous speed of the active migration events ($v_{inst.\ act.}$) decreased over development (Kruskal-Wallis, E15.5 vs E15.5, P<0.001). **(E)** Cumulative probability plots of the data presented in (D) showing a shift to lower instantaneous speeds at E17.5. Sample size (C) as n=cells/N=slices/M=mothers at E13.5: 150/18/12; E15.5: 170/10/8; E17.5: 349/14/9. n (cells) was used as sample size in statistical tests. Sample size (D) as n=steps from cells in (C) at E13.5: n=832; E15.5: n=972; E17.5: n=1740. n (steps) was used as sample size in statistical tests. Scale bar=30 µm.

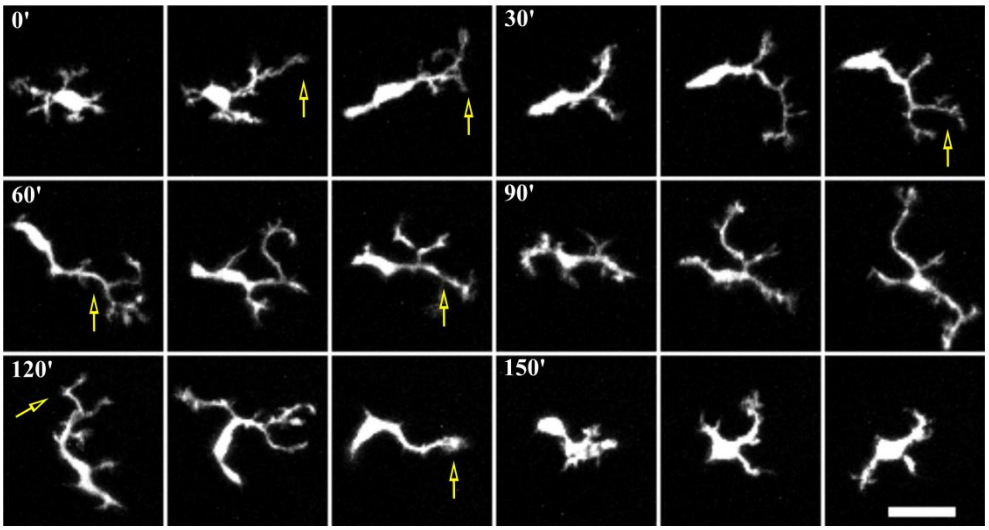

Fig 3.3. Microglial morphology changes during saltatory migration in the cortex at E13.5. Zoom-ins from the microglial cell in Fig. 3.2. Yellow arrows point to the process that is chosen to initiate directive migration. Frame interval=10 min. Scale bar=15 μm.

3.4.3 Cortical fibronectin presence decreases over development

Developmental changes in microglial migration might result from changes in the microenvironment. ECM proteins, such as fibronectin, are developmentally regulated [296]. Nevertheless, the deposition pattern of fibronectin in the embryonic mouse brain remains controversial [296, 439, 440]. To bring clarity on this pattern at the ages relevant for this study, fibronectin's deposition pattern in the embryonic cortex during the microglial colonization phase from E13.5 to E17.5 was analysed using immunostaining **(Fig. 3.4A)** and cortical mean grey value quantification **(Fig. 3.4B)**. Fibronectin was localized throughout the entire cortex at E13.5 as thick aggregates (Fig. 3.4 A, a1-a4). At E15.5 **(Fig. 3.4A, b1-b4)** and E17.5 **(Fig. 3.4A, c1-c4)**, fibronectin staining was less dense when compared to staining at E13.5. Mean grey value assessment (gray value scale 0-255; immunostaining intensity) indicated that fibronectin deposition decreased **(Fig. 3.4B)** during the microglial colonization phase of the embryonic cortex. The median cortical fibronectin grey values were 13.8 [IQR: 11.7-7.2] at E13.5, 8.5 [IQR: 6.2-11.5] at E15.5 and 2.9 [IQR: 1.4-5.4] on E17.5, which all significantly differ from each other **(Fig. 3.4B)**. To confirm the mean grey value measurements, the fibronectin protein content was determined on isolated embryonic cortices using western blotting **(Fig. 3.4C)**. Quantification of fibronectin relative to β-actin showed that the cortical fibronectin contents at E13.5 (51.6 [IQR:33.1-77.3]) and at E15.5 (32 [IQR:22.9-37.9]) were significantly higher than at E17.5 (7.6 [IQR:4.3-17]) **(Fig. 3.4D).**

Though fibronectin was diffusely localized in the parenchyma, developing blood vessels marked by isolectin-GS-IB_4 (Fig. 3.4 E, e4) were highly immunoreactive for fibronectin (**Fig. 3.4E**, yellow arrowheads in e1, e3 for zoom-in), as reported extensively in literature [296, 354, 439, 440]. As previously described [37, 52, 92, 99] microglia were often found in close proximity with blood vessels **(Fig. 3.4E**).

Thus, cortical fibronectin decreases with development and it is also deposited along blood vessels.

3.4.4 Fibronectin receptor α5β1 is expressed by microglia and is developmentally downregulated

Microglia-ECM contacts are likely to be mediated by fibronectin-integrin interactions. *In vitro* adhesion of microglia to a fibronectin coated surface is regulated through fibronectin receptors, such as α5β1 integrin [356, 358, 359, 361]. This integrin heterodimer is described as the major fibronectin receptor and is well characterized on the molecular as well as the signaling level [278, 308]. To determine the expression of α5β1 integrin on embryonic microglia *in vivo*, E13.5, E15.5 and E17.5 cortices were isolated and the fibronectin receptor was immediately analysed after isolation using flow cytometry. Because the α5 integrin subunit exclusively associates with the β1 subunit, a monoclonal antibody raised against α5 was used to identify α5β1 expression on microglial cells [337]. Microglial cells were gated based on eGFP expression, after exclusion of dead cells (Fig. 3.4 F). At E13.5, 99.8% [IQR: 98.8-100.0] of the microglial population expressed the α5 subunit **(Fig. 3.4G)**. This percentage did not change at E15.5 (99.9% [IQR: 99.5-100.0]), but it was significantly different at E17.5 (98.9% [IQR: 97.6-99.4]) compared to E15.5 **(Fig. 3.4G)**. The median fluorescence intensity (MFI), an indicator of the expression level per cell, of the α5 positive microglia significantly decreased from E13.5 (12356 MFI [IQR: 11678-14330]) to E15.5 (9558 MFI [IQR: 8825-10207]) and to E17.5 (4479 MFI [IQR: 4202-4796]) **(Fig. 3.4H)**.

In conclusion nearly all embryonic microglia expressed the α5β1 integrin receptor but the expression level decreased in the course of development.

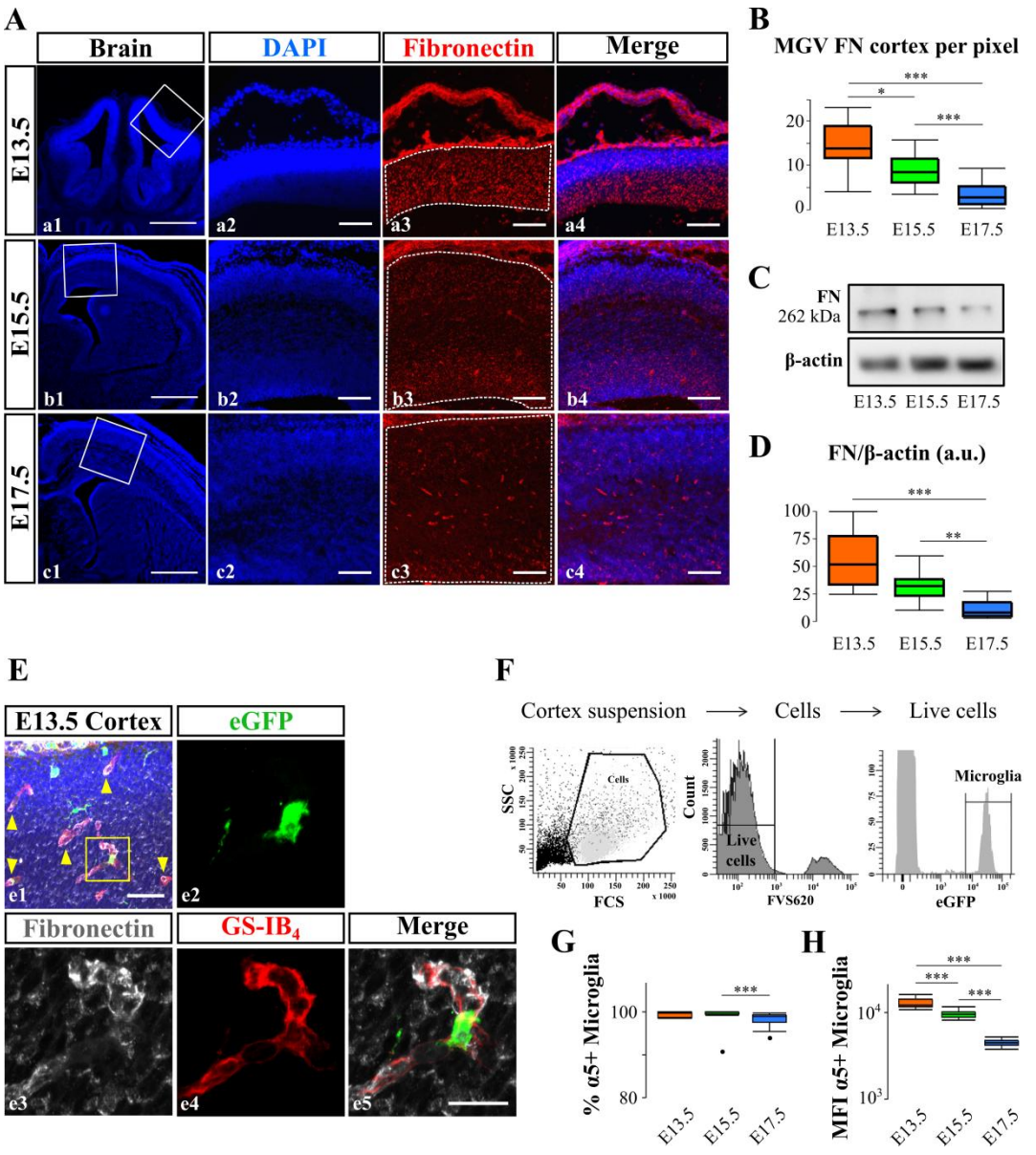

Fig. 3.4. Cortical fibronectin and fibronectin receptor on microglia decrease over development. (A) E13.5 (a1-4), E15.5 (b1-4), E17.5 (c1-4) coronal brain sections (DAPI, blue) with insets zooming in on the cortex (a2, b2, c2), indicating ROIs for analysis (white dotted lines in a3, b3, c3) and fibronectin staining (red, a4, b4, c4). Fibronectin was detectable as dense aggregates at E13.5 and with lower density at E15.5 and E17.5. **(B)** Mean grey value (MGV, 0-255) quantifications of the fibronectin immunostainings in the cortical areas marked in a3, b3 and c3. Fibronectin presence was significantly higher at E13.5 than at E15.5 (P=0.041) and E17.5 (P<0.001), while presence at E15.5 was significantly higher than at E17.5 (P<0.001) (Kruskal-Wallis with Dunn's). **(C)** Representative western blotting for fibronectin deposition in the cortex at E13.5, E15.5 and E17.5 with β-actin as loading control. **(D)** Fibronectin western blotting quantification relative to β-actin. Fibronectin deposition was significantly higher at E13.5 compared to E17.5 (P<0.001), while deposition at E15.5 was significantly higher compared to E17.5 (P=0.001) (ANOVA with Tukey HSD on log10 transformed data). **(E)** Laser scanning microscopy images (Z-projections) showing E13.5 cortex (e1) with microglia (eGFP, green, e2), nuclear staining (DAPI, blue), fibronectin (greys, e3) and blood vessels (GS-IB_4, red, e4). Microglia are frequently observed in the vicinity of blood vessels (inset zoom) and blood vessels show high fibronectin reactivity (e5, yellow arrowheads in e1). **(F)** Flow cytometry gating strategy to assess α5 integrin (fibronectin receptor) expression on microglial cells in panels G and H. **(G)** The percentage of α5 positive microglial cells subtly, however significant, decreased from E15.5 to E17.5 (Kruskal-Wallis with Dunn's, P<0.001). **(H)** The expression level (median fluorescence intensity, MFI) of the α5 positive population significantly decreased from E13.5 to E15 to E17.5 (ANOVA with Tukey HSD on log10 transformed data, all P<0.001). At E13.5 embryos were pooled per 2-3 and at E15.5-E17.5 individual embryos were analysed. Sample size (B) as

n=slices/N=embryos/M=mothers at E13.5: 28/3/3; E15.5: 21/3/3; E17.5: 39/3/2. n (slices) was used as sample size in statistical tests. Sample size (D) as N=embryos/M=mothers at E13.5: 8/3; E15.5: 9/3; E17.5: 9/3. N (embryos) was used as sample size in statistical tests. Sample size (G,H) as N=embryos/M=mothers at E13.5: 8/3; E15.5: 16/3; E17.5: 20/3. N (embryos) was used as sample size in statistical tests. FN, Fibronectin. Scale bar (A)=500 µm in a1, b1, c1; 100 µm in insets (all other panels). Scale bar (E) =50 µm in e1, 20 µm in e5.

3.4.5 α5β1 integrin is dispensable for microglia contact with blood vessels

Microglia are often observed in contact with blood vessels in the developing and adult CNS and in physiologic as well as in pathologic conditions [21, 92, 99]. However, the mechanical basis for this contact is unknown [21, 92, 456]. Based on our previous findings, the α5β1 integrin was suspected to mediate microglia attachment to blood vessels. Since microglia were reported to migrate along blood vessels after injury in rat postnatal slice preparations [99] and they made transient contacts with blood vessels in the developing zebrafish from 6 to 10 days post fertilization (dpf) [457], it was first determined whether α5β1 integrin could be important in the capability of microglia to migrate along blood vessels. Time-lapse imaging showed that microglia can use blood vessels as substrates to migrate in the cortex of the mouse embryo (**Fig. 3.5A** upper panel). However, α5β1 blockage using a blocking antibody specifically targeting the α5β1 integrin dimer did not impair this capability of microglia to migrate along the surface of blood vessels (**Fig. 3.5A** lower panel). To confirm this observation, the percentage of microglia contacting a blood vessel was determined in the time-lapse sequences starting from 3 h after application of the α5β1 blocking. Two modes of contact were observed: full soma alignment (**Fig. 3.5B** left panel) and "touching" contacts between blood vessels and microglial cell processes (**Fig. 3.4B** middle panel). Because the process contact mode was less frequently observed, both contact modes were grouped under "microglia-blood vessel contact". For comparison purposes, a free microglia not contacting a blood vessel is shown in **Fig. 3.5B** (right panel). At E13.5 and E17.5, 50.0% [IQR: 36.7-81.3] and 100% [IQR: 85.1-100.0] of microglial cells contacted blood vessels in the presence of the isotype and the percentage did not change after α5β1 blockage (E13.5: 50.0% [IQR: 40.0-66.7], E17.5: 86.6% [IQR: 61.1-100.0]) **(Fig. 3.5C)**. The percentage of microglia contacting blood vessels significantly increased with development **(Fig. 3.5C)**.

Blocking α5β1 might have subtle effects on microglia behaviour, such as dynamic changes in contacts with blood vessels, which cannot be revealed by the analysis described above. Therefore we next investigated the percentage of time that each cell spent on contacting blood vessels - either by full soma contact, process contact or no contact as illustrated in **Fig. 3.5B**. The percentage of time spent on a particular contact was highly variable **(Fig. 3.5 D)**. At E13.5 in control conditions, the median percentage of time microglia spent on contacting a blood vessel using their soma or using processes was 0.0% [IQR: 0.0-92.1] and 0.0% [IQR: 0.0-5.3], respectively. 84.2% [0.0-100.0] of the time, the cells made no contact. These values did not change after α5β1 blockage (5.3% [0.0-89.9], 0.0% [0.0-5.8] and 84.2% [5.6-100.0], for Soma, Process or no contact, respectively). At E17.5 in control conditions, the median percentage of time microglia spent on contacting a blood vessel using their soma or using processes was 21.1% [IQR: 0.0-80.3] and 21.1% [IQR: 0.0-48.7], respectively. 23.7% [0.0-63.2] of the time, the cells made

no contact. These values did not change after α5β1 blockage (20.5% [0.0-59.2], 25.7% [0.0-54.0] and 10.5% [0.0-79.0], for Soma, Process or no contact, respectively).

All together, these results indicate that α5β1 integrin is neither essential for the capability of microglia to migrate along blood vessels nor for microglia-blood vessel contact.

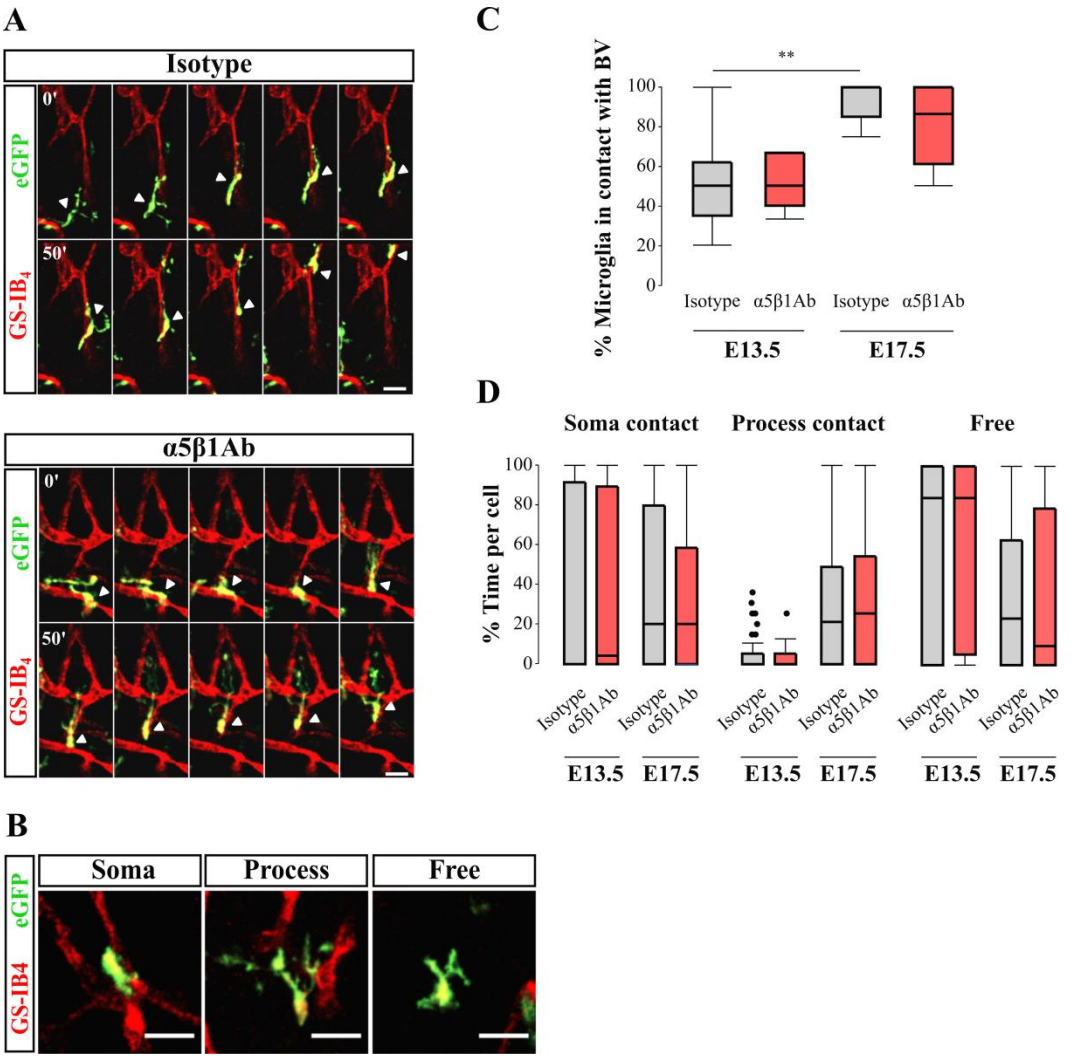

Fig. 3.5. α5β1 integrin is not essential for microglia–blood vessel contact. (A) Time-lapse sequences (30 µm Z-projections) at E17.5 showing microglial cells (eGFP, green) capable to migrate (arrowheads) along the surface of blood vessels (GS-IB$_4$, red) in control as well as after α5β1 integrin blockage in acute brain slices. Frame interval=10 min. **(B)** Modes of microglia-blood vessel contact: Full soma (left panel), touching with a process (middle panel) and free or no contact (right panel). **(C)** The percentage of microglia that made contact with a blood vessel during time-lapse recordings (3-6 hours after blocking onset) was not significantly different after α5β1 integrin blockage compared to isotype at E13.5 (Student *t*-test, *P*=0.813) nor at E17.5 (Mann-Whitney, *P*=0.169). The percentage of microglia that made contact with a blood vessel rose significantly from E13.5 to E17.5 (Mann- Whitney, *P*=0.003). **(D)** The percentage of time spent per cell on a particular contact was not significantly affected by α5β1 blockage (Mann-Whitney, *P*=0.683; 0.802; 1.000 for % Soma; % Process; % Free at E13.5 and *P*=0.173; 0.343; 0.974 for % Soma; % Process; % Free at E17.5, respectively). Sample size (C) as N=slices/M=mothers at E13.5: 9/7 (Iso) and 7/3 (Ab); E17.5: 10/7 (Iso) and 12/3 (Ab). N (slices) was used as sample size in statistical tests. Sample size (D) as n=cells/N=slices/M=mothers at E13.5: 41/9/7 (Iso) and 33/7/3 (Ab); E17.5: 86/10/7 (Iso) and 82/12/3 (Ab). n (cells) was used as sample size in statistical tests. Scale bar (A,B)= 30 µm.

3.4.6 α5β1 integrin blockage has opposite effects on microglia migration during the embryonic cortical development

Based on the parallel decrease in microglial average migration speed, cortical fibronectin deposition and α5β1 integrin expression level on microglia during the developmental period analysed, it was hypothesized that the functional importance of this receptor during microglial migration would diminish over time. To address this issue, the same migration parameters as analysed for control migration **(Figs. 3.1 and 3.2)** were assessed, but in the presence of the α5β1 blocking antibody or isotype control in E13.5, E15.5 and E17.5 acute brain slices **(Fig. 3.6)**. Representative time-lapse Z-projections overlaid with migration tracks are shown in Fig. 6A. There was no effect of isotypes on migration **(Fig. 3.6B, Fig. 3.7, Fig. 3.1B)**.

At E13.5 α5β1 integrin blockage caused a significant reduction (~25%) of the average migration speed (23.5 μm/h [IQR: 15.7-37.8]) when compared to isotype control (31.5 μm/h [IQR: 19.6-44.0]) **(Figs. 6B and D)**. Conversely, α5β1 integrin blockage at E15.5 and E17.5 significantly increased the migration speed to 41.3 μm/h [IQR: 27.8-56.7] (~14%) and 31.6 μm/h [IQR: 19.7-50.9] (~17%) compared to isotype (E15.5: 36.2 μm/h [IQR: 23.7-49.3], E17.5: 27.0 μm/h [IQR: 17.7-37.2]) **(Figs. 6B, 6D)**. The effect of the antibody was indeed significantly different across ages (dotted lines with asterisks, **Fig. 3.6B**). Upon α5β1 blockage, the immobile fraction was 0.0% [IQR: 0.0-9.1] at E13.5, 0.0% [IQR: 0.0-8.3] at E15.5 and 3.1% [IQR: 0.0-8.0] at E17.5, which were not significantly different from isotype (0.0% [IQR: 0.0-13.2] at E13.5; 5.0% [IQR 0.0-7.7] at E15.5 and 5.0% [IQR: 0.0-10.9] at E17.5) **(Fig. 3.6C)**. The effect of the antibody did not differ across ages. After exclusion of the immobile fraction in the average speed analysis, we found the same significant differences between isotype and α5β1 blockage (E13.5: P=0.016, E15.5: P=0.013, E17.5: P<0.001, Kruskal-Wallis with Dunn's post test) (data not shown). This confirms that α5β1 blockage does not affect the immobile microglial population.

These results indicate that α5β1 integrin blockage affects the microglial average migration speed in opposite ways depending on the embryonic age, without affecting the proportion of immobile microglia.

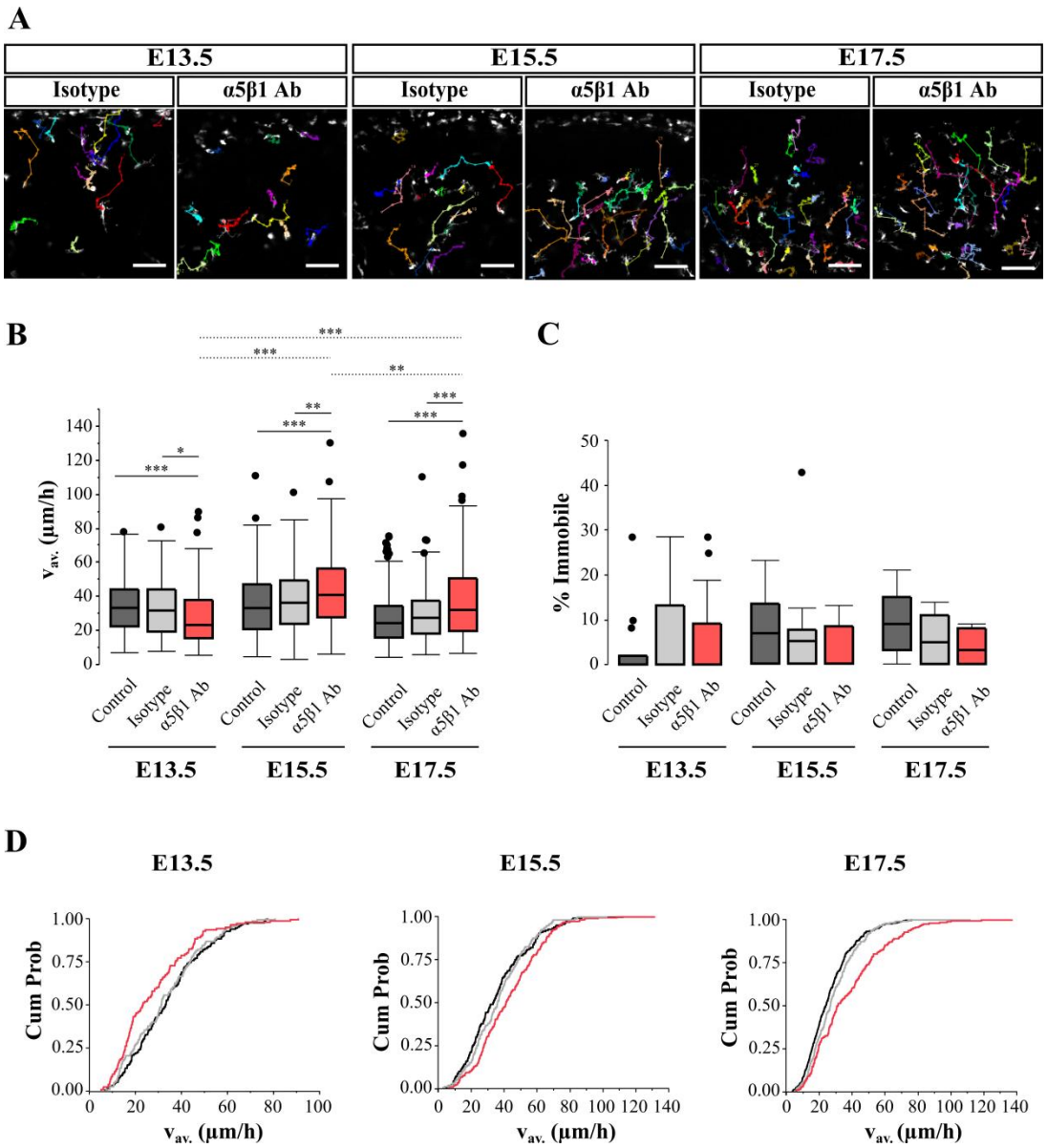

Fig. 3.6. α5β1 integrin blockage at E13.5 decreases while at E15.5 and E17.5 it increases microglial migration speed. Microglia movement was recorded in acute brain slices in the presence of an α5β1 blocking antibody or isotype control during 6 h using 2-photon time-lapse imaging. Cell somas were manually tracked. **(A)** Representative microglial (eGFP, greys) migration tracks in different colors at E13.5, E15.5 and E17.5. The meninges is located at the top of the image and the ventricle at the bottom (not visible at E15.5 and E17.5). **(B)** At E13.5 α5β1 integrin blockage significantly diminished microglial migration speed $v_{av.}$ (µm/h) compared to isotype (P=0.017) while it caused an increase in migration speed at E15.5 (P=0.009) and at E17.5 (P<0.001) (all Kruskal-Wallis with Dunn's). The effect of the blocking antibody was significantly different across ages (dotted lines; E13.5 vs. E15.5: P<0.001; E13.5 vs. E17.5: P<0.001; E15.5 vs. E17.5: P=0.001; all Kruskal-Wallis with Dunn's). **(C)** Immobile fractions after α5β1 integrin blockage at E13.5, E15.5 and E17.5 did neither differ significantly from isotype (all ages P=1.000), nor from control (E13.5 P=1.000; E15.5 P=0.525; E17.5 P=0.146) (all Kruskal-Wallis with Dunn's). The effect of the blocking antibody did not differ across ages (all ages P=1.000; all Kruskal-Wallis with Dunn's). **(D)** Cumulative probability distributions (control in black, isotype in grey and α5β1 Ab in red) of average migration speed data in α5β1 blockage conditions show clear shifts from isotype and control distributions. Sample size as n=cells/N=embryos/M=mothers at E13.5: 135/15/8 (Ab), 128/16/11 (Iso); E15.5: 227/11/6 (Ab), 180/11/7 (Iso); E17.5: 213/11/6 (Ab), 246/10/5 (Iso). n (cells) was used as sample size in statistical tests. For sample size control condition see Fig. 3.1. Isotypes did not affect normal (control) migration. Scale bar=100 µm.

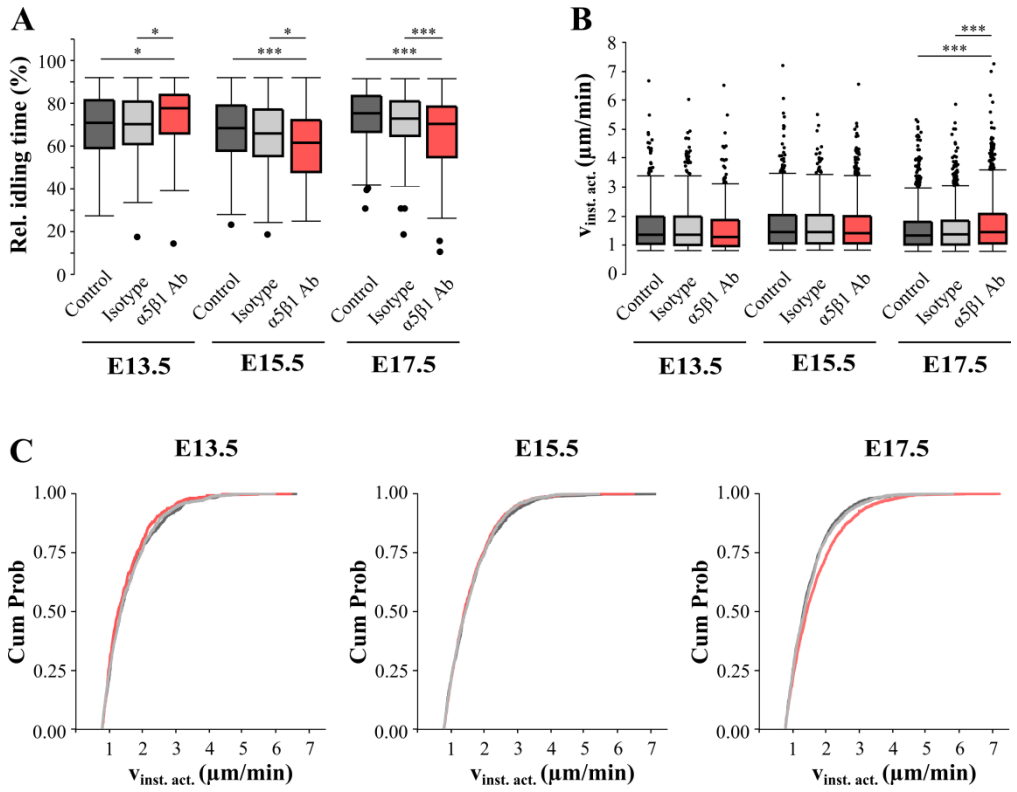

Fig. 3.7. α5β1 integrin blockage affects idling and instantaneous speed. Experimental set-up see Fig. 3.7. **(A)** α5β1 blockage at E13.5 significantly increased relative idling time compared to isotype, while at E15.5 and E17.5 it significantly decreased idling (Kruskal-Wallis with Dunn's, E13.5 P=0.013; E15.5 P=0.015; E17.5 P<0.001). **(B)** Instantaneous speed of the active migration events ($v_{inst.\ act.}$) significantly increased at E17.5 after blockage compared to isotype (Kruskal-Wallis with Dunn's, P<0.001). **(C)** Cumulative probability plots (control in black, isotype in grey and α5β1 Ab in red) of the data presented in (B) at E13.5, E15.5 and E17.5 showing a shift to higher instantaneous speeds at E17.5 after α5β1 blockage. Sample size (A) as n=cells/N=slices/M=mothers at E13.5: 121/15/8 (Ab), 134/16/11 (Iso); E15.5: 228/11/6 (Ab), 178/11/7 (Iso); E17.5: 222/11/6 (Ab), 247/10/5 (Iso). n (cells) was used as sample size in statistical tests. Sample size (B) as n=steps from cells in (C) at E13.5: 605 (Ab), 795 (Iso); E15.5: 1749 (Ab), 1076 (Iso); E17.5: 1399 (Ab), 1338 (Iso). n (steps) was used as sample size in statistical tests. For sample size control condition see Fig. 3.1. Isotypes did not affect normal (control) idling and instantaneous speed.

To determine whether the change in average speed was due to the cells spending more or less time idling and/or to a change in instantaneous speed, we determined the median relative idling time and the median instantaneous speed of the events above the idling threshold **(Fig. 3.7)**. After α5β1 blockage, the median relative idling time was 84.6% [IQR: 72.1-91.7] at E13.5, 67.4% [IQR: 51.9-78.9] at E15.5 and 77.0% [IQR: 60.1-86.2] at E17.5 **(Fig. 3.7A)**. They were all significantly different compared to isotype (76.9% [IQR: 66.6-88.3] at E13.5, 71.8% [IQR: 60.0-83.8] at E15.5 and 80.0% [IQR: 70.6-88.9] at E17.5). After α5β1 blockage the instantaneous velocities of migration events were 1.3 µm/min [IQR: 1.0-1.9] at E13.5, 1.4 µm/min [IQR: 1.1-2.0] at E15.5 and 1.4 µm/min [IQR: 1.1-2.1] at E17.5 **(Fig. 3.7B and C)**. Only at E17.5, after blockage microglia migrated with a significantly higher instantaneous speed compared to isotype control (1.4 µm/min [IQR: 1.0-2.0] at E13.5, 1.5 µm/min [IQR: 1.1-2.0] at E15.5, 1.4 µm/min [IQR: 1.0-1.8] at E17.5) **(Fig. 3.7B and C)**. Additionally, after α5β1 blockage at all ages, microglia still migrated

saltatory (see Supplementary Movies). In conclusion, α5β1 blockage mainly affects the time the cells spend idling without affecting the saltatory migration pattern.

3.4.7 α5β1 integrin zone-specifically regulates microglial migration at E15.5

Given the unexpected though intriguing effects of α5β1 blockage on microglial migration speed depending on the embryonic age, we next aimed to clarify the cause of this change in function over embryonic development. Since the micro-environment has a major influence on the microglial gene expression profile and possibly their function as well [31, 124], and fibronectin deposition decreases markedly in the cortex from E13.5 to E17.5 **(Fig. 3.4A-D)**, we speculated that the fibronectin density might influence the function of the integrin. It was shown indeed that integrins can sense the density of glycoproteins in the ECM followed by changes in cell signaling [458, 459]. More importantly, recent evidence points to a role of fibronectin concentration in the substrate since this factor determined whether α5β1 integrin promoted or inhibited migration of glioblastoma cells in culture [460]. Blandin *et al.* showed that in glioblastoma cells cultured in spheroids on a high fibronectin density (10μg/ml), α5 integrin promoted migration out of the spheroid. Using α5 shRNA or function blocking antibodies, this egression decreased. When fibronectin was absent from the microenvironment, α5 integrin limited migration out of the spheroid or in other words, it promoted cell-cell and/or cell-matrix interactions inside the spheroid. When α5 was depleted in this setting, cells started to egress from the spheroid [460].

Though fibronectin deposition decreases with embryonic age **(Fig. 3.4A-D)**, its dispersion over the cortex is not uniform and this might affect the effect of blocking α5β1 integrin [460]. At E13.5, fibronectin deposition is high and homogenous throughout the cortex **(Fig 3.4A-D)**. In contrast, cortical fibronectin deposition at E15.5 and E17.5 is decreased and not distributed uniformly **(Fig. 3.4A-D)**. From E15.5 three well defined anatomical zones can be distinguished based on a nuclear DAPI staining or a transmission image, namely the ventricular zone (VZ), closest to the ventricle, the intermediate zone (IZ) and the cortical plate (CP) **(Fig. 3.8A)** [72]. These zones markedly differ in their presence of fibronectin **(Fig. 3.8A)** with a notably lower deposition in the IZ. In time-lapse recordings at E13.5 the entire cortex was imaged, while from E15.5 mostly the CP and IZ, in were imaged due to field of view restrains. Since microglia from E15.5 avoid the CP **(Fig. 3.6A)** [72], we can state that we recorded microglial migration at E13.5 in a fibronectin-high environment, while at E15.5 and E17.5 we recorded migration in a fibronectin-low environment. Based on the fibronectin concentration-dependent effects on microglial migration upon α5β1 blockage observed by Blandin *et al.* in glioblastoma spheres [460], we speculated that the outcome of α5β1 blockage might be zone (thus fibronectin density) related. More specifically, we expected the microglial cells in the VZ at E15.5 to migrate slower upon blockage, comparable to E13.5, while the cells in the IZ would increase their migration speed. We assessed this question at E15.5, because at that age the fibronectin deposition is at an intermediate level and the effect of the blocking antibody is most clearly opposite to the one at E13.5 **(Fig. 3.4 and 3.6)**. Microglial migration speed after α5β1 blockage was indeed significantly lower in the VZ than in the IZ, with a median speed of 29.7 μm/h [IQR: 20.6-39.7] and 43.3 μm/h [IQR:31.6-58.0] respectively **(Fig. 3.8B)**. However, migration speed in the VZ after α5β1 blockage did not differ from treatment with isotype control (25.3 μm/h [IQR: 18.8-38.9] **(Fig. 3.8A)**.

Together, these results show that at E15.5 in contrast to microglia residing in the IZ (low fibronectin), microglia of the VZ (high fibronectin) do not rely on α5β1 integrin for regulating migration speed.

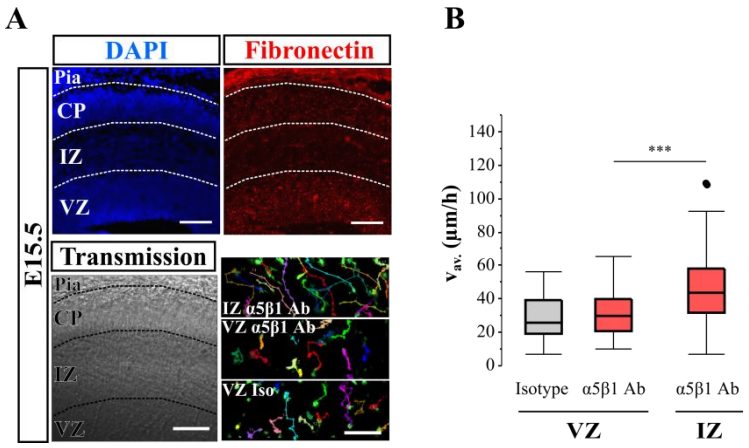

Fig. 3.8. α5β1 integrin blockage does not affect microglial migration speed in the ventricular zone. Experimental set-up see Fig. 3.7. **(A)** Zone-specific fibronectin deposition and effect of α5β1 integrin blockage on microglial migration. Anatomical distinction of different zones (Ventricular zone, VZ; Intermediate zone; IZ; Cortical plate, CP) in the E15.5 dorsal forebrain using DAPI (blue, top left), differential deposition of fibronectin in these zones (red, top right), transmission image of the dorsal forebrain (bottom left) and 6h time-lapse recording of microglial migration in the VZ and IZ under blockage and isotype conditions. **(B)** α5β1 blockage did not change microglial migration speed in the VZ (Kruskal-Wallis with Dunn's, P=0.682). Effects of α5β1 blockage differ significantly between zones (Kruskal-Wallis with Dunn's, P<0.001). Sample size as n=cells/N=slices/M=mothers: 67/4/4 (VZ iso), 95/8/4 (VZ Ab), 117/4/4 (IZ Ab). n (cells) was used as sample size in statistical tests. Scale bar =100 μm.

3.4.8 Fibronectin concentration does not influence the outcome of α5β1 integrin blockage *in vitro*

Given the observation that microglia in different cortical zones that harbor different fibronectin densities, reacted differentially to the α5β1 blocking antibody **(Fig. 3.8)**, we next aimed to find out whether this could be due to the fibronectin concentration. We tackled this question in a simple *in vitro* transwell migration assay, in which basal mobility of the microglia-like BV-2 cell line was measured on different concentrations of fibronectin coating (0, 0.1 and 10 μg/ml) and in the presence of the α5β1 function blocking antibody or isotype control **(Fig. 3.9)**. In the absence of fibronectin (0 μg/ml), median relative to control migration indices were 159.1% [IQR: 128.4-189.3] with α5β1 antibody and 122.0% [IQR: 102.0-139.9] with isotype. On low density fibronectin coating (0.1 μg/ml), the indices were 136.8% [IQR: 124.5-149.9] with antibody and 108.7% [IQR: 96.2-118.6] with isotype. On high density fibronectin coating, the indices were 129.0% [IQR: 118.1-133.8] with antibody and 100.7% [IQR: 93.3-110.8] with isotype. Irrespective of the fibronectin coating, α5β1 blockage caused a significant (or a trend towards, in case of fibronectin absence) increase in the relative migration index compared to control and isotype, while the isotype itself did not induce a change in relative migration index compared to control **(Fig. 3.9A and B)**. The fibronectin density however did not affect the extent to which the α5β1 Ab caused increased migration relative to the isotype treatment **(Fig. 3.9C)**. Relative

medians were 126.4% [IQR: 120.5-142.0], 123.1% [IQR: 116.8-127.8] and 122.9% [IQR: 110.6-141.7] for 0, 0.1 and 10 µg/ml fibronectin, respectively.

To determine whether the fibronectin concentration affected migration, migration indices were determined relative to the 0 µg/ml fibronectin coating **(Fig. 3.9D)**. In control treatment, median migration indices were 118.1% [IQR: 99.9-124.2] for 0.1 µg/ml FN and 130.1% [IQR: 101.8-134.1] for 10 µg/ml FN, of which the high density almost (trend) significantly differed from the condition without fibronectin. Upon isotype treatment, median migration indices were 97.6% [IQR: 92.1-102.0] for 0.1 µg/ml FN and 105.0% [IQR: 102.5-115.3] for 10 µg/ml FN, of which the high density was significantly different from the two others. Upon α5β1 blockage median migration indices were 99.5% [IQR: 91.5-101.5] for 0.1 µg/ml FN and 108.6% [IQR: 96.2-110.9] for 10 µg/ml FN, which were not significantly different, neither from 0 µg/ml FN **(Fig. 3.9D)**.

Together, these results show that α5β1 integrin blockage in microglia-like cells induces increased migration and that the fibronectin concentration in the microenvironment does not influence this process *in vitro*.

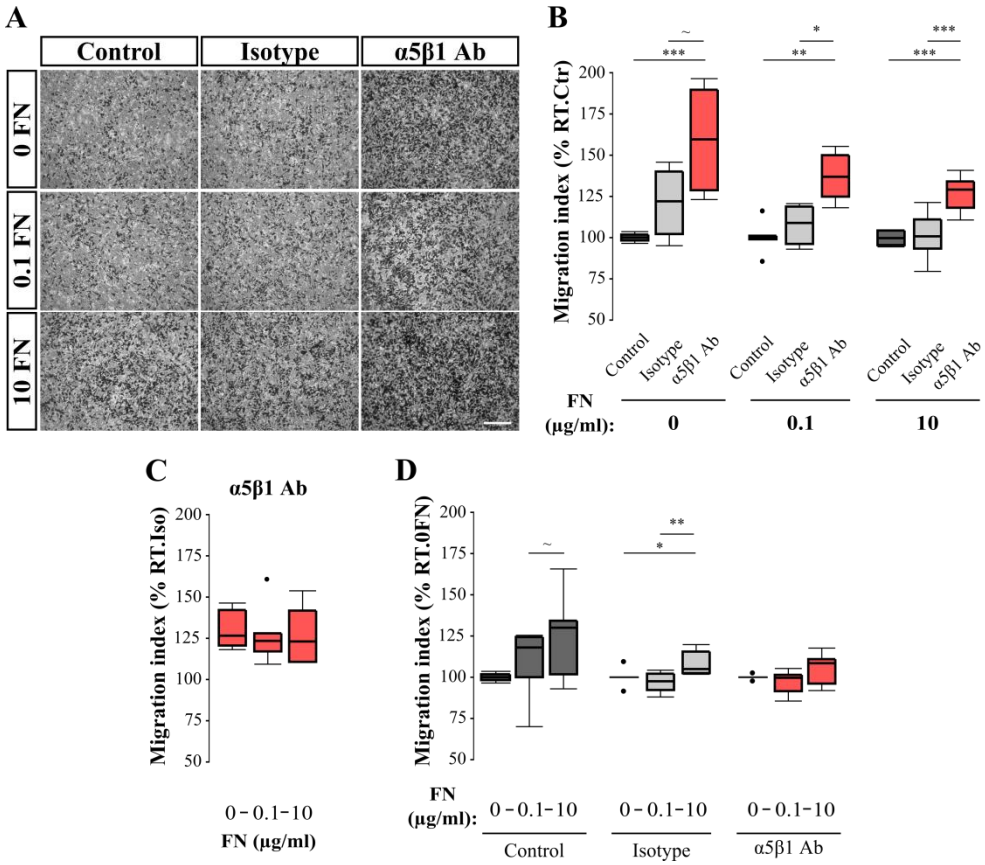

(previous page) **Fig. 3.9. α5β1 integrin blockage increases migration *in vitro*.** BV-2 cell basal migration was assessed in transwell assays in the presence of the α5β1 function blocking antibody (Ab). Membranes were coated with different concentrations of FN (0, 0.1 and 10 µg/ml). The migration index is an indirect measure for the quantity of migrated cells and it is calculated from the median grey values of pictures from the bottom of the insert relative to a control or to 0 µg/ml fibronectin. **(A)** Representative pictures of migrated cells at the bottom of the membrane. **(B)** The relative to control migration index (RT.Ctr) significantly increased in the presence of the α5β1 Ab compared to isotype on 0.1 and 10µg/ml FN coatings (Kruskal-Wallis with Dunn's at 0.1 FN P=0.027; ANOVA with Tukey HSD at 10 FN P=0.0001). A trend towards an increase was observed in the absence of FN (Kruskal-Wallis with Dunn's, 0 FN P=0.065). **(C)** FN concentration did not change the effect size of α5β1 blockage relative to the isotype (RT.Iso) (ANOVA with Tukey HSD on log10 transformed data, all P>0.863). **(D)** A high FN concentration significantly increased the relative to 0 FN (RT.0FN) migration index in comparison to low or absent FN in case of isotype treatment (Kruskal-Wallis with Dunn's, 10 vs. 0 FN P=0.044; 10 vs. 0.1 FN P=0.004), and induced a trend towards increased migration in the control treatment (Kruskal-Wallis with Dunn's, 10 vs. 0 FN P=0.056). FN concentration did not affect migration in the presence of the α5β1 Ab (Kruskal-Wallis wit Dunn's, all P>0.107). Sample size as n=inserts/N=independent experiments: 8/4 in all cases expect 7/4 for 0.1 FN Ab and 10 FN control. n (inserts) was used as sample size in statistical tests. Isotypes did not affect migration. FN, Fibronectin; RT., Relative To. Scale bar (A, white)=200 µm.

3.5 Discussion

In this study, we show that during early colonization of the embryonic cortex microglia migrate in a saltatory fashion and that their average migration speed is developmentally regulated. We demonstrate that the adhesion molecules fibronectin and its receptor the α5β1 integrin play an important role in regulating embryonic microglial migration. The presence of cortical fibronectin and the expression of α5β1 integrin on microglia decreased throughout development, but as a paradox we found that α5β1 integrin has opposite functions in microglial migration depending on the embryonic age. Blockage of the α5β1 integrin decreased migration speed at E13.5 while it led to an increased migration speed at E15.5 and E17.5, without affecting the size of the immobile fraction.

3.5.1 Microglia exhibit a saltatory migration behaviour while speed decreases during embryonic corticogenesis

The behaviour of microglial cells invading the embryonic cortex from E13.5 to E17.5 is characterized by a saltatory migration pattern. This pattern consists of pausing phases during which the microglial cell explores its surroundings interspersed with active phases of migration in the direction of a selected protrusion. This saltatory migration pattern of microglia in the mouse embryonic brain, which is maintained during the developmental period studied here, is similar to the migration behaviour of microglia described *in vivo* in the developing zebrafish larvae [461], suggesting that this particular behaviour of microglia during brain development is evolutionary conserved over species.

We observed a decrease in the microglial average migration speed over embryonic development and this resulted from both an increased idling time and a lower instantaneous speed. Our observations are similar to what has been observed between postnatal ages P2 and P6 in the mouse hippocampus [70] and between 3.5 and 5 dpf in the zebrafish optic tectum [457]. The decrease in average speed at E17.5 coincided with an increase in the immobile fraction of microglial cells and could indicate that some microglial cells acquire their final locations in the cortex between E13.5 and E17.5. However, we cannot exclude that the rise in immobile fraction

over early development reflects a long lasting transitory resting state between active migration phases, since the cortical development proceeds postnatally [462, 463]. The immobile fraction was insensitive to α5β1 blockage from E13.5 to E17.5. This suggests that α5β1 does not essentially contribute to the integrin-ECM interactions tightly anchoring the cell in place. The decrease in microglial migration speed is likely to result from changes in the local environment. We show that the fibronectin deposition and the expression of fibronectin receptor α5β1 integrin on microglia, decrease from E13.5 to E17.5 in the cortex. Indeed, changes in ECM composition alter microglial adhesion to substrates, which could impact their migration [294, 337]. Accordingly microglial migration speed was decreased in the newborn rabbit brain as a consequence of *in utero* inflammation and it was suspected to result from changes in adhesion molecule expression after inflammation [454].

3.5.2 Developmental decrease in fibronectin and microglial fibronectin receptor α5β1 integrin expression in the embryonic cortex

All three parameters, microglial average migration speed, the cortical fibronectin deposition and microglial α5β1 integrin expression levels decreased from E13.5 to E17.5. This concurrent decrease indicates that the interaction between fibronectin and α5β1 integrin might regulate microglia migration speed supporting the hypothesis that the ECM plays an important role in migration during early colonization of the cortex by these immune cells. Throughout development, fibronectin is highly expressed by blood vessels and along radial glial processes [296, 354, 439, 440], which makes these structures ideal scaffolds to guide microglial migration. Accordingly, changes in microglial migration speed observed in the presence of the α5β1 integrin blocking antibody may result from an alteration of interactions between microglia, blood vessels and/or radial glial fibers.

3.5.3 No essential role for α5β1 integrin in mediating microglial contact with blood vessels

Contact between microglia and blood vessels during development has been reported in zebrafish, quails, mice, rats as well as humans [92]. Although α5β1 integrin is implicated in the adhesion of CNS endothelial cells to fibronectin [354], we did not find any evidence for a major role of this receptor in the dynamic interaction between microglia and blood vessels during the developmental period investigated here. Neither the capability of microglia to use blood vessels as guiding substrates for migration, nor the fraction of these cells contacting blood vessels, nor the time spent on soma or process contact was altered in the presence of the blocking antibody. Other ECM proteins, such as laminin or Intercellular Adhesion Molecule (ICAM)-1 or 2, expressed along developing blood vessels might mediate contact [98, 464] as microglia *in vitro* do express the receptors for these ligands [98, 356]. Alternatively, integrins other than α5β1, such as α4β1 and/or αvβ1 might be working in concert with α5β1 to mediate adhesion to fibronectin expressed by blood vessels [356, 358]. Lack of effect of the blocking antibody on microglia interaction with blood vessels does not preclude disturbances of microglial interactions with other cell types, such as radial glia which produce and align fibronectin along their processes [296, 301, 465]. Dense packing of these radial glial fibers may however hamper reliable quantification of interactions with microglia in the cortex.

3.5.4 Age-specific role of α5β1 integrin in microglial migration

Although almost all microglia from E13.5 to E17.5 expressed α5β1 integrin, its expression level decreased over development. This might indicate that embryonic microglia are capable to interpret changes in fibronectin deposition. This idea is supported by *in vitro* work showing that after cultivation on fibronectin primary microglia upregulate α5β1 integrin [356]. Based on the developmental decrease in both adhesion molecules, we expected that blocking α5β1 would largely decrease migration speed at E13.5 while it would affect migration less at E17.5. Surprisingly our experiments indicate that this is not the case. After α5β1 blockage, migration speed indeed decreased at E13.5, but it increased at E17.5.

As observed here at E13.5, a decrease in migration after either α5β1 or general β1 integrin blockage was also reported *in vitro* in microglial chemotaxis and wound healing assays [370, 373, 374]. Integrin blockage has led to various outcomes on migration depending on the cell type, the integrin heterodimer and the environmental dimensions. For example α5β1 depletion inhibited neuronal migration during mouse embryonic corticogenesis *in vivo* [351]. On the contrary, integrin blocking antibodies increased migration in platelets [466], neutrophiles [467], cancer cells (3D matrix) [468] and trophoblast cells [469] *in vitro*, as observed in our experiments at E17.5.

Variations in fibronectin affecting its function in migration?

The age-specific function of the α5β1 integrin could be related to the decreasing amount and cortical zone-related presence of fibronectin from E13.5 to E17.5. In cultured glioblastoma cells, the fibronectin coating concentration determined whether α5β1 integrin promoted or inhibited migration [460]. On the contrary, we found that α5β1 blockage induced an increase in migration of BV-2 cells in transwell assays irrespective of the used fibronectin coating concentration and that the effect size did not differ between fibronectin concentrations. The increase in migration after α5β1 blockage is in line with the results of the *ex vivo* time-lapse studies at E15.5 and E17.5 Additionally, in *ex vivo* slices at E15.5 we show that α5β1 integrin only plays an obvious role in microglia migrating in the IZ, while microglial cells of the VZ remained unaffected by the blocking antibody. Since both the E13.5 whole cortex and the E15.5 VZ are rich in fibronectin, and the α5β1 blocking antibody only affected migration at E13.5, it is tempting to state that the fibronectin concentration does not seem to influence the function of α5β1 integrin. However, we did not determine the *in situ* zone-specific fibronectin concentrations, so we cannot rule out that E13.5 whole cortex and E15.5 VZ harbor different fibronectin densities and thus do affect α5β1 integrin function. For example the E15.5 VZ fibronectin concentration could be intermediate between the one at E13.5 and at E15.5 IZ and could represent therefore a transition phase between high fibronectin causing the integrin to naturally promote migration (E13.5), and low fibronectin (E15.5 IZ) causing the integrin to inhibit migration.

In addition to the possible effect of fibronectin concentration on microglial migration, alternative splicing of fibronectin mRNA might alter its biological function and thereby influence its role in migration. Fibronectin is assembled as a dimer and its two chains are not necessarily identical. Each chain is folded and consists of a linear arrangement of repeating units of amino acids,

classified as type I, II and III repeats. Each of these repeating units contain regions that can interact with a variety of molecules, such as fibrin, collagen, heparin, integrins and fibronectin itself [470]. The type III repeats include important domains involved in promoting cell adhesion such as the arg-gly-asp-ser (RGDS) amino acid sequence and the synergistic sequence pro-his-ser-arg-asn (PHSRN), which are recognized by the α5β1 integrin. Two exons code for type III repeats known as EIIIA and EIIIB - in between which the repeat (III10) containing the RGDS sequence is located - and are spliced to be either totally included or excluded. The III connecting segment (IIICS), also known as the variable (V) region, may be spliced at several locations to completely/partially/not exclude the V region depending on the species and cell type [438, 470, 471]. Splicing of the LDV cell binding sequence (also known as CS1) within the V region appears an evolutionary conserved property of fibronectin during development and has been attributed important roles in migration though binding to the α4β1 integrin. Loss of this LDV sequence after development, could allow for a form of fibronectin more appropriate in cell stability than in dynamic processes such as migration [471]. Alternative splicing of fibronectin can influence its cell binding properties through a variety of mechanisms. First, splicing of the EIIIA, EIIIB and V regions can alters the integrin's affinity for the RGD sequence (presence of a synergistic site (PHSRN sequence) in between the EIIIA and EIIIB regions) or simply alter recognition by α4β1 integrin (for the V region). Second, splice regions can alter the conformation of the RGD sequence, with one conformation favouring binding to α5β1 integrin and the other favouring binding to αvβ3. Third, incorporation of extra repeats with a certain rotation might alter the spatial relationship between the RGD sequence and any adjacent synergistic sites and thereby affect the affinity of integrin binding [471]. Given the fact that expression of isoforms changes during embryogenesis (with during embryogenesis in rodents a higher expression of the splice variants containing the regions EIIIA, EIIIB and V and thus the binding sites for α5β1), the function of fibronectin in mediating cell adhesion/migration might be altered as well [278, 288, 471-475].

In addition, cellular traction forces can alter the tensional state of the fibronectin molecule so as to expose cryptic integrin-binding sites that induce changes in cell behavior. In its turn, tensed fibronectin induces activation of α5β1 integrin through traction forces within the cell [278, 279, 476]. Fibronectin can also autocrosslink into multimers known as superfibronectin with functional consequences as to enhance cell adhesion and to reduce cell migration [477]. However, since we did not assess the presence of different isoforms, conformations or tensional states of fibronectin in the cortex of E13.5-E17.5 mouse embryos, we cannot exclude that fibronectin has different functions in cell adhesion/migration over development.

Why paradoxical functions of α5β1 during CNS development?

On a molecular level, the observed opposite functions of α5β1 integrin during cortical development might be explained by a maturation of the adhesion involving α5β1. Generally, cell migration involves unstable nascent adhesion (physical interaction between the ECM, the integrin and the cytoskeleton) formation which undergoes rapid turnover. When a protrusion rests, the nascent adhesion can "mature" into a highly stable focal adhesion. This means the adhesion grows in size and stability by attraction and posttranslational modifications of intracellular adaptor proteins that constitute the link between the integrin and the cytoskeleton. When the cell migrates further, the

ECM-cytoskeleton link is disrupted [272, 478]. The stability of the adhesion is important for overall cell migration speed and can be regulated at the level of the ECM, the integrin and the adaptor proteins [272, 273, 283, 478]. Interestingly, adhesion strength has a biphasic effect on migration speed: the speed increases between low and intermediate adhesion strength and slows down between intermediate and high adhesion strength [272, 336]. We therefore speculate that at E13.5 α5β1 is involved in unstable adhesions which favor migration while from E15.5 onwards, the integrin is linked to more stable, mature adhesions that cause tighter anchoring of the cell body. When the ability to form these unstable adhesions is impaired upon blockage at E13.5, the cell will not find an anchor point to transduce force in order to migrate. At E17.5 α5β1 linked adhesions would be more stable, causing a decrease in migration speed. When the integrin-matrix link is disrupted by the blocking antibody, microglia could be released and could be free to migrate faster using other integrins. Plausible candidates for mediating migration could be α4β1, α6β1, αvβ1, αvβ3, αvβ8, αLβ2 or αMβ2, since microglia express these integrins at least *in vitro* [356, 359, 361]. Alternatively, the paradoxical effects of α5β1 antibody-mediated blockage on migration speed might reflect not changes in adhesion strength over development but rather variations in the balance of α4β1/α5β1 function. α4β1 (binding to the CS1 site) was shown to work in concert with α5β1 (binding amongst others to the RGDS site) in order to promote migration along fibronectin by binding to the V region of fibronectin in neurcal crest and lymphoma cell migration [479, 480]. Migration experiments including the blockage of α4β1 integrin as well would aid in sorting out whether these integrins work together at different ages and what their functions are.

3.5.5 α5β1 integrin might sense fibronectin concentration

When α5β1 integrin was blocked in *in vitro* transwell assays, migration increased on all fibronectin concentrations but the effect of the fibronectin concentration as observed in control conditions was lost. This suggests that α5β1 integrin mediates the fibronectin concentration-specific effect on migration, while the integrin itself is not involved in the migration process itself. Our results thus point to an intracellular signaling function of α5β1 leading to increased mobility. For example, α5β1 could be involved in sensing the fibronectin density in the environment through translating the amount of integrin clustering to intracellular signaling (also called mechanotransduction) leading to increased cytoskeletal dynamics [276]. In an environment lacking fibronectin, α5β1 could mediate cell-cell interactions via binding to other α5β1 integrins, as reported for mesenchymal cells in the in vivo developing zebrafish larvae [481], or it could mediate direct interactions with the polycarbonate insert membranes, which has not been described in literature yet. In these cases, α5β1 would promote cell cohesion and thus limit migration. Since the fibronectin concentration-dependent effect is lost upon α5β1 blockage, we assume that fibronectin concentration sensing and signaling occurs through this integrin only.

3.5.6 Fibronectin affecting microglial reactivity?

Interestingly, in the control BV-2 transwell assays the high fibronectin coating caused increased migration. It must be noted that we did not rule out the possibility that the fibronectin coating or blockage of α5β1 integrin induces proliferation in BV-2 cells, so the increase in migration should be interpreted with caution. In any case, these phenomenons might be related to the transformation

of the cell into a more alerted or immune-active state as shown by the upregulation of integrins, MHC class I, the production of MMPs and an amoeboid morphology after exposure to fibronectin coating [294, 356]. The increase in migration on fibronectin is in accordance with the increased activation of microglia at sites of fibronectin upregulation in case of lesions and blood-brain barrier breakdown during neuroinflammation [294].

3.5.7 Study limitations

This study is the first to dig deeper into molecular mechanisms of physiologic migration of microglia during development. A limitation of the use of brains slices in this study might be that microglial migration in slice preparations does not reflect the true physiologic behaviour during development. Microglia at the slice surface could be activated in terms of phagocytosis and velum-like pseudopod formation as observed in slices of rat facial nucleus following peripheral axotomy [449]. Nevertheless, microglia within the tissue depth did not show such behaviours. This indicates that deep tissue imaging, as performed in our study, is likely to allow analyzing behaviour of the microglial population close to physiologic conditions [70, 71, 449]. It is important to note that microglial mobility in the *in vivo* developing zebrafish was also high [457, 461]. Finally, an *in utero* embryonic brain imaging [482, 483], although challenging, would be required to fully confirm that the intense microglial migration behaviour we observed in slices truly reflects the microglial behaviour in the developing brain of the intact embryo.

Migrating neurons, radial glia and blood vessels in the developing brain are known to express the α5β1 integrin [351, 354, 484] which could indirectly interfere with the alteration of microglia migration we observed in the presence of the blocking antibody. This is unlikely to be the case at the blood vessel level since we did not observed any difference in microglia-blood vessels interactions in the presence of the blocking antibody. Knock-down of this integrin in neural precursors resulted in a decreased radial migration and affected their morphology and differentiation capacity [351]. To our knowledge it is yet unknown if neuronal migration can affect microglia mobility. So far it has been shown that SDF-1-expressing basal progenitors in the ventricular/subventricular zone promote microglia recruitment into the subventricular [62]. Nevertheless, we cannot completely exclude that interactions between developing neurons and microglia might be altered after blockage. Finally β1 integrins in radial glia control the morphological differentiation of both glia and neurons [345] but the alterations of these processes by impairing β1 integrin expression occur in a time scale that is incompatible with the time scale observed for microglia behaviour alteration.

Changes in microglial migration speed observed in the presence of the blocking antibody are apparently modest (14-25% changes), but they are in the range of those observed on neurons migration speed after blocking glycine receptors [485] or on microglia migration after blocking the CC chemokine receptor 5 [486]. It is likely that α5β1 integrin is not the sole integrin dimer to play a role in microglial migration [354]. The long term consequences of defective integrin dependent microglial migration on brain development and neuronal network functionality remain unknown and require further attention. This might be a challenging task regarding the fact that genetically

engineered integrin knock-outs can suffer from functional compensation of other integrins [314, 338].

3.5.8 Conclusion

Our results strongly indicate that α5β1 integrin regulates the microglial migration process during embryonic microglial colonization of the mouse cortex, without playing an essential role in contact with blood vessels. We report for the first time opposing age-dependent functions of the α5β1 integrin. At E13.5 the α5β1 integrin promotes while at E15.5 and E17.5 it inhibits microglial migration. We hypothesize that during development, the stability of the α5β1-linked adhesion changes and therefore blockage of the fibronectin receptor leads to different outcomes. What causes microglial migration to decrease and how changes in α5β1 integrin function are molecularly regulated - cell intrinsically and/or environmentally - are questions that require further investigation.

CHAPTER 4:

The CXCL12/CXCR4/integrinß1 signaling axis in microglial migration:

an exploratory study

Partially based on: experiments performed by Kaline Arnauts during her master thesis "The link between Cxcl12/CxcR4 and integrin ß1 in microglia migration during brain development in mice".

Own contribution: Design of experiments, supervision of the master thesis, flow cytometry integrin subunits on cortical microglia and time-lapse experiments, all data analyses, figure production and manuscript writing

4.1 Abstract

During embryonic brain development microglia, myeloid-derived cells originating from the yolk sac, already invade the brain at E10.5 in mice. CXCL12 signaling through its receptor CXCR4 was found to recruit microglial cells to the cortex, but the underlying mechanisms were not clarified. We previously demonstrated the involvement of α5β1 integrin during microglial migration in the embryonic mouse cortex and β1 integrin is a downstream target of CXCR4 in cancer and immune cells and increases adhesion and invasion after CXCL12 signaling. We therefore hypothesized that the CXCL12/CXCR4/β1 integrin signaling axis drives microglial migration during embryonic brain development. We found that BV-2 cells, a microglia/macrophage cell line, showed increased migration towards CXCL12 in the presence of fibronectin, which was inhibited by blocking CXCR4. This was not observed in primary cultures of microglia. Blockage of integrin β1, PI3K and MEK1/2 reduced BV-2 cell migration towards control levels, while β2 integrin blockage did not affect migration. Blockage of integrin β1, PI3K and MEK1/2 in acute brain slices at embryonic day (E)13.5 and E17.5 differentially affected microglial migration speed, while CXCR4 blockage did not have any effect. Our results support the presence of a CXCL12/CXCR4/β1 integrin signaling axis in BV-2 cells *in vitro* only. They argue against an involvement of CXCR4 signaling in regulating microglial migration speed *in vivo* after these cells have invaded the brain parenchyma in the developing embryo.

4.2 Introduction

Microglia are highly migratory in the embryonic brain cortex and this behaviour most likely relates to their plentiful physiological tasks in CNS development [16, 72, 93, 487]. Microglia originate from myeloid progenitors in the yolk sac and invade the parenchyma tissue around E10.5 in mice [20, 72]. Several molecules were shown to be involved in establishing the microglial population inside the CNS, such as colony stimulating factor 1 (CSF-1), interleukin (IL)-34 and their receptor CSF1R, Matrix metalloproteinases, Fractalkine receptor (CX3CR1), NADPH oxidase-2 (NOX2) and CXCL12 (alternatively Stromal derived factor-1 (SDF-1)) and are therefore thought to recruit microglia to the brain [59, 62]. It is however not clear whether these molecules either attract microglial progenitors towards the brain and enable their invasion, or mediate their dispersion once inside the brain parenchyma.

CXCL12 is a chemokine with multiple functions in the developing CNS, such as regulating neural progenitor cell proliferation and migration, maintaining tangential migration of interneurons, maintaining radial glial scaffold integrity and mediating axonal guidance and pathfinding [488-490]. Additionally, CXCL12/CXCR4 signaling was recently demonstrated to impact on the microglial density in the embryonic cortex, where this chemokine is produced by basal progenitors in the ventricular (VZ) and subventricular (SVZ) zones [62]. However, the downstream effects of this CXCR4 activation in microglia are unknown. Upon CXCL12 binding to CXCR4, which is a Gi protein coupled receptor, intracellular signaling pathways might be activated that lead to the binding of talin and kindlin to the intracellular portion of integrins. This association will induce a

conformational stretching of the integrin which enhances extracellular matrix (ECM) binding, a process called inside-out signaling [314].

Studies in cancer cells have demonstrated a clear link between CXCR4 signaling and β1 integrin activation and subsequent adhesion to ECM molecules, including fibronectin [319-321]. For example, Hartmann *et al.* found that CXCL12-CXCR4 signaling induced β1-integrin activation in small lung cancer cells and this resulted in an increased adhesion to the ECM adhesive protein fibronectin. They determined that the adhesion was mediated by α2, α4, α5 and β1-integrins, along with CXCR4 activation and this could be inhibited by CXCR4 antagonists. Blocking the α5 subunit led to a stronger decrease in adhesion to fibronectin than blocking of the α4 subunit [319]. In acute lymphoblastic leukemia, lymphoblasts show increased migration towards bone marrow fibroblasts by ß1 integrin induced adhesion following CXCL12 stimulation [321]. Also in ovarian cancer cells and prostate cancer cells the CXCL12/β1 integrin axis enhances invasion of cancer cells by upregulation of ß1 integrins [491-493]. Human lung cancer cells increase their migration, as well as their expression of ß1 and ß3 integrins by regulation of the ERK and NF-κB dependent pathway following CXCL12 stimulation [494]. In addition CXCR4 couples to Gi proteins and activated Gi is able to, amongst others, activate the Src family of tyrosine kinases [320] while in its turn, Src can phosphorylate tyrosines of the NpxY motif of β-integrin tails and thereby mediate talin-integrin interactions, which are indispensable for integrin inside out activation [314]. Further, CXCL12 binding also induces activation of PI3K, resulting in the activation of more downstream targets such as PyK2, Akt, the downstream NF-κB pathway and MAPK pathways including ERK, JNK and p38 signaling. All these induced pathways are involved in chemotaxis, transcription, proliferation and cell survival [489, 494-497]. Also in hematopoietic, immune and radial glial cells evidence was found for CXCR4/β1 crosstalk. In hematopoietic stem cells, CXCL12 induced activation of αLβ2 and α4β1 integrins to bind their ligand and mediate migration [498]. In neutrophils, CXCL12/CXCR4 signaling mediates adhesion to VCAM-1 and bone marrow retention through α4β1, which can be blocked by CXCR4 and α4 antagonists [499]. In radial glial cells, CXCL12/CXCR4 signaling promoted their adhesion to pial basement membrane components through β1 integrin activation [490]. Also, we recently showed that microglia inside the embryonic cortical parenchyma can interact with fibronectin and age-specifically rely on integrin α5β1 during microglial migration in embryonic development [487]. Together, these studies suggest that CXCL12/CXCR4/β1-integrin signaling drives microglial migration along fibronectin inside the parenchyma.

In this exploratory study, we aim to analyse the presence of a functional CXCL12/CXCR4/β1-integrin signaling axis in the process of microglial migration. To this end, we study the role of CXCR4, β1 integrin, PI3K/Akt and Raf-ERK signaling pathways during migration of cultured microglia in transwell assays and during embryonic microglial migration *ex vivo* in acute brain slices using multiphoton excitation time-lapse microscopy. To functionally block the signaling axis, we use a CXCR4 blocker (AMD3100), a general β1 integrin function blocking antibody and PI3K and MEK1/2 (ERK) inhibitors throughout the study.

4.3 Materials and Methods

4.3.1 BV-2 cell line

The immortalized murine microglial BV-2 cell line was cultured in Dulbecco's Modified Eagle's medium (DMEM (D5796), Sigma) supplemented with 10% fetal bovine serum (FBS, Gibco) and 1% penicillin-streptomycin (P/S, Invitrogen) at 37°C in a humidified atmosphere with 5% CO_2. Confluent cell cultures were passaged by trypsin-EDTA treatment (T3924, Sigma) after rinsing with 1x Phosphate Buffered Saline (PBS, Lonza). The trypsin reaction was stopped by the addition of supplemented DMEM. Cells were used until passage 10. Cells were placed on serumfree medium (DMEM 5796) supplemented with 1% P/S overnight preceding an experiment.

4.3.2 Primary microglia

Primary microglia were obtained from brain isolation of C57BL/6 wildtype pups at postnatal day 2. Pups were decapitated and brains were isolated in ice-cold HBSS buffer (Gibco) supplemented with 7 mM HEPES buffer solution (Gibco). Brains were transferred to DMEM D5796 with 1% P/S and kept on ice. Tissue was titruated in 1 ml DMEM supplemented with 1% P/S using glass pipets precoated with horse serum (HS, ThermoFisher). The cell suspension was passed through a 70 µm cell strainer and centrifugated for 5 min at 400g at 4°C. Cell pellets were resolved in DMEM supplemented with 10% FBS, 10% HS and 1% P/S (DMEM 10.10.1) preheated at 37°C and seeded in poly-D-lysine (PDL, 20µg/ml, Sigma) precoated T175 flasks, at a concentration of 2 brains/flask. Cells were cultured for 7-10 days in DMEM 10.10.1 in a humidified atmosphere with 5% CO_2 at 37°C. After 10 days, the medium was changed for fresh medium supplemented with 10 ml conditioned colony stimulating factor 1 (CSF-1) medium. CSF-1 was produced in-house, as described below (Point 4.3.3). After 3-5 days, a shake-off was performed for 3 h at 230 rpm at 37°C. Medium containing detached cells was collected and passed through a 70 µm cell strainer. The cell suspension was centrifugated for 10 min at 300g, resuspended in 37°C preheated DMEM 10.10.1 and seeded in a 24 well plate precoated with PDL at 2.10^5 cells/well or immediately used for experiments.

4.3.3 In-house Colony stimulating factor 1 production

The mouse fibroblast cell line L929 was cultured in DMEM supplemented with 10% FBS, 1% P/S, 1% non-essential amino acids (NEAA, M7145, Sigma) and 1% L-glutamine (G7513, Sigma). Cells were cultured in T175 as a confluent monolayer and excreted CSF-1. The medium containing CSF-1 was collected after 10-11 days of culturing, sterile filtered (0.2µm) and stored at -20°C.

4.3.4 Animals

All protocols for animal experiments were conducted following the European Community guiding principles about the care and use of animals and with the approval of the Ethical Committee on Animal Research of Hasselt University. Mice were maintained in the animal facility of the Hasselt University in accordance with the guidelines of the Belgian Law and the European Council Directive. For flow cytometry and time-lapse imaging experiments, embryos were obtained by mating transgenic Cx3cR1-eGFP knock-in males [403] (European Mouse Mutant Archive (EMMA) with

approval of Stephen Jung) with C57BL/6 wild type females. In these knock-in mice the Cx3cR1 gene is exchanged for eGFP, hence all macrophages, including microglial cells, express eGFP [403]. In order to produce primary microglia cultures, wildtype C57BL/6 males and females were crossed. Mice were mated overnight and females with vaginal plugs the next morning were designated E0.5.

4.3.5 Flow cytometry

BV-2 and primary microglial cells

Cells were washed with PBS and centrifugated for 5 min at 400 g at 4°C followed by staining for 30 min on ice with the monoclonal antibodies anti-CD29 and anti-CD184 **(Table 4.1)** in FACS buffer (PBS, 2% FCS, sodium azide, 50 µl/well). After 2 washes, the pellet was resolved in FACS buffer. Cells were analysed with a FACS Aria II and the FACS Diva 6.1.3 software (BD Biosciences). Each tube of cells is considered as a sample (N=1).

Embryonic microglia

Cortical microglia from CX3CR1$^{+/eGFP}$ E13.5, E15.5 and E17.5 brains were isolated as described before in Smolders *et al.* (2015) with modifications **(Chapter 5)** [451]. Cortical tissue freed from meninges was mechanically homogenized in neurobasal medium (Gibco, Thermo Fisher Scientific) supplemented with 2mM L-glutamine, N2 supplement, B27 supplement and 1% penicillin/streptomycin (all from Thermo Fisher Scientific). The homogenate was centrifugated 5 min at 700 g at 4°C, the pellet was resuspended in cold PBS and stained with Fixable Viability stain 620 (FVS620) (BD Biosciences) during 10 min at room temperature (RT). Cell suspensions were fixed in 4% PFA during 10 min, washed in PBS by centriguation at 400 g for 5 min and resuspended in PBS. Cells were incubated for 15 min on RT with a panel of monoclonal antibodies against α integrin subunits known to pair up with the β1-subunit, and against β1 integrin (listed in **Table 4.1**) in 50µl PBS/well in a V-bottom shaped 96 well plate. After 2 washes in PBS cells were acquired in a FACS Fortessa (BD Biosciences) and analysed with FACS Diva 8.0.1 software (BD Biosciences). Within the living cell population (FVS620 low) the eGFP positive microglia (110-4799 cells per tube) were gated. Within the microglial population, the percentage of α-subunit positive microglia and their median fluorescence intensity (MFI) were analysed. Fluorescence-minus-one (FMO) controls (for justification see (Maecker and Trotter 2006)) were used to gate the positive cell population. At E13.5, embryos were pooled per 2 or 3 (N=8). At E15.5 (N=16) and E17.5 (N=20), embryos were analysed separately. Data were obtained from 3 different mothers (M=3).

Table 4.1: Antibodies and isotypes used for flow cytometry.

Antibody	Fluorescent label	Dilution cells	Dilution embryo	Company	Cat. nr.	Isotype
CD29 (β1)	APC-Cy7	1:1000	1:250	Biolegend	102225	Ham IgG
CD184 (CXCR4)	Alexa Fluor 647	1:100	1:25	Biolegend	146503	Rat IgG2b
CD49d (α4)	PE-Cy7	/	1:250	Biolegend	103617	Rat IgG2b
CD49e (α5)	PE	/	1:25	BD	557447	Rat IgG2a
CD49f (α6)	APC	/	1:250	eBioscience	17-0495	Rat IgG2a
CD51 (αv)	BV421	/	1:250	BD	740062	Rat IgG1

4.3.6 Transwell migration assay

BV-2 cells

Migration assays were performed using Corning transwell membrane filters (8 µm pore size, Corning Costar, New York, USA). BV-2 cells were serum starved overnight on DMEM 5796 with 1 % P/S, from now on referred to as serumfree medium, and harvested the next morning by trypsinisation, centrifugation for 10 min at 400 g, washes in PBS and resuspension in serumfree medium. If mentioned, inserts were precoated with fibronectin (10 µg/ml) for 1 h at 37 °C before the start of the assay. After 1 h filters were washed twice in PBS and placed in a 24 well plate containing 400 µl serumfree medium. Cells were seeded at a density of 1.10^5 cells/insert in 100 µl serum free medium with or without blockers and isotypes. Cells were preincubated for 30 min with the following blockers or the matching isotype: AMD3100 (4 µM, A5602, Sigma), ß1 function blocking antibody (5 µg/ml, clone HMB-1, #102210, Biolegend), ß1 isotype (5 µg/ml, Hamster IgG isotype control, #400916, Biolegend), ß2 function blocking antibody (5 µg/ml, clone GAME-46, #557440, BD Biosciences), ß2 isotype (5 µg/ml, Rat IgG1 isotype control, #53922, BD Biosciences), LY294002 (10 µM, Sigma) or U0126 (10 µM, Sigma). After 30min, serumfree medium in the bottom well was changed for medium containing CXCL12 (100 ng/ml, Peprotech) [62, 497] or serumfree medium (control). Cells were allowed to migrate for 6 h at 37°C in a humidified atmosphere with 5 % CO_2. Cells were fixed for 5 min in 4 % PFA, washed with PBS and stained with for 2 min with 0,05 % crystal violet. Migrated cells were present at the bottom side of the filter and filter tops were cleaned with cotton buds. From each filter pictures were taken on 10X magnification in black and white modus at three different non-overlapping locations using a Zeiss Primovert microscope and Axiocam camera. Pictures were thresholded using the Default threshold and manual adjustments in Fiji and the mean grey value of the total picture measured. Mean grey values were averaged per filter (migration index (MI)) and calculated relative to the control MI. Each filter is considered as a sample (N=1).

Primary microglia

Migration assays with primary microglia were performed similarly as described for BV-2 cells. Cells were seeded immediately after shake-off on filters precoated with fibronectin (10 µg/ml) in DMEM (D5796) supplemented with 10 % FCS, 10 % horse serum (HS) and 1 % P/S. Migration assays were conducted for 24 h at 37°C in a humidified atmosphere with 5 % CO_2. MI was determined as described for BV-2 cells.

4.3.7 Adhesion assay

Serum starved BV-2 cells were harvested as described above. A flat bottom-96 well plate was uncoated or precoated during 1 h at 37 °C with fibronectin (10 µg/ml, Sigma) or 1 % BSA. Wells were washed twice with PBS after coating. Cells were seeded at a concentration of 5.10^4 cells in 100 µl serumfree medium. The assay was performed in the presence or absence of CXCL12 (100 ng/ml) in combination with either AMD3100 (4 µM), a ß1 function blocking antibody (5µg/ml) or Hamster IgG isotype control (5 µg/ml). Cells were allowed to attach for 6 h. Non-adherent cells were washed away with PBS, adherent cells were fixed for 5 min with 4 % PFA and stained with crystal violet. One overview picture/well was taken at 4X magnification with the Zeiss Primovert microscope. Pictures were processed and adhesion relative to fibronectin coating only was calculated as described for the MI. Each filter is considered as a sample (N=1).

4.3.8 *ex vivo* time-lapse imaging

Time-lapse imaging was performed as described before [487]. For blocking experiments, the recording medium was supplemented with either AMD3100 (40 µM), LY294002 (20 µM), U0126 (20 µM), a β1 function blocking antibody (10 µg/ml, clone HMB-1), an α5β1 function blocking antibody (clone BMC5, 10µl/ml, #NBP2-29788, Novus), a combination of α5β1 and β1 antibodies or matching isotype controls (Hamster IgG isotype control for β1 or clone RTK4174 for α5β1, 10µl/ml, #400710, Biolegend). Microglial soma tracking and quantification of the average migration speed (µm/h) occurred as described before in Fiji using the MTrackJ Plugin written by Erik Meijering [487]. Average speed was calculated as the total length of the traveled path divided by the duration of the track. The number of cells is referred to as "n", the number of slices as "N" and the number of mother animals corresponding to independent experiments as "M".

4.3.9 Statistics

Sample sizes are described in the figure legends as n=cells/N=tubes, filters or wells/M=independent experiments or mother animals. The reader is referred to the figure legends for details about the sample size and the statistical test, and to the supplement p155 for population descriptors per figure. Data are presented as scatter plots were each dots corresponds to 1 sample, the horizontal line to the median and bars to the interquartile ranges (IQR). In case of box plots (used when sample size exceeded 25), whiskers extend to 1.5x the IQR (Tukey representation). Statistical analyses were performed using SAS JMP® Pro 12.1.0. Data distributions were assessed for normality (Shapiro-Wilk) and equality of variance (Brown-Forsythe). In case these assumptions were met for all groups, a Student *t*-test in case of 2 groups or ANOVA was performed in case of

three groups followed by Tukey HSD post-hoc, correcting for multiple comparisons. **In Fig. 2D and 9C**, data were transformed on a log10 scale to meet the equality of variance assumption, though the original data were used for presentation for ease of interpretation. When the distribution of at least one group was non-gaussian, nonparametric tests such as Mann-Whitney in case of two groups or Kruskal-Wallis with Dunn's multiple comparison post-hoc in case of three groups were performed. *P*-values smaller than 0.05 were considered significant with * $P<0.05$, ** $P<0.01$ and *** $P<0.001$.

4.4 Results

4.4.1 CXCL12/CXCR4 signaling evokes β1 integrin-dependent migration in microglia-like cells *in vitro*

In order to explore the CXCL12/CXCR4/β1 signaling axis and associated intracellular signaling pathways in microglia, we first assessed whether BV-2 cells and primary microglia express CXCR4 and β1 integrin. The BV-2 cell line, although highly debated with regard to its low resemblance to *in vivo* microglia [113], is a practical and easy first approach to study this signaling axis in microglia-like cells. Using flow cytometry, we found that more or less 90% of BV-2 and at least 70% of primary microglial cells express both receptors **(Fig. and Suppl. Table 4.1.)**.

We next assessed whether CXCL12 could attract BV-2 cells and primary mouse microglia and whether this effect was mediated through CXCR4. Since we hypothesized that microglia use the CXCL12/CXCR4/β1 signaling axis to migrate along fibronectin, we coated the surfaces in the *in vitro* experiments with fibronectin. Using transwell assays and a well known inhibitor specifically targeting CXCR4, AMD3100, we demonstrated that CXCL12 works as an effective chemoattractant in BV-2 cells leading to increased migration to the bottom of the filter compared to the control condition, which contained only serumfree medium in the bottom well **(Fig. 4.2 A, B)**. This increased migration was fully abolished by co-administration of AMD3100 **(Fig. and Suppl. Table 4.2A, B)**. In primary microglia we did not find a chemoattractive effect of CXCL12, though AMD3100 induced a decrease in migration compared to CXCL12 administration and control **(Fig. and Suppl. Table 4.2C)**. When transwell assays were conducted in the absence of fibronectin (uncoated filters), primary microglia did not migrate at all (data not shown) and CXCL12 did no longer attract BV-2 cells **(Fig. and Suppl. Table 4.2D)**. These results show that CXCL12 is an effective chemoattractant for BV-2 cells only. Migration towards CXCL12 necessitates the presence of extracellular matrix supporting β1 integrin binding, such as fibronectin.

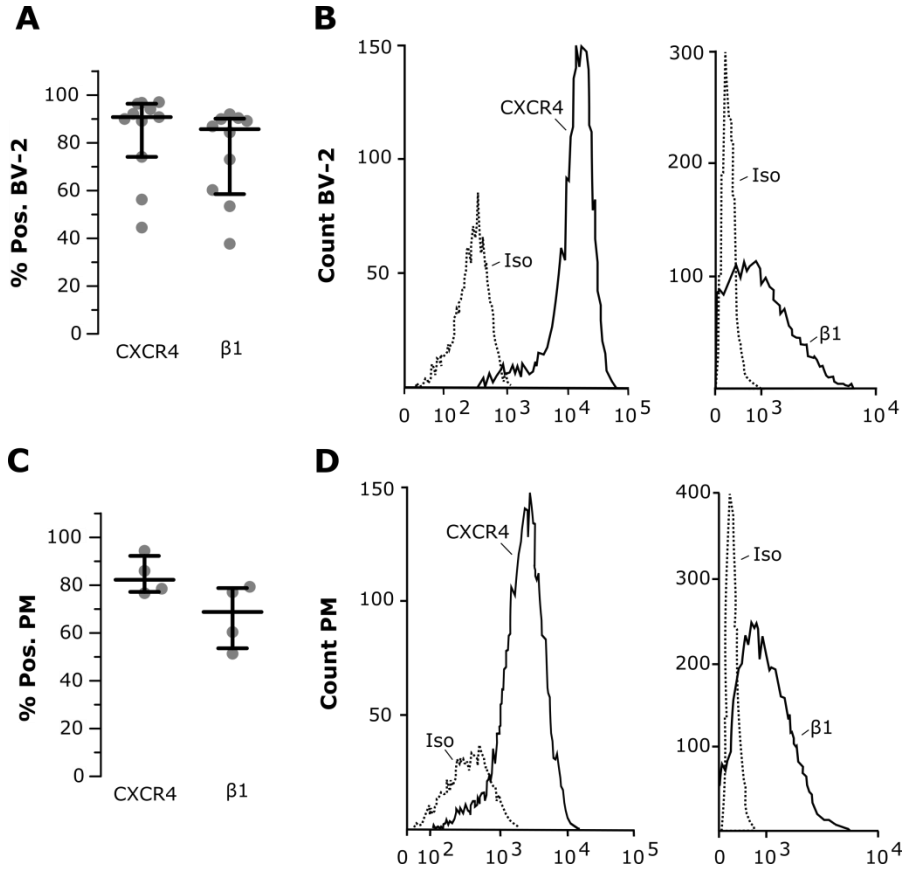

Fig. 4.1. Cultured microglia-like cells express CXCR4 and β1 integrin. Percentage of **(A)** BV-2 cells and **(C)** Primary microglia positive for CXCR4 or β1 integrin evaluated by flow cytomtery. **(B, D)** Representative fluorescence intensity histograms. Sample size BV-2: CXCR4 N=11/M=4; β1 N=10/M=4); and PM N=4/M=2. Iso,Isotype; Pos., Positive; PM, Primary microglia.

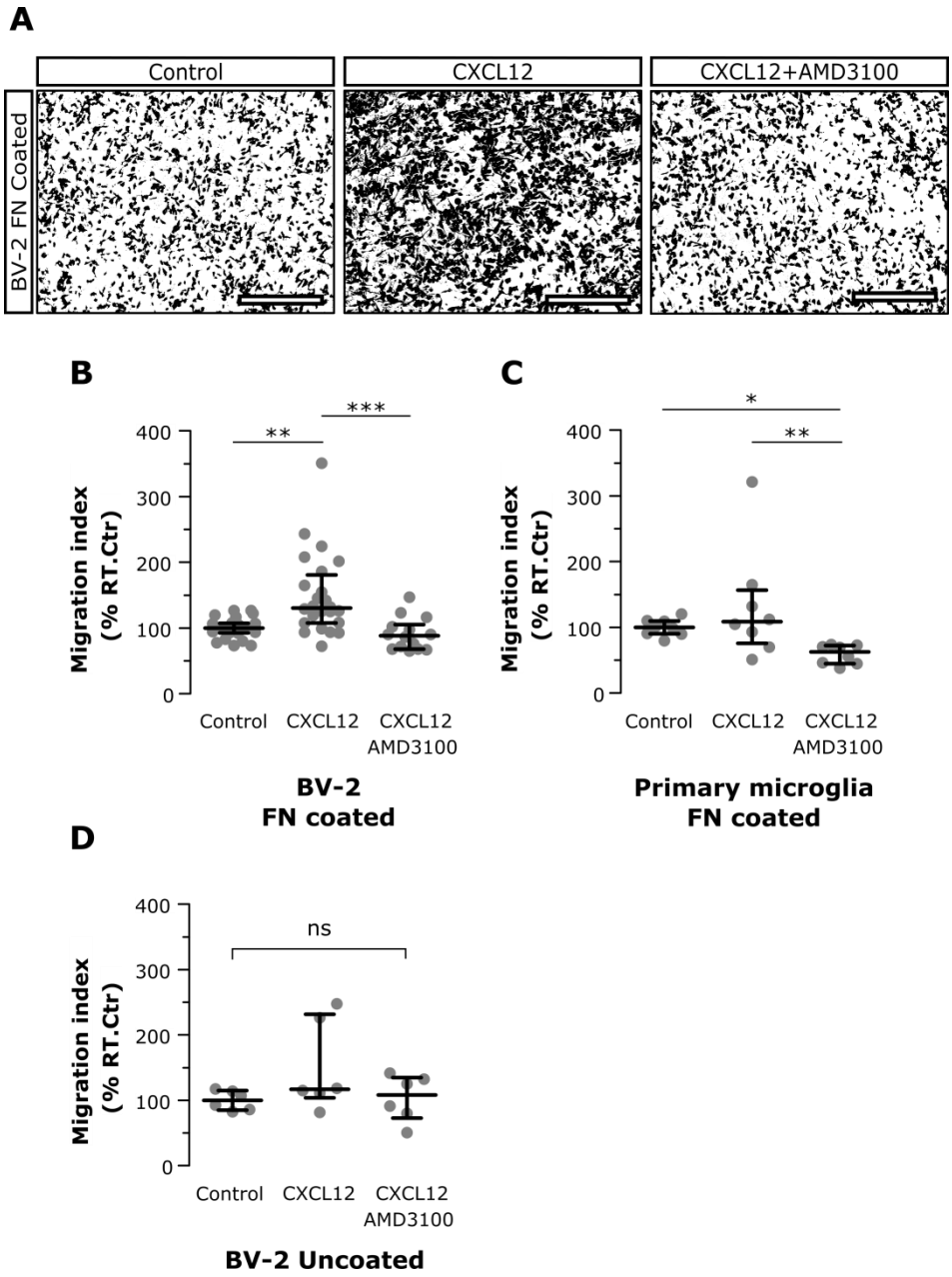

Fig. 4.2. CXCL12 attracts microglia-like cells in the presence of fibronectin coating. (A) Transwell assay of BV-2 cells on fibronectin coating in serumfree (control), CXCL12 and CXCR4 blocking (AMD3100) conditions showing thresholded pictures of filter bottoms. **(B-D)** Quantifications of transwell assays depicting the migration index (MI) relative to control on fibronectin coated and uncoated filters in BV-2 and primary microglial cells. **(B)** AMD3100 attenuated CXCL12-induced migration of BV-2 cells on fibronectin. **(C)** AMD3100 inhibited migration of primary microglia on fibronectin in the presence of CXCL12 while the latter did not elicit increased migration. **(D)** In the absence of fibronectin, CXCL12 had no attractive properties on BV-2 cells. BV-2 and PM FN coated and PM: Kruskal-Wallis test with Dunn's. BV-2 uncoated: ANOVA + Tukey on Log10 transformed values of Migration index RT.Ctr. Sample size BV-2 FN coated: control N=25/M=4; CXCL12 N=24/M=14; AMD N=14/M=7; Primary microglia: all N=8/M=4; BV-2 uncoated: all N=6/M=3. PM, primary microglia; RT.Ctr, Relative to control; FN, Fibronectin. Scale bar=300µm

To determine whether CXCL12-induced migration of BV-2 cells involved primarily β1 integrin, we performed transwell assays in the presence of β1 and β2 function blocking antibodies. We found that co-administration of CXCL12 and an antibody targeting β1, fully abolished CXCL12-induced migration of BV-2 cells compared to isotype application, as was also reported for CXCR4 blockage using AMD3100 **(Fig. and Suppl. Table 4.2A, B)**. On the contrary, a β2 targetting antibody did not influence CXCL12 induced migration **(Fig and Suppl. Table 4.3)**. Thus, BV-2 cells specifically rely on β1 and not on β2 integrin signaling for migrating towards a CXCL12 source.

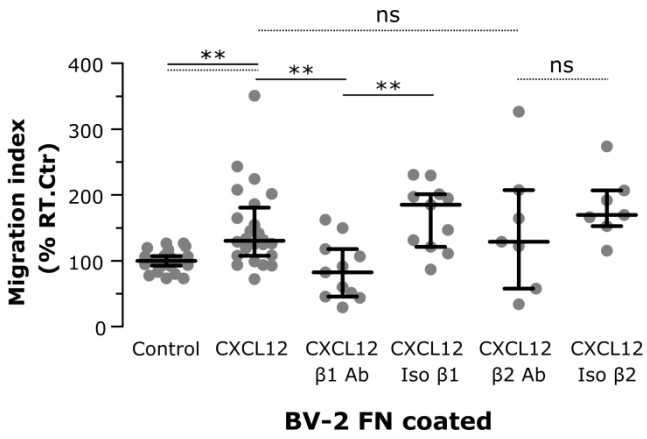

Fig. 4.3. CXCL12-induced migration specifically involves β1 integrin. Transwell assay during 6 h in BV-2 cells. The β1 blocking antibody inhibited BV-2 cell migration induced by CXCL12 compared to isotype, while a β2 blocking antibody did not (Kruskal-Wallis tests with Dunn's for β1 -full lines- and β2 -dotted lines- separately). Sample size control N=25/M=14; CXCL12 N=24/M=14; β1 Ab N=11/M=7; Iso β1 N=11/M=7; β2 Ab N=7/M=5; Iso β2 N=7/M=5. Ab, antibody, FN, Fibronectin, RT.Ctr, Relative to control, ns, not significant.

It must be noted that the observed decreased migration after inhibitor application in transwell assays could be a consequence of decreased adhesion of the cells to the filter instead of a decreased capacity to migrate. To rule out this possibility, we performed adhesion assays in the same conditions as for transwell assays (6 hours). To ensure that the adhesion was not an artifact of the duration of the assay, we included a negative control (1% BSA coating) in which BV-2 adhesion should be impaired. As a control we used fibronectin coating only and calculated the others conditions relative to this one. We found that in case wells were coated with fibronectin, cell adherence more than doubled compared to 1% BSA coating **(Fig. and Suppl. Table 4.3)**. Administration of CXCL12, AMD3100, β1 blocking antibodies or isotype did not result in changes in adhesion **(Fig. and Suppl. Table 4.3)**. Therefore, we assume that the decrease in migration after inhibitor application is truly due to an impairment in migration capacity and not to a decreased cell adherence to the filter.

All together, this set of *in vitro* experiments show that BV-2 cells use β1 integrins in order to migrate along fibronectin towards CXCL12 and that this signaling occurs through CXCR4. This was however not the case for primary microglia, which could indicate the absence of a CXCL12/CXCR4/β1 signaling axis for migration of primary microglial cells.

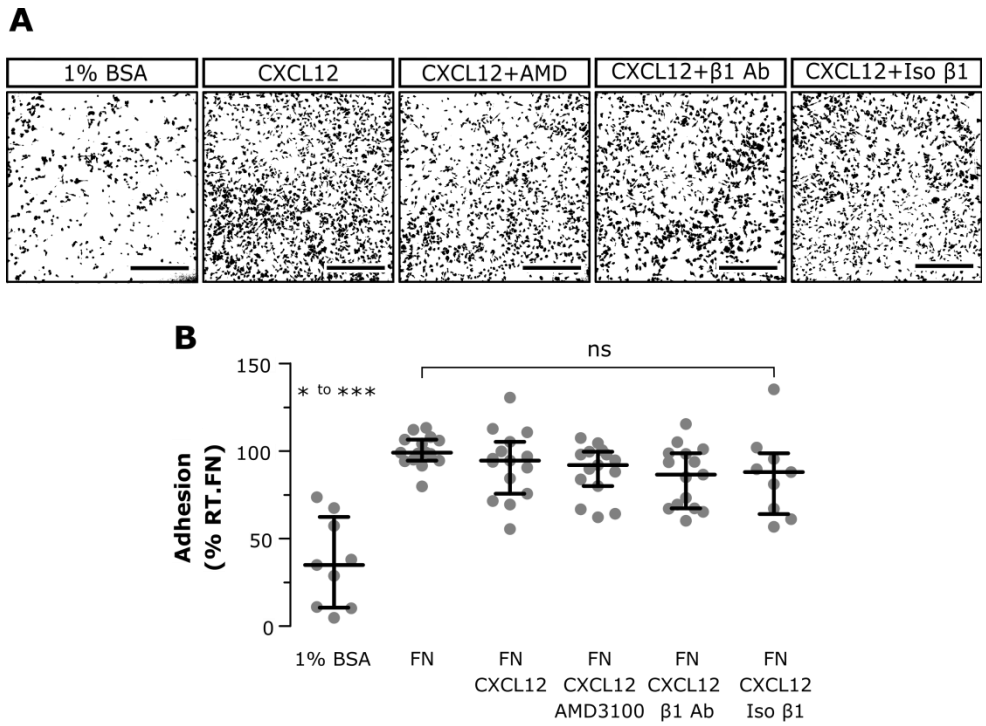

Fig. 4.4. AMD3100 and β1 function blocking antibody do not impair BV-2 cell adhesion to the FN coating. (A) Thresholded pictures of BV-2 cells adhesion assay on 1% BSA (negative control), only FN, FN with CXCL12 and the latter condition supplemented with the different blockers or isotype control. **(B)** 1% BSA coating impaired BV-2 adhesion in comparison to other conditions. No significant difference in pairwise comparsions between all other groups. Kruskal-Wallis test with Dunn's. Sample size 1% BSA and Iso N=9/M=3; rest N=15/M=4. Ab, antibody, FN, Fibronectin, Iso, Isotype, RT.Ctr, Relative to control, ns, not significant. Scale bar=500µm.

4.4.2 CXCL12 induced migration is regulated by PI3K-Akt and Ras-ERK signaling pathways in microglia-like cells *in vitro*

To further shed light on the molecular signaling pathways involved in CXCL12-induced BV-2 cell migration, we investigated the functions of PI3K (part of the PI3K-Akt pathway, using Ly294002) and MEK1/2 (part of the Ras-ERK pathway, using U0126) using transwell assays **(Fig. & Suppl. Table 4.5)**. Both kinases have been described to regulate the activation of integrins downstream of CXCR4 signaling [319, 321, 495], but they also signal downstream of integrins [314, 500]. For example PI3K signaling through Rac influences cytoskeleton dynamics which allows the cell to migrate [272, 501]. In addition, the PI3K-Akt and Ras-ERK signaling pathways are the main mechanisms of the cell to control processes from cell survival to metabolism and motility in response to extracellular cues [502]. Co-administration of CXCL12 and Ly294002 or U0126 fully abolished migration to control levels **(Fig. & Suppl. Table 4.5)**. These results show that both the PI3K-Akt and Ras-ERK pathways play essential roles in CXCL12-induced BV-2 cell migration.

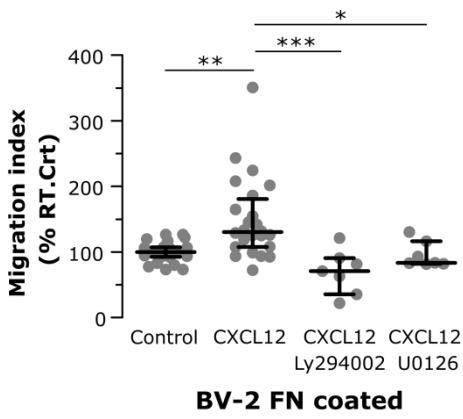

Fig. 4.5. PI3K-Akt and Ras-ERK signaling are necessary for migration in BV-2 cells. Transwell assay during 6 h in BV-2 cells in the presence of PI3K and MEK 1/2 inhibitors, Ly294002 and U0126. Both inhibitors attenuated CXCL12-induced migration (Kruskal-Wallis test with Dunn's). Sample size control N=25/M=14; CXCL12 N=24/M=14; Ly249004 and U0126 N=7/M=5. FN, Fibronectin, RT.Ctr, Relative to control.

4.4.3 β1 integrins, but not CXCR4, age-specifically regulate microglial migration speed in acute brain slices

To investigate the role of CXCR4 signaling in migration of embryonic microglia during their colonization of the embryonic cortex, we first determined the presence of CXCR4 and β1 integrin on the cell surface of acutely isolated embryonic microglia. We found that around half or less of the microglial population at E15.5 and E17.5 expressed CXCR4, which is in contrast with our observations in primary microglia. The percentage of CXCR4 positive microglia was highly variable at E17.5 **(Fig. and Suppl. Table 4.6)**. To the contrary, almost all microglial cells expressed the β1 subunit at E13.5, E15.5 and E17.5 **(Fig. and Suppl. Table 4.6)**. These findings suggest that targeting these receptors would affect some to all embryonic microglia.

Arno *et al.* [62] established in various ways that CXCL12/CXCR4 signaling is involved in establishing the microglial density in the embryonic cortex. They found that CXCL12 production by basal progenitors in the ventricular zones attract microglia. However, from this study it is not clear whether CXCL12/CXCR4 signaling instructs the microglial precursors to invade the brain or whether it functions in attracting microglial cells that are already present in the brain or a combination of both. To determine whether CXCR4 influences migration of microglia that already have invaded the brain, we administered AMD3100 to acute live CX3CR1$^{+/eGFP}$ embryonic brain slices at E13.5 and E17.5. This live tissue was imaged during 6 hours, starting within 3 hours after sacrificing the mother animal. Microglial cells (eGFP positive) were tracked in 3D and average migration speeds were calculated per cell ($v_{av.}$ in μm/h). At neither of both ages AMD3100 influenced migration speed **(Fig. and Suppl. Table 4.7)**. These results indicate that CXCR4 signaling does not play a role in regulating microglial migration speed in the developing embryonic mouse brain.

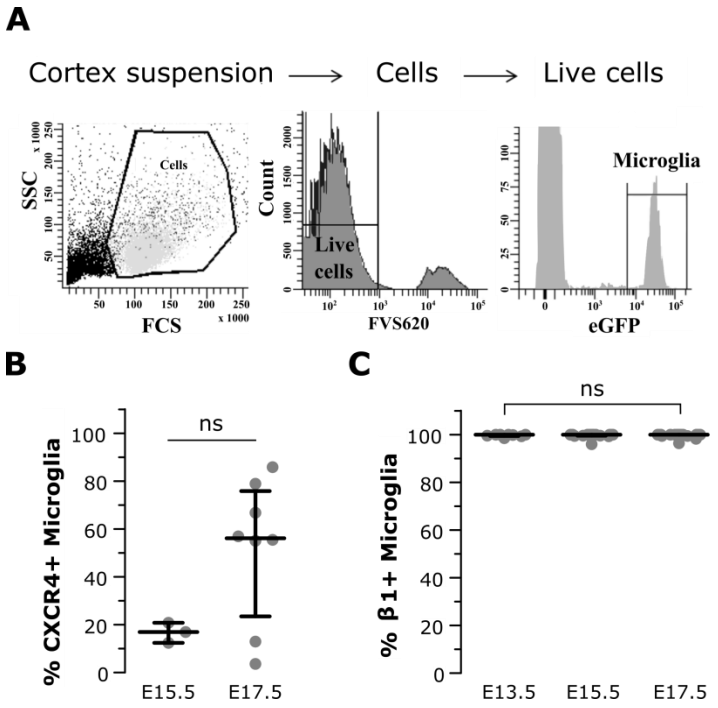

Fig. 4.6. A modest fraction of the embryonic microglia population expresses CXCR4, while all express β1 integrins *ex vivo.* (A) Flow cytometry gating strategy to assess receptor expression on microglial cells in panels B and C. **(B)** The percentage of CXCR4 positive microglial cells does not change from E15.5 to E17.5 (Mann-Whitney test), nor does the percentage positive for β1 (Kruskal-Wallis test with Dunn's). **(C)** All microglia at different embryonic ages express β1 integrins (Kruskal-Wallis test with Dunn's). Sample size CXCR4: E15 N=3/M=1; E17 N=8/M=3; β1: E13 N=8/M=3; E15 N=16/M=3; E17 N=20/M=3.

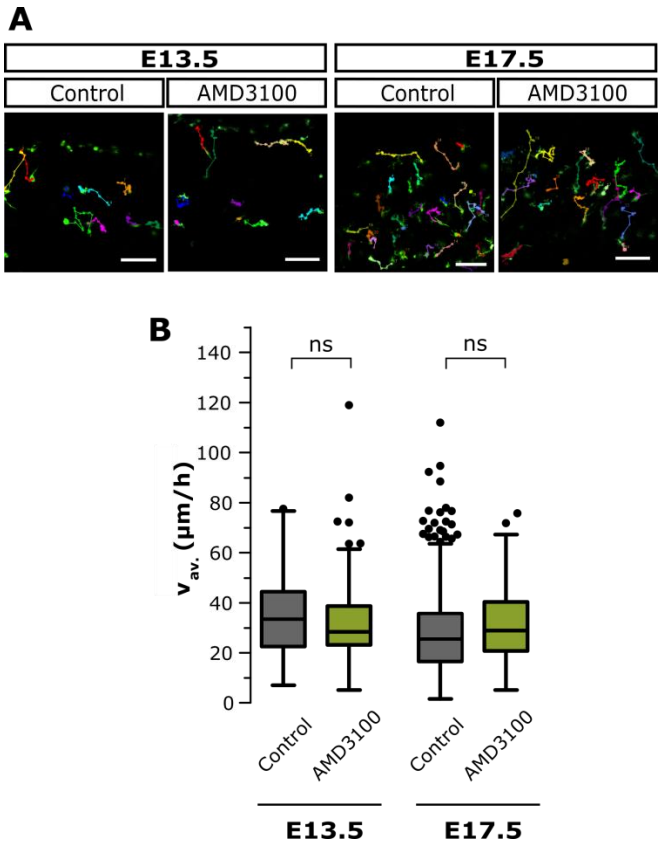

Fig. 4.7. CXCR4 is not involved in regulating microglial migration speed in acute embryonic brain slices. Microglia movement was recorded in acute brain slices during 6 h using 2-photon time-lapse imaging and cell somas were manually tracked. **(A)** Representative Z-projections of microglial migration tracks at E13.5 and E17.5 (eGFP/ microglia, green). Each cell track has its own color. The meninges is located at the top of the image and the ventricle at the bottom (not visible at E17.5). **(B)** Microglial average migration speed $v_{av.}$ (µm/h) did not change at either age in the presence of a CXCR4 inhibitor (AMD3100) (Student *t*-test). Sample size as n=cells/N=slices/M=mothers at E13.5: control n=161/N=18/M=12; AMD3100 n=68/N=6/M=5; at E17.5: control n=501/N=22/M=13; AMD3100 n=87/N=4/M=4. Scale bar=100 µm.

We then quantified microglial migration speed in acute embryonic brain slices in the presence of the β1 function blocking antibody or its isotype at E13.5, E15.5 and E17.5 **(Fig. and Suppl. Table 4.8)**. Treatment with the β1 blocking antibody resulted in a decreased migration speed compared to controls. Surprisingly and in contrast to what we found in a previous study using an α5β1 antibody, general β1 blockage at E15.5 led to a decreased migration speed compared to isotype and control (Chapter 3) [487]. In contrast to E15.5, but in accordance with the α5β1 antibody, general β1 blockage at E17.5 resulted in a small but significant increase in migration speed compared to controls **(Fig. and Suppl. Table 4.8)**, which we also observed previously upon α5β1 antibody application at E17.5 (Chapter 3) [487]. It must be noted that at E13.5, general β1 blockage resulted in a higher decrease in speed compared to α5β1 blockage (P<0.001, Welch's Test for unequal variances). On the contrary, at E17.5 general β1 blockage resulted in a lower increase in speed compared to α5β1 blockage (P<0.001, Welch's Test for unequal variances).

To determine which specific β1 integrins could mediate these functions, we analysed the expression of α integrin subunits that pair up with β1 and that have been previously identified in primary microglial cells [361], on acutely isolated embryonic microglia using flow cytometry (**Fig. and Suppl. Table 4.9**). From E13.5 to E17.5 almost all microglia express α5, α6, and αv integrins, while their expression level decreases over development. On the contrary, about 15% of the embryonic microglia stably expressed the α4 subunit over development. In order for these α subunits to be expressed, β1 should be expressed as well and this was the case as shown in **Fig. 4.6**. Thus based on expression, α5β1, α6β1, and αvβ1 integrins are likely to play more prominent roles in regulating migration when compared to α4β1.

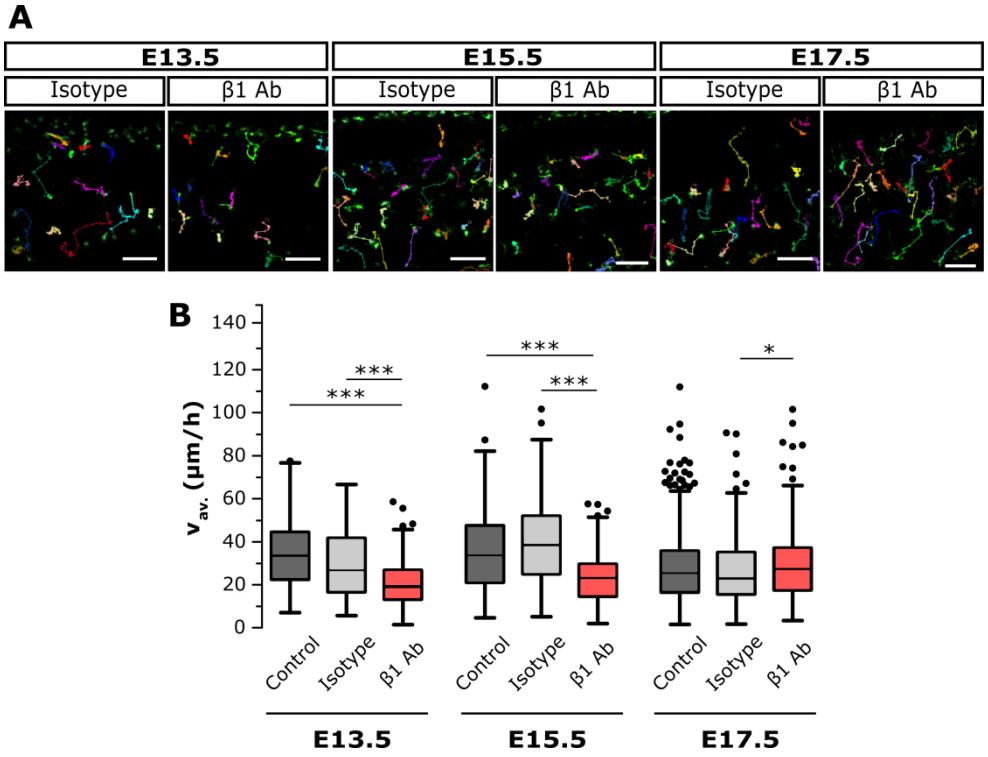

Fig. 4.8. Age-specific effects of β1 integrin blockage on microglial migration speed in acute embryonic brain slices. Experimental set-up see Fig. 4.7. **(A)** Representative Z-projections of microglial migration tracks at E13.5, E15.5 and E17.5 (eGFP/ microglia, green). Each cell track has its own color. The meninges is located at the top of the image and the ventricle at the bottom (not visible from E15.5 onwards). **(B)** Treatment of slices with a β1 integrin function blocking antibody resulted in a decreased microglial average migration speed $v_{av.}$ (µm/h) at E13.5 and E15.5 while it elicited a subtle but significant increase in speed at E17.5, compared to isotype treatment (Kruskal-Wallis with Dunn's at all ages). Sample size as n=cells/N=slices/M=mothers at E13.5: n=161/N=18/M=12 (control), n=91/N=8/M=5 (iso), n=83/N=9/M=5 (Ab); at E15.5: n=170/N=10/M=8 (control), n=233/N=11/M=6 (iso), n=218/N=11/M=5 (Ab); at E17.5: n=501/N=22/M=13 (control), n=254/N=12/M=7 (iso), n=322/N=13/M=6 (Ab). Ab, antibody. Scale bar=100 µm.

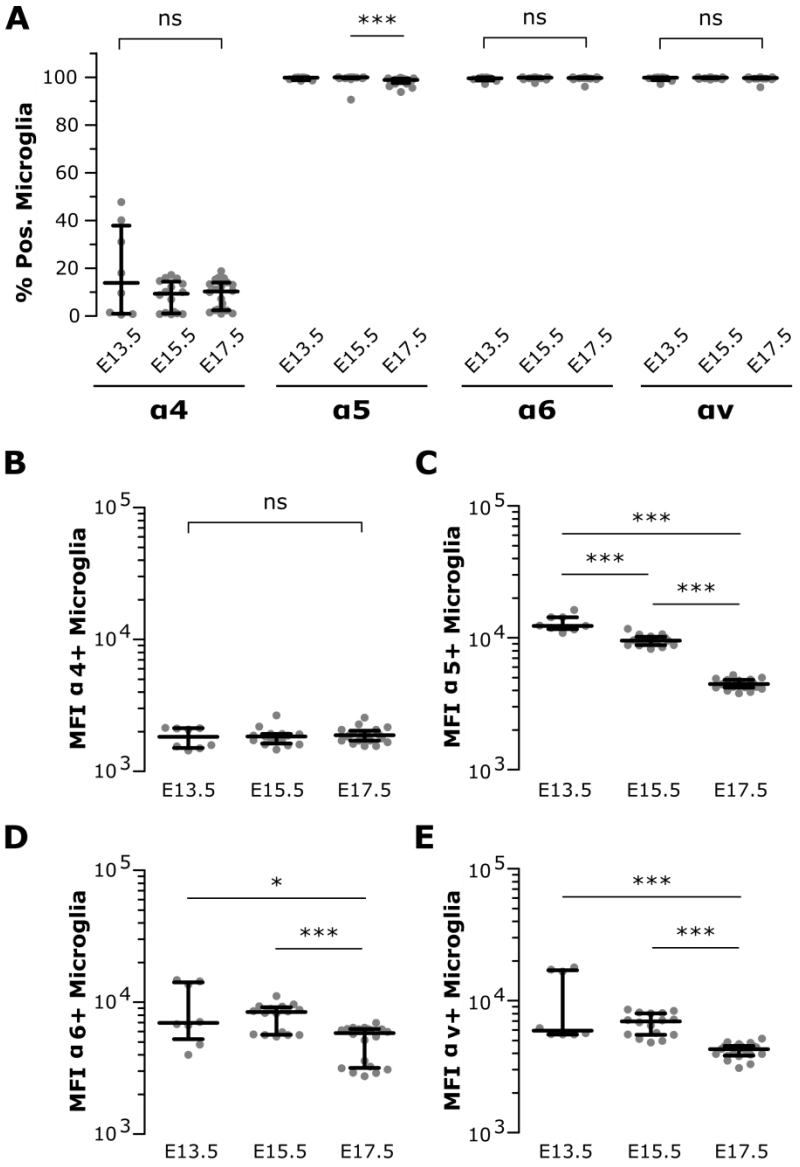

Fig. 4.9. Embryonic microglia express several types of β1 integrins. Flow cytometric analysis of α integrin subtypes known to pair up with β1 and previously identified in primary microglial cells. For gating strategy and β1 analysis see Fig. 4.6. **(A)** Percentage of microglial cells positive for different α subunits. Almost all microglia expressed α5, α6 and αv-integrins from E13.5 to E17.5 and the percentage of α5 integrin expressing microglia subtly decreased over development (Kruskal-Wallis with Dunn's). α4 integrin was present on a small subset of microglial cells from E13.5 to E17.5. **(B-E)** The expression level (median fluorescence intensity, MFI) of all but α4 integrins decreased from E13.5 to E17.5 (All Kruskal-Wallis test with Dunn's per α subunit except for α5: ANOVA with Tukey on log10 transformed data). Sample size E13 N=8/M=3; E15 N=16/M=3; E17 N=20/M=3. MFI, Median fluorescence intensity; ns, not significant.

The β1 function blocking antibody targets all β1 dimers, including α5β1. To validate our current and previous results (Chapter 3) [487], we combined α5β1 and β1 function blocking antibody treatment at E15.5. At this particular age the effects of both antibodies were clearly opposite: blocking α5β1 resulted in a vast increase in migration speed (Chapter 3) [487], while β1 blockage resulted in a prominent decrease **(Fig and Suppl. Table 4.8)**. Since the β1 antibody in theory blocks α5β1 integrins along with other integrins, applying both blocking antibodies at the same time should still mimic the effect of a β1 blockage only. We found that indeed a combined application of both antibodies mimicked the effect of sole β1 antibody treatment **(Fig and Suppl. Table 4.10)**. Migration speed upon combined treatment did not differ from β1 antibody application only, but did

differ from α5β1 antibody or combined isotype treatment. It must be noted that application of both isotypes together increased migration speed as well compared to control. Neverthless, these results certify that the β1 antibody functionally targets more integrins than only the α5β1 integrin and that β1 integrins other than α5β1, all together play a more prominent -and opposite - role in microglial migration than α5β1 at E15.5.

All together, these *ex vivo* migration experiments argue against a role of CXCR4 in regulating embryonic microglial migration *in vivo*, though they reveal a surprising age-specific function of β1 integrins in regulation microglial migration speed in the embryonic brain.

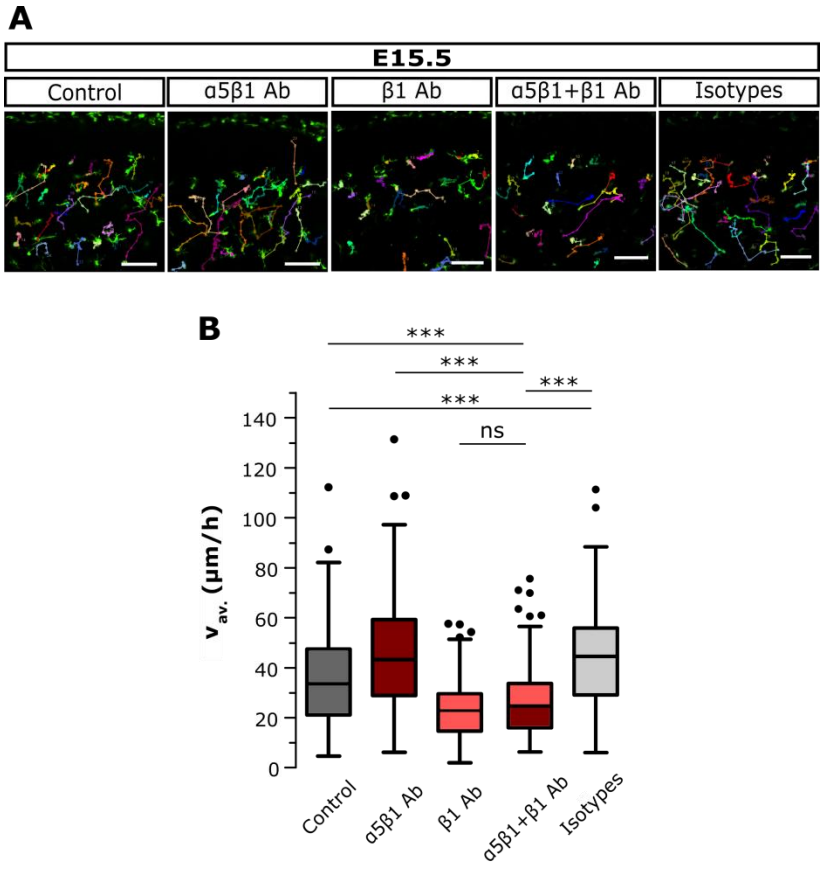

Fig. 4.10. β1 blockage overrules the effects of α5β1 blockage on microglial migration speed upon combined treatment in acute embryonic brain slices. Experimental set-up see Fig. 4.7. **(A)** Representative Z-projections of microglial migration tracks at E15.5 (eGFP/ microglia, green) in control conditions and upon treatment with function blocking antibodies or isotypes. Each cell track has its own color. The meninges is located at the top of the image and the ventricle at the bottom (not visible). **(B)** Treatment of slices with both α5β1 and β1 function blocking antibodies resulted in an effect on migration speed that was different (opposite) compared to treatment with α5β1 alone, control and both isotypes but not different compared to application of β1 alone. Treatment with both isotypes did not influence migration speed compared to control. All Kruskal-Wallis tests with Dunn's. Sample size as n=cells/N=slices/ M=mothers: control n=170/N=10/M=8; α5β1 Ab n=252/N=11/M=6; β1 Ab n=218/N=11/M=5; α5β1+β1 Ab n=150/N=7/M=3; Isos n=140/N=6/M=2. Ab, antibody. Scale bar=100 µm.

4.4.4 PI3K and MEK 1/2 differentially regulate microglial migration speed in acute brain slices dependent on the embryonic age

To further shed light on the molecular signaling pathways involved in microglial migration, conform the transwell assays in BV-2 cells **(Fig. 4.5)**, we investigated the functions of PI3K (using Ly294002) and MEK1/2 (using U0126) at E13.5 and E17.5 in embryonic brain slices **(Fig. & Suppl. Table 4.11)**. In both E13.5 and E17.5 embryonic brain slices Ly294002 treatment strongly decreased migration speed. In accordance, U0126 treatment at E13.5 also diminished migration speed, however this was not the case at E17.5 where U0126 had the opposite effect and augmented migration speed **(Fig. & Suppl. Table 4.11)**. These results imply that the signaling pathways involved in microglial migration have different outcomes in terms of promoting or inhibiting the migration process in microglial cells during embryonic development.

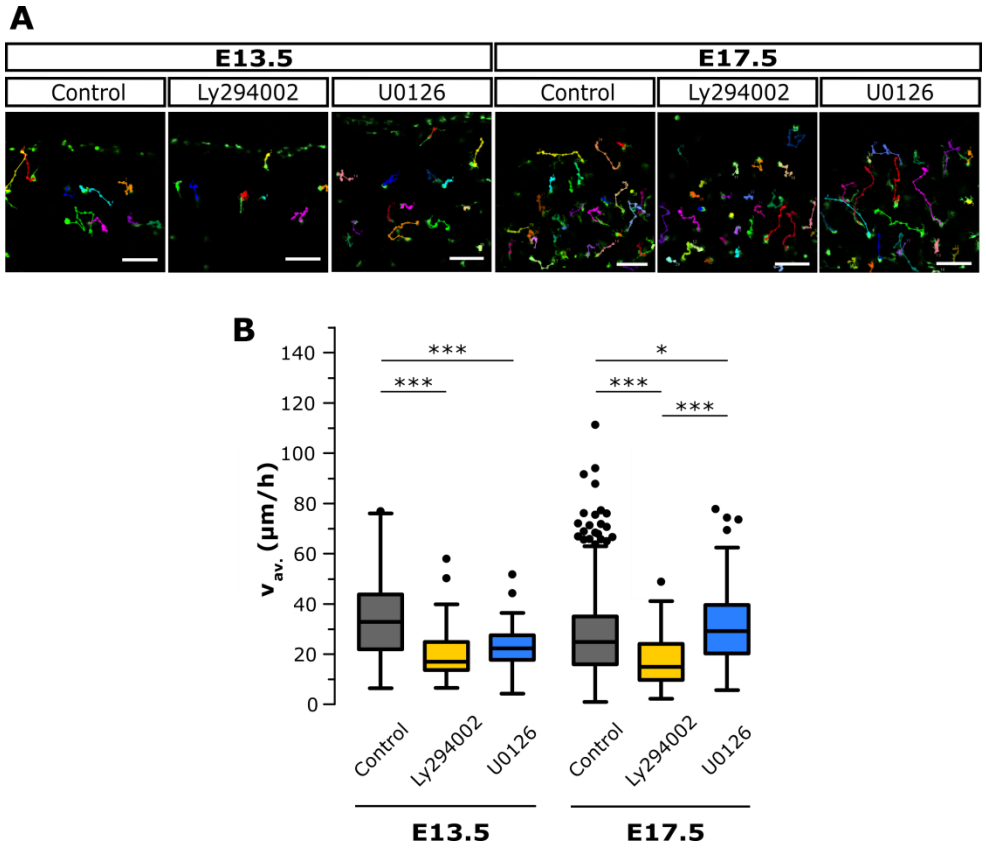

Fig. 4.11. PI3K-Akt and Ras-ERK pathways have age specific functions in regulating microglial migration speed in acute embryonic brain slices. Experimental set-up see Fig. 4.7. **(A)** Representative Z-projections of microglial migration tracks at E13.5 and E17.5 (eGFP/ microglia, green) in control conditions and upon treatment with inhibitors for PI3K (Ly294002) or MEK1/2 (U0126). Each cell track has its own color. The meninges is located at the top of the image and the ventricle at the bottom (not visible at E17.5). **(B)** Treatment with Ly294002 at E13.5 and E17.5 resulted in a reduced migration speed compared to control. Treatment with U0126 decreased migration speed at E13.5 while it increased migration speed at E17.5 compared to control. At E17.5 Ly294002 and U0126 elicited opposite effects on microglial migration speed. All Kruskal-Wallis tests with Dunn's. Sample size as n=cells/N=slices/M=mothers at E13.5: n=161/N=18/M=12 (control), n=35/N=4/M=4 (Ly294002), n=44/N=4/M=4 (U0126); at E17.5: n=501/N=22/M=13 (control), n=110/N=5/M=5 (Ly294002), n=92/N=5/M=5 (U0126). Scale bar=100 µm.

4.5 Discussion

During development, microglia migrate from the yolk sac to the brain and subsequently invade and disperse throughout the parenchyma. CXCL12/CXCR4 signaling was previously shown to attract microglial cells and to establish the microglial density in the normal developing embryonic mouse cortex [62]. In this exploratory study, we found indications for the presence of a CXCL12/CXCR4/β1 signaling axis in BV-2 cells that allows migration on β1-binding ECM substrates such as fibronectin. In cultured primary microglia and in the embryonic brain *ex vivo*, we found no evidence for a function of CXCR4 in determining the microglial migration speed, though for migration these cells rely on β1 integrins and their function changes throughout development. Further, we demonstrated that PI3K and MEK1/2 are part of important molecular signaling pathways involved in microglial migration.

4.5.1 The CXCL12/CXCR4/β1 signaling axis in cultured microglia

In this study, we showed that BV-2 cells efficiently migrate towards CXCL12 in case a fibronectin substrate is present and this attraction was fully reliant on CXCR4 function. Our results in BV-2 cells are in accordance with previous reports showing functional CXCR4 and CXCL12-induced migration in both microglial cell lines and primary cultures [497, 503, 504]. It must be noted that although CXCR4 was long thought to be unique amongst chemokine receptors because it exclusively interacted with CXCL12, migration inhibitory factor was demonstrated to compete with CXCL12 for binding to CXCR4 [505]. In its turn, CXCL12 was also long considered to interact only with CXCR4 until recently CXCR7 was revealed as an alternative receptor for CXCL12 [504, 506, 507]. However, CXCR4 still seems the most important receptor for signaling as CXCR7 could not compensate for the loss of CXCR4 [504]. Further it is noteworthy that in the developing and adult rat brain no expression of CXCR7 expression was found on microglial cells, which indicates that CXCL12 signaling through CXCR7 in the embryo is not very likely [507].

Our findings in primary microglia are however in conflict with previous studies in which primary microglial cells did migrate towards CXCL12 and this could be blocked by AMD3100 [62, 504]. Nevertheless, since our sample size is rather small and variation is high, additional experiment should be performed. Further, it should be clarified whether primary microglia in our hands (effect of the used culture media) already produce CXCL12 themselves. Indeed, previous studies show that rat primary microglia express mRNA transcripts of CXCL12 [508] and produce 3 ng/ml CXCL12 in control culture conditions [509]. In contrast, another study could not detect expression of CXCL12 in unstimulated human fetal microglial cultures using conventional immunocytochemistry [510]. If primary microglia in our transwell migration assays produce CXCL12, the endogenous CXCL12 could saturate their CXCR4 which explains the absence of a chemoattractive effect upon supplemental CXCL12 application. When CXCR4 is blocked, migration is inhibited to a level even lower than control without CXCL12, which might point to CXCL12 induced chemokinesis, although this effect was excluded in a previous study [504]. Additional work is necessary to dissect out the contribution of CXCL12-induced proliferation in migration assays and to confirm the effects of CXCL12 and involved pathways in primary microglia. Proliferation and dose-response transwell assays would help in solving these issues.

In case fibronectin was absent, CXCL12 did not attract BV-2 cells. Since interaction with fibronectin occurs amongst others through ß1 integrins [511], migration of microglia-like cells along fibronectin is the first indication of ß1 involvement in CXCL12-induced migration. In order to confirm that CXCL12 signaling induces migration exclusively along fibronectin, migration along additional ECM molecules, such as laminin (another β1 binding ECM molecule), ICAM1 (β2 binding ECM). Further, we showed that CXCL12 stimulation concomitant with ß1 integrin blockage induced a complete abolishment of migration to control levels, while ß2 blockage did not affect migration at all, which points to a full dependency on integrin ß1 during CXCL12-induced migration. Here as well, additional migration blockage experiments using integrins binding fibronectin, but not through β1 such as αvβ3 and αvβ8 should be performed to conclusively state that the CXCL12 effect on microglia attraction is both fibronectin as well as β1 integrin specific. In any case, the ß1 subtypes involved in mediating CXCL12-induced migration remain to be determined. Our flow cytometry analyses on embryonic microglia and antibody titrations on BV-2 cells (not shown) suggest that α5, α6, αv integrins likely play a major role, while a minor role for α4 is envisioned, based on the percentage of microglia that express these markers. It should be noted however that not integrin expression level, but rather the conformation, or in other words activation state of the integrin, is functionally relevant[318, 322]. However, involvement of other α subunits cannot be excluded since our analysis was limited to the abovementioned α subunits. Nevertheless, cultured microglia were reported to only specifically express the β1 dimerizing α-subunits investigated in our study [356].

Although various studies in cancer and neuronal stem cells report on a link between CXCR4 and an increase of β1 integrin affinity or clustering followed by alterations in adhesion and/or migration [319, 321, 490, 494, 512, 513], this link is not established yet in microglial cells at embryonic stages, although our results provide indications for a link in BV-2 cells at least. In any case, the results obtained in this study were according to expectation based on findings in previous literature and have paved the way for additional experiments investigating whether CXCL12 induces β1 integrin activation and subsequent intracellular signaling involved in cell migration.

4.5.2 No role for CXCR4 in parenchymal migration of microglia in the embryo

Using various *in vivo* approaches to disturb CXCL12/CXCR4 signaling, Arno *et al.* found a decreased microglial density in the embryonic cortex [62]. Their findings point to a function of CXCL12 in recruiting microglial cells into the brain and/or in regulating migration speed inside the parenchyma. In our *ex vivo* time lapse experiments in embryonic brain slices, only migration speed of microglia that have already entered the parenchyma could be analysed since all connections with the surrounding tissue and blood vessels were lost after isolating the brain. We found no influence of blocking CXCR4 on microglial migration speed at E13.5 neither at E17.5. In contrast to our findings in embryonic brain slices, CXCL12/CXCR4 signaling was previously shown to stimulate mobility of microglia in the neonatal retina [161]. Additionally, systemic application of agents that block CXCL12/CXCR4 signaling resulted in reduced numbers of macrophages/microglia in this study [161]. Further, the direction of migration might be affected instead of speed. Additional analyses with regard to directionality of migration and experiments in attempt to redirect microglial migration in slices after exogenous CXCL12 application will shed light on this matter. So, we

believe that the function of CXCR4 is most likely related to the recruitment of microglial cells into the brain.

Given the fact that microglial recruitment was not completely abolished after suppressing CXCL12 signaling in the study by Arno *et al.* it must be noted that only around one third of embryonic microglial cells expressed CXCR4 [62], other attractive cues are likely to regulate microglial migration into the brain. In that respect, microglial density was transiently altered in CX3CR1 KO mice [111], and in Nox2 and VEGFR1 impaired mice [63], which renders these proteins plausible candidates as well. Nevertheless, the effects observed in these studies were also transient and did not elicit complete abolishment of microglial presence in the brain. Microglial migration into and inside the brain is likely to be supported by a complex interplay between various chemoattractants and/or repellants, which still need to be identified.

The lack of effect of CXCR4 blockage on microglial migration speed at E13.5 could be due to the lack of CXCR4 expression at this age. CXCR4 expression on microglial cells has been reported before [497, 503, 504]. However, expression levels of this receptor during embryonic development has never been examined, except at E15.5 by Arno et al who found similar results to our study [62]. In case the microglial CXCR4 expression at E13.5 is lower than at E15.5, it is not surprising that no change is observed after blockage.

4.5.3 Age-specific role of β1 integrins in microglial migration

Blockage of ß1 integrins resulted in a decreased microglial migration speed at E13.5 and E15.5 in embryonic brain slices, while at E17.5 ß1 blockage led to a subtle increase in migration speed. Thus, the sum of all ß1 integrins promotes migration at E13.5 and E15.5, while overall they exert a net migration inhibiting function at E17.5. We cannot explain what causes this shift in function, but a similar shift was also reported in a previous study of our group concerning the function of α5β1 integrin, which occurred earlier between E13.5 and E15.5 [487]. Remarkably, α5β1 and β1 blocking antibodies elicited opposing effects at E15.5: α5β1 blockage augmented migration speed while general β1 blockage reduced migration speed. Additionally, the β1 antibody did not perfectly mimic the effect size of the α5β1 antibody. This discrepancy could be explained by the putative blockage of other integrins, reported to be expressed by microglia in culture such as α4β1, α5β1, αvβ1 and α6β1 [356, 358, 511] and which we also identified on embryonic microglia from E13.5 to E17.5 as well. Apparently, the net function of all β1 integrin heterodimers summed together at E13.5 and E15.5, seems to be migration promoting versus slightly migration inhibiting at E17.5. As already brought forward in our previous study [487], we hypothesize that the stability of the adhesion coupled to the integrin changes over development from an unstable adhesion supporting fast migration on E13.5 to a more stabile adhesion causing the cell to gradually anchor in the ECM at E17.5. This change could cause different outcomes of integrin blockage on migration speed depending on the embryonic age [487].

In addition to β1 integrins, β2 integrins could play a role in microglial migration [514]. However, they are unlikely to be essential during microglial migration, because microglial activation and homing to injured neurons was unaffected in β2 integrin deficient mice [376]. Instead, integrins of

the β1, as shown in this study, or αv family are good candidates of modulating microglial morphology and migration along ECM proteins such as fibronectin [294, 361, 370, 374].

4.5.4 Roles of PI3K-Akt and Ras-ERK signaling in microglial migration

The PI3K-Akt pathway is a well studied signaling pathway associated with growth factor and chemokine signaling that amongst other through communication with Rac can regulate cytoskeleton dynamics and migration [501, 502, 515]. Contradictory results have been obtained with regard to the role of this pathway in cell migration. PI3K is involved in the regulation of migration speed in neutrophils and in zebrafish during development [516, 517] and it was established that specifically PI3Kγ regulates migratory activity in BV-2 cells [518]. Although this enzyme seems to be a nodal point in the control of microglial motility, Lipfert *et al.* demonstrated that CXCL12-induced chemotaxis of microglial cells solely depends on Erk1/2 signaling (MAPK pathway) and not on PI3K signaling [504]. In this study, we found clear evidence for a prominent role of the PI3K-Akt pathway in facilitating both BV-2 cell migration and microglial migration in *ex vivo* in acute embryonic brain slices. We therefore expect when β1 antibody and Ly294002 (the PI3K blocker we used) are administered together, the effect of blocking PI3K would remain, since the cell needs cytoskeleton dynamics in order to migrate.

The Ras-ERK signaling chain, similar to the PI3K-Akt pathway, is a chief pathway for regulating divergent cell responses to extracellular ligands, ranging from cell survival to motility [502]. We here demonstrated a prominent role of the Ras-ERK pathway in facilitating BV-2 cell migration after CXCL12 stimulation. In *ex vivo* brain slices at E13.5, Ras-ERK signaling accordingly promotes microglial migration. At E17.5 on the contrary, this pathway is negatively involved in microglial migration. The discrepancy between the role of Ras-ERK signaling in microglial migration *in vitro* and *ex vivo* (at E17.5) might be due to the type of readout and the cue that is used, since molecular pathways might depend on the specific mechanism, cell type and environment studied. For example, Peled *et al.* showed that the processes of adhesion and migration are differentially regulated on a molecular level, so the importance of integrins during these processes can vary [498]. Recently, Meller *et al*. showed that molecular mechanisms for microglial migration differed between *in vitro* and *in vivo* settings, and that microglial motility processes *in vivo* also required different molecular signaling [519]. More in particular, *in vivo* Kindlin3-mediated integrin signaling was required for timely advancement of microglial protrusions towards the site of brain damage while Kindlin3 was dispensable for *in vivo* microglial migration in development as well as in chronic inflammation of the CNS [519]. Thus *in vitro* microglia-related findings should be interpreted with extreme caution. Indeed, it was recently shown that upon cultivation, microglia rapidly lose their signature gene expression profile [520, 521]. Nevertheless, it is very suprising that Ras-ERK signaling has opposite functions in microglial migration over development and this phenomen should be investigated further at other ages as well and using a microglia specific approach to rule out a microglia response secondary to changes in metabolism of the neighboring cells, since pharmacological blockage using U0126 (as for Ly249002) is not microglia specific (discussed in **Point 4.5.5**).

Going further into "specificity of effects", Lipfert *et al.* found that CXCL12-induced proliferation of primary microglia is mediated through Erk1/2 and Akt signaling [504] and another study showed that CXCL12 slightly induced proliferation of BV-2 cells at the concentration we used in our study [497] **(Chapter 4)**. This means that the effect we observed in BV-2 cells upon blockage of PI3K and MEK1/2 might arise from inhibition of CXCL12-induced proliferation and thus asks for additional experiments to rule out a proliferation effect of CXCL12 that could be interpreted as increased migration.

In summary, these results imply that the PI3K-Akt and Ras-ERK signaling pathways have different functions in terms of promoting and inhibiting the migration process in microglial cells during embryonic development. Although *in vitro* work might yield helpful mechanistic information, verification with a microglia-specific approach *in vivo* is necessary, since microglial responses *in vitro* differ from *in vivo*.

4.5.5 Study limitations

An important point of attention of this preliminary study is the use of pharmacological or antibody mediated blockage on slices. Although our *in vitro* experiments show that a direct effect of these different compounds on migration of a microglia cell line is entirely possible, it must be taken into account that the changes in migration speed we observed in the *ex vivo* embryonic brain slices might not be microglia specific but rather a consequence of blockage of these proteins in on other cells present in the slice.

CXCL12/CXCR4 signaling is implicated in multiple developmental processes such as neurogenesis, migration of interneurons and angiogenesis [161, 522, 523]. Further, CXCR4 signaling in astrocytes and microglia leads to tumournecrosis factor-α (TNF- α) production and subsequent glutamate release by astrocytes, which is involved in the regulation of neuronal apoptosis in rodent adult hippocampal slices [524]. Also, in developing spinal cord radial glia, CXCL12 controls the integrity of the radial glial scaffold by inducing adhesion of the radial cells to the ECM through β1 integrin activation [490]. Accordingly, β1 integrins play key roles during embryonic development, such as during neural stem cell differentiation, maintenance of the radial glial scaffold and neuronal migration [343, 345-350]. Since microglia possess an arsenal of receptors to monitor the status of their surroundings [32], we cannot exclude that changes in microglial mobility are secondary to impairments in neuronal (progenitor) physiology. To overcome these possible non-specific effects, conditional knockout mice may be used to delete or alter Cxcr4 and/or β1 integrin specifically in microglia. Alternatively, slices may be electroporated to induce overexpression or a non-functional form of CXCL12 in radial glial cells and subsequently study the effect on microglial migration. However, since we did not observe an effect of general CXCR4 blockage on microglial migration speed in brain slices, we do not expect to observe effects in a microglia specific knockout either. It should also not be neglected that compensation mechanisms might occur after integrin knock out.

4.6 Conclusion

In this exploratory work we have paved the way for further research to connect CXCL12/CXCR4 signaling to β1 integrin-dependent migration en intracellular siganling in cultured microglial cells. In the embryo however, CXCR4 does not seem to be implicated in regulating microglial dispersion inside the healthy parenchyma, after the cells have invaded the brain. Nevertheless, our results point to the necessity for PI3K-Akt signaling and to a complex and age dependent regulation of β1 integrin function and Ras-ERK signaling during microglial migration in the embryonic brain *ex vivo*.

4.7 Supplemental data description

Suppl. Table 4.1. Statistical descriptors of data in Fig. 4.1 "Cultured microglia-like cells express CXCR4 and β1 integrin". Values correspond to percentage of population positive for a marker.

	(A) BV-2		(B) Primary microglia	
	% CXCR4+	% β1+	% CXCR4+	% β1+
Median	90.7	85.7	82.3	68.8
25% Quant.	74.1	58.5	77.2	53.7
75% Quant.	96.4	90.0	92.2	78.8
Mean	83.7	75.7	83.9	67.1
Std. Dev	17.9	19.0	8.0	13.4
Std. Error	5.4	6.0	4.0	6.7
Sample size	N=11/M=4	N=10/M=4	N=4/M=2	N=4/M=2
Stat. Test	None		None	
***P*-values**	NA		NA	

NA, not applicable; Sample size: N=measured tubes, M=independent experiments

Suppl. Table 4.2. Statistical descriptors of data in Fig. 4.2 "CXCL12 attracts microglia-like cells in the presence of fibronectin coating". Values correspond to the migration index calculated relative to control.

	BV-2						Primary microglia		
	(B) FN Coated			(D) Uncoated			(C) FN Coated		
	Control	CXCL12	CXCL12+AMD	Control	CXCL12	CXCL12+AMD	Control	CXCL12	CXCL12+AMD
Median	100.0	130.3	88.3	100.0	116.8	108.2	100.0	108.5	62.5
25% Quant.	92.8	107.7	68.1	85.1	103.8	72.9	90.2	75.9	45.0
75% Quant.	107.2	180.9	105.3	114.9	231.7	134.9	109.8	156.9	72.2
Mean	100.0	149.2	90.7	100.0	150.1	103.6	100.0	131.3	58.8
Std. Dev	15.2	61.8	24.7	14.8	69.0	35.4	13.2	84.5	14.5
Std. Error	3.0	12.6	6.6	6.1	28.2	14.4	4.7	29.9	5.1
Sample size	N=25/M=4	N=24/M=14	N=14/M=7	N=6/M=3	N=6/M=3	N=6/M=3	N=8/M=4	N=8/M=4	N=8/M=4
Stat. Test	Kruskal-Wallis with Dunn's			ANOVA + Tukey HSD on Log10 MI RT.Ctr			Kruskal-Wallis with Dunn's		
***P*-values**	CXCL12 vs control: $P = 0.0022$ **			CXCL12 vs control: $P = 0.2598$			CXCL12 vs control: $P = 1$		
	AMD vs control: $P = 0.4629$			AMD vs control: $P = 0.9977$			AMD vs control: $P = 0.0140$ *		
	AMD vs CXCL12: $P < 0.0001$ ***			AMD vs CXCL12: $P = 0.2358$			AMD vs CXCL12: $P = 0.0071$ **		

Sample size: N=filters, M=independent experiments

Suppl. Table 4.3. Statistical descriptors of data in Fig. 4.3 "CXCL12-induced migration specifically involves β1 integrin**"**. Values correspond to the migration index calculated relative to control.

	BV-2 FN Coated					
	Control	**CXCL12**	**CXCL12+β1 Ab**	**CXCL12+Iso β1**	**CXCL12+β2 Ab**	**CXCL12+Iso β2**
Median	100.0	130.3	82.5	185.2	128.9	169.9
25% Quant.	92.8	107.7	45.9	121.2	57.7	153.0
75% Quant.	107.2	180.9	118.1	201.4	207.4	206.8
Mean	100.0	149.2	85.6	167.0	148.8	182.5
Std. Dev	15.2	61.8	44.6	49.5	98.3	49.7
Std. Error	3.0	12.6	13.4	14.9	37.2	18.8
Sample size	N=25/M=4	N=24/M=14	N=11/M=7	N=11/M=7	N=7/M=5	N=7/M=5
Stat. Test	Kruskal-Wallis with Dunn's (control-CXCL12-β1 Ab-Iso β1) & (control-CXCL12-β2 Ab-Iso β2)					
***P*-values**	CXCL12 vs control: *P* = 0.0037 **				For β2:	*P* = 0.0025 **
	CXCL12 vs β1 Ab: *P* = 0.0042 **					*P* = 1
	Iso β1 vs β1 Ab: *P* = 0.0014 **					*P* = 0.7765

Sample size: N=filters, M=independent experiments

Suppl. Table 4.4. Statistical descriptors of data in Fig. 4 "AMD3100 and β1 function blocking antibody do not impair BV-2 cell adhesion to the FN coating". Values correspond to the adhesion index calculated relative to the fibronectin (FN) only condition.

	BV-2					
	1% BSA	**FN**	**FN+CXCL12**	**FN+CXCL12+AMD3100**	**FN+CXCL12+β1 Ab**	**FN+CXCL12+iso β1**
Median	34.9	99.1	94.6	91.9	86.6	87.9
25% Quant.	10.6	94.5	75.7	80.1	67.4	64.1
75% Quant.	62.4	106.5	105.2	99.6	98.8	98.7
Mean	36.2	100.0	92.4	88.6	85.3	86.2
Std. Dev	25.4	8.7	19.1	14.6	17.2	24.1
Std. Error	8.5	2.2	4.9	3.8	4.4	8.0
Sample size	N=9/M=3	N=15/M=4	N=15/M=4	N=15/M=4	N=15/M=4	N=9/M=3
Stat. Test *P*-values	Kruskal-Wallis with Dunn's (BSA-FN-CXCL12-AMD) & (BSA-FN-CXCL12-β1 Ab-Iso β1) BSA vs FN: *P* <0.0001 *** BSA vs CXCL12: *P*= 0.0018 ** BSA vs AMD: *P*= 0.0098 ** All other pairwise comparisons: ns (P>0.3067) For β1: BSA vs β1: *P* = 0.0292 * BSA vs Iso β1: P= 0.1130					

Sample size: N=wells, M=independent experiments

Suppl. Table 4.5. Statistical descriptors of data in Fig. 4.5 "PI3K and MEK1/2 signaling are necessary for migration in BV-2 cells". Values correspond to the migration index calculated relative to control.

	BV-2 FN Coated			
	Control	**CXCL12**	**CXCL12+Ly294002**	**CXCL12 U0126**
Median	100.0	130.3	70.7	83.6
25% Quant.	92.8	107.7	35.6	82.0
75% Quant.	107.2	180.9	90.9	116.4
Mean	100.0	149.2	69.3	95.8
Std. Dev	15.2	61.8	33.5	19.8
Std. Error	3.0	12.6	12.7	7.5
Sample size	N=25/M=4	N=24/M=14	N=7/M=5	N=7/M=5
Stat. Test	Kruskal-Wallis with Dunn's			
***P*-values**	CXCL12 vs control: *P* = 0.0043 **			
	CXCL12 vs Ly294002: *P* < 0.0001 ***			
	CXCL12 vs U0126: *P* = 0.0305 *			

Sample size: N=filters, M=independent experiments

Suppl. Table 4.6. Statistical descriptors of data in Fig. 4.6 "A modest fraction of the embryonic microglia population expresses CXCR4, while all express β1 integrins *ex vivo"*. Values correspond to the percentage of microglia positive for the marker.

	% CXCR4+		% β1+		
	E15.5	**E17.5**	**E13.5**	**E15.5**	**E17.5**
Median	17.0	56.2	99.9	99.9	99.9
25% Quant.	12.5	23.5	99.4	99.5	99.9
75% Quant.	20.8	75.9	100.0	100.0	100.0
Mean	16.8	51.9	99.7	99.6	99.6
Std. Dev	4.2	29.3	0.5	1.0	0.9
Std. Error	2.4	10.4	0.2	0.2	0.2
Sample size	N=3/M=1	N=8/M=3	N=8/M=3	N=16/M=3	N=20/M=3
Stat. Test	Mann Whitney test				
***P*-values**	CXCR4 E15.5 vs E17.5: P= 0.1939				

Sample size: N=tubes with single or pooled embryonic brains, M=independent experiments

Suppl. Table 4.7. Statistical descriptors of data in Fig. 4.7 "CXCR4 is not involved in regulating microglial migration speed in acute embryonic brain slices". Values correspond to average migration speeds per cell (μm/h).

	E13.5		E17.5	
	Control	**AMD3100**	**Control**	**AMD3100**
Median	33.5	28.4	25.4	28.9
25% Quant.	22.5	23.2	16.6	20.8
75% Quant.	44.3	38.6	35.7	40.3
Mean	34.6	33.3	28.5	30.4
Std. Dev	16.2	19.0	16.2	14.6
Std. Error	1.3	2.3	0.7	1.6
Sample size	n=161/N=18/M=12	n=68/N=6/M=5	n=501/N=22/M=13	n=87/N=4/M=4
Stat. Test	Student *t*-test		Student *t*-test	
***P*-values**	Control vs AMD: *P* = 0.6103		Control vs AMD: *P* = 0.2842	

Sample size: n=cells, N=slices, M=mothers

Suppl. Table 4.8. Statistical descriptors of data in Fig 4.8 "Age-specific effects of β1 integrin blockage on microglial migration speed in acute embryonic brain slices". Values correspond to average migration speeds per cell (μm/h). *Table continues on next page.*

	E13.5		
	Control	**Isotype**	**β1 Ab**
Median	33.5	26.8	19.2
25% Quant.	22.5	16.7	13.2
75% Quant.	44.3	41.6	26.8
Mean	34.6	30.4	21.1
Std. Dev	16.2	16.4	11.6
Std. Error	1.3	1.7	1.3
Sample size	n=161/N=18/M=12	n=91/N=8/M=5	n=83/N=9/M=5
Stat. Test	Kruskal-Wallis with Dunn's		
***P*-values**	Control vs Iso: *P* = 0.1		
	Control vs β1 Ab: *P*< 0.0001 ***		
	Iso vs β1 Ab: *P* = 0.0003 ***		

Sample size: n=cells, N=slices, M=mothers

	E15.5		
	Control	**Isotype**	**β1 Ab**
Median	33.6	38.4	22.9
25% Quant.	21.2	25.1	14.7
75% Quant.	47.4	51.9	29.6
Mean	36.2	40.0	23.5
Std. Dev	19.7	19.0	11.5
Std. Error	1.5	1.2	0.8
Sample size	n=170/N=10/M=8	n=233/N=11/M=6	n=218/N=11/M=5
Stat. Test	Kruskal-Wallis with Dunn's		
***P*-values**	Control vs Iso: $P = 0.0787$		
	Control vs β1 Ab: $P < 0.0001$ ***		
	Iso vs β1 Ab: $P < 0.0001$ ***		

	E17.5		
	Control	**Isotype**	**β1 Ab**
Median	25.4	22.9	27.2
25% Quant.	16.6	15.7	17.5
75% Quant.	35.7	35.0	37.0
Mean	28.5	26.4	29.4
Std. Dev	16.2	15.4	15.6
Std. Error	0.7	1.0	0.9
Sample size	n=501/N=22/M=13	n=254/N=12/M=7	n=322/N=13/M=6
Stat. Test	Kruskal-Wallis with Dunn's		
***P*-values**	Control vs Iso: $P = 0.1779$		
	Control vs β1 Ab: $P = 0.5450$		
	Iso vs β1 Ab: $P = 0.0124$ *		

Sample size: n=cells, N=slices, M=mothers

Suppl. Table 4.9. Statistical descriptors of data in Fig. 4.9 "Embryonic microglia express several types of β1 integrins". Values correspond to percentage of microglia positive for a marker or to the median fluorescence intensity (MFI), corresponding to the expression level of the marker on average per cell. *Table continues on next page.*

	(A) % α4+			(A) % α5+		
	E13.5	**E15.5**	**E17.5**	**E13.5**	**E15.5**	**E17.5**
Median	13.9	9.5	10.3	99.8	99.9	98.9
25% Quant.	1.0	1.2	2.5	98.8	99.5	97.6
75% Quant.	37.9	14.4	14.0	100.0	100.0	99.4
Mean	18.7	8.3	8.9	99.5	99.2	98.3
Std. Dev	18.8	6.3	6.0	0.6	2.3	1.6
Std. Error	6.7	1.6	1.3	0.2	0.6	0.3
Sample size	N=8/M=3	N=16/M=3	N=20/M=3	N=8/M=3	N=16/M=3	N=20/M=3
Stat. Test	Kruskal-Wallis with Dunn's			Kruskal-Wallis with Dunn's		
***P*-values**	All ages compared: $P = 1$			E13.5 vs E15.5 $P = 1$ E13.5 vs E17.5 $P = 0.4423$ E15.5 vs E17.5: $P < 0.0007$ ***		

	(A) % α6+			(A) % αv+		
	E13.5	**E15.5**	**E17.5**	**E13.5**	**E15.5**	**E17.5**
Median	99.6	99.8	99.7	99.8	99.8	99.7
25% Quant.	98.7	99.5	99.5	98.8	99.5	99.4
75% Quant.	100.0	99.9	99.9	100.0	99.9	99.9
Mean	99.2	99.6	99.5	99.3	99.6	99.5
Std. Dev	1.0	0.6	0.8	1.0	0.3	0.9
Std. Error	0.3	0.2	0.2	0.4	0.1	0.2
Sample size	N=8/M=3	N=16/M=3	N=20/M=3	N=8/M=3	N=16/M=3	N=20/M=3
Stat. Test	Kruskal-Wallis with Dunn's			Kruskal-Wallis with Dunn's		
***P*-values**	All ages compared: $P = 1$			All ages compared: $P = 1$		

Sample size: N=tubes with single or pooled embryonic brains, M=independent experiments

	(B) MFI α4+			(C) MFI α5+		
	E13.5	**E15.5**	**E17.5**	**E13.5**	**E15.5**	**E17.5**
Median	1832.0	1838.0	1882.0	12356.0	9558.0	4479.0
25% Quant.	1509.0	1633.0	1709.0	11678.0	8825.0	4202.0
75% Quant.	2125.0	1923.0	2037.0	14330.0	10207.0	4796.0
Mean	1818.0	1844.0	1887.0	13012.0	9585.0	4462.0
Std. Dev	323.0	278.7	250.6	1801.0	913.8	383.1
Std. Error	114.2	69.7	56.0	636.7	228.4	85.7
Sample size	N=8/M=3	N=16/M=3	N=20/M=3	N=8/M=3	N=16/M=3	N=20/M=3
Stat. Test	Kruskal-Wallis with Dunn's			ANOVA with Tukey HSD on Log10		
***P*-values**	All ages compared: $P = 1$			All ages compared: $P < 0.0001$ ***		

	(D) MFI α6+			(E) MFI αv+		
	E13.5	**E15.5**	**E17.5**	**E13.5**	**E15.5**	**E17.5**
Median	6972.0	8417.0	5854.0	5941.0	6983.0	4291.0
25% Quant.	5258.0	5673.0	3184.0	5566.0	5528.0	3841.0
75% Quant.	14190.0	9192.0	6264.0	17073.0	8038.0	4537.0
Mean	9015.0	7801.0	5060.0	10047.0	6732.0	4194.0
Std. Dev	4462.0	1827.0	1529.0	5992.0	1300.0	539.1
Std. Error	1578.0	456.8	341.9	2119.0	325.0	120.6
Sample size	N=8/M=3	N=16/M=3	N=20/M=3	N=8/M=3	N=16/M=3	N=20/M=3
Stat. Test	Kruskal-Wallis with Dunn's			Kruskal-Wallis with Dunn's		
***P*-values**	E13.5 vs E15.5: $P = 1$			E13.5 vs E15.5: $P = 1$		
	E13.5 vs E17.5: $P = 0.0281$ *			E13.5 vs E17.5: $P < 0.0001$ ***		
	E15.5 vs E17.5: P= 0.0077 **			E15.5 vs E17.5: $P < 0.0001$ ***		

Sample size: N=tubes with single or pooled embryonic brains, M=independent experiments

Suppl. Table 4.10. Statistical descriptors of data in Fig. 4.10 "β1 blockage overrules the effects of α5β1 blockage on microglial migration speed upon combined treatment in acute embryonic brain slices". Values correspond to average migration speeds per cell (μm/h).

	E15.5				
	Control	**α5β1 Ab**	**β1 Ab**	**α5β1+β1 Ab**	**Isotypes**
Median	33.6	43.3	22.9	25.1	44.9
25% Quant.	21.2	28.8	14.7	16.4	29.5
75% Quant.	47.4	59.3	29.6	34.1	56.2
Mean	36.2	44.9	23.5	27.5	45.0
Std. Dev	19.7	20.6	11.5	14.1	19.9
Std. Error	1.5	1.3	0.8	1.2	1.7
Sample size	n=170/N=10/M=8	n=252/N=11/M=6	n=218/N=11/M=5	n=150/N=7/M=3	n=140/N=6/M=2
Stat. Test	Kruskal-Wallis with Dunn's				
***P*-values**	Control vs Isos: *P* = 0.0006 ***		α5β1+β1 Ab vs β1 Ab: *P* = 0.3851		
	Control vs α5β1+β1 Ab: *P* = 0.0005 ***		α5β1+β1 Ab vs α5β1 Ab: *P*< 0.0001 ***		
	Isos vs α5β1+β1 Ab: *P*< 0.0001 ***				

Sample size: n=cells, N=slices, M=mothers

Suppl. Table 4.11. Statistical descriptors of data in Fig. 4.11 "PI3K and MEK1/2 have age specific functions in regulating microglial migration speed in acute embryonic brain slices". Values correspond to average migration speeds per cell (μm/h).

	E13.5			E17.5		
	Control	**Ly294002**	**U0126**	**Control**	**Ly294002**	**U0126**
Median	33.5	17.6	23.0	25.4	15.6	29.8
25% Quant.	22.5	14.3	18.4	16.6	10.3	20.8
75% Quant.	44.3	25.4	28.1	35.7	24.7	40.2
Mean	34.6	21.6	23.7	28.5	18.1	32.2
Std. Dev	16.2	11.3	8.9	16.2	9.8	15.5
Std. Error	1.3	1.9	1.3	0.7	0.9	1.6
Sample size	n=161/N=18/M=12	n=35/N=4/M=4	n=44/N=4/M=4	n=501/N=22/M=13	n=110/N=5/M=5	n=92/N=5/M=5
Stat. Test	Kruskal-Wallis with Dunn's			Kruskal-Wallis with Dunn's		
***P*-values**	Control vs Ly294002: *P* < 0.0001 ***			Control vs Ly294002: *P* < 0.0001 ***		
	Control vs U0126: *P* = 0.0002 ***			Control vs U0126: *P* = 0.0315 *		
	U0126 vs Ly294002: *P* = 0.8854			U0126 vs Ly294002: *P*< 0.0001 ***		

Sample size: n=cells, N=slices, M=mothers

CHAPTER 5:

Maternal immune activation evoked by polyinosinic:polycytidylic acid does not evoke microglial cell activation in the embryo

Based on: Smolders S*, Smolders SMT*, Swinnen N, Gärtner A, Rigo JM°, Legendre P°, Brône B°. Maternal immune activation evoked by polyinosinic:polycytidylic acid does not evoke microglial cell activation in the embryo. Front Cell Neurosci, 2015. Aug 5;9:301.*° equally contributing.

Own contribution: Participation in P(I:C) injections, sample collections, immunofluorescent stainings and their quantification, flow cytometry on brain suspension. Participation in figure preparation and writing of the manuscript.

5.1 Abstract

Several studies have indicated that inflammation during pregnancy increases the risk for the development of neuropsychiatric disorders in the offspring. Morphological brain abnormalities combined with deviations in the inflammatory status of the brain can be observed in patients of both autism and schizophrenia. It was shown that acute infection can induce changes in maternal cytokine levels which in turn are suggested to affect fetal brain development and increase the risk on the development of neuropsychiatric disorders in the offspring. Animal models of maternal immune activation reproduce the etiology of neurodevelopmental disorders such as schizophrenia and autism. In this study the Poly (I:C) model was used to mimic viral immune activation in pregnant mice in order to assess the activation status of fetal microglia in these developmental disorders. Because microglia are the resident immune cells of the brain they were expected to be activated due to the inflammatory stimulus.

Microglial cell density and activation level in the fetal cortex and hippocampus were determined. Despite the presence of a systemic inflammation in the pregnant mice, there was no significant difference in fetal microglial cell density or immunohistochemically determined activation level between the control and inflammation group. These data indicate that activation of the fetal microglial cells is not likely to be responsible for the inflammation induced deficits in the offspring in this model.

5.2 Introduction

Schizophrenia and autism are neurodevelopmental disorders that can arise early during postnatal life. Although genetic deficits are important risk factors, perturbations of local environment, especially during pregnancy, are suspected to play a central role in the occurrence of these neurodevelopmental disorders. Maternal immune activation during pregnancy is considered as a risk factor for schizophrenia and autism in the offspring [525]. To study the mechanisms behind this association several animal models were developed in which pregnant rodents were infected with the influenza virus, polyinosinic:polycytidylic acid [Poly (I:C)] or lipopolysaccharide (LPS) [526]. These models confirmed that prenatal infection leading to maternal immune activation (MIA) can lead to behavioural and neurological disorders in the offspring [151, 222, 248, 527-530]. During MIA evoked by Poly (I:C), an elevated maternal serum cytokine, interleukin-6 (IL-6), was found to be critical for the development of these neurological deficits in the offspring [217, 531]. Differences in behavioural abnormalities observed in the offspring at adult age are critically dependent on the time of maternal Poly (I:C) challenge, being related to differences in cytokine responses in the fetal brain shortly after the induction of MIA [248, 532]. However, the source of the cytokine response in the fetal brain remains a matter of debate as it can originate from maternal, placental and/or embryonic tissue. An endogenous increase in fetal brain cytokine production was demonstrated using mRNA analysis of the cytokine expression level upon maternal Poly (I:C) challenge during the late gestation stage in mice (17 embryonic days, E17) [248]. This was not oberved when maternal Poly (I:C) challenge was performed at mid gestation stage (E9) [248], a developmental age at which immature microglia, the resident immune cells of the brain, have not yet invaded the fetal central nervous system (CNS) [20, 37, 72].

Microglia colonize the brain early during embryonic development (E11.5 in the mouse embryo) [20, 37, 72] and are known to control several developmental processes in the brain at perinatal developmental stages [73, 144, 151]. First, embryonic microglia have been shown to be involved in angiogenesis through close contact with vessel sprouts and endothelial tip cells and the secretion of soluble factors that stimulate angiogenesis during development [159, 162]. Secondly, during CNS development microglial cells clear cellular debris and induce programmed cell death in developing neurons via the production of superoxide ions [141, 142] and tumour necrosis factor (TNF)-α [533]. Thirdly, several studies have pointed towards an important role for microglia in synaptic remodeling and synapse elimination [64, 156, 174, 534]. Finally, microglial cells can also influence the development and differentiation of neural cells. Microglia-conditioned media can influence embryonic precursor migration and differentiation in primary cultures [535, 536]. In addition, microglial cells can regulate cortical precursor proliferation and astrogenesis [252]. Primary culture experiments on embryonic precursor cultures showed that microglial cells are important for precursor proliferation and astrogenesis. In microglia-depleted cultures and cultures from PU.1 knock out embryos proliferation and astrogenesis were decreased. Addition of microglia to these cultures restored both processes and an abnormal increase in microglial cell numbers resulted in increased astrogenesis [400]. Deactivation of embryonic microglia with tetracyclines or elimination via the macrophages suicide technique led to an increase in neural precursor cells, while microglial activation had the opposite effect [144].

MIA induces an imbalance in cytokines levels, of which maternal IL-6 has been shown to be a critical mediator in inducing the effects of MIA on brain development and behavioural changes [217]. IL-6 is known to induce activation of adult microglial cells; leading to the production of pro-inflammatory factors, such as nitric oxide, reactive oxygen species, proteolytic enzymes and TNF-α by microglial cell cultures [537], microglial proliferation (*in vitro*) [538] and infiltration (*in vivo*) [539] or the upregulation of microglial CX3CR1, making them more sensitive to fractalkine signaling [540]. An imbalance in cytokine levels caused by MIA might thus be able to activate embryonic microglia, even at early developmental stages, and alter their normal functions. This can trigger a cascade of events that could lead to developmental defects observed in the offspring of LPS or Poly (I:C) treated pregnant mice. Indeed, MIA evoked by LPS injection evoked microglia activation and enhanced phagocytosis of neural precursors by microglia at prenatal stages in rats [144]. However, the question remains whether an endogenous increase in fetal brain cytokine production in response to maternal Poly (I:C) challenge is of microglial origin. Accordingly it remains unclear whether Poly (I:C)-induced MIA results in the activation of embryonic microglia during fetal development.

To determine to what extent MIA evoked by Poly (I:C) can alter cortex invasion by microglia and/or change embryonic microglial cell activation state, we evoked MIA using a single (at E11.5) or a double injection (at E11.5 and E15.5) of Poly (I:C) [248, 541]. This developmental time window is an important time point for cortex invasion by immature microglia as their cell density dramatically increases during this period [72]. We show that Poly (I:C)-induced MIA does not affect microglial density and activation level during embryonic development suggesting that pathological activation

of embryonic microglial cells at the onset of their colonization processes cannot explain neurological deficits observed at postnatal stages in offspring after Poly (I:C)-induced MIA

5.3 Materials and Methods

5.3.1 BV-2 cell culture

The immortalized mouse microglial cell line BV-2 (kindly provided by Dr. F. Stassen, Maastricht, The Netherlands) was cultured in Dulbecco's Modified Eagle Medium containing 10% fetal calf serum, 2mM glutamine and 1 % penicillin streptomycin (all from Life Technologies). Cells were detached by incubation with PBS-EDTA 20 mM for 10 minutes at room temperature before proceeding with filtering for flow cytometry.

5.3.1 Animals

All experiments were conducted in accordance with the European Community guiding principles on the care and use of animals and with the approval of the Ethical Committee on Animal Research of Hasselt University. Mice were maintained in the animal facility of the Hasselt University in accordance with the guidelines of the Belgian Law and the European Council Directive. To visualize microglia in the embryonic cortex the transgenic CX3CR1-eGFP knock-in mice [403] were used. The heterozygous CX3CR1-eGFP +/- embryos used in this study were obtained by crossing wild type C57BL/6 females with homozygous CX3CR1-eGFP +/+ male mice (obtained from the European Mouse Mutant Archive – EMMA with the approval of Stephen Jung [403]). The day of conception was designated as embryonic day 0.5 (E0.5).

5.3.2 Maternal immune activation

At day E11.5 (single injection) or at E11.5 and E15.5 (double injection) mice received i.p. a dose of Poly (I:C) (20mg/kg) (Polyinosinic–polycytidylic acid potassium salt; Sigma-Aldrich, Bornem, Belgium) or vehicle (saline). Five hours after injection the maternal blood was collected, the serum was aliquoted and stored at -80°C until the IL-6 assay was performed [217, 222]. The maternal IL-6 concentrations were determined using the Mouse IL-6 ELISA Kit from Thermo Scientific (Rockford, Illinois, USA), following the manufacturer's instructions. The analysis was conducted using a FLUOstar OPTIMA plate reader (BMG Labtech, Ortenberg, Germany).

5.3.3 Fluorescent immunostaining of embryonic brains

Pregnant mice were sacrificed and embryonic tissue processed as described before [72]. The heads of E11.5 and E12.5 embryos were fixed in 4% paraformaldehyde for 3 hours at 4°C and 5 hours for E17.5 embryos. After fixation, the embryonic heads were cryoprotected overnight in phosphate-buffered saline (PBS) + 30% sucrose, frozen in optimal cutting temperature compound (Tissue-Tek) and stored at -80°C until sectioned. Ten micrometer-thick coronal tissue sections were cut on a Leica CM1900 uv cryostat, mounted on Superfrost Plus glasses and stored at -20°C until staining.

To check whether embryonic microglia can be directly activated by Poly (I:C), IL-6 or LPS, 300-µm thick coronal brain slices (E15.5) were cultured for 24 hours with either saline, Poly (I:C) (50

µg/ml), IL-6 (10 ng/ml) or LPS (1 µg/ml). To this end, pregnant mothers were euthanized at E15.5. Embryonic brains were isolated in ice-cold PBS-glucose (pH 7.4; 25mM), embedded in 3% low melting agarose (Fisher Scientific) and sliced coronally at a thickness of 300 µm using a Microm HM650V Vibrating Blade Microtome. Slices were mounted on MilliCell organotypic inserts (Millipore) and maintained in semi-hydrous conditions at 37°C and 5% CO2 for 24 hours. The media consisted of Neurobasal medium supplemented with 2mM L-glutamine, B27 supplement, N2 supplement and 0.5% penicillin-streptomycin (all from Invitrogen) with either saline, Poly (I:C) (50 µg/ml), IL-6 (10 ng/ml) or LPS (1 µg/ml) added. Afterwards slices were fixed for 1 hour in 4% PFA and cryoprotected overnight in PBS + 30% sucrose, frozen in optimal cutting temperature compound (Tissue-Tek) and stored at -80°C until sectioned. Ten micrometer-thick coronal tissue sections were cut on a Leica CM1900 uv cryostat, mounted on Superfrost Plus glasses and stored at -20°C until staining.

In order to determine the activation state of the microglia, we used antibodies against interleukin (IL)-1β, inducible nitric oxide synthase (iNOS) and Mac-2/Galectin-3 [37, 144]. All primary antibodies and working solutions are listed in **Table 5.1**.

Table 5.1. Overview of the antibodies used for immunostainings and flow cytometry experiments.

Antibody	Company	Reference	Dilution
Immunohistochemistry			
Anti-IL1β (rabbit polycl.)	Abcam	ab9722	1:100
Anti-iNOS (rabbit polycl.)	Abcam	ab15323	1:250
Anti-Mac-2 (rat monocl.)	American Type Culture Collection	TIB-166	1:250
Flow cytometry			
Anti-IL1β PE (rat monocl.)	LifeSpan BioSciences	LS-C184791	1:300
Anti-iNOS PE-Cy7 (rat monocl.)	eBioscience	25-5920	1:300
Anti-Mac-2 PE (rat monocl.)	eBioscience	12-5301	1:300

5.3.4 Isolation of microglia and flow cytometry experiments

Brains were isolated from CX3CR1-eGFP +/- E17.5 embryos from mothers subjected to a single saline or Poly (I:C) injection on E11.5, or a double Poly (I:C) injection on E11.5 and E15.5. All steps occurred at 4°C or on ice, unless stated otherwise, to avoid microglia activation. Meninges were removed, the cortical area identical to the immunohistochemical analysis was dissected out and incubated during 30min at 30°C in DMEM/F-12(1:1) + GlutaMAX (Life Technologies) containing 48U/ml Papain from papaya latex (Sigma). Papain containing supernatants was discarded and the tissue was mechanically disrupted in medium through fast pipetting using a 1 ml pipet. Afterwards, the homogenate was centrifuged at 400g during 5 min, resuspended in 40% isotonic Percoll (GE Healthcare) and centrifuged at 700g during 10min without break. The pellet was resuspended in PBS and filtered through a 35µm cell strainer. Cell suspensions were fixed and permeablized in Cytofix/Cytoperm buffer (BD Cytofix/Cytoperm™ Plus Fixation/Permeabilization Kit, BD Biosciences) during 20 min on ice, washed and incubated on ice for 30 min in Perm/Wash buffer

with a mix of fluorochrome-conjugated rat anti-mouse antibodies: iNOS-PE-Cy7 (clone CXNFT, eBioscience), Mac-2-PE (clone eBioM3/38, eBioscience) and IL1β-PE (clone 11n92, LifeSpan BioSciences) **(Table 5.1)**. The following isotype controls were used: Rat IgG2aκ PE-Cy7, Rat IgG2aκ PE and Rat IgG2b PE (all from eBioscience). After washes, cells were resuspended in FACS buffer (PBS, 2% FCS, sodium azide), acquired in a FACS Aria II and analysed with FACS Diva 6.1.3 software (BD Biosciences). Isotype-marker overlay graphs were created in FlowJo 10.0.8 Software. Inside the singlet population, the eGFP positive microglia (1000-12000 cells per experiment) were gated **(Fig. 5.5A)**, and within this population, the percentage of Mac-2, iNOS and IL1β positive microglia was analysed. Isotype controls were used to gate the positive cell population (Fig. 5.5 B). Per group, embryos were derived from one to three different mothers (saline, single Poly (I:C), double Poly(I:C)). BV-2 cells **(Suppl. Data)** were used as positive controls for the different antibodies (Fig. 5.6).

5.3.5 Analysis and statistics

Quantitative analysis of microglial cells was performed on images of coronal embryonic brain sections. We focused our analysis on the cerebral cortex area located dorsally to the lateral ganglionic eminences (LGE) and medial ganglionic eminences (MGE), containing the frontal and pariental cortex on E11.5 and E12.5, and the somatosensory and motor cortex at E17.5. This region of the cortex is well characterized on the functional and cellular level and the two GE structures are the major sources of cortical interneurons during embryonic neurogenesis [416, 418]. For the quantifications of the hippocampal area at E17.5 only the dorsal hippocampus was included in the analysis.

Images were taken with a Nikon Eclipse 80i microscope and a Nikon digital sight camera DS-2MBWc (10x Nikon plan objective (numerical aperture (NA) of 0.25) and a 20x Plan Fluor objective (NA of 0.5)). Images (1600 x 1200) were analysed with ImageJ 1.45e software (NIH, USA; http://rsb.info.nih.gov/ij/). Only eGFP-positive cell bodies were taken into account for the measurements. Density analysis was performed by counting the number of eGFP positive cell bodies per mm² [72]. For analysis of activation state we calculated the percentage of the eGFP positive cells that were also showing immunoreactivity for the activation marker. All values are expressed as mean ± S.E.M. The number of sections used is indicated as n, the number of embryos or blood samples as N; # sections/# embryos is thus designated in the text as n/N. Statistical significance was assessed by nonparametric Mann Whitney test or Kruskal-Wallis test, *P*-values smaller than 0.05 were considered significant.

5.4 Results

An increase in IL-6 level in the maternal blood is a crucial factor in the development of MIA-induced deficits and changes observed in the offspring [217]. To control that the Poly (I:C) injection procedure we used evoked an increase in IL-6 level in the maternal blood, we analysed the IL-6 level in the maternal serum samples 5 hours after injection of either saline or Poly (I:C). We found a significant increase ($P < 0.0001$; Mann Whitney test) in the level of IL-6 in the sera of female mice primed with Poly (I:C) (1876 ± 389.2 pg/ml, N = 22) when compared to those injected with

saline (14.8 ± 3.3 pg/ml, N = 26), thus indicating that the mice in the Poly (I:C) group effectively suffered from a systemic immune response.

In response to brain injury, microglia proliferate and shift to beneficial or detrimental activation states depending on the local environment. When activated, microglial cells adopt a phagocytic phenotype in order to clear dying cells [32]. In pathological conditions, such as in the mouse model of LPS-induced MIA, phagocytosis of neuronal precursor cells by microglia was also increased, which resulted in a decrease in the size of the precursor cell pool in the cerebral cortex [144]. It must also be noted that microglial disturbances were also observed in patients suffering from autistic or schizophrenic disorders. Microglial activation has been observed in the brains of autistic [229, 230] and schizophrenic patients [226, 542, 543]. Recent studies also indicated that there is an increase in microglial density in different brain regions in the adult Poly (I:C) MIA offspring [544, 545].

To determine if Poly (I:C)-evoked MIA alters the embryonic microglial cell colonization process in the fetal brain we compared cell density after single injection of Poly (I:C), double injection of Poly (I:C) or saline treatments, in the cortex at E11.5, E12.5 and at E17.5 (single injection) or at E17.5 (double injections) and in the hippocampal area at E17.5 (single and double injections). At all ages tested we did not find any significant difference in microglia cell density (Mann Whitney test; $P > 0.05$, for detailed *P*-values see **Table 5.2**) in the cortex or in the hippocampus after a single or after double injections **(Fig. 5.1 and Table 5.2)**, thus suggesting that Poly (I:C)-evoked MIA does not alter early invasion of the cortex and the hippocampus by microglial cells in the embryo.

Table 5.2. Microglial cell density in the cortex and hippocampal area of embryos derived from the control group and the group that was subjected to maternal inflammation at E11.5 or at E11.5 and E15.5.

	Single injection at E11.5			
Brain structure	*Cortex*			*Hippocampus*
Embryonic age	*E11.5*	*E12.5*	*E17.5*	*E17.5*
Saline	48.6 ± 8.8	34.9 ± 2.8	59.6 ± 5.8	122.5 ± 4.9
Poly (I:C)	32.2 ± 5.7	37.8 ± 2.9	56.5 ± 4.3	111.6 ± 5.7
***P* value**	*0.191*	*0.375*	*0.573*	*0.435*
	Double injection at E11.5 and E15.5			
Brain structure	*Cortex*			*Hippocampus*
Embryonic age	*E17.5*			*E17.5*
Saline	59.8 ± 3.1			95.3 ± 4.8
Poly (I:C)	57.8 ± 2.2			91.0 ± 5.7
***P* value**	*0.931*			*0.699*

Values are mean ± SEM of the number of microglial cells per mm², Mann Whitney test was used for statistical analysis. When injected at E11.5 the numbers of embryonic brains in the saline and Poly (I:C) group were respectively: E11.5 = 4/5; E12.5 = 12/7; E17.5 cortex = 6/8; E17.5 hippocampus = 5/8. When injected at E11.5 and E15.5 numbers of embryonic brains in the saline and Poly (I:C) group were respectively: E17.5 cortex = 5/6; E17.5 hippocampus = 6/6.

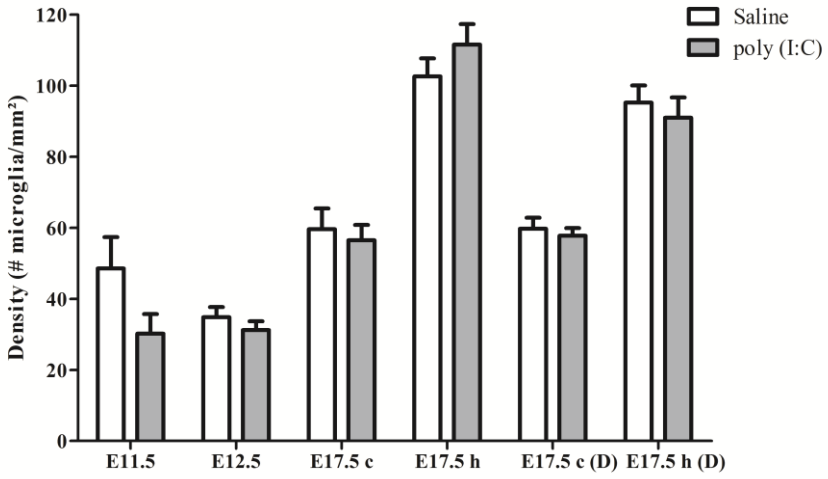

Fig. 5.1. Embryonic microglial cell density is not increased after single and double injection of Poly (I:C). Microglial cell density in the cortex and hippocampal area was not affected after Poly (I:C)-induced MIA. Values are mean ± SEM of the number of microglial cells per mm², Mann Whitney test was used for statistical analysis. When injected at E11.5 the numbers of embryonic brains in the saline and Poly (I:C) group were respectively: E11.5 = 4/5; E12.5 = 12/7; E17.5 cortex = 6/8; E17.5 hippocampus = 5/8. When injected at E11.5 and E15.5 numbers of embryonic brains in the saline and Poly (I:C) group were respectively: E17.5 cortex = 5/6; E17.5 hippocampus = 6/6. c, cortex; h, hippocampal area; (D), double injection.

To determine if MIA induced a change in microglial activation level after a single Poly (I:C) injection (E11.5), we performed an immunostaining for three different activation markers: Mac-2/Galectin-3, iNOS and IL1β at E11.5 and E17.5.Mac-2/Galectin-3 is a marker of microglial phagocytic activation state [188, 546] while iNOS and IL1β are markers of a cytotoxic activation state [144]. At E11.5 none of the microglia located in the cortex was immmunopositive for Mac-2 staining both after saline injection (n/N = 14/3) and after Poly (I:C) challenge (n/N = 18/3) **(Fig. 5.2B1 and B2)**. At E17.5, 2.5 ± 0.5% (n/N = 38/4) of the microglia in the cortex **(Fig. 5.2A1 and A2)** and 3.2 ± 0.7% (n/N = 27/4) of the microglia in the hippocampal area expressed Mac-2 after saline injection. We did not find any significant difference ((Kruskal-Wallis test; *P* = 0.448) after Poly (I:C) challenge. After Poly (I:C) challenge, 1.9 ± 0.7% (n/N = 23/4) of the microglia in the cortex and 2.5 ± 1% (n/N = 15/4) of microglia in hippocampal area expressed Mac-2 **(Fig. 5.2C1, C2, D1 and D2)**. We next investigated the expression of IL1β and iNOS [144] to determine if embryonic microglia can adopt a cytotoxic activation state after a single injection of Poly (I:C). Induction of MIA by a single injection of Poly (I:C) did not result in a significant increase in the percentage of microglia expressing IL1β either at E11.5 and E17.5 (Kruskal-Wallis test; *P* = 0.136). In control conditions, 0 ± 0% (n/N = 6/3) and 2.2 ± 1% (n/N = 15/4) of microglia located in the cortex expressed IL1β at E11.5 and E17.5 **(Fig. 5.3A1 and A2)** respectively while 3.1 ± 1.3% (n/N = 17/4) expressed IL1β in the hippocampal area (E17.5). After Poly (I:C) challenge, 3.3 ± 3.3% (n/N = 10/3) and 3.5 ± 1% (n/N = 19/4) of microglia located in the cortex expressed IL1β at E11.5 **(Fig. 5.3 B1 and B2)** and at E17.5 **(Fig. 5.3C1 and C2)** respectively, while 7.2 ± 2.6 % (n/N = 17/4) expressed IL1β in the hippocampal area (E17.5) **(Fig. 5.3D1 and D2)**. We found similar results when analyzing iNOS expression at E11.5 and E17.5 in the cortex and in the hippocampal area (E17.5). Cortical iNOS expression in control conditions (E11.5: 8.3 ± 5.7%, n/N = 10/3; E17.5: 2.0 ± 1.1%, n/N = 15/4 **(Fig. 5.4A1 and A2)**) was not significantly different when compared to the Poly (I:C) condition (E11.5: 0 ± 0%, n/N = 8/3 (Fig. 5.4 B1 and B2); E17.5 :1.9 ± 1.1%, n/N = 12/4 **(Fig. 5.4C1 and C2)** (Kruskal-Wallis test; *P* = 0.471). In the hippocampal

area, 1.5 ± 1.0% of microglia (n/N = 14/4) express iNOS in control conditions while 0 ± 0%, of microglia (n/N = 10/4) express iNOS after Poly (I:C) challenge (Fig. 5.4 D1 and D2, being not significantly different (Kruskal-Wallis test; $P = 0.471$)).

This lack of change in embryonic microglia activation state after a single Poly (I:C) injection could possibly lead only to a "primed" microglial state. Indeed, two injections of LPS were necessary in rat to elicit MIA induced microglia dysfunction during phagocytosis of cortical neural precursor cells [144], suggesting that the microglial phenotype could become only fully altered after the second inflammatory challenge. To determine if this is also the case for Poly (I:C) we reanalysed microglial density and activation level after a repeated injection of Poly (I:C). Consequently, the mothers suffered from a double immune stimulation (on E11.5 as well as on E15.5). Despite the presence of a maternal immune response after both injections, there was no significant increase in microglial cell density (Mann Whitney test; $P > 0.05$, for detailed *P*-values see **Table 5.2**) **(Fig. 5.1 and Table 5.2)**. Microglial activation states were analysed at E17.5 as described above. We did not find any significant difference (Kruskal-Wallis test; Mac-2, $P = 0.139$; IL1β, $P = 0.945$; iNOS, $P = 0.093$) in the percentage of microglia expressing Mac-2, IL1β or iNOS between control conditions and after double injections of Poly (I:C). After double injections of Poly (I:C) the percentage of microglia immunoreactive for Mac-2 antibody was 0 ± 0% (n/N = 29/6) in the cortex **(Fig. 5.2E1 and E2)** and 2.0 ± 0.7% (n/N = 22/6) in the hippocampal area **(Fig. 5.2F1 and F2)**. In the cortex **(Fig. 5.3E1 and E2)** and hippocampal area **(Fig. 5.3F1 and F2)** 1.4 ± 0.7% (n/N = 34/6) and 1.4 ± 1.0% (n/N = 25/6) of the microglial cells showed immunoreactivity for the IL1β antibody, while 1.8 ± 0.7% (n/N = 34/6) and 0 ± 0% (n/N = 23/6) of the microglia were positive for iNOS in the cortex **(Fig. 5.4E1 and E2)** and hippocampal area **(Fig. 5.4F1 and F2)**, respectively. These results indicate that even double injections of Poly (I:C) did not evoke microglia activation in the embryo.

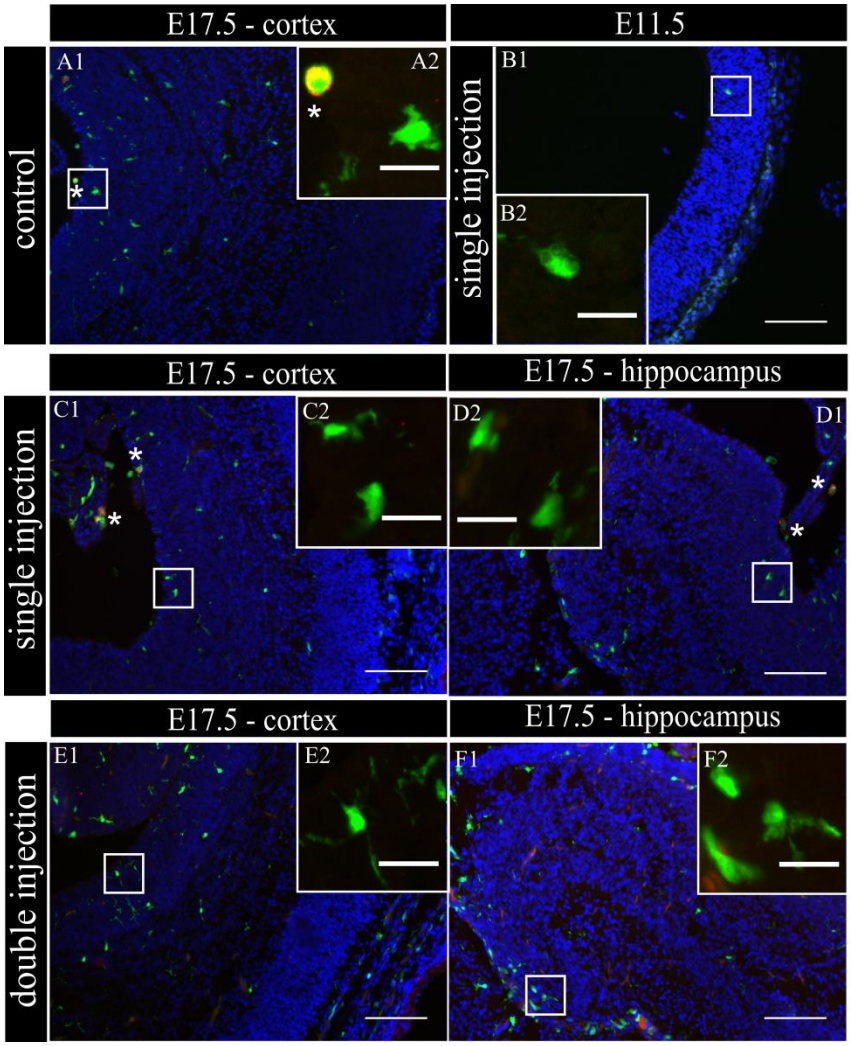

Fig. 5.2. Embryonic microglial cell population is poorly immunoreactive to the Mac-2/Galectine-3 antibody after single and double injection of Poly (I:C). (A-F1) Coronal sections of embryonic brains, with cell nucleus staining in blue (DAPI) and microglial (CX3CR1-eGFP) cells in green. Immunohistochemical staining using a Mac-2 antibody (red) showed that at E17.5 almost no microglial cells in the cortex were immunoreactive for Mac-2 **(A2)** after injection with saline. At E11.5 **(B2)** and E17.5 **(C2 and E2)** in the cortex and E17.5 hippocampal area **(D2 and F2)** there was no increased percentage of microglial cells expressing the activation marker after Poly (I:C) challenge compared to control. White square indicates the location of the cells in the tissue showed in the inset; * indicates a Mac-2 positive eGFP cell. Examples of one control brain area and Poly (I:C) group only as they were not significantly different. Scale bar = 100 μm and for insets = 20 μm.

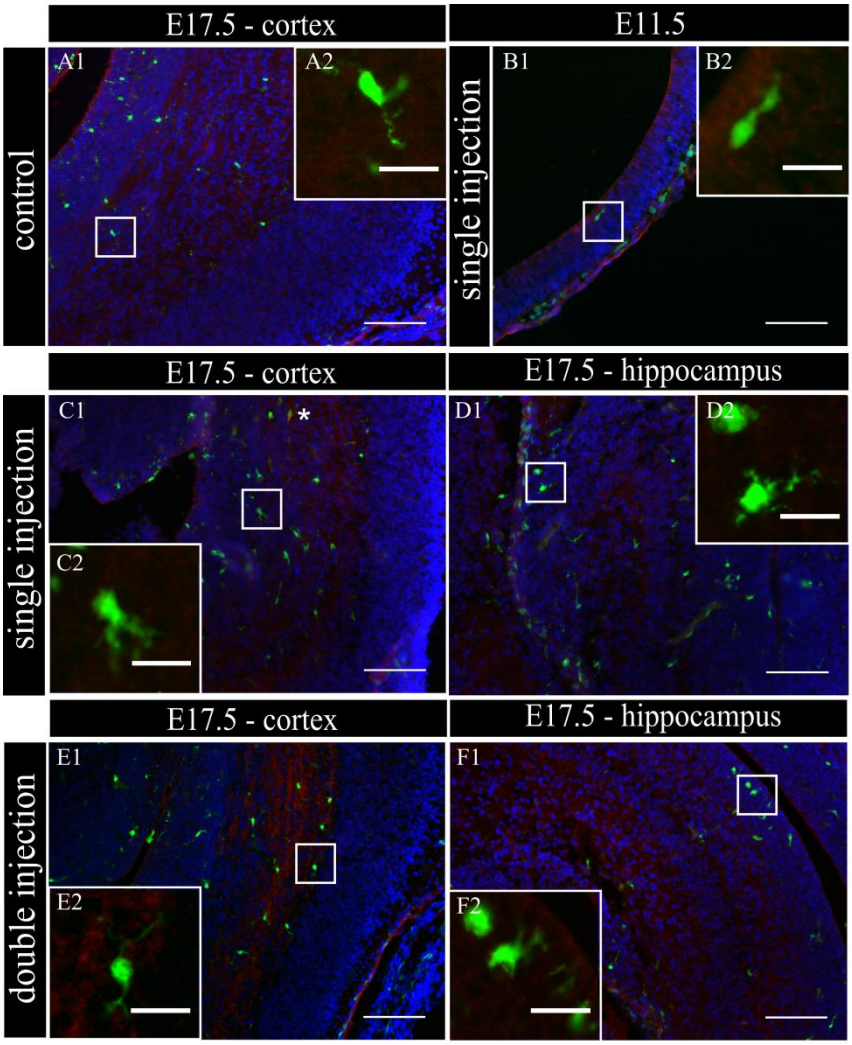

Fig. 5.3. Embryonic microglia show no increased expression of IL1β after single and double injection of Poly (I:C). (A-F1) Coronal sections of embryonic brains, with cell nucleus staining in blue (DAPI) and microglial (CX3CR1-eGFP) cells in green. Immunohistochemical staining using an IL1β antibody (red) showed that at E17.5 almost no microglial cells in the cortex were immunoreactive for IL1β **(A2)** after injection with saline. At E11.5 **(B2)** and E17.5 **(C2 and E2)** in the cortex and E17.5 hippocampal area **(D2 and F2)** there was no increased percentage of microglial cells expressing the activation marker after Poly (I:C) challenge compared to control. White square indicates the location of the cells in the tissue showed in the inset; * indicates an IL1β positive eGFP cell. Examples of one control brain area and Poly (I:C) group only as they were not significantly different. Scale bar = 100 μm and for insets = 20 μm.

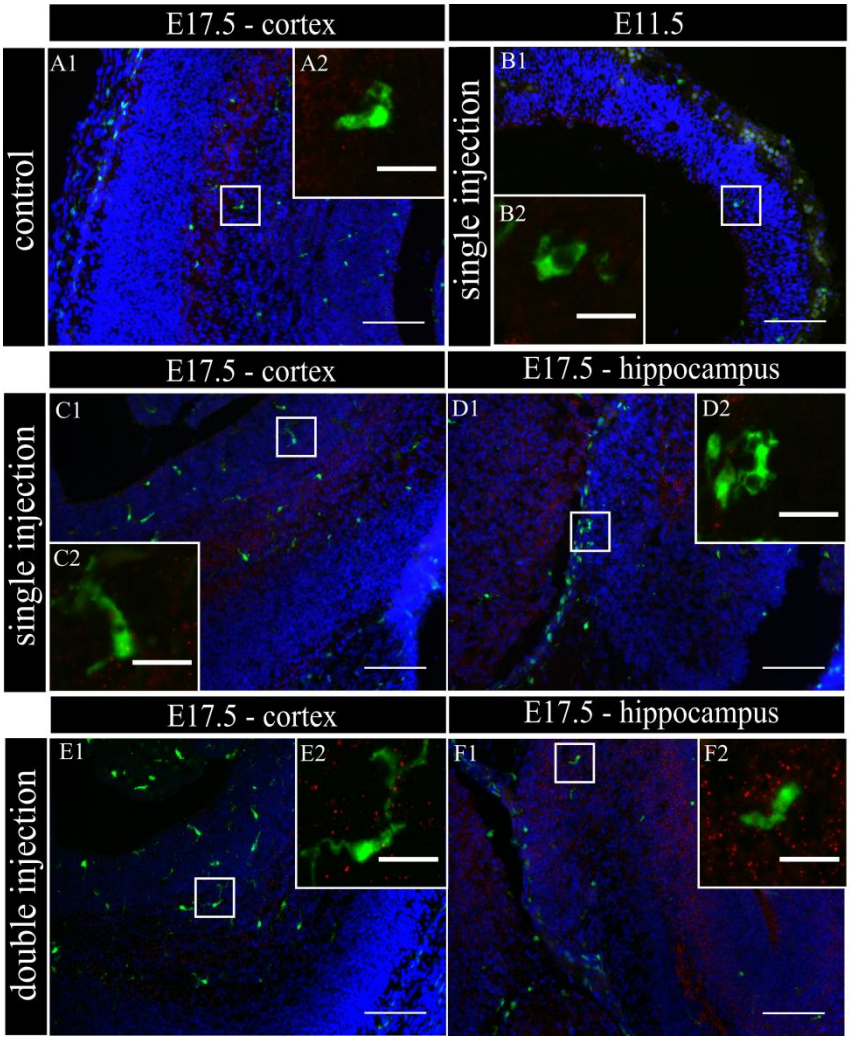

Fig. 5.4. Embryonic microglia cell population is poorly immunoreactive to the iNOS antibody after single and double injection of Poly (I:C). (A-F1) Coronal sections of embryonic brains, with cell nucleus staining in blue (DAPI) and microglial (CX3CR1-eGFP) cells in green. Immunohistochemical staining using an iNOS antibody (red) showed that at E17.5 almost no microglial cells in the cortex were immunoreactive for iNOS **(A2)** after injection with saline. At E11.5 **(B2)** and E17.5 **(C2 and E2)** in the cortex and E17.5 hippocampal area **(D2 and F2)** there was no increased percentage of microglial cells expressing the activation marker after Poly (I:C) challenge compared to control. White square indicates the location of the cells in the tissue showed in the inset. Examples of one control brain area and Poly (I:C) group only as they were not significantly different. Scale bar = 100 μm and for insets = 20 μm.

In addition to the immunohistochemical stainings, the presence of the activation markers on microglial cells at E17.5 was investigated by flow cytometry. The gating strategy and positive controls are shown in **Fig. 5.5A,B and Fig 5.6**. The results of the flow cytometric quantifications were similar to those obtained by immunohistochemistry. There was no significant difference in the proportion of microglial cells that were positive for Mac-2 after single Poly (I:C) injection (16.8 ± 0.0 %; N = 10) or double Poly (I:C) injection (27.0 ± 4.6 %; N = 10) when compared to the control group (15.5 ± 4.3; N = 5) (**Fig. 5.5C**, left panel; Kruskal-Wallis test, $P = 0.161$). The proportion of microglial cells that were positive for IL1β in the control group (14.2 ± 3.1 %; N = 10) was not significantly different (**Fig. 5.5C**, middle panel; Kruskal-Wallis test, $P = 0.093$) to the percentage of microglia that was positive for IL1β after a single (22.3 ± 3.9 %; N = 8) or double Poly (I:C) injection (16.0 ± 2.1 %; N = 6). The percentage of microglial cells positive for iNOS in the control group was 9.1 ± 2.8 % (N = 5). There was no significant effect (**Fig. 5.5C**, right panel; Kruskal-Wallis test, $P = 0.816$) of a single Poly (I:C) (7.1 ± 1.5 %; N = 10) or double Poly (I:C) challenge (9.9 ± 2.7 %; N = 10) on the percentage of microglia expressing this marker.

(next page) **Fig. 5.5. Flow cytometry reveals that embryonic microglial cells show a poor expression of activation markers Mac-2, IL1β and iNOS. (A)** Gating strategies for the microglial cells. In the whole embryonic cortex cell suspension, a gate was created on the non-debris population (left). Inside this population, single cells were selected (middle) and within this population, the microglial cells were gated based on CX3CR1-eGFP intensity (right). SSC, Side scatter; FSC, Forward scatter. **(B)** Gating strategies for positive Mac-2, iNOS and IL1β populations. Microglial cell count of representative samples is shown for Mac-2 (left), IL1β (middle) and iNOS (right; full lines) for embryos derived from saline, single Poly (I:C) and double Poly (I:C) injected mothers. Gates for positive populations were drawn based on the isotype fluorescence intensity (dotted lines). FI, fluorescence intensity. **(C)** Left panels: At E17.5 only a small percentage of microglial cells shows reactivity for Mac-2. There is no significant effect of Poly (I:C) injection on this percentage. Number of embryos tested: Saline N = 5; single Poly (I:C) N = 10 and double Poly (I:C) N = 10. Middle panels: In control conditions, less than 15 % of the microglial cells is positive for IL1β. There is no significant effect of Poly (I:C) injection on this proportion. Number of embryos tested: Saline N = 10; single Poly (I:C) N = 8 and double Poly (I:C) N = 6. Right panels: At E17.5 less than 10 % of the microglial cells is positive for iNOS. Poly (I:C) challenge has no significant effect on this percentage. Number of embryos tested: Saline N = 5; single Poly (I:C) N = 10 and double Poly (I:C) N = 10.

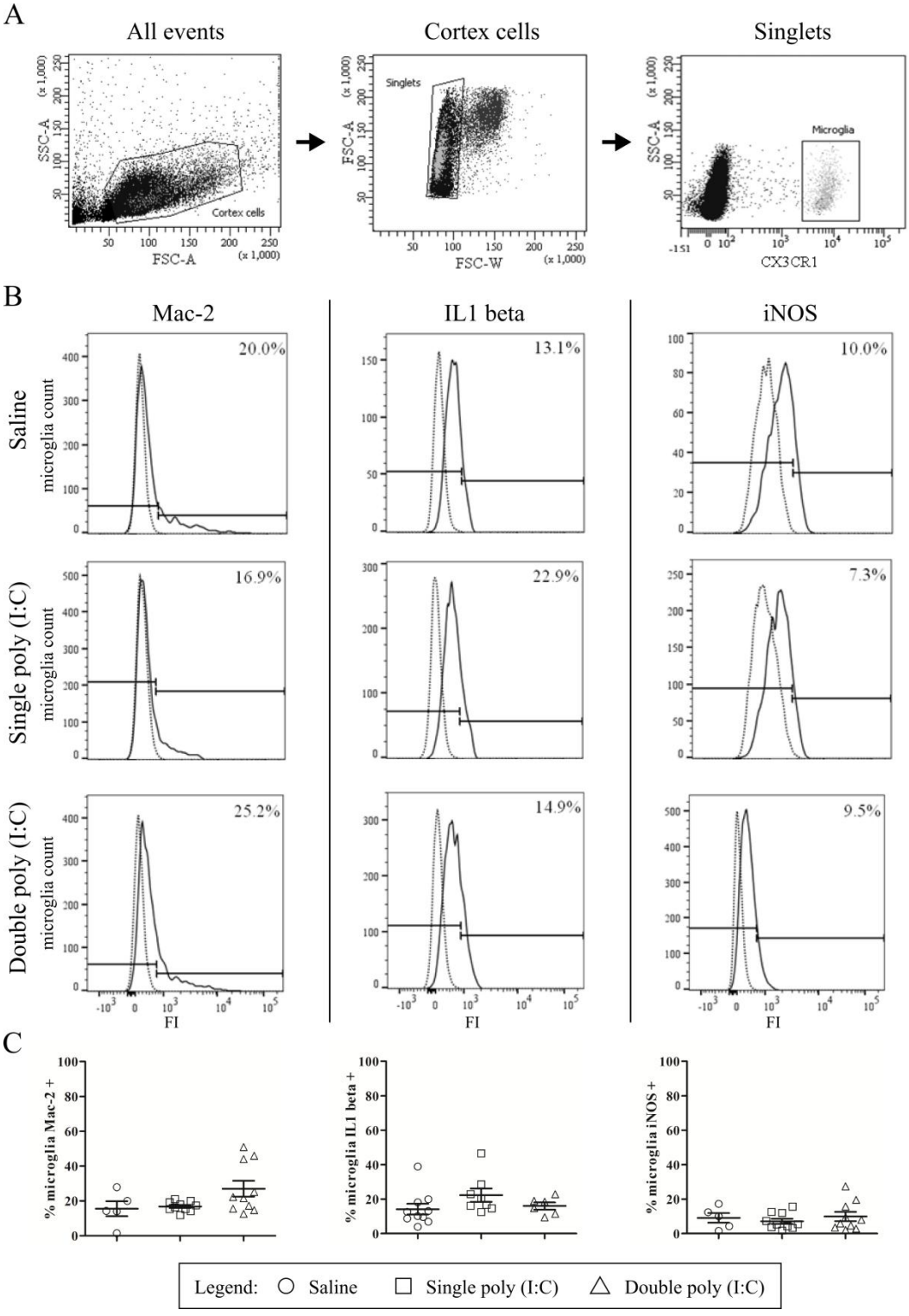
A
All events
Cortex cells
Singlets
SSC-A
FSC-A
Cortex cells
FSC-A
FSC-W
Singlets
SSC-A
CX3CR1
Microglia
B
Mac-2
IL1 beta
iNOS
Saline
Single poly (I:C)
Double poly (I:C)
microglia count
20.0%
13.1%
10.0%
16.9%
22.9%
7.3%
25.2%
14.9%
9.5%
FI
C
% microglia Mac-2 +
% microglia IL1 beta +
% microglia iNOS +
Legend: Saline Single poly (I:C) Double poly (I:C)

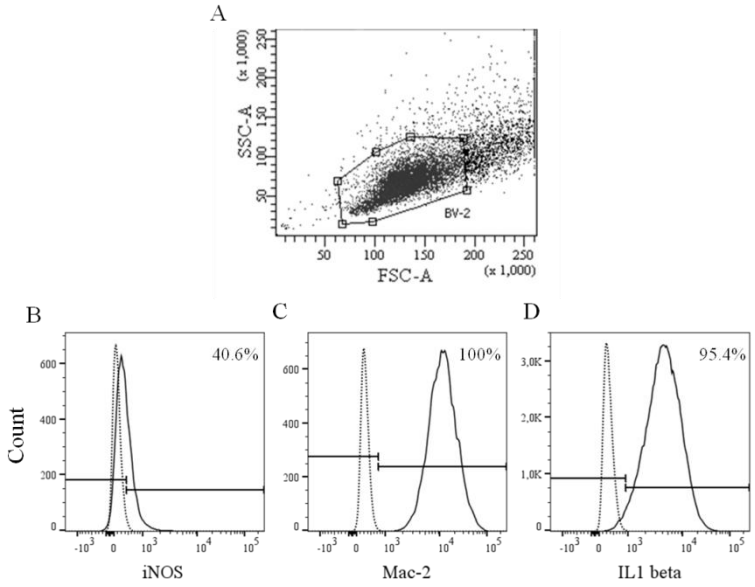

Fig. 5.6. BV-2 cells are positive for iNOS, Mac-2 and IL1 beta (A-D). BV-2 cells **(A)** were processed identical to the embryonic cortex cell suspension for flow cytometric staining. Using the same antibody concentration we find immune reactivity for iNOS (40.6%, **B**), Mac-2 (100%, **C**) and IL1 beta (95.4%, **D**) (full lines), which indicates that the antibody is capable to recognize the antigens. Gates for positive populations were drawn based on the isotype fluorescence intensity (dotted lines).

The absence of activation marker expression by microglia after Poly (I:C) challenge raised the question whether fetal microglia can be directly activated by a Poly (I:C) challenge as suspected for LPS [144] and IL-6 [217]. To address this issue we analysed the activation state of microglia in short-term cultured embryonic brain slices (E15.5) after exposure to IL-6, Poly (I:C) or LPS. The percentage of microglial cells expressing Mac-2/Galectin-3, iNOS and IL1β were analysed 24 hours after immune challenge of the slices **(Fig. 5.7D)**. Fig. 5.7 insets show examples of microglial cells that did **(Fig. 5.7A-C2)** or did not show immunoreactivity **(Fig. 5.7A-C3)** for the activation markers tested (Mac-2, IL1β and iNOS). In control conditions 31 ± 5.9%, (n/N = 23/4) of microglia were immunoreactive for Mac-2 antibody. This percentage was significantly higher (Kruskal-Wallis test; $P < 0.0001$) than that observed *in vivo* indicating that an *in vitro* environment promotes microglia phagocytic activation state. However there was no significant effect (Kruskal-Wallis test; $P = 0.274$) of IL-6, Poly (I:C) or LPS treatment on the percentage of microglia being immunoreactive to Mac-2 antibody **(Fig. 5.7D)**, being 34 ± 5.5% (n/N = 22/4) after IL-6 exposure, 32 ± 6.7%, (n/N = 18/5) after Poly (I:C) exposure and 47 ± 7.5% (n/N = 21/5) after LPS exposure **(Fig. 5.7D)**. As observed for Mac-2, the percentage of IL1β immunoreactive microglia was significantly higher than in *in vivo* conditions (in control conditions 52 ± 6.8%, (n/N = 27/4) (Kruskal-Wallis test; $P < 0.0001$)) and for iNOS a trend to a higher percentage was observed under control conditions (in control conditions 18 ± 5.7%, (n/N = 23/4) (Kruskal-Wallis test; $P = 0.091$)). As shown in **Fig. 5.7D** treatment with IL-6 or Poly (I:C) did not significantly change the percentage of microglia immunoreactive for IL1β or iNOS antibodies. When looking at IL1β immunoreactivity, 36 ± 7.2% (n/N = 16/4) of the microglia was positive after IL-6 exposure and 54 ± 7.5%, (n/N = 19/5) after Poly (I:C) exposure **(Fig. 5.7D)**. For iNOS they were 30 ±

6.5% (n/N = 19/4) after IL-6 exposure and 25 ± 3.9%, (n/N = 25/5) after Poly (I:C) exposure **(Fig. 5.7D)**. However we found that LPS, contrary to IL-6 or Poly (I:C), can directly activate microglia to a detrimental activation state. Indeed LPS exposure significantly increased the percentage of microglia immunoreactive for IL1β (Kruskal-Wallis test; P = 0.025) or iNOS antibodies (Kruskal-Wallis test; P = 0.025). In the presence of LPS 66 ± 5.5 (n/N= 22/5) and 42 ± 7.1% (n/N = 21/5) of microglia were immunoreactive for IL1β antibody or iNOS antibody, respectively.

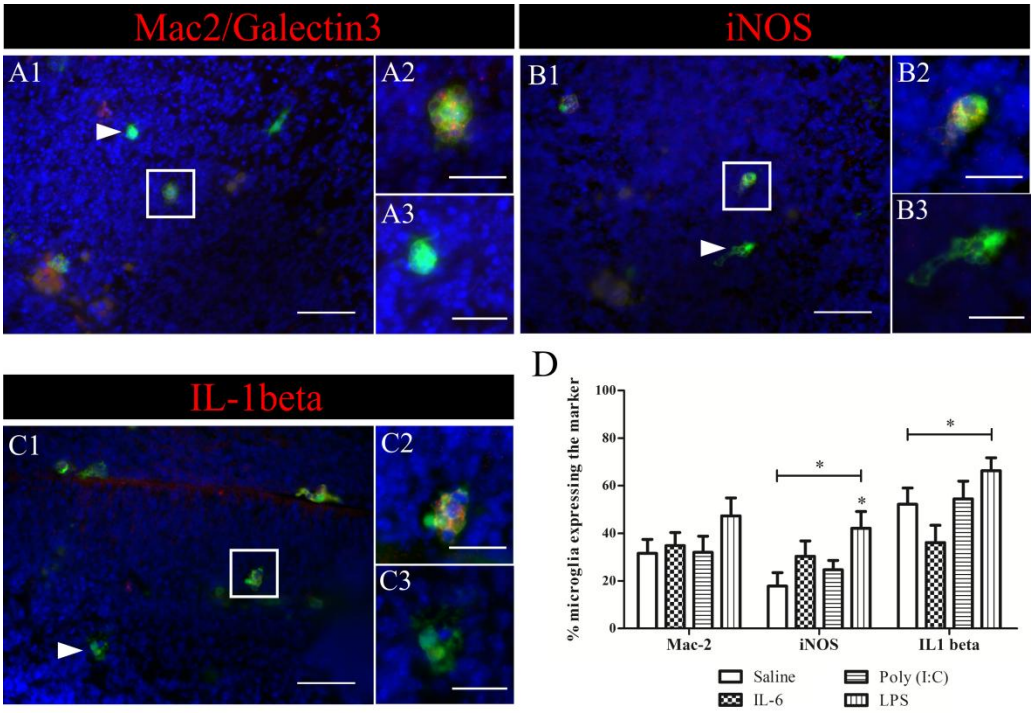

Fig. 5.7. Microglial activation in short-term cultured brain slices. Example of activation marker stainings on short-term cultured slices treated with LPS. **(A)** Immunohistochemical staining for Mac-2/Galectin-3 (red), nuclei were visualized with DAPI (blue) (A1). Microglia (green) positive (A1 white square, A2) for Mac-2/Galectin-3 (red) and microglia that do not express the marker (white triangle, A3) were present in the slice. **(B)** Immunohistochemical staining for for iNOS (red), nuclei were visualized with DAPI (blue) (B1). Microglial cells that were positive (white square B1, B2) and negative (white triangle B1, B3) for iNOS (red) were observed in the slice after LPS treatment. **(C)** Immunohistochemical staining for IL1β (red), nuclei were visualized with DAPI (blue) (C1). Microglial cells that were positive (white square C1, C2) and negative (white triangle C1, C3) for IL1β (red) were observed in the slice after LPS treatment. Examples of the different immunostainings were taken from slices treated for 24 hours with 1 µg/ml LPS. Scale bar = 50 µm and for inserts = 20 µm. White squares indicate the microglia positive for the marker and shown in higher magnification (A-C2), white triangles indicate microglia negative for the marker and shown in higher magnification (A-C3). **(D)** Quantification of the expression of three activation markers (Mac-2, iNOS and IL1β) by microglia in E15.5 brain slices cultured for 24 hours with IL-6 (10 ng/ml), Poly (I:C) (50 µg/ml) or LPS (1 µg/ml). Kruskal Wallis test was used for statistical analysis. Number of treated slices in control and IL-6 group N = 4; LPS and Poly (I:C) group N = 5. Number of cryosections for Mac-2/iNOS/IL1β in: saline group n = 23/23/27; IL-6 group n = 22/19/16; Poly (I:C) group n = 18/25/19; LPS group n = 21/21/22 (all derived from 3 different embryos). (* $p < 0.05$).

5.5 Discussion

MIA-induced behavioural and neurological alterations observed in the offspring at juvenile and adult stages in animals are supposed to be correlated with the etiology of neuropsychiatric disorders in humans [226, 229, 230, 542, 543]. Our study in mice demonstrates, for the first time, that MIA evoked by single or double Poly (I:C) injections does not change microglia density and their activation state in the embryo *in vivo.* This suggests that the behavioural and neurological alterations in the offspring cannot be related to the alteration of the activation state of embryonic microglial cells. Our *in vitro* studies indicated that microglia cannot be directly activated by Poly (I:C) or IL-6 exposure, contrary to the activation observed upon LPS application.

5.5.1 Direct effects of infectious triggers on microglia

Several observations suggest that the different infectious triggers induce differences in activation of embryonic microglia. The cytokine IL-6 can cross the placenta barrier *in vivo* when maternal inflammation was induced during mid-gestation [547-549], but it is not clear whether Poly (I:C) as well can cross the placenta [550]. LPS is shown to cross the placenta barrier *in vivo* when maternal inflammation was induced during early gestation [547, 551], but this was not the case when LPS was injected at late gestation [549]. Although extrapolation of these results to a Poly (I:C) challenge would suggest that embryonic microglia are directly or indirectly activated in response to Poly (I:C)-induced MIA at mid gestation, we could not find any evidence for microglia activation in this study. In addition our results suggest a different response of the embryonic brain to MIA depending on the trigger used.

5.5.2 Microglial alterations following Poly (I:C) or LPS induced MIA

Until now, only the study of Pratt *et al*. assessed microglial density in the embryonic mouse brain following maternal Poly (I:C) challenge and like us, report no changes in this aspect [552]. Changes in microglial number/density following Poly (I:C) challenge in the pregnant mice have only been found at postnatal or adult stages in a handful of studies and not necessarily in the same brain regions [544, 553-555]. On the contrary, other studies found no change in postnatal or adult microglial density [88, 556, 557]. The study of Pratt et al. showed changes in embryonic (E16.5) microglial IL1α, IL4, IL9, GM-CSF and M-CSF expression, but not in a series of other cytokines and chemokines, including IL1β similar to our findings [552]. Postnatal microglia in the offspring of Poly(I:C) injected pregnant mice neither show changes in immune-related protein expression [557-559].

More extensive literature exists on microglial alterations in the embryo following LPS challenge in the pregnant mother. In the fetal sheep brain, microglial cell numbers increased as well as the number of activated/amoeboid cells [241, 560, 561]; in the rat embryo the percentage of microglia expressing iNOS and IL1β was increased [144] and postnatally a changed immunoreactivity by microglial cells was still observed [551]; and in mice Iba-1 reactivity was increased during late embryonic and early postnatal stages [562]. It must be noted that the whole of MIA studies are in general characterized by a high variation in the protocol to induce MIA, with regard to gestational age of MIA trigger, dose, administration route and species exists between studies (both for Poly

(I:C) als for LPS). These variations might contribute to the contrasting results on microglial alterations. Also some studies use the mRNA and/or protein expression level of different cytokines as read-out [88] while others use immunohistochemistry [144, 530] or cell number [241, 553] to investigate microglial cell activation after MIA. In addition, the effect of MIA is studied on several different postnatal and adult time points. In that way it is of interest to compare in parallel the effect of MIA induced by different infectious agents using the same protocol on microglia at different time points ranging from embryonic development to postnatal development and adult life in different species.

5.5.3 Effects of Poly(I:C)-induced MIA on CNS physiology

MIA induces not only a cytokine response in the maternal unit but also alters several cytokine levels in the placenta and in the fetus [218, 552]. Under normal conditions cytokines are present in the placental unit where they play an important role in controlling the tissue homeostasis and balance of the different T-cell types present in this structure. In addition, toll-like receptors (TLR), such as TLR-2 and 4, are expressed on human chorionic villi [563]. Maternal injection with IL-6 is known to lead to endocrine changes in the placenta [564] and injection of a high dose of LPS results in placental inflammation [565] and induction of pro-inflammatory cytokines in the amniotic fluid [566]. In addition, a direct injection of LPS into the uteroplacental circulation leads to a reaction in the embryonic brain, suggesting the placental unit can contribute to perinatal brain damage through the induction of an inflammatory reaction as a response to infection during pregnancy [241]. This complicates elucidating the site where the cytokines act upon to potentially alter brain development since they can act directly on neural progenitors and neurons [250, 251]. For example, IL-6 and LIF can influence the differentiation of neural progenitor cells [252].

These data, in combination with the lack of microglial activation in our MIA study suggests that the acute maternal inflammation induced by Poly (I:C) could affect other systems or cell types during embryonic stages. These MIA-induced early abnormalities might result in an altered CNS environment in the offspring that in turn affects the microglial cells at later developmental stages. This hypothesis is supported by the observed changes in neurotransmitter systems in the adult offspring and not in the pre-pubertal period after challenge with Poly (I:C) [553]. GABAergic gene expression, like GABA receptor subunits and vesicular transporters, can be altered in the adult prefrontal cortex after Poly (I:C)-induced MIA [567]. In addition, serotonin and glutamate signaling was altered [568]. These changes were not present at pre-pubertal ages.

It is also important to note that, although microglia do not invade the CNS of mouse embryo at E9 [37, 72], Poly (I:C) challenge at this gestation stage resulted in the suppression of spatial exploration in the adult [248]. This reinforces the idea that embryonic microglia dysfunction, if any, is unlikely to be the main mechanism inducing developmental disorders featuring pathological behaviour. Accordingly, Poly (I:C) challenge at E9 did not evoke any increase in cytokine mRNA level in the fetal brain [248]. Poly (I:C) might thus induce developmental deficits via direct action on neuronal development.

5.5.4 Second hit hypothesis

Our results cannot exclude that Poly (I:C) evokes an embryonic microglia priming resulting in an exaggerated response of microglia to homeostatic disturbances at postnatal or adult stages and subsequently aggravating neuronal dysfunction. In some neurodegenerative disease models in rodents (for example Alzheimer's, Parkinson's and prion disease) the injection of LPS or Poly (I:C) leads to a more severe pathology. The combined exposure of a prenatal immune challenge (Poly (I:C) at E9) and peripubertal stress (from P30 to 40) resulted in the development of sensorimotor gating deficiencies and led to increased dopamine levels in the adult hippocampus [530]. At peripubertal age of P41, the combination of both stressors resulted in altered neuroimmune responses, presented as increased microglial cell number and elevated levels of IL1β and TNFα in the hippocampus and prefrontal cortex [530]. These latter changes were transient, as they were not longer present in the adult. Finally, low doses of Poly (I:C) worsened the deficits in pre-pulse inhibition and latent inhibition in 16 week old mice with mutations in a schizophrenia susceptibility gene but had no effect in wild-type animals, thus indicating that genetic and environmental factors can interact to worsen the schizophrenia-related behaviour [569].

CHAPTER 6:

General discussion and perspectives

Microglia are the immune cells of the brain and it is now established that they perform essential tasks during brain development and homeostasis. Microglial progenitors arise in the yolk sac and start to colonize the brain slightly before neurogenesis and neuronal migration begins. Despite of the recent advances in understanding the plentiful roles of microglia in brain development, many aspects of their physiology and mechanisms underpinning their migration behaviour remain unresolved.

In this dissertation, we first described the colonization pattern and phenotype of microglia in the embryonic mouse brain based on the expression of surface markers **(Chapter 2)**. Second, we characterized the microglial migration behaviour over development and herein assessed the role of extracellular matrix (ECM) (fibronectin)-integrin interactions **(Chapter 3)**. Third, we investigated the presence of a chemotactic C-X-C motif chemokine (CXCL)-12/ C-X-C chemokine receptor type (CXCR)-4/β1 integrin signaling axis during microglial migration **(Chapter 4)**. Fourth, the effect of maternal immune activation on the activation profile of microglia residing in the cortex and hippocampus of the embryonic offspring was investigated **(Chapter 5)**. **Fig. 6.1** shows a summary of the main results obtained in this work.

In this last chapter, I critically reflect on the data generated in this dissertation with respect to the current state of knowledge in the field of developmental neuroscience. By integrating results from different chapters, I place our findings in a broader context and bring forward new points for discussion. Throughout this chapter, new questions pop up and I try to briefly suggest how these can be tackled from an experimental point of view. These outstanding questions are listed at the end of the chapter in **Box 6.1.**

6.1 Properties of microglia during colonization of the embryonic brain

In **Chapter 2** we have demonstrated that the microglial colonization process occurs in three phases: in the first phase from E10.5 to E14.5 the microglial cell numbers increases modestly, followed by a steep increase from E14.5 to E15.5 and again a slow phase from E15.5 to E17.5. We also show that microglia proliferate mainly before entering the central nervous system (CNS) parenchyma, which was also observed in spinal cord [37]. Proliferation rates inside the cortical parenchyma decrease steadily to considerably low levels already at E15.5, which indicates that microglia colonize the cortex mainly through intensive migration instead of proliferation. We further demonstrate that microglia populate the brain mainly from hot spots near the pial membrane and the parenchyma lining the ventricle towards the inner zones of the cortex, but avoiding the cortical plate zone as of E15.5. This finding is further discussed in **Point 6.4**.

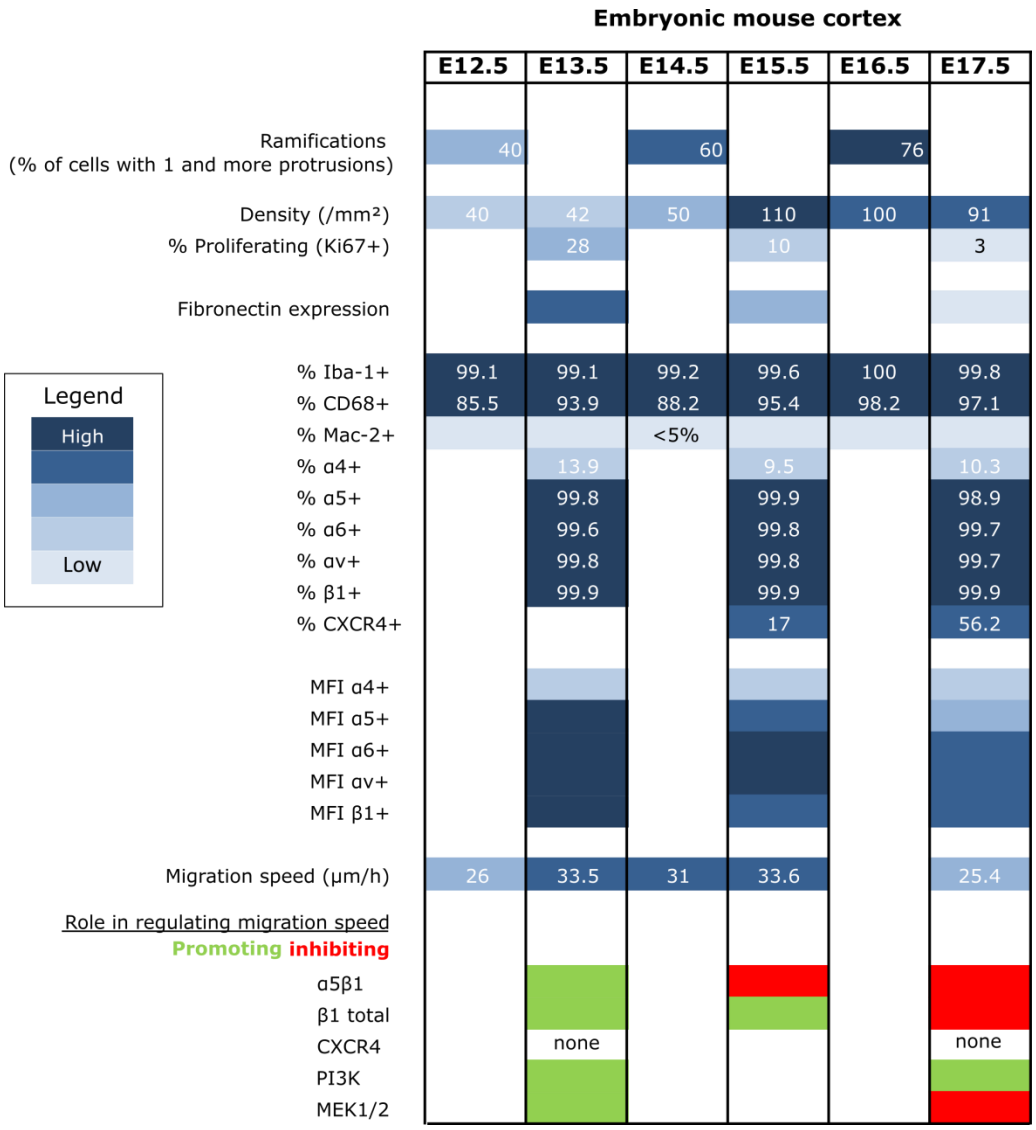

Fig. 6.1. Summary results dissertation. The blue gradient represents low (light blue) to high numbers (dark blue). White space = not studied. E, embryonic day; MFI, Median fluorescence intensity.

6.1.1 Morphology and protein markers

During early development, microglia in the cortical parenchyma show a more amoeboid morphology, with an oval cell body and few short and thick protrusions. With increasing embryonic age, microglia in the cortical wall gradually acquire protrusions **(Chapter 2)**. The amoeboid morphology might be, but is not necessarily correlated with activation of the cell in terms of pro- or anti-inflammatory reactivity [35, 38-41]. This morphology could also point to an immature status of the cell, which was also suggested for microglia in the developing barrel cortex [35]. Indeed, in the embryonic cortex microglia show no signs of classical inflammatory activation such as Mac-2, inducible nitric oxide synthase (iNOS) or interleukin-1β (IL-1β) expression **(Chapter 5)**. For Mac-2, cortical microglia show lower expression levels than microglia residing in the choroid plexus primordium, which are actually choroid plexus macrophages [126], or in the spinal cord [37] **(Chapter 2)**. Nevertheless, all - or almost all in case of cluster of differentiation 68 (CD68) - these

cells are all immunoreactive for the classical microglia/macrophage markers Iba-1, CD11b (alternatively integrin αM, part of complement receptor 3; unpublished observations) and CD68 **(Chapter 2)** [37, 570]. We further show that all cortical embryonic microglia express the β1 class integrins α5, α6 and αV from E13.5 to E17.5, while a minority expresses α4 integrin **(Chapters 3 and 4)**. While microglia remain positive for these integrins throughout embryonic development, their expression level of α5, α6 and αV decreases. The expression of α4β1, α5β1, αLβ2 integrins was found to correlate with activation status in primary microglia [361], but the decrease in integrin expression level could also relate to a progressing maturation of these cells over development, as observed for integrin expression on cortical neuronal progenitor cells [484].

6.1.2 Maturation and the microenvironment

The proposed microglial maturation could be steered by the microenvironment since primary microglia in culture adapt their integrin expression according to the type of extracellular matrix (ECM) present in their local environment [356] and we showed that the cortical fibronectin, an ECM protein, content diminishes with increasing embryonic age **(Chapter 3)**. Unfortunately**,** we lack detailed information about the ECM composition during brain development in different CNS regions. Since the ECM is a major determinant of cell identity, phenotype and behaviour, and microglia express various receptors (integrins) that bind the ECM **(Chapter 4)** [356, 358, 359, 361], it is not unlikely that differences in ECM composition evoke microglial heterogeneity amongst brain regions. Indeed recent studies underscore the heterogeneity of the *microglial transcriptome* with regard to various brain areas and age in adult rodents, but these *profiles are not yet known for embryonic developmental stages* [39, 112, 113, 116, 117, 124, 127, 130]. Subsequent to invasion of the CNS microglia likely adopt tissue-specific signatures and functions imposed locally by the rapidly changing microenvironment during development [112, 571, 572]. Hence, we propose to describe the microglial phenotype during early development as "customized" or simply "embryonic" instead of "immature".

In summary, our results show a three-wave microglial invasion process of the embryonic brain and underscore that during CNS colonization the microglial phenotype and probably their function as well, is tailored to the CNS's local environment. In the cortical parenchyma at least, embryonic microglia display a "resting" phenotype in terms of immune function-related protein expression.

6.2 The microglial migration behaviour in the embryonic brain

Although we found that *in situ* embryonic microglia display a "resting" phenotype, we show that these cells are not resting at all in terms of behaviour. Our *ex vivo* time-lapse imaging experiments in acute slice preparations show that embryonic microglia migrate throughout the cortical parenchyma, while scanning their surroundings. Their morphology rapidly changes every 2 minutes **(Chapters 2 and 3)**. This active scanning behaviour is also a hallmark of microglia in the healthy adult mouse brain *in vivo* [34, 36]. *Ex vivo*, embryonic microglia adopt a saltatory motion pattern with intermittent phases of active migration and pauses during which the cell seem to scan its environment **(Chapter 3)**. The vast majority of the cells are mobile. The movements of the embryonic microglia in our studies closely resemble those of microglia studied in late postnatal

cultured rat hippocampal slices [445]. In that study, Grinberg *et al.* describe the movements of a mobile microglial cell - of note, only 3% of the microglial cells are mobile in control conditions postnatally - as "Lévy flights". Lévy flight motion consists of a random walk characterized by many small step-lengths with occasional relatively large step-lengths. This movement is associated with an optimal search pattern, which is also observed in organisms searching for food [445, 573]. Carbonell *et al.* also modeled microglial migration induced by injury in slice preparations as a random walk [486]. Microglia could adopt this Lévy flight search strategy to efficiently carry out their functions as sculptors and guardians of the brain [16, 574] **(Chapter 1, Point 1.2.7)**. *In order to know whether microglia in the embryonic brain adopt such patterns as well for migration, mathematical modeling should be applied to the XYZ-coordinates of our migration database.*

6.2.1 Microglial settlement during embryogenesis

Our *ex vivo* time-lapse recordings also reveal a decrease in microglial migration speed over embryonic development **(Chapters 2 and 3)**, which might indicate that microglia gradually acquire their final positions with increasing age. This reasoning is however in contrast with the measurements of Eyo *et al.* in hippocampal slices that point to a transient rise in microglial migration speed at postnatal ages. Migration speed at postnatal day (P)2 (~36 µm/h) was reported to be higher than in our E17.5 cortex measurements (~25 µm/h) and to decrease to ~17µm/h at P6 [70]. Because embryonic hippocampal migration was not measured in our studies and the cortex was not studied in Eyo and co-workers' experiments, we cannot rule out that *migration speed is influenced by region-specific ongoing developmental processes as well*, as was already discussed for the heterogeneity in microglial phenotypes and transcriptional profiles in **Point 6.1.2**. *Single cell transcriptomic and proteomic studies of microglia obtained from different regions of the brain and cortical zones, and at a one day interval during embryonic mouse brain development would certainly aid in finding correlations with changes in migration speed over development.*

If it is true that by E17.5 microglia start to acquire their final locations in the cortex, one might expect that the immobile cells in our slices show a more ramified morphology, which we did not observe. Literature states that microglia increase their amount of protrusions during embryonic development in mice [72], in zebrafish larvae [457] and in humans [57], but it does not seem to coincide with definitive settlement inside the parenchyma. Altough literature often postulates that microglia migrate to achieve their final location and start to ramify, *the time point at which microglia become truly immobile* (even regardless of the brain region) was never investigated in mammals. In developing zebrafish larvae settlement occurs at 5 days post fertilization [457]. The true ramification process might be triggered after E18 in mice when cortical neuronal migration has ceased and neuronal network maturation begins [575]. In the early mouse hippocampus microglial morphology was stable during the first postnatal week (2-3 primary ramifications) [70], so the complex ramification process has to start later. Indeed, the actual transformation from "amoeboid" to "ramified" was reported to start around P10, when transcription factor *Runx1* is lost [102]. By P28 the ramification process is complete [102, 104]. The acquisition of a morphologic "adult/ramified" phenotype seems to coincide with the establishment of an adult gene expression profile in microglia by P28 in mice [112]. *Time-lapse experiments in postnatal brain slices, or*

ideally in the in vivo pup, at 1 day interval might aid to pinpoint the age at which microglia are fully settled in the brain.

6.2.2 Regulation of microglial migration speed

Microglial migration speed is likely influenced by changes in the local environment. Developmental neuronal apoptosis does not seem to instruct the decrease in microglial migration speed during development [70]. Interestingly, Zhang *et al.* reported a decrease in speed as a consequence of bacterial endotoxin-induced *in utero* inflammation in the newborn rabbit brain [454]. These findings concur with the results of Grinberg *et al.* who showed in cultured postnatal rat hippocampal slices that synaptic activity influences microglial migration speed [445]. More in particular, they found that microglial movement was significantly decreased by enhanced neuronal activity through lipopolysaccharide (LPS) administration or chemical long-term potentiation, and significantly increased by neuronal activity blockade using Tetrodotoxin (TTX). Thus, synaptic activity seems to restrain microglial cells in their current micro-territories and absence of synaptic activity sends them away to explore other parts of the parenchyma [445]. However, the observed effect of the administered compounds on microglial migration might occur through a direct effect on these cells and not necessarily through a change in synaptic activity since LPS was found to suppress migration and process extension in primary microglia cultures [365, 576, 577] and primary rat microglia might - though controversial - express TTX-sensitive voltage-operated Na^+ channels [32]. Nevertheless, it is intriguing to speculate that in our experiments microglia migration speed might slow down between E15.5 and E17.5 **(Chapter 3)** because local spontaneous activity starts to emerge in the cortex. Indeed, the ventricular zone (VZ) of mouse embryonic slice preparations already shows spontaneous calcium transients, and already at E16 some neurons in the mouse neocortex (marginal zone) show repetitive action potential discharges and spontaneous glutamatergic and γ-Aminobutyric acid (GABA)-ergic synaptic inputs [578]. If microglial migration speed is dependent on local depolarizing activity, this might explain the slow migration speed in the VZ at E15.5 **(Chapter 3)**. Also, subplate neurons show functional thalamocortical synaptic transmission at E19 in rats [578], which means that towards the end of gestation synaptic activity increases. This finding is in favor of our *hypothesis that with increasing neuronal activity, microglial migration speed decreases*. *A way to tackle this question might be to use optogenetic approaches to induce local neuronal firing and study simultaneously the microglial migration behavior in the in vivo animal [579].*

Alternatively and additionally, regional and temporal differences in the expression of chemokines, cytokines and adhesion molecules might play a role in regulating microglial migration speed [62, 283, 294, 337, 361, 442, 486, 580]. For example, microglial migration speed in the adult mouse hippocampus increases dependent on the stimulus type (stab lesion versus viral activation) and can be reduced by pharmacological blockade of the cysteine–cysteine chemokine receptor (CCR) 5 [486]. Additionally, changes in ECM composition were found to alter microglial adhesion, morphology and surface marker expression which might impact on migration speed [294, 337]. A change in ECM protein expression seems a plausible explanation for the decrease in microglial migration speed since it is known that the ECM environment rapidly changes during embryonic development [296] **(Chapter 1, Point 1.3.1)**.

We thus demonstrate that embryonic microglia are highly migratory cells that survey their microenvironment. They migrate in a saltatory fashion and their migration speed diminishes with increasing embryonic age, possibly reflecting the upcoming end of their colonization process. Their mobility is likely to be influenced by a combination of the local ECM composition and neuronal activity. *Whether the intense microglial migration behaviour in slices truly reflects the microglial behaviour in the developing brain of the intact embryo*, *remains to be confirmed through in utero imaging [482, 483]*.

6.3 Complex regulation of integrin function in microglial migration during development

We propose a hypothetical model of varying function of different β1 integrin subtypes with embryonic age. We suggest that at E13.5, all or subsets of β1 integrins known to be expressed by microglia (α4β1, α5β1, αvβ1 and α6β1) **(Chapter 4)** are involved in nascent adhesion formation (as discussed in **Points 1.3.2 and 3.5.4**), since general β1 blockage decreased migration speed to a higher extend than α5β1 blockage did. At E15.5, the migration promoting role of α5β1 would shift to a migration inhibiting role. At that age, the function of α5β1 integrin is however still inferior to the migration promoting (opposite) roles of the ensemble of β1 integrins, because general β1 blockage caused a decrease in migration speed. By E17.5, we speculate that the α5β1-linked adhesion has undergone maturation which translates to a more tightly anchored cell body into the ECM. When this tight connection is disrupted, microglia are released and free to migrate towards a yet unknown source, possibly using integrins of the β2, β3, β5 and/or β8 class as their presence was shown in primary cultured microglial cells [294, 356, 358, 359, 361]. At E17.5, the role of α5β1 is still migration inhibiting, but has become superior to a net migration promoting role of the ensemble of β1 integrins, because general β1 blockage resulted in an increased migration speed, but to a lower extent than α5β1 blockage **(Chapter 4)**. Integrin usage is known to be dynamic: other integrins can take over the functions of the ones that are absent or functionally impaired [314, 338, 581]. Moreover, as brought forward in the introduction in **Point 1.3.2**, it is the *conformation of the integrin that is biologically relevant for adhesion mechanisms, so this should be assessed as well in future experiments using for example conformation sensitive antibodies*. Of note, we cannot exclude contributions of other β1 integrins such as α1, α2, α3 and so on [511] since we did not assess their presence on embryonic microglia. Nevertheless their involvement seems less likely because these integrins were not expressed by primary microglia [356, 358, 359, 361]. It must also be noted that our integrin blockage approach (similar to pharmacological blockage of CXCR4, Phosphatidylinositol-4,5-bisphosphate 3-kinase (PI3K) and Mitogen-activated protein kinase kinase (MEK) described in **Chapter 4**) is not specific for microglia. In order to fully exclude the possibility of indirect effects on microglial migration via possibly disturbed neural progenitor cells, neurons and endothelial cells, additional research using microglia specific knockouts is warranted. Our experiments in BV-2 cells **(Chapters 3 and 4)** do however show that migration of microglia-like cells can be directly affected by the integrin antibodies, and therefore strengthen our conclusion towards direct effects of the blocking antibodies on microglia in acute slices. Nevertheless, an effect observed in cultured microglia does not necessarily correlate with or predict the effect *in vivo* [519] (as discussed in **Chapter 4**).

Microglial migration in the embryo might alternatively be independent of integrins according to recent findings of Meller *et al.* [519]. The authors found that specific deletion of Kindlin3 (an intracellular protein involved in integrin activation, comparable to the function of Talin [314]) in microglia had no effect on microglial migration and population of the CNS during embryonic development [519]. However, it must be noted that compensation by Kindlin1 and/or 2 might have occurred, which could mask the true involvement of Kindlin3. Furthermore, since already 5% of total Kindlin3 level might be sufficient to be functional, proof that these animals are complete knockouts is necessary [582].

Altogether our results indicate that microglial migration in the embryonic cortical parenchyma is dependent on β1 integrins. Notably, integrin-mediated functions (migration promoting vs. inhibiting) seem to vary amongst integrin subtypes and likely switch and/or change importance during embryonic development. Such a switch might occur for α5β1 integrin and is in that case likely at E14, which is the age reported for mouse microglia to shift gene expression profile from "early microglia (E10.5-E14)" to "pre-microglia (E14-P9)" [112]. *Which event or factor is causing this shift in integrin function remains an open question and additional research is essential to test this hypothesis on the molecular level. In order to test the plausibility of the change in nature of adhesion the α5β1 integrin is involved in, one might assess its activation state using antibodies recognizing the stretched conformation of the integrin, as well as degree of clustering* [376]*. The amount of focal adhesion proteins, such as zyxin and vinculin associated with the α5β1 integrin could be assessed since their presence is involved in regulating migration speed* [273, 583]*. Also, the long term consequences of defective integrin-dependent microglial migration on brain development and neuronal network functionality remain unknown and require further attention*. *In this respect, it should be first determined which molecules are essential in promoting parenchymal microglial migration in the embryo. The use of a series of microglia-specific conditional integrin or chemokine receptor knockouts (see* ***Point 6.4.1****) will aid in pinpointing targets. Then it will be important to inhibit the spreading of microglia during development and subsequently assess the effect of defective microglial migration on radial glia differentiation into neurons, astrocytes and oligodendrocytes, synaptogenesis, myelination and the functionality of neuronal networks postnatally and in the adult.*

6.4 Candidate cues for steering parenchymal microglial migration during development

6.4.1 Chemoattractants and chemorepellants

A few studies have shed light on the cues that attract microglia towards the CNS at embryonic stages, but could not pinpoint whether these molecules steer the parenchymal colonization of the cells [52, 62, 63, 67]. In acute embryonic brain slices we did not find a role for CXCR4 in regulating microglial migration speed, while β1 integrins are age-specifically involved in determining microglial migration speed **(Point 6.3) (Chapter 4)**, so as to conclude that β1 integrin function is not downstream of CXCR4 signaling during microglial migration in the embryo *ex vivo*. Though it remains to be assessed whether CXCR4 signaling is involved in regulating directive migration, we

currently assume that CXCR4 most likely plays a role in solely recruiting microglial precursors towards the brain [62, 161].

Interestingly, we observe that from E15.5 the cortical plate is devoid of microglia **(Chapter 2)** and microglia avoid migrating through this zone (time-lapse imaging **Chapter 2, 3 and 4**). Instead it seems that microglia accumulate in the layers ventrally to the cortical plate, thus in the subplate, intermediate zone and ventricular zone, as if they are waiting for a launch signal to populate the cortical layers. This transient microglial absence in the cortical plate has been reported in the human, macaque and rat developing cortex as well [56, 57, 82, 144], but the signals leading to this phenomenon have never been disclosed. The specific localization of chemoattractive and chemorepellant molecules might underlie the transient absence of microglia in the cortical plate. Rezaie *et al.* suggested that in the human embryonic brain microglia could follow the gradient of C-C motif chemokine ligand (CCL)-5 (also known as regulated on activation, normal T cell expressed and secreted (RANTES)) and CCL2 (also known as Monocyte chemotactic protein-1 (MCP-1)) which together form an increasing gradient from the subventricular zone to a peak in the subplate followed by low levels in the cortical plate [82]. After focal brain injury, as well as *in vitro*, microglial migration speed was dependent on CCR5 signaling, which is a receptor for CCL5 [486, 584]. Also, the specific complementary expression of IL-34 and CSF1 during development might play in the role in the specific distribution of microglial cells [61]. At E15.5, IL-34 is restricted to the marginal zone while CSF-1 is present in the subventricular and the ventricular zone. From P0-P20, IL-34 is found in cortical layers V to II, while CSF-1 expression is restricted to layer VI. This fits with the postnatal invasion of the cortical layers by microglia. Further, semaphorins could act as chemorepellants for microglia based on their repellant properties on axonal outgrowth and specific absence of mRNA from the intermediate zone and subplate between E16 and P0 in rats [585]. More in particular Semaphorin B mRNA is the only Semaphorin mRNA that is present in the cortical plate from E15 until E19 in rats, without concurrent expression in the neuroepithelium, where microglia tend to reside. Also, microglia can express plexin-B1, the receptor for Semaphorin 4A and 4D, in pathologic settings, but it is not known whether embryonic microglia express these receptors [586]. Further, Slit1, another chemorepellant, is specifically expressed in the cortical plate around E15 in mice [587] and might also repel microglia through Robo signaling, the receptor for Slit proteins, since primary rat microglia were shown to express Robo2 [588].

6.4.2 Cell death and synaptogenesis

In addition, the subplate is the first layer where developmental cell death occurs and where the first thalamocortical synapses are formed starting earliest at E15.5, which might attract microglial cells [11, 15, 16, 589]. However, we think the former event is not likely to underlie the specific distribution pattern of microglia, because as a first argument we did not detect any cleaved capsase-3 immunoreactivity in that region around E15.5 **(Chapter 2)**. It must be noted however that the absence of cleaved caspase-3 immunoreactivity is no conclusive evidence for absence of apoptosis, since also caspase-independent apoptosis can occur [590]. As a second argument, microglia in the vicinity of dying cells, such as in the choroid plexus primordium **(Chapter 2)**, mostly show a phagocytic morphology and Mac-2 immunoreactivity [37, 434], which we neither observed in the layers ventral to the cortical plate at E15.5 and E17.5. Alternatively,

synaptogenesis in the subplate layer might be a more plausible event leading to the temporary accumulation of microglia, since microglia can sense neuronal activity [167, 168] and their migration speed is likely inversely correlated with neuronal and synaptic activity [445].

Altogether, CXCL12/CXCR4 signaling likely plays a role solely in recruiting microglial cells to the CNS, although a role for this chemokine axis in directional microglial migration in the embryonic cortex remains to be assessed. *Other factors steering parenchymal microglial migration likely include chemoattractants, chemorepellants and synaptic activity*, but require further investigation. *In utero imaging of conditional microglia-specific knock-out animals might be valuable in addressing the chemokine pathways involved in steering microglial migration. More feasible approaches for a first-base screening might be to the use of several chemoattractant/chemorepellant knockout or functional mutation (loss and gain of expression) models to determine the microglial dispersion within in the brain.*

6.5 Microglial interactions with blood vessels

In **Chapter 3** we aimed to disrupt the microglia-blood vessel contact by interfering with α5β1 integrin and its ligand fibronectin, but neither the capability of microglia to use blood vessels as guiding substrates for migration, nor the fraction of these cells contacting blood vessels, nor the time spent on soma or process contact were altered in the presence of the α5β1 blocking antibody**.**

6.5.1 Mechanisms of interaction

Next to alternative integrins and ECM molecules acting in concert **(Chapters 3 and 4)** in mediating mechanical contact between microglia and blood vessels, Notch1-Dll4 signaling might be involved in microglia-endothelial cell interaction [21]. Notch1 signaling in microglia could induce the expression of integrins leading to attachment to blood vessels, similar to what is reported for vascular smooth muscle cells adhering to endothelial cells during vascular maturation [591]. Further, the involvement of cadherin-based cell-cell adhesion between microglia and blood vessels cannot be excluded, as cadherin expression was found in macrophages, though to our knowledge not reported yet in microglial cells [592-594]. Of note, cadherins are transmembrane receptors that mediate cell-cell adhesion and catenin-dependent intracellular signalling by reciprocal binding [595]. However, how microglial contact with blood vessels is manifested mechanically, is unknown and needs further clarification.

6.5.2 Attraction towards blood vessels

The study of Rymo *et al.* demonstrated a strong directed migration of microglia towards blood vessels in aortic ring explants *in vitro* [162], but the factors that contribute to this chemotaxis remain generally unknown. In the postnatal rat brain, CXCL12 transcripts and protein were detected in endothelial cells [596]. So, microglia might be attracted towards CXCL12-producing developing blood vessels. Once arrived, microglia might attach to the blood vessel and downregulate CXCR4, conform a mechanism described in leukemic precursor-B cells [321] and in granular cells of the dendate gyrus [597]. This mechanism might explain why not all microglia express CXCR4 **(Chapter 4)**. One would then expect all microglial cells to be stuck to blood

vessels around late embryonic development when the microglial colonization process is getting closer to its end, concomitant with a downregulation of the microglial CXCR4 expression. Indeed, we show that during late embryongenesis almost all microglia have made contact with blood vessels in a time span of six hours and that the majority of this time was spent on contacting blood vessels using their soma and/or protrusions **(Chapter 3)**. Additional experiments at postnatal ages are necessary to determine whether microglia downregulate CXCR4. Further, we demonstrate an increasing microglia-blood vessel contact with increasing embryonic age, which indicates that microglia are gradually attracted by developing blood vessels during embryonic development **(Chapter 3)**. It must be noted that we also observed microglia escaping from blood vessels (unpublished observations), which suggests that microglial cells can shift function and leave the blood vessels after fulfilling their tasks. To know if this hypothesis is plausible, it would be interesting to know the percentage of microglia in contact with blood vessels in adult mice, but this question was never assessed.

Further, given the significant amount of time spent on contacting blood vessels, microglial cells likely use the developing vasculature as migration highways **(Chapter 3)**. This possibility was also noted by del Rio-Hortega who stated *"In its migration, it follows more or less closely the direction of the vessels"* [82, 598]. *More precise tracking analyses are necessary to assess how well the direction of migrating microglia relates with the direction of blood vessels in the developing cortex. In addition, specifically targeting factors secreted by the developing vasculature will help in elucidating what causes the attraction of microglia towards blood vessels.*

6.5.3 Mechanisms of influencing blood vessel branching

The results of Rymo *et al.* suggest that although microglia-blood vessel contact enhances, it is not essential to induce branching [162]. However, it must be noted that in this study "contact" refers to the cells being present or absent at the aortic ring cultures. The authors did not test whether nearby presence or direct contact of microglial cells with angiogenic sprouts differentially affected branching [162]. The function of this direct and dynamic microglia-blood vessel contact deserves further investigation.

The mechanisms or factors through which microglia influence vessel branching were questioned for a long time. Research clearly pointed to soluble factors secreted by microglia, but excluded microglial vascular endothelial growth factor (VEGF) [159, 162]. Recently, some of these secreted factors were identified [599, 600]. In the *in vivo* developing mouse brain Chen *et al.* found that signaling between CD95L secreted by microglia on one hand and its receptor CD95R on neurons and endothelial cells on the other hand promoted neurovascular development, including blood vessel branching, through intracellular signaling of src-family kinase (SFK) and PI3K intracellular signaling [599]. Another recent study, carried out mainly *in vitro*, points to the involvement of microglial basigin-2, an extracellular matrix metalloproteinase inducer, in angiogenesis [600]. In addition, it was recently discovered that γ3-containing laminins in the vascular basal membrane during postnatal mouse retinal angiogenesis under normal circumstances restrict branching, through tempering microglial recruitment and activation via β1 integrins (here, activation refers to

an increased percentage of amoeboid and CD68 expressing microglia and down-regulation of microglial TGF-β1 expression) [601].

In summary, microglia mediate blood vessel branching during CNS development and the underlying signaling mechanisms start to emerge. However, the importance of direct microglia-blood vessel contact and the molecules mechanistically involved in this process remain unknown. Nevertheless, we excluded an essential role for α5β1 integrin in the contact between microglia and blood vessels in the *ex vivo* embryonic brain. *Light can be shed on these questions through the use of microglia-specific integrin knockouts followed by electron microscopy assessment of contact between both. Once these molecues are identified, the effect of contact disruption can be studied on blood vessel branching.*

6.6 Does microglial activation by maternal immune activation lead to neurodevelopmental disorders?

Until now, although deletion or mutations in microglia specific genes have been associated with neurodevelopmental and neurological disorders [8] **(Point 1.2.8)**, it remains unclear whether microglial alterations after MIA lie on the basis of neuronal disorders or reflect a normal microglia response to neural dysfunctions. Several authors have speculated over such MIA-induced developmental dysfunctional microglia that could lead to neurodevelopmental disorders [8, 16, 208, 211, 602-604]. In **Chapter 5**, we did not find evidence for MIA evoked by single or double Poly (I:C) injections to change microglial density or microglial expression of classical immune activation proteins. Our *in vitro* results also demonstrate that embryonic microglia cannot be directly activated by Poly (I:C) or IL-6 exposure, contrary to the activation observed upon LPS application **(Chapter 5)**. Our results suggest that the behavioural and neurological alterations in the offspring cannot be related to the alteration of the activation state of embryonic microglial cells. It must be noted that we did not test whether our MIA offspring developed cognitive and behavioural deficits, although this model is validated and our pregnant mothers did show increased IL-6 serum levels, a hallmark and predictor for behavioural deficits in the offspring [207, 217, 526].

6.6.1 Priming of microglia

Yet, our results cannot exclude that the embryonic microglial cells become primed, which could result in a disturbed cytokine and neurotrophic factor production in response to a subsequent inflammatory stimulus or stressor during postnatal or juvenile life [208, 509, 605-607]. Most interestingly, the presence of microglia during the first two weeks of postnatal development is crucial for brain development and behaviour [266]. The early postnatal period is also the critical time window during which a second stimulus generates an altered microglial response [228, 530, 608]. The first stimulus does not necessarily have to be of immune origin, but could also be genetic susceptibility, which illustrates the interaction between genetic and environmental factors in the etiology of neurodevelopmental disorders [569]. In this early postnatal time frame, the microglial density steeply increases, synaptic pruning by microglia is ongoing and microglia in the hippocampus between P14 and P28 undergo significant changes, such as reduced cell density,

decreased *ex vivo* phagocytic activity, and an increase in the expression of genes involved in inflammation and cell migration [174, 609].

6.6.2 Reported alterations in microglia upon MIA

Possibly, microglial function during development is altered upon MIA, but is not per se detectable with the common classical activation markers and density/morphology analyses. Many recent studies point indeed to MIA-induced changes in the microglial epigenetics [214, 610] and transcriptomics associated with genes involved in the developmental functions of microglia, such as synaptogenesis and neuronal network formation [112, 151, 152, 611]. Of note, even prenatal stress can affect microglial morphology and functions from motility to cytokine, chemokine and growth factor production, which indicates that microglial function is extremely sensitive to environmental conditions [509, 612-615]. Matcovitch-Natan *et al*. describe that microglia from mice subjected to MIA and analysed at the pre-microglia stage (E14 to early postnatal weeks) were transcriptionally shifted towards a more advanced developmental stage [112]. This implies that MIA renders microglia more "mature", which is in accordance with a recent microglial transcriptomics study suggesting an accelerated development of these cells in autism patients [116]. Interestingly, postmortem studies suggest that neurogenesis in ASD might be accelareted as well, based on higher neuronal density and accelerated brain growth in ASD subjects [616]. It is not clear how accelerated microglial development and accelerated neurogenesis relate to each other. Also, perturbed microglial maturation was reported upon early life stress [609].

6.6.3 Controversies in microglial activation following MIA

Although the prenatal intraperitoneal Poly (I:C) injection in the pregnant mother used in this work **(Chapter 5)** is a well established model to induce MIA, results between studies are not consistent with regard to effects on microglia. Despite the presence of synaptic or behavioural deficits, both absence [88, 247, 617] and presence [555, 618, 619] of microglial "activation" has been reported in MIA animal models. It must be noted that these few references used in this section only serve to illustrate the controversy and by no means encompass all "microglia during MIA" findings in literature. This controversy is caused by the high level of variation in the readout and the protocols of MIA studies. A first and major issue is the use of the term "microglial activation" as a readout. This term is vague and is often (mis)used to report increases in microglial density and changes in morphology [241, 553]. As discussed before, morphology does not correlate per se with function [35, 38-42]. In accordance, another study suggests that morphological changes observed in "activated" microglia are likely associated with an underlying change in transcriptome maturity and not necessarily "reactivity" [116]. So whenever microglia with fewer or thicker ramifications are detected, it does not mean that these cells have a detrimental cytokine secretion profile and disturb every cell in their vicinity. Some studies do use mRNA and/or protein expression level of different cytokines [88] or immunohistochemistry [144, 530] to assess whether the cells are immune-activated. Unfortunately, even then some studies fail to use inflammation markers such as TNFα, IL1β, IL-6, iNOS and Mac-2, and instead use Iba-1 and CD68 which are merely general markers to identify microglia/macrophages and are not specific for immune activation. Second and third sources of variations are the time and location of readout after MIA. The effect of MIA on

microglia is studied in different brain regions and on several different embryonic, postnatal and adult time points. Microglial alterations may only be detected transiently at specific locations and only during postnatal and/or adult stages [88, 544, 553, 555]. Other sources of variations are the dosage and time of injection of the MIA-evoking trigger, since differences in behavioural abnormalities observed in the offspring at adult age are critically dependent on these factors [248, 532]. This phenomenon might be related to the varying presence of other neural cells at different gestational time points, as demonstrated recently in co-cultures [620] and to the severity of the cytokine storm in the mother. Next, the trigger itself varies, which is mostly Poly (I:C) or LPS, sometimes IL-6 or a virus [241, 560, 561]. Lastly, the investigated species also varies from mice, to rats, to sheep, to pigs, and to macaques [144, 151, 241, 617].

As already brought forward by others, attention should be paid to the involvement of astrocytes in MIA-induced pathology as well [16, 212, 621, 622]. After all, a complex interplay exist between microglia and astrocytes and the latter are important players of neural circuit development through their contribution in synaptogenesis, synapse elimination and functional modulation of synapses [623]. Additionally, astrocytic markers are altered upon MIA [624] and in schizophrenia [625].

Altogether, MIA studies measuring microglial "activation" are almost impossible to compare due to high variations in the readout (type, location and timing) and MIA model (type, dosage, timing of MIA induction and species). The field would benefit from a thorough systematic review, that bundles all these different approaches and aims at discovering correlations between the sources of variation and microglial anomalies. We hope future research with regard to MIA-induced microglial dysfunction will describe the precise readout, and not jump to any rash conclusions labeling microglia with "activated" or "not activated". *Hence, a broader readout is necessary which in addition to the analysis of morphology, density and immune protein expression, encompasses transcriptomic and functional studies on microglia. Simultaneously analyzing the transcriptional profile of other cell populations in the brain, and this over multiple time points during embryonic and postnatal development, might aid in pinpointing which cell type is affected first by MIA. To assess whether dysfunctional microglia drive the neurological deficits following MIA, microglia depletion and repopulation with functional cells or a pharmacological approach specifically targeted at restoring homeostatic functions of microglia might aid in solving this question.* Nevertheless, there is no smoke without a fire: accumulating evidence strongly points in the direction of at least a partially shared causative role for microglia in MIA-induced cognitive and behavioural deficits. In this respect, the interplay with astrocytes may not be forgotten.

6.7 Limitations of this work

The results presented in this work add considerable value to the field of developmental neuroscience and might aid on the long run in unraveling pathological mechanisms of neurological diseases. We hope that these data will contribute to the identification of new targets to treat or prevent neurological disorders or to the development of tools for early diagnosis. Nevertheless, it is important to keep in mind that the work presented here was conducted in mice and that the human brain and its development is far more complex and longer lasting than that of rodents. For example, P0-5 development in rats is estimated to correspond to the whole third trimester of

human brain development, P7-10 to the first year of life and P21 to the transition to the early juvenile stage in man [626, 627]. Although the overall structural and functional development of the cortex and several microglial characteristics are similar in humans and rodents, some important differences in microglial physiology have be noted as well and this might have implications for the extrapolation of findings on rodent microglia towards the human setting [9, 578, 628].

Several features of the development of the microglial population are highly similar between rodents and humans such as their specfic distribution pattern (e.g transient absence from the cortical plate) and contact with radial glial cells and blood vessels in the developing brain [2, 56, 80, 402, 431]. Both in mice and in humans, microglia turn over several times during the organisms' life span [86]. Also many genes and their products on the transcriptional and protein level are similarly expressed in both species under control circumstances, such as Iba-1, PU.1, DAP12, CD11b, TMEM119 and P2Y12R (Reviewed in [132, 521, 628-630]. In contrast, a number of immune genes, including TLR, Fcγ and Sialic Acid-Binding Immunoglobulin-Like Lectin receptors, as well as cell cycle regulator proteins such as TAL1 and IFI16, were abundantly expressed in human microglia but not in their mouse counterparts or the other way around [521, 630]. These findings demonstrate that human microglia have their own specific gene signature. Interestingly, the sex difference in transcriptomic microglial maturation and immune reactivity profiles in mice is also found in humans, with even mouse models for neurodevelomental disorders showing the same transcriptomic anomalies as their human counterparts [116]. On the other hand, major discrepancies between both species' microglial signatures arise during aging or in pro-inflammatory conditions [236, 630]. Further, important discrepancies in microglial gene expression profiles between mouse models for neurodegeneration and the corresponding human neurodegenerative diseases were identified, questioning the validity of mouse models for neurodegenerative diseases [631]. Thus, with the eye on development of therapeutics, it is vital to be aware of and to assess similarities and dissimilarities between rodent and human microglia. The use of the latest technological advances such as single cell transcriptomics and proteomics will certainly aid in clarifying these issues.

A second "limit" - though at the same time an advantage - of this study is the use of acute brain slices. Slice preparations are optically accessible and convenient to study and manipulate cell behavior and molecular interactions while preserving the native 3D brain environment and thus mimic the *in vivo* situation [441, 442, 632]. Accordingly, microglial behavior and reaction to compounds is highly comparable between acute slice preparations and *in vivo (*cranial window) in the adult brain [366, 448]. While in case of *in vivo* imaging only superficial cortical layers can be imaged, brain slice preparations allow to study all brain structures. Most importantly, 2D molecular mechanisms involved in cell migration differ considerably from 3D, so in order to extrapolate results to the *in vivo* setting, studies in a physiological 3D environment are necessary [283, 633]. One might argue that microglial migration in slice preparations is a consequence of tissue damage and does not reflect the true physiological behavior during development. However, the fact that microglia in the *in vivo* developing zebrafish are highly mobile as well, is in favor of considering microglial migration in slices as physiological [457, 461]. Further, the fact that microglial migration is not observed in acute brain slices from adult mice, indicates that tissue injury due to slicing

alone is not enough to induce microglial mobilization [70]. Nevertheless, *in utero* embryonic brain imaging is of key importance to confirm the intense microglial migration behavior in the intact mammalian developing brain [70]. Although technically challenging, already some *in utero* embryonic brain imaging studies have been performed previously [482, 483].

In conclusion, the use of rodent models and acute slice preparations is indispensable to unravel key features of microglial physiology during embryonic development, but the validation of these findings *in vivo* and in humans is an important step towards identifying targets for intervention in the clinic.

6.8 Outstanding questions

Box 6.1. List of outstanding questions brought forward in the discussion

Microglial colonization of the brain

- Which cues guide microglial migration once inside the CNS parenchyma?
- What signals are retaining microglia transiently from the cortical plate?
- At which age do microglia become settled in the parenchyma?

Microglial migration behaviour

- Is the direction of microglial migration random?
- Is the direction of migration determined by the arrangements of blood vessels?
- Is the changing migration speed predicted by specific transcriptional signatures?
- Is the changing migration speed caused by changes in neuronal activity over development?
- Does *the ex vivo* migration behaviour of microglia correspond well to the *in vivo* behaviour?
- What is the purpose of the intensive microglial migration?*! Use of microglia-specific approaches*

Age-specific integrin functions

- How can the shift in integrin function be explained at a molecular level?
- What determines whether integrins exert migration promoting or inhibiting functions?
- Does CXCR4 cross talk to β1 integrin causing changes in migration in microglial cells?

Microglia and blood vessel interactions

- What are the underlying mechanisms for microglia to attach to blood vessels?
- What signals attract microglia towards blood vessels?
- What is the function of the molecular contact with blood vessels?

Microglia and neurodevelopmental disorders

- Can microglial dysfunction during development cause behavioural and cognitive deficits during later life, alone or in combination with other factors?
- Are microglial alterations merely a reaction to an already changed neuronal network after maternal immune activation?
- Do microglia work together with astrocytes in shaping neuronal networks?

List of references

1. Stiles, J. and T.L. Jernigan, *The basics of brain development.* Neuropsychol Rev, 2010. **20**(4): p. 327-48.
2. Silbereis, J.C., et al., *The Cellular and Molecular Landscapes of the Developing Human Central Nervous System.* Neuron, 2016. **89**(2): p. 248-68.
3. Tremblay, M.E., et al., *From the Cajal alumni Achucarro and Rio-Hortega to the rediscovery of never-resting microglia.* Front Neuroanat, 2015. **9**: p. 45.
4. Reemst, K., et al., *The Indispensable Roles of Microglia and Astrocytes during Brain Development.* Front Hum Neurosci, 2016. **10**: p. 566.
5. Lyck, L., et al., *An empirical analysis of the precision of estimating the numbers of neurons and glia in human neocortex using a fractionator-design with sub-sampling.* J Neurosci Methods, 2009. **182**(2): p. 143-56.
6. Martinez-Garay, I., et al., *Cadherin 2/4 signaling via PTP1B and catenins is crucial for nucleokinesis during radial neuronal migration in the neocortex.* Development, 2016. **143**(12): p. 2121-34.
7. Pelvig, D.P., et al., *Neocortical glial cell numbers in human brains.* Neurobiol Aging, 2008. **29**(11): p. 1754-62.
8. Frost, J.L. and D.P. Schafer, *Microglia: Architects of the Developing Nervous System.* Trends Cell Biol, 2016. **26**(8): p. 587-97.
9. Clancy, B., R.B. Darlington, and B.L. Finlay, *Translating developmental time across mammalian species.* Neuroscience, 2001. **105**(1): p. 7-17.
10. Tong, C.K. and S. Vidyadaran, *Role of microglia in embryonic neurogenesis.* Exp Biol Med (Maywood), 2016. **241**(15): p. 1669-75.
11. Stolp, H., et al., *The Long and the Short of it: Gene and Environment Interactions During Early Cortical Development and Consequences for Long-Term Neurological Disease.* Front Psychiatry, 2012. **3**: p. 50.
12. Verkhratsky, A., V. Parpura, and J.J. Rodriguez, *Where the thoughts dwell: the physiology of neuronal-glial "diffuse neural net".* Brain Res Rev, 2011. **66**(1-2): p. 133-51.
13. Gotz, M. and W.B. Huttner, *The cell biology of neurogenesis.* Nat Rev Mol Cell Biol, 2005. **6**(10): p. 777-88.
14. Kanold, P.O. and H.J. Luhmann, *The subplate and early cortical circuits.* Annu Rev Neurosci, 2010. **33**: p. 23-48.
15. Ferrer, I., et al., *Cell death and removal in the cerebral cortex during development.* Prog Neurobiol, 1992. **39**(1): p. 1-43.
16. Mosser, C.A., et al., *Microglia in CNS development: Shaping the brain for the future.* Prog Neurobiol, 2017.
17. Cooper, J.A., *A mechanism for inside-out lamination in the neocortex.* Trends Neurosci, 2008. **31**(3): p. 113-9.
18. Kelsom, C. and W. Lu, *Development and specification of GABAergic cortical interneurons.* Cell Biosci, 2013. **3**(1): p. 19.
19. Marin, O. and J.L. Rubenstein, *Cell migration in the forebrain.* Annu Rev Neurosci, 2003. **26**: p. 441-83.
20. Ginhoux, F., et al., *Fate mapping analysis reveals that adult microglia derive from primitive macrophages.* Science, 2010. **330**(6005): p. 841-5.
21. Arnold, T. and C. Betsholtz, *The importance of microglia in the development of the vasculature in the central nervous system.* Vasc Cell, 2013. **5**(1): p. 4.
22. Hagan, N. and A. Ben-Zvi, *The molecular, cellular, and morphological components of blood-brain barrier development during embryogenesis.* Semin Cell Dev Biol, 2015. **38**: p. 7-15.
23. Ginhoux, F., et al., *Origin and differentiation of microglia.* Front Cell Neurosci, 2013. **7**: p. 45.
24. Qian, X., et al., *Timing of CNS cell generation: a programmed sequence of neuron and glial cell production from isolated murine cortical stem cells.* Neuron, 2000. **28**(1): p. 69-80.
25. Kriegstein, A. and A. Alvarez-Buylla, *The glial nature of embryonic and adult neural stem cells.* Annu Rev Neurosci, 2009. **32**: p. 149-84.
26. Nikodemova, M., et al., *Microglial numbers attain adult levels after undergoing a rapid decrease in cell number in the third postnatal week.* J Neuroimmunol, 2015. **278**: p. 280-8.

27. Del Rio, J.A., et al., *Developmental history of the subplate and developing white matter in the murine neocortex. Neuronal organization and relationship with the main afferent systems at embryonic and perinatal stages.* Cereb Cortex, 2000. **10**(8): p. 784-801.

28. Squarzoni, P., M.S. Thion, and S. Garel, *Neuronal and microglial regulators of cortical wiring: usual and novel guideposts.* Front Neurosci, 2015. **9**: p. 248.

29. Kettenmann, H., F. Kirchhoff, and A. Verkhratsky, *Microglia: new roles for the synaptic stripper.* Neuron, 2013. **77**(1): p. 10-8.

30. Pfisterer, U. and K. Khodosevich, *Neuronal survival in the brain: neuron type-specific mechanisms.* Cell Death Dis, 2017. **8**(3): p. e2643.

31. Sousa, C., K. Biber, and A. Michelucci, *Cellular and Molecular Characterization of Microglia: A Unique Immune Cell Population.* Front Immunol, 2017. **8**: p. 198.

32. Kettenmann, H., et al., *Physiology of microglia.* Physiol Rev, 2011. **91**(2): p. 461-553.

33. Kozlowski, C. and R.M. Weimer, *An automated method to quantify microglia morphology and application to monitor activation state longitudinally in vivo.* PLoS One, 2012. **7**(2): p. e31814.

34. Nimmerjahn, A., F. Kirchhoff, and F. Helmchen, *Resting microglial cells are highly dynamic surveillants of brain parenchyma in vivo.* Science, 2005. **308**(5726): p. 1314-8.

35. Arnoux, I., et al., *Adaptive phenotype of microglial cells during the normal postnatal development of the somatosensory "Barrel" cortex.* Glia, 2013. **61**(10): p. 1582-94.

36. Davalos, D., et al., *ATP mediates rapid microglial response to local brain injury in vivo.* Nat Neurosci, 2005. **8**(6): p. 752-8.

37. Rigato, C., et al., *Pattern of invasion of the embryonic mouse spinal cord by microglial cells at the time of the onset of functional neuronal networks.* Glia, 2011. **59**(4): p. 675-95.

38. Karperien, A., H. Ahammer, and H.F. Jelinek, *Quantitating the subtleties of microglial morphology with fractal analysis.* Front Cell Neurosci, 2013. **7**: p. 3.

39. Hanisch, U.K., *Functional diversity of microglia - how heterogeneous are they to begin with?* Front Cell Neurosci, 2013. **7**: p. 65.

40. Olah, M., et al., *Microglia phenotype diversity.* CNS Neurol Disord Drug Targets, 2011. **10**(1): p. 108-18.

41. Scheffold, A., et al., *Telomere shortening leads to an acceleration of synucleinopathy and impaired microglia response in a genetic mouse model.* Acta Neuropathol Commun, 2016. **4**(1): p. 87.

42. Streit, W.J., et al., *Microglial pathology.* Acta Neuropathol Commun, 2014. **2**: p. 142.

43. Hagemeyer, N., et al., *Microglia contribute to normal myelinogenesis and to oligodendrocyte progenitor maintenance during adulthood.* Acta Neuropathol, 2017.

44. McKercher, S.R., et al., *Targeted disruption of the PU.1 gene results in multiple hematopoietic abnormalities.* EMBO J, 1996. **15**(20): p. 5647-58.

45. Beers, D.R., et al., *Wild-type microglia extend survival in PU.1 knockout mice with familial amyotrophic lateral sclerosis.* Proc Natl Acad Sci U S A, 2006. **103**(43): p. 16021-6.

46. McGrath, K.E., J.M. Frame, and J. Palis, *Early hematopoiesis and macrophage development.* Semin Immunol, 2015. **27**(6): p. 379-87.

47. Perdiguero, E.G. and F. Geissmann, *The development and maintenance of resident macrophages.* Nat Immunol, 2016. **17**(1): p. 2-8.

48. Ginhoux, F. and S. Jung, *Monocytes and macrophages: developmental pathways and tissue homeostasis.* Nat Rev Immunol, 2014. **14**(6): p. 392-404.

49. Yoder, M.C., *Inducing definitive hematopoiesis in a dish.* Nat Biotechnol, 2014. **32**(6): p. 539-41.

50. Ginhoux, F. and M. Guilliams, *Tissue-Resident Macrophage Ontogeny and Homeostasis.* Immunity, 2016. **44**(3): p. 439-49.

51. Xu, J., et al., *Temporal-Spatial Resolution Fate Mapping Reveals Distinct Origins for Embryonic and Adult Microglia in Zebrafish.* Dev Cell, 2015. **34**(6): p. 632-41.

52. Kierdorf, K., et al., *Microglia emerge from erythromyeloid precursors via Pu.1- and Irf8-dependent pathways.* Nat Neurosci, 2013. **16**(3): p. 273-80.

53. Schulz, C., et al., *A lineage of myeloid cells independent of Myb and hematopoietic stem cells.* Science, 2012. **336**(6077): p. 86-90.

54. Erblich, B., et al., *Absence of colony stimulation factor-1 receptor results in loss of microglia, disrupted brain development and olfactory deficits.* PLoS One, 2011. **6**(10): p. e26317.

55. Tay, T.L., et al., *Microglia across the lifespan: from origin to function in brain development, plasticity and cognition.* J Physiol, 2017. **595**(6): p. 1929-1945.

56. Verney, C., et al., *Early microglial colonization of the human forebrain and possible involvement in periventricular white-matter injury of preterm infants.* J Anat, 2010. **217**(4): p. 436-48.

57. Monier, A., et al., *Entry and distribution of microglial cells in human embryonic and fetal cerebral cortex.* J Neuropathol Exp Neurol, 2007. **66**(5): p. 372-82.

58. Elmore, M.R., et al., *Colony-stimulating factor 1 receptor signaling is necessary for microglia viability, unmasking a microglia progenitor cell in the adult brain.* Neuron, 2014. **82**(2): p. 380-97.

59. Ueno, M. and T. Yamashita, *Bidirectional tuning of microglia in the developing brain: from neurogenesis to neural circuit formation.* Curr Opin Neurobiol, 2014. **27**: p. 8-15.

60. Wei, S., et al., *Functional overlap but differential expression of CSF-1 and IL-34 in their CSF-1 receptor-mediated regulation of myeloid cells.* J Leukoc Biol, 2010. **88**(3): p. 495-505.

61. Nandi, S., et al., *The CSF-1 receptor ligands IL-34 and CSF-1 exhibit distinct developmental brain expression patterns and regulate neural progenitor cell maintenance and maturation.* Dev Biol, 2012. **367**(2): p. 100-13.

62. Arno, B., et al., *Neural progenitor cells orchestrate microglia migration and positioning into the developing cortex.* Nat Commun, 2014. **5**: p. 5611.

63. Lelli, A., et al., *The NADPH oxidase Nox2 regulates VEGFR1/CSF-1R-mediated microglial chemotaxis and promotes early postnatal infiltration of phagocytes in the subventricular zone of the mouse cerebral cortex.* Glia, 2013. **61**(9): p. 1542-55.

64. Paolicelli, R.C., et al., *Synaptic pruning by microglia is necessary for normal brain development.* Science, 2011. **333**(6048): p. 1456-8.

65. Hoshiko, M., et al., *Deficiency of the microglial receptor CX3CR1 impairs postnatal functional development of thalamocortical synapses in the barrel cortex.* J Neurosci, 2012. **32**(43): p. 15106-11.

66. Ueno, M., et al., *Layer V cortical neurons require microglial support for survival during postnatal development.* Nat Neurosci, 2013. **16**(5): p. 543-51.

67. Walsh, C.E. and P.F. Hitchcock, *Progranulin regulates neurogenesis in the developing vertebrate retina.* Dev Neurobiol, 2017.

68. Xu, J., et al., *Microglia Colonization of Developing Zebrafish Midbrain Is Promoted by Apoptotic Neuron and Lysophosphatidylcholine.* Dev Cell, 2016. **38**(2): p. 214-22.

69. Martin-Estebane, M., et al., *Onset of microglial entry into developing quail retina coincides with increased expression of active caspase-3 and is mediated by extracellular ATP and UDP.* PLoS One, 2017. **12**(8): p. e0182450.

70. Eyo, U.B., et al., *Developmental changes in microglial mobilization are independent of apoptosis in the neonatal mouse hippocampus.* Brain Behav Immun, 2016. **55**: p. 49-59.

71. Eyo, U.B. and M.E. Dailey, *Microglia: key elements in neural development, plasticity, and pathology.* J Neuroimmune Pharmacol, 2013. **8**(3): p. 494-509.

72. Swinnen, N., et al., *Complex invasion pattern of the cerebral cortex bymicroglial cells during development of the mouse embryo.* Glia, 2013. **61**(2): p. 150-63.

73. Michell-Robinson, M.A., et al., *Roles of microglia in brain development, tissue maintenance and repair.* Brain, 2015. **138**(Pt 5): p. 1138-59.

74. Ashwell, K., *Development of microglia in the albino rabbit retina.* J Comp Neurol, 1989. **287**(3): p. 286-301.

75. Ashwell, K.W., et al., *The appearance and distribution of microglia in the developing retina of the rat.* Vis Neurosci, 1989. **2**(5): p. 437-48.

76. Billiards, S.S., et al., *Development of microglia in the cerebral white matter of the human fetus and infant.* J Comp Neurol, 2006. **497**(2): p. 199-208.

77. Dalmau, I., et al., *Dynamics of microglia in the developing rat brain.* J Comp Neurol, 2003. **458**(2): p. 144-57.

78. Marin-Teva, J.L., et al., *Tangential migration of ameboid microglia in the developing quail retina: mechanism of migration and migratory behavior.* Glia, 1998. **22**(1): p. 31-52.

79. Marin-Teva, J.L., et al., *Proliferation of actively migrating ameboid microglia in the developing quail retina.* Anat Embryol (Berl), 1999. **200**(3): p. 289-300.

80. Rezaie, P., K. Patel, and D.K. Male, *Microglia in the human fetal spinal cord--patterns of distribution, morphology and phenotype.* Brain Res Dev Brain Res, 1999. **115**(1): p. 71-81.

81. Sanchez-Lopez, A., et al., *Radial migration of developing microglial cells in quail retina: a confocal microscopy study.* Glia, 2004. **46**(3): p. 261-73.

82. Rezaie, P. and D. Male, *Colonisation of the developing human brain and spinal cord by microglia: a review.* Microsc Res Tech, 1999. **45**(6): p. 359-82.

83. Rezaie, P., et al., *Microglia in the cerebral wall of the human telencephalon at second trimester.* Cereb Cortex, 2005. **15**(7): p. 938-49.

84. Rigato, C., et al., *Microglia proliferation is controlled by P2X7 receptors in a Pannexin-1-independent manner during early embryonic spinal cord invasion.* J Neurosci, 2012. **32**(34): p. 11559-73.

85. Alliot, F., I. Godin, and B. Pessac, *Microglia derive from progenitors, originating from the yolk sac, and which proliferate in the brain.* Brain Res Dev Brain Res, 1999. **117**(2): p. 145-52.

86. Askew, K., et al., *Coupled Proliferation and Apoptosis Maintain the Rapid Turnover of Microglia in the Adult Brain.* Cell Rep, 2017. **18**(2): p. 391-405.

87. Kim, I., et al., *A postnatal peak in microglial development in the mouse hippocampus is correlated with heightened sensitivity to seizure triggers.* Brain Behav, 2015. **5**(12): p. e00403.

88. Garay, P.A., et al., *Maternal immune activation causes age- and region-specific changes in brain cytokines in offspring throughout development.* Brain Behav Immun, 2012.

89. Xavier, A.L., et al., *Ontogeny of CX3CR1-EGFP expressing cells unveil microglia as an integral component of the postnatal subventricular zone.* Front Cell Neurosci, 2015. **9**: p. 37.

90. Eyo, U.B., et al., *Developmental changes in microglial mobilization are independent of apoptosis in the neonatal mouse hippocampus.* Brain Behav Immun, 2015.

91. Navascues, J., et al., *Entry, dispersion and differentiation of microglia in the developing central nervous system.* An Acad Bras Cienc, 2000. **72**(1): p. 91-102.

92. Pont-Lezica, L., et al., *Physiological roles of microglia during development.* J Neurochem, 2011. **119**(5): p. 901-8.

93. Herbomel, P., B. Thisse, and C. Thisse, *Zebrafish early macrophages colonize cephalic mesenchyme and developing brain, retina, and epidermis through a M-CSF receptor-dependent invasive process.* Dev Biol, 2001. **238**(2): p. 274-88.

94. Cuadros, M.A. and J. Navascues, *The origin and differentiation of microglial cells during development.* Prog Neurobiol, 1998. **56**(2): p. 173-89.

95. Navascues, J., et al., *Origin of microglia in the quail retina: central-to-peripheral and vitreal-to-scleral migration of microglial precursors during development.* J Comp Neurol, 1995. **354**(2): p. 209-28.

96. Cuadros, M.A., et al., *Development of microglia in the quail optic tectum.* J Comp Neurol, 1994. **348**(2): p. 207-24.

97. Cuadros, M.A., et al., *Microglia development in the quail cerebellum.* J Comp Neurol, 1997. **389**(3): p. 390-401.

98. Dalmau, I., et al., *Expression of LFA-1alpha and ICAM-1 in the developing rat brain: a potential mechanism for the recruitment of microglial cell precursors.* Brain Res Dev Brain Res, 1997. **103**(2): p. 163-70.

99. Grossmann, R., et al., *Juxtavascular microglia migrate along brain microvessels following activation during early postnatal development.* Glia, 2002. **37**(3): p. 229-40.

100. Tanaka, J. and N. Maeda, *Microglial ramification requires nondiffusible factors derived from astrocytes.* Exp Neurol, 1996. **137**(2): p. 367-75.

101. Matyash, M., et al., *The adenosine generating enzymes CD39/CD73 control microglial processes ramification in the mouse brain.* PLoS One, 2017. **12**(4): p. e0175012.

102. Nayak, D., T.L. Roth, and D.B. McGavern, *Microglia development and function.* Annu Rev Immunol, 2014. **32**: p. 367-402.

103. Zusso, M., et al., *Regulation of postnatal forebrain amoeboid microglial cell proliferation and development by the transcription factor Runx1.* J Neurosci, 2012. **32**(33): p. 11285-98.

104. Miyamoto, A., et al., *Microglia contact induces synapse formation in developing somatosensory cortex.* Nat Commun, 2016. **7**: p. 12540.

105. Schilling, T., et al., *Upregulation of Kv1.3 K(+) channels in microglia deactivated by TGF-beta.* Am J Physiol Cell Physiol, 2000. **279**(4): p. C1123-34.

106. Nutile-McMenemy, N., A. Elfenbein, and J.A. Deleo, *Minocycline decreases in vitro microglial motility, beta1-integrin, and Kv1.3 channel expression.* J Neurochem, 2007. **103**(5): p. 2035-46.

107. Artym, V.V. and H.R. Petty, *Molecular proximity of Kv1.3 voltage-gated potassium channels and beta(1)-integrins on the plasma membrane of melanoma cells: effects of cell adherence and channel blockers.* J Gen Physiol, 2002. **120**(1): p. 29-37.

108. Levite, M., et al., *Extracellular K(+) and opening of voltage-gated potassium channels activate T cell integrin function: physical and functional association between Kv1.3 channels and beta1 integrins.* J Exp Med, 2000. **191**(7): p. 1167-76.

109. Svahn, A.J., et al., *miR-124 Contributes to the functional maturity of microglia.* Dev Neurobiol, 2016. **76**(5): p. 507-18.

110. Saika, R., et al., *MicroRNA-101a regulates microglial morphology and inflammation.* J Neuroinflammation, 2017. **14**(1): p. 109.

111. Pagani, F., et al., *Defective microglial development in the hippocampus of Cx3cr1 deficient mice.* Front Cell Neurosci, 2015. **9**: p. 111.

112. Matcovitch-Natan, O., et al., *Microglia development follows a stepwise program to regulate brain homeostasis.* Science, 2016. **353**(6301): p. aad8670.

113. Butovsky, O., et al., *Identification of a unique TGF-beta-dependent molecular and functional signature in microglia.* Nat Neurosci, 2014. **17**(1): p. 131-43.

114. Wong, K., et al., *Mice deficient in NRROS show abnormal microglial development and neurological disorders.* Nat Immunol, 2017. **18**(6): p. 633-641.

115. Erny, D., et al., *Host microbiota constantly control maturation and function of microglia in the CNS.* Nat Neurosci, 2015. **18**(7): p. 965-77.

116. Hanamsagar, R., et al., *Generation of a microglial developmental index in mice and in humans reveals a sex difference in maturation and immune reactivity.* Glia, 2017.

117. Tay, T.L., et al., *A new fate mapping system reveals context-dependent random or clonal expansion of microglia.* Nat Neurosci, 2017.

118. Reu, P., et al., *The Lifespan and Turnover of Microglia in the Human Brain.* Cell Rep, 2017. **20**(4): p. 779-784.

119. Bruttger, J., et al., *Genetic Cell Ablation Reveals Clusters of Local Self-Renewing Microglia in the Mammalian Central Nervous System.* Immunity, 2015. **43**(1): p. 92-106.

120. Lavin, Y., et al., *Tissue-resident macrophage enhancer landscapes are shaped by the local microenvironment.* Cell, 2014. **159**(6): p. 1312-26.

121. Gosselin, D., et al., *Environment drives selection and function of enhancers controlling tissue-specific macrophage identities.* Cell, 2014. **159**(6): p. 1327-40.

122. Gautier, E.L., et al., *Gene-expression profiles and transcriptional regulatory pathways that underlie the identity and diversity of mouse tissue macrophages.* Nat Immunol, 2012. **13**(11): p. 1118-28.

123. Buttgereit, A., et al., *Sall1 is a transcriptional regulator defining microglia identity and function.* Nat Immunol, 2016. **17**(12): p. 1397-1406.

124. Grabert, K., et al., *Microglial brain region-dependent diversity and selective regional sensitivities to aging.* Nat Neurosci, 2016. **19**(3): p. 504-16.

125. Crotti, A. and R.M. Ransohoff, *Microglial Physiology and Pathophysiology: Insights from Genome-wide Transcriptional Profiling.* Immunity, 2016. **44**(3): p. 505-15.

126. Goldmann, T., et al., *Origin, fate and dynamics of macrophages at central nervous system interfaces.* Nat Immunol, 2016. **17**(7): p. 797-805.

127. Hart, A.D., et al., *Age related changes in microglial phenotype vary between CNS regions: grey versus white matter differences.* Brain Behav Immun, 2012. **26**(5): p. 754-65.

128. Schnell, L., et al., *Acute inflammatory responses to mechanical lesions in the CNS: differences between brain and spinal cord.* Eur J Neurosci, 1999. **11**(10): p. 3648-58.

129. Flowers, A., et al., *Proteomic anaysis of aged microglia: shifts in transcription, bioenergetics, and nutrient response.* J Neuroinflammation, 2017. **14**(1): p. 96.

130. De Biase, L.M., et al., *Local Cues Establish and Maintain Region-Specific Phenotypes of Basal Ganglia Microglia.* Neuron, 2017.

131. Zrzavy, T., et al., *Loss of 'homeostatic' microglia and patterns of their activation in active multiple sclerosis.* Brain, 2017. **140**(7): p. 1900-1913.

132. Bennett, M.L., et al., *New tools for studying microglia in the mouse and human CNS.* Proc Natl Acad Sci U S A, 2016. **113**(12): p. E1738-46.

133. Harrison, S.J., et al., *Sall1 regulates cortical neurogenesis and laminar fate specification in mice: implications for neural abnormalities in Townes-Brocks syndrome.* Dis Model Mech, 2012. **5**(3): p. 351-65.

134. Holtman, I.R., D. Skola, and C.K. Glass, *Transcriptional control of microglia phenotypes in health and disease.* J Clin Invest, 2017.

135. Prinz, M., D. Erny, and N. Hagemeyer, *Ontogeny and homeostasis of CNS myeloid cells.* Nat Immunol, 2017. **18**(4): p. 385-392.

136. Hickman, S.E., et al., *The microglial sensome revealed by direct RNA sequencing.* Nat Neurosci, 2013. **16**(12): p. 1896-905.

137. Italiani, P. and D. Boraschi, *From Monocytes to M1/M2 Macrophages: Phenotypical vs. Functional Differentiation.* Front Immunol, 2014. **5**: p. 514.

138. Yona, S., et al., *Fate mapping reveals origins and dynamics of monocytes and tissue macrophages under homeostasis.* Immunity, 2013. **38**(1): p. 79-91.

139. Chiu, I.M., et al., *A neurodegeneration-specific gene-expression signature of acutely isolated microglia from an amyotrophic lateral sclerosis mouse model.* Cell Rep, 2013. **4**(2): p. 385-401.

140. Kierdorf, K., et al., *Development and function of tissue resident macrophages in mice.* Semin Immunol, 2015. **27**(6): p. 369-78.

141. Marin-Teva, J.L., et al., *Microglia promote the death of developing Purkinje cells.* Neuron, 2004. **41**(4): p. 535-47.

142. Wakselman, S., et al., *Developmental neuronal death in hippocampus requires the microglial CD11b integrin and DAP12 immunoreceptor.* J Neurosci, 2008. **28**(32): p. 8138-43.

143. Antony, J.M., et al., *Endogenous microglia regulate development of embryonic cortical precursor cells.* J Neurosci Res, 2011. **89**(3): p. 286-98.

144. Cunningham, C.L., V. Martinez-Cerdeno, and S.C. Noctor, *Microglia regulate the number of neural precursor cells in the developing cerebral cortex.* J Neurosci, 2013. **33**(10): p. 4216-33.

145. Cunningham, C., *Microglia and neurodegeneration: the role of systemic inflammation.* Glia, 2013. **61**(1): p. 71-90.

146. Garden, G.A. and T. Moller, *Microglia biology in health and disease.* J Neuroimmune Pharmacol, 2006. **1**(2): p. 127-37.

147. Masuda, T. and M. Prinz, *Microglia: A Unique Versatile Cell in the Central Nervous System.* ACS Chem Neurosci, 2016. **7**(4): p. 428-34.

148. Shigemoto-Mogami, Y., et al., *Microglia enhance neurogenesis and oligodendrogenesis in the early postnatal subventricular zone.* J Neurosci, 2014. **34**(6): p. 2231-43.

149. Mosher, K.I., et al., *Neural progenitor cells regulate microglia functions and activity.* Nat Neurosci, 2012. **15**(11): p. 1485-7.

150. Bechade, C., et al., *Nitric oxide regulates astrocyte maturation in the hippocampus: involvement of NOS2.* Mol Cell Neurosci, 2011. **46**(4): p. 762-9.

151. Squarzoni, P., et al., *Microglia modulate wiring of the embryonic forebrain.* Cell Rep, 2014. **8**(5): p. 1271-9.

152. Pont-Lezica, L., et al., *Microglia shape corpus callosum axon tract fasciculation: functional impact of prenatal inflammation.* Eur J Neurosci, 2014. **39**(10): p. 1551-7.

153. Chamak, B., V. Morandi, and M. Mallat, *Brain macrophages stimulate neurite growth and regeneration by secreting thrombospondin.* J Neurosci Res, 1994. **38**(2): p. 221-33.

154. Chamak, B., A. Dobbertin, and M. Mallat, *Immunohistochemical detection of thrombospondin in microglia in the developing rat brain.* Neuroscience, 1995. **69**(1): p. 177-87.

155. Wu, Y., et al., *Microglia: Dynamic Mediators of Synapse Development and Plasticity.* Trends Immunol, 2015. **36**(10): p. 605-13.

156. Zhan, Y., et al., *Deficient neuron-microglia signaling results in impaired functional brain connectivity and social behavior.* Nat Neurosci, 2014. **17**(3): p. 400-6.

157. Checchin, D., et al., *Potential role of microglia in retinal blood vessel formation.* Invest Ophthalmol Vis Sci, 2006. **47**(8): p. 3595-602.

158. Kubota, Y., et al., *M-CSF inhibition selectively targets pathological angiogenesis and lymphangiogenesis.* J Exp Med, 2009. **206**(5): p. 1089-102.

159. Fantin, A., et al., *Tissue macrophages act as cellular chaperones for vascular anastomosis downstream of VEGF-mediated endothelial tip cell induction.* Blood, 2010. **116**(5): p. 829-40.

160. Stefater, J.A., 3rd, et al., *Regulation of angiogenesis by a non-canonical Wnt-Flt1 pathway in myeloid cells.* Nature, 2011. **474**(7352): p. 511-5.

161. Unoki, N., et al., *SDF-1/CXCR4 contributes to the activation of tip cells and microglia in retinal angiogenesis.* Invest Ophthalmol Vis Sci, 2010. **51**(7): p. 3362-71.

162. Rymo, S.F., et al., *A two-way communication between microglial cells and angiogenic sprouts regulates angiogenesis in aortic ring cultures.* PLoS One, 2011. **6**(1): p. e15846.

163. Outtz, H.H., et al., *Notch1 controls macrophage recruitment and Notch signaling is activated at sites of endothelial cell anastomosis during retinal angiogenesis in mice.* Blood, 2011. **118**(12): p. 3436-9.

164. Wolf, S.A., H.W. Boddeke, and H. Kettenmann, *Microglia in Physiology and Disease.* Annu Rev Physiol, 2017. **79**: p. 619-643.

165. Hughes, V., *Microglia: The constant gardeners.* Nature, 2012. **485**(7400): p. 570-2.

166. Brown, A., *Understanding the MIND phenotype: macrophage/microglia inflammation in neurocognitive disorders related to human immunodeficiency virus infection.* Clin Transl Med, 2015. **4**: p. 7.

167. Wake, H., et al., *Resting microglia directly monitor the functional state of synapses in vivo and determine the fate of ischemic terminals.* J Neurosci, 2009. **29**(13): p. 3974-80.

168. Li, Y., et al., *Reciprocal regulation between resting microglial dynamics and neuronal activity in vivo.* Dev Cell, 2012. **23**(6): p. 1189-202.

169. Fontainhas, A.M., et al., *Microglial morphology and dynamic behavior is regulated by ionotropic glutamatergic and GABAergic neurotransmission.* PLoS One, 2011. **6**(1): p. e15973.

170. Tremblay, M.E., et al., *Effects of aging and sensory loss on glial cells in mouse visual and auditory cortices.* Glia, 2012. **60**(4): p. 541-58.

171. Parkhurst, C.N., et al., *Microglia promote learning-dependent synapse formation through brain-derived neurotrophic factor.* Cell, 2013. **155**(7): p. 1596-609.

172. Bessis, A., et al., *Microglial control of neuronal death and synaptic properties.* Glia, 2007. **55**(3): p. 233-8.

173. Stevens, B., et al., *The classical complement cascade mediates CNS synapse elimination.* Cell, 2007. **131**(6): p. 1164-78.

174. Schafer, D.P., et al., *Microglia sculpt postnatal neural circuits in an activity and complement-dependent manner.* Neuron, 2012. **74**(4): p. 691-705.

175. Bialas, A.R. and B. Stevens, *TGF-beta signaling regulates neuronal C1q expression and developmental synaptic refinement.* Nat Neurosci, 2013. **16**(12): p. 1773-82.

176. Bahrini, I., et al., *Neuronal exosomes facilitate synaptic pruning by up-regulating complement factors in microglia.* Sci Rep, 2015. **5**: p. 7989.

177. Czirr, E., et al., *Microglial complement receptor 3 regulates brain Abeta levels through secreted proteolytic activity.* J Exp Med, 2017.

178. Rogers, J.T., et al., *CX3CR1 deficiency leads to impairment of hippocampal cognitive function and synaptic plasticity.* J Neurosci, 2011. **31**(45): p. 16241-50.

179. Tsuda, M., et al., *P2X4 receptors induced in spinal microglia gate tactile allodynia after nerve injury.* Nature, 2003. **424**(6950): p. 778-83.

180. Coull, J.A., et al., *BDNF from microglia causes the shift in neuronal anion gradient underlying neuropathic pain.* Nature, 2005. **438**(7070): p. 1017-21.

181. Sipe, G.O., et al., *Microglial P2Y12 is necessary for synaptic plasticity in mouse visual cortex.* Nat Commun, 2016. **7**: p. 10905.

182. Schafer, D.P., E.K. Lehrman, and B. Stevens, *The "quad-partite" synapse: microglia-synapse interactions in the developing and mature CNS.* Glia, 2013. **61**(1): p. 24-36.

183. Cantaut-Belarif, Y., et al., *Microglia control the glycinergic but not the GABAergic synapses via prostaglandin E2 in the spinal cord.* J Cell Biol, 2017.

184. Sato, K., *Effects of Microglia on Neurogenesis.* Glia, 2015. **63**(8): p. 1394-405.

185. Ribeiro Xavier, A.L., et al., *A Distinct Population of Microglia Supports Adult Neurogenesis in the Subventricular Zone.* J Neurosci, 2015. **35**(34): p. 11848-61.

186. Sierra, A., et al., *Microglia shape adult hippocampal neurogenesis through apoptosis-coupled phagocytosis.* Cell Stem Cell, 2010. **7**(4): p. 483-95.

187. Chew, L.J., A. Takanohashi, and M. Bell, *Microglia and inflammation: impact on developmental brain injuries.* Ment Retard Dev Disabil Res Rev, 2006. **12**(2): p. 105-12.

188. Rotshenker, S., *The role of Galectin-3/MAC-2 in the activation of the innate-immune function of phagocytosis in microglia in injury and disease.* J Mol Neurosci, 2009. **39**(1-2): p. 99-103.

189. Colonna, M. and O. Butovsky, *Microglia Function in the Central Nervous System During Health and Neurodegeneration.* Annu Rev Immunol, 2017.

190. Hanisch, U.K. and H. Kettenmann, *Microglia: active sensor and versatile effector cells in the normal and pathologic brain.* Nat Neurosci, 2007. **10**(11): p. 1387-94.

191. Ransohoff, R.M., *A polarizing question: do M1 and M2 microglia exist?* Nat Neurosci, 2016. **19**(8): p. 987-91.

192. Ginhoux, F., et al., *New insights into the multidimensional concept of macrophage ontogeny, activation and function.* Nat Immunol, 2016. **17**(1): p. 34-40.

193. Jin, X. and T. Yamashita, *Microglia in central nervous system repair after injury.* J Biochem, 2016. **159**(5): p. 491-6.

194. Shechter, R., et al., *Infiltrating blood-derived macrophages are vital cells playing an anti-inflammatory role in recovery from spinal cord injury in mice.* PLoS Med, 2009. **6**(7): p. e1000113.

195. Rolls, A., R. Shechter, and M. Schwartz, *The bright side of the glial scar in CNS repair.* Nat Rev Neurosci, 2009. **10**(3): p. 235-41.

196. Rolls, A., et al., *Two faces of chondroitin sulfate proteoglycan in spinal cord repair: a role in microglia/macrophage activation.* PLoS Med, 2008. **5**(8): p. e171.

197. Kawabori, M. and M.A. Yenari, *The role of the microglia in acute CNS injury.* Metab Brain Dis, 2015. **30**(2): p. 381-92.

198. Zhou, X., X. He, and Y. Ren, *Function of microglia and macrophages in secondary damage after spinal cord injury.* Neural Regen Res, 2014. **9**(20): p. 1787-95.

199. Madsen, D.H. and T.H. Bugge, *Imaging collagen degradation in vivo highlights a key role for M2-polarized macrophages in extracellular matrix degradation.* Oncoimmunology, 2013. **2**(12): p. e27127.

200. Shechter, R., et al., *The glial scar-monocyte interplay: a pivotal resolution phase in spinal cord repair.* PLoS One, 2011. **6**(12): p. e27969.

201. Madsen, D.H., et al., *M2-like macrophages are responsible for collagen degradation through a mannose receptor-mediated pathway.* J Cell Biol, 2013. **202**(6): p. 951-66.

202. Kigerl, K.A., et al., *Identification of two distinct macrophage subsets with divergent effects causing either neurotoxicity or regeneration in the injured mouse spinal cord.* J Neurosci, 2009. **29**(43): p. 13435-44.

203. Domingues, H.S., et al., *Oligodendrocyte, Astrocyte, and Microglia Crosstalk in Myelin Development, Damage, and Repair.* Front Cell Dev Biol, 2016. **4**: p. 71.

204. Miron, V.E., et al., *M2 microglia and macrophages drive oligodendrocyte differentiation during CNS remyelination.* Nat Neurosci, 2013. **16**(9): p. 1211-1218.

205. Ren, Y. and W. Young, *Managing inflammation after spinal cord injury through manipulation of macrophage function.* Neural Plast, 2013. **2013**: p. 945034.

206. Hu, X., et al., *Microglial and macrophage polarization-new prospects for brain repair.* Nat Rev Neurol, 2015. **11**(1): p. 56-64.

207. Reisinger, S., et al., *The poly(I:C)-induced maternal immune activation model in preclinical neuropsychiatric drug discovery.* Pharmacol Ther, 2015. **149**: p. 213-26.

208. Knuesel, I., et al., *Maternal immune activation and abnormal brain development across CNS disorders.* Nat Rev Neurol, 2014. **10**(11): p. 643-60.

209. Fernandez de Cossio, L., et al., *Prenatal infection leads to ASD-like behavior and altered synaptic pruning in the mouse offspring.* Brain Behav Immun, 2017. **63**: p. 88-98.

210. Kim, H.J., et al., *Deficient autophagy in microglia impairs synaptic pruning and causes social behavioral defects.* Mol Psychiatry, 2016.

211. Paolicelli, R.C. and M.T. Ferretti, *Function and Dysfunction of Microglia during Brain Development: Consequences for Synapses and Neural Circuits.* Front Synaptic Neurosci, 2017. **9**: p. 9.

212. Petrelli, F., L. Pucci, and P. Bezzi, *Astrocytes and Microglia and Their Potential Link with Autism Spectrum Disorders.* Front Cell Neurosci, 2016. **10**: p. 21.

213. Werling, D.M., *The role of sex-differential biology in risk for autism spectrum disorder.* Biol Sex Differ, 2016. **7**: p. 58.

214. Nardone, S. and E. Elliott, *The Interaction between the Immune System and Epigenetics in the Etiology of Autism Spectrum Disorders.* Front Neurosci, 2016. **10**: p. 329.

215. Alexopoulou, L., et al., *Recognition of double-stranded RNA and activation of NF-kappaB by Toll-like receptor 3.* Nature, 2001. **413**(6857): p. 732-8.

216. Choi, G.B., et al., *The maternal interleukin-17a pathway in mice promotes autism-like phenotypes in offspring.* Science, 2016. **351**(6276): p. 933-9.

217. Smith, S.E., et al., *Maternal immune activation alters fetal brain development through interleukin-6.* J Neurosci, 2007. **27**(40): p. 10695-702.

218. Patterson, P., Xu, W., Smith, S., Devarman, B., *Maternal Immune Activation, Cytokines and Autism*, in *Autism*, A.W. Zimmerman, Editor 2008, Humana Press: Totowa, NJ.

219. Malkova, N.V., et al., *Maternal immune activation yields offspring displaying mouse versions of the three core symptoms of autism.* Brain Behav Immun, 2012.

220. Bauman, M.D., et al., *Activation of the maternal immune system during pregnancy alters behavioral development of rhesus monkey offspring.* Biol Psychiatry, 2014. **75**(4): p. 332-41.

221. Machado, C.J., et al., *Maternal immune activation in nonhuman primates alters social attention in juvenile offspring.* Biol Psychiatry, 2015. **77**(9): p. 823-32.

222. Shi, L., et al., *Maternal influenza infection causes marked behavioral and pharmacological changes in the offspring.* J Neurosci, 2003. **23**(1): p. 297-302.

223. Patterson, P.H., Xu W, Smith S.E.P, Devarman B.E, *Maternal Imunne Activation, Cytokines and Autism.* A.W. Zimmerman (ed.), Autism, 2008.

224. Mondelli, V., et al., *Brain microglia in psychiatric disorders.* Lancet Psychiatry, 2017. **4**(7): p. 563-572.

225. Bayer, T.A., et al., *Evidence for activation of microglia in patients with psychiatric illnesses.* Neurosci Lett, 1999. **271**(2): p. 126-8.

226. Radewicz, K., et al., *Increase in HLA-DR immunoreactive microglia in frontal and temporal cortex of chronic schizophrenics.* J Neuropathol Exp Neurol, 2000. **59**(2): p. 137-50.

227. Upthegrove, R., N. Manzanares-Teson, and N.M. Barnes, *Cytokine function in medication-naive first episode psychosis: a systematic review and meta-analysis.* Schizophr Res, 2014. **155**(1-3): p. 101-8.

228. Howes, O.D. and R. McCutcheon, *Inflammation and the neural diathesis-stress hypothesis of schizophrenia: a reconceptualization.* Transl Psychiatry, 2017. **7**(2): p. e1024.

229. Vargas, D.L., et al., *Neuroglial activation and neuroinflammation in the brain of patients with autism.* Ann Neurol, 2005. **57**(1): p. 67-81.

230. Morgan, J.T., et al., *Microglial activation and increased microglial density observed in the dorsolateral prefrontal cortex in autism.* Biol Psychiatry, 2010. **68**(4): p. 368-76.

231. Suzuki, K., et al., *Microglial activation in young adults with autism spectrum disorder.* JAMA Psychiatry, 2013. **70**(1): p. 49-58.

232. Hafizi, S., et al., *Imaging Microglial Activation in Individuals at Clinical High Risk for Psychosis: An In-Vivo PET Study with [18F]FEPPA.* Neuropsychopharmacology, 2017.

233. Loth, M.K., et al., *TSPO in a murine model of Sandhoff disease: presymptomatic marker of neurodegeneration and disease pathophysiology.* Neurobiol Dis, 2016. **85**: p. 174-86.

234. Roncaroli, F., et al., *TSPO expression in brain tumours: is TSPO a target for brain tumour imaging?* Clin Transl Imaging, 2016. **4**: p. 145-156.

235. Veronese, M., et al., *Kinetic modelling of [11C]PBR28 for 18 kDa translocator protein PET data: A validation study of vascular modelling in the brain using XBD173 and tissue analysis.* J Cereb Blood Flow Metab, 2017: p. 271678X17712388.

236. Owen, D.R., et al., *Pro-inflammatory activation of primary microglia and macrophages increases 18 kDa translocator protein expression in rodents but not humans.* J Cereb Blood Flow Metab, 2017: p. 271678X17710182.

237. Voineagu, I., et al., *Transcriptomic analysis of autistic brain reveals convergent molecular pathology.* Nature, 2011. **474**(7351): p. 380-4.

238. Patterson, P.H., *Maternal infection: window on neuroimmune interactions in fetal brain development and mental illness.* Curr Opin Neurobiol, 2002. **12**(1): p. 115-8.

239. Fatemi, S.H., et al., *Glial fibrillary acidic protein and glutamic acid decarboxylase 65 and 67 kDa proteins are increased in brains of neonatal BALB/c mice following viral infection in utero.* Schizophr Res, 2004. **69**(1): p. 121-3.

240. Golan, H.M., et al., *Specific neurodevelopmental damage in mice offspring following maternal inflammation during pregnancy.* Neuropharmacology, 2005. **48**(6): p. 903-17.

241. Hutton, L.C., et al., *Microglial activation, macrophage infiltration, and evidence of cell death in the fetal brain after uteroplacental administration of lipopolysaccharide in sheep in late gestation.* Am J Obstet Gynecol, 2008. **198**(1): p. 117 e1-11.

242. Butovsky, O., et al., *Activation of microglia by aggregated beta-amyloid or lipopolysaccharide impairs MHC-II expression and renders them cytotoxic whereas IFN-gamma and IL-4 render them protective.* Mol Cell Neurosci, 2005. **29**(3): p. 381-93.

243. Fatemi, S.H., et al., *Prenatal viral infection leads to pyramidal cell atrophy and macrocephaly in adulthood: implications for genesis of autism and schizophrenia.* Cell Mol Neurobiol, 2002. **22**(1): p. 25-33.

244. Fatemi, S.H., et al., *Prenatal viral infection causes alterations in nNOS expression in developing mouse brains.* Neuroreport, 2000. **11**(7): p. 1493-6.

245. Fatemi, S.H., et al., *Defective corticogenesis and reduction in Reelin immunoreactivity in cortex and hippocampus of prenatally infected neonatal mice.* Mol Psychiatry, 1999. **4**(2): p. 145-54.

246. Fatemi, S.H., et al., *Human influenza viral infection in utero increases nNOS expression in hippocampi of neonatal mice.* Synapse, 1998. **29**(1): p. 84-8.

247. Giovanoli, S., et al., *Late prenatal immune activation causes hippocampal deficits in the absence of persistent inflammation across aging.* J Neuroinflammation, 2015. **12**: p. 221.

248. Meyer, U., et al., *The time of prenatal immune challenge determines the specificity of inflammation-mediated brain and behavioral pathology.* J Neurosci, 2006. **26**(18): p. 4752-62.

249. Frick, L.R., K. Williams, and C. Pittenger, *Microglial dysregulation in psychiatric disease.* Clin Dev Immunol, 2013. **2013**: p. 608654.

250. Bauer, S., B.J. Kerr, and P.H. Patterson, *The neuropoietic cytokine family in development, plasticity, disease and injury.* Nat Rev Neurosci, 2007. **8**(3): p. 221-32.

251. Deverman, B.E. and P.H. Patterson, *Cytokines and CNS development.* Neuron, 2009. **64**(1): p. 61-78.

252. Nakanishi, M., et al., *Microglia-derived interleukin-6 and leukaemia inhibitory factor promote astrocytic differentiation of neural stem/progenitor cells.* Eur J Neurosci, 2007. **25**(3): p. 649-58.

253. Koyama, R. and Y. Ikegaya, *Microglia in the pathogenesis of autism spectrum disorders.* Neurosci Res, 2015. **100**: p. 1-5.

254. Roumier, A., et al., *Impaired synaptic function in the microglial KARAP/DAP12-deficient mouse.* J Neurosci, 2004. **24**(50): p. 11421-8.

255. Paloneva, J., et al., *Loss-of-function mutations in TYROBP (DAP12) result in a presenile dementia with bone cysts.* Nat Genet, 2000. **25**(3): p. 357-61.

256. Roumier, A., et al., *Prenatal activation of microglia induces delayed impairment of glutamatergic synaptic function.* PLoS One, 2008. **3**(7): p. e2595.

257. Kaifu, T., et al., *Osteopetrosis and thalamic hypomyelinosis with synaptic degeneration in DAP12-deficient mice.* J Clin Invest, 2003. **111**(3): p. 323-32.

258. McKim, D.B., et al., *Microglial recruitment of IL-1beta-producing monocytes to brain endothelium causes stress-induced anxiety.* Mol Psychiatry, 2017.

259. Chen, S.K., et al., *Hematopoietic origin of pathological grooming in Hoxb8 mutant mice.* Cell, 2010. **141**(5): p. 775-85.

260. Krabbe, G., et al., *Microglial NFkappaB-TNFalpha hyperactivation induces obsessive-compulsive behavior in mouse models of progranulin-deficient frontotemporal dementia.* Proc Natl Acad Sci U S A, 2017.

261. Derecki, N.C., et al., *Wild-type microglia arrest pathology in a mouse model of Rett syndrome.* Nature, 2012. **484**(7392): p. 105-9.

262. Cronk, J.C., et al., *Methyl-CpG Binding Protein 2 Regulates Microglia and Macrophage Gene Expression in Response to Inflammatory Stimuli.* Immunity, 2015. **42**(4): p. 679-91.

263. Wang, J., et al., *Wild-type microglia do not reverse pathology in mouse models of Rett syndrome.* Nature, 2015. **521**(7552): p. E1-4.

264. Schafer, D.P., et al., *Microglia contribute to circuit defects in Mecp2 null mice independent of microglia-specific loss of Mecp2 expression.* Elife, 2016. **5**.

265. Paolicelli, R.C., et al., *TDP-43 Depletion in Microglia Promotes Amyloid Clearance but Also Induces Synapse Loss.* Neuron, 2017.

266. VanRyzin, J.W., et al., *Temporary Depletion of Microglia during the Early Postnatal Period Induces Lasting Sex-Dependent and Sex-Independent Effects on Behavior in Rats.* eNeuro, 2016. **3**(6).

267. Nissen, J.C., *Microglial Function across the Spectrum of Age and Gender.* Int J Mol Sci, 2017. **18**(3).

268. Nelson, L.H., S. Warden, and K.M. Lenz, *Sex differences in microglial phagocytosis in the neonatal hippocampus.* Brain Behav Immun, 2017.

269. Lenz, K.M. and M.M. McCarthy, *A starring role for microglia in brain sex differences.* Neuroscientist, 2015. **21**(3): p. 306-21.

270. Lenz, K.M., et al., *Microglia are essential to masculinization of brain and behavior.* J Neurosci, 2013. **33**(7): p. 2761-72.

271. Rozario, T. and D.W. DeSimone, *The extracellular matrix in development and morphogenesis: a dynamic view.* Dev Biol, 2010. **341**(1): p. 126-40.

272. Vicente-Manzanares, M. and A.R. Horwitz, *Cell migration: an overview.* Methods Mol Biol, 2011. **769**: p. 1-24.

273. Fraley, S.I., et al., *A distinctive role for focal adhesion proteins in three-dimensional cell motility.* Nat Cell Biol, 2010. **12**(6): p. 598-604.

274. Theocharis, A.D., et al., *Extracellular matrix structure.* Adv Drug Deliv Rev, 2016. **97**: p. 4-27.

275. Ahmed, M. and C. Ffrench-Constant, *Extracellular Matrix Regulation of Stem Cell Behavior.* Curr Stem Cell Rep, 2016. **2**: p. 197-206.

276. Barnes, J.M., L. Przybyla, and V.M. Weaver, *Tissue mechanics regulate brain development, homeostasis and disease.* J Cell Sci, 2017. **130**(1): p. 71-82.

277. Stoffels, J.M., et al., *Fibronectin aggregation in multiple sclerosis lesions impairs remyelination.* Brain, 2013. **136**(Pt 1): p. 116-31.

278. Bachman, H., et al., *Utilizing Fibronectin Integrin-Binding Specificity to Control Cellular Responses.* Adv Wound Care (New Rochelle), 2015. **4**(8): p. 501-511.

279. Zollinger, A.J. and M.L. Smith, *Fibronectin, the extracellular glue.* Matrix Biol, 2016.

280. Engler, A.J., et al., *Matrix elasticity directs stem cell lineage specification.* Cell, 2006. **126**(4): p. 677-89.

281. Caiazzo, M., et al., *Defined three-dimensional microenvironments boost induction of pluripotency.* Nat Mater, 2016. **15**(3): p. 344-52.

282. Dalby, M.J., N. Gadegaard, and R.O. Oreffo, *Harnessing nanotopography and integrin-matrix interactions to influence stem cell fate.* Nat Mater, 2014. **13**(6): p. 558-69.

283. Doyle, A.D. and K.M. Yamada, *Mechanosensing via cell-matrix adhesions in 3D microenvironments.* Exp Cell Res, 2016. **343**(1): p. 60-6.

284. Lau, L.W., et al., *Pathophysiology of the brain extracellular matrix: a new target for remyelination.* Nat Rev Neurosci, 2013. **14**(10): p. 722-9.

285. Soleman, S., et al., *Targeting the neural extracellular matrix in neurological disorders.* Neuroscience, 2013. **253**: p. 194-213.

286. Gordon, M.K. and R.A. Hahn, *Collagens.* Cell Tissue Res, 2010. **339**(1): p. 247-57.

287. Jones, F.S. and P.L. Jones, *The tenascin family of ECM glycoproteins: structure, function, and regulation during embryonic development and tissue remodeling.* Dev Dyn, 2000. **218**(2): p. 235-59.

288. Ffrench-Constant, C. and R.O. Hynes, *Alternative splicing of fibronectin is temporally and spatially regulated in the chicken embryo.* Development, 1989. **106**(2): p. 375-88.

289. Domogatskaya, A., S. Rodin, and K. Tryggvason, *Functional diversity of laminins.* Annu Rev Cell Dev Biol, 2012. **28**: p. 523-53.

290. Ruoslahti, E., *Brain extracellular matrix.* Glycobiology, 1996. **6**(5): p. 489-92.

291. Bruckner, G., et al., *Postnatal development of perineuronal nets in wild-type mice and in a mutant deficient in tenascin-R.* J Comp Neurol, 2000. **428**(4): p. 616-29.

292. De Luca, C. and M. Papa, *Looking Inside the Matrix: Perineuronal Nets in Plasticity, Maladaptive Plasticity and Neurological Disorders.* Neurochem Res, 2016. **41**(7): p. 1507-15.

293. Suttkus, A., M. Morawski, and T. Arendt, *Protective Properties of Neural Extracellular Matrix.* Mol Neurobiol, 2016. **53**(1): p. 73-82.

294. Milner, R., et al., *Fibronectin- and vitronectin-induced microglial activation and matrix metalloproteinase-9 expression is mediated by integrins alpha5beta1 and alphavbeta5.* J Immunol, 2007. **178**(12): p. 8158-67.

295. Lathia, J.D., et al., *Patterns of laminins and integrins in the embryonic ventricular zone of the CNS.* J Comp Neurol, 2007. **505**(6): p. 630-43.

296. Sheppard, A.M., S.K. Hamilton, and A.L. Pearlman, *Changes in the distribution of extracellular matrix components accompany early morphogenetic events of mammalian cortical development.* J Neurosci, 1991. **11**(12): p. 3928-42.

297. Liesi, P., *Do neurons in the vertebrate CNS migrate on laminin?* EMBO J, 1985. **4**(5): p. 1163-70.

298. Margolis, R.U., et al., *Glycosaminoglycans of brain during development.* Biochemistry, 1975. **14**(1): p. 85-8.

299. Yasuhara, O., et al., *Immunohistochemical localization of hyaluronic acid in rat and human brain.* Brain Res, 1994. **635**(1-2): p. 269-82.

300. Bignami, A. and R. Asher, *Some observations on the localization of hyaluronic acid in adult, newborn and embryonal rat brain.* Int J Dev Neurosci, 1992. **10**(1): p. 45-57.

301. Sheppard, A.M., et al., *Neuronal production of fibronectin in the cerebral cortex during migration and layer formation is unique to specific cortical domains.* Dev Biol, 1995. **172**(2): p. 504-18.

302. Anlar, B., et al., *Expression of adhesion and extracellular matrix molecules in the developing human brain.* J Child Neurol, 2002. **17**(9): p. 707-13.

303. Koser, D.E., et al., *Mechanosensing is critical for axon growth in the developing brain.* Nat Neurosci, 2016. **19**(12): p. 1592-1598.

304. Sekine, K., et al., *Reelin controls neuronal positioning by promoting cell-matrix adhesion via inside-out activation of integrin alpha5beta1.* Neuron, 2012. **76**(2): p. 353-69.

305. Garcion, E., A. Faissner, and C. ffrench-Constant, *Knockout mice reveal a contribution of the extracellular matrix molecule tenascin-C to neural precursor proliferation and migration.* Development, 2001. **128**(13): p. 2485-96.

306. Sobeih, M.M. and G. Corfas, *Extracellular factors that regulate neuronal migration in the central nervous system.* Int J Dev Neurosci, 2002. **20**(3-5): p. 349-57.

307. Takada, Y., X. Ye, and S. Simon, *The integrins.* Genome Biol, 2007. **8**(5): p. 215.

308. Hynes, R.O., *Integrins: bidirectional, allosteric signaling machines.* Cell, 2002. **110**(6): p. 673-87.

309. Luo, B.H., C.V. Carman, and T.A. Springer, *Structural basis of integrin regulation and signaling.* Annu Rev Immunol, 2007. **25**: p. 619-47.

310. Shattil, S.J., C. Kim, and M.H. Ginsberg, *The final steps of integrin activation: the end game.* Nat Rev Mol Cell Biol, 2010. **11**(4): p. 288-300.

311. Takagi, J., et al., *Global conformational rearrangements in integrin extracellular domains in outside-in and inside-out signaling.* Cell, 2002. **110**(5): p. 599-11.

312. Takagi, J., et al., *Structure of integrin alpha5beta1 in complex with fibronectin.* EMBO J, 2003. **22**(18): p. 4607-15.

313. Tanzer, M.L., *Current concepts of extracellular matrix.* J Orthop Sci, 2006. **11**(3): p. 326-31.

314. Zent, R.P., A. (Eds.), *Cell-Extracellular Matrix Interactions in Cancer*. Vol. XII. 2010: Springer. 314.

315. Adair, B.D., et al., *Three-dimensional EM structure of the ectodomain of integrin {alpha}V{beta}3 in a complex with fibronectin.* J Cell Biol, 2005. **168**(7): p. 1109-18.

316. Campbell, I.D. and M.J. Humphries, *Integrin structure, activation, and interactions.* Cold Spring Harb Perspect Biol, 2011. **3**(3).

317. Kinashi, T., *Intracellular signalling controlling integrin activation in lymphocytes.* Nat Rev Immunol, 2005. **5**(7): p. 546-59.

318. Bouvard, D., et al., *Integrin inactivators: balancing cellular functions in vitro and in vivo.* Nat Rev Mol Cell Biol, 2013. **14**(7): p. 430-42.

319. Hartmann, T.N., et al., *CXCR4 chemokine receptor and integrin signaling co-operate in mediating adhesion and chemoresistance in small cell lung cancer (SCLC) cells.* Oncogene, 2005. **24**(27): p. 4462-71.

320. Busillo, J.M. and J.L. Benovic, *Regulation of CXCR4 signaling.* Biochim Biophys Acta, 2007. **1768**(4): p. 952-63.

321. Shen, W., et al., *The chemokine receptor CXCR4 enhances integrin-mediated in vitro adhesion and facilitates engraftment of leukemic precursor-B cells in the bone marrow.* Exp Hematol, 2001. **29**(12): p. 1439-47.

322. Pan, L., et al., *Research advances on structure and biological functions of integrins.* Springerplus, 2016. **5**(1): p. 1094.

323. Changede, R., et al., *Nascent Integrin Adhesions Form on All Matrix Rigidities after Integrin Activation.* Dev Cell, 2015. **35**(5): p. 614-21.

324. Choi, C.K., et al., *Actin and alpha-actinin orchestrate the assembly and maturation of nascent adhesions in a myosin II motor-independent manner.* Nat Cell Biol, 2008. **10**(9): p. 1039-50.

325. Vicente-Manzanares, M. and A.R. Horwitz, *Adhesion dynamics at a glance.* J Cell Sci, 2011. **124**(Pt 23): p. 3923-7.

326. Iwamoto, D.V. and D.A. Calderwood, *Regulation of integrin-mediated adhesions.* Curr Opin Cell Biol, 2015. **36**: p. 41-7.

327. Valdembri, D. and G. Serini, *Regulation of adhesion site dynamics by integrin traffic.* Curr Opin Cell Biol, 2012. **24**(5): p. 582-91.

328. Horton, E.R., et al., *Definition of a consensus integrin adhesome and its dynamics during adhesion complex assembly and disassembly.* Nat Cell Biol, 2015. **17**(12): p. 1577-87.

329. Harburger, D.S. and D.A. Calderwood, *Integrin signalling at a glance.* J Cell Sci, 2009. **122**(Pt 2): p. 159-63.

330. Doyle, A.D., et al., *Local 3D matrix microenvironment regulates cell migration through spatiotemporal dynamics of contractility-dependent adhesions.* Nat Commun, 2015. **6**: p. 8720.

331. Mendoza, P., et al., *Rab5 activation promotes focal adhesion disassembly, migration and invasiveness in tumor cells.* J Cell Sci, 2013. **126**(Pt 17): p. 3835-47.

332. Petrie, R.J. and K.M. Yamada, *Multiple mechanisms of 3D migration: the origins of plasticity.* Curr Opin Cell Biol, 2016. **42**: p. 7-12.

333. Palecek, S.P., et al., *Integrin-ligand binding properties govern cell migration speed through cell-substratum adhesiveness.* Nature, 1997. **385**(6616): p. 537-40.

334. Huttenlocher, A. and A.R. Horwitz, *Integrins in cell migration.* Cold Spring Harb Perspect Biol, 2011. **3**(9): p. a005074.

335. Vicente-Manzanares, M., C.K. Choi, and A.R. Horwitz, *Integrins in cell migration--the actin connection.* J Cell Sci, 2009. **122**(Pt 2): p. 199-206.

336. Barnhart, E.L., et al., *An adhesion-dependent switch between mechanisms that determine motile cell shape.* PLoS Biol, 2011. **9**(5): p. e1001059.

337. Milner, R. and I.L. Campbell, *The integrin family of cell adhesion molecules has multiple functions within the CNS.* J Neurosci Res, 2002. **69**(3): p. 286-91.

338. Schmid, R.S. and E.S. Anton, *Role of integrins in the development of the cerebral cortex.* Cereb Cortex, 2003. **13**(3): p. 219-24.

339. Park, Y.K. and Y. Goda, *Integrins in synapse regulation.* Nat Rev Neurosci, 2016. **17**(12): p. 745-756.

340. Kerrisk, M.E., L.A. Cingolani, and A.J. Koleske, *ECM receptors in neuronal structure, synaptic plasticity, and behavior.* Prog Brain Res, 2014. **214**: p. 101-31.

341. Almutairi, M.M., et al., *Factors controlling permeability of the blood-brain barrier.* Cell Mol Life Sci, 2016. **73**(1): p. 57-77.

342. del Zoppo, G.J. and R. Milner, *Integrin-matrix interactions in the cerebral microvasculature.* Arterioscler Thromb Vasc Biol, 2006. **26**(9): p. 1966-75.

343. Loulier, K., et al., *beta1 integrin maintains integrity of the embryonic neocortical stem cell niche.* PLoS Biol, 2009. **7**(8): p. e1000176.

344. Long, K., et al., *Integrin signalling regulates the expansion of neuroepithelial progenitors and neurogenesis via Wnt7a and Decorin.* Nat Commun, 2016. **7**: p. 10354.

345. Belvindrah, R., et al., *Beta1 integrins in radial glia but not in migrating neurons are essential for the formation of cell layers in the cerebral cortex.* J Neurosci, 2007. **27**(50): p. 13854-65.

346. Georges-Labouesse, E., et al., *Essential role of alpha 6 integrins in cortical and retinal lamination.* Curr Biol, 1998. **8**(17): p. 983-6.

347. Anton, E.S., J.A. Kreidberg, and P. Rakic, *Distinct functions of alpha3 and alpha(v) integrin receptors in neuronal migration and laminar organization of the cerebral cortex.* Neuron, 1999. **22**(2): p. 277-89.

348. Graus-Porta, D., et al., *Beta1-class integrins regulate the development of laminae and folia in the cerebral and cerebellar cortex.* Neuron, 2001. **31**(3): p. 367-79.

349. Murase, S. and A.F. Horwitz, *Deleted in colorectal carcinoma and differentially expressed integrins mediate the directional migration of neural precursors in the rostral migratory stream.* J Neurosci, 2002. **22**(9): p. 3568-79.

350. Emsley, J.G. and T. Hagg, *alpha6beta1 integrin directs migration of neuronal precursors in adult mouse forebrain.* Exp Neurol, 2003. **183**(2): p. 273-85.

351. Marchetti, G., et al., *Integrin alpha5beta1 is necessary for regulation of radial migration of cortical neurons during mouse brain development.* Eur J Neurosci, 2010. **31**(3): p. 399-409.

352. Webb, D.J., et al., *alpha5 integrin signaling regulates the formation of spines and synapses in hippocampal neurons.* J Biol Chem, 2007. **282**(10): p. 6929-35.

353. Michaluk, P., et al., *Matrix metalloproteinase-9 controls NMDA receptor surface diffusion through integrin beta1 signaling.* J Neurosci, 2009. **29**(18): p. 6007-12.

354. Milner, R. and I.L. Campbell, *Developmental regulation of beta1 integrins during angiogenesis in the central nervous system.* Mol Cell Neurosci, 2002. **20**(4): p. 616-26.

355. Osada, T., et al., *Interendothelial claudin-5 expression depends on cerebral endothelial cell-matrix adhesion by beta(1)-integrins.* J Cereb Blood Flow Metab, 2011. **31**(10): p. 1972-85.

356. Milner, R. and I.L. Campbell, *The extracellular matrix and cytokines regulate microglial integrin expression and activation.* J Immunol, 2003. **170**(7): p. 3850-8.

357. Kloss, C.U., et al., *Integrin family of cell adhesion molecules in the injured brain: regulation and cellular localization in the normal and regenerating mouse facial motor nucleus.* J Comp Neurol, 1999. **411**(1): p. 162-78.

358. Welser-Alves, J.V., et al., *Microglia use multiple mechanisms to mediate interactions with vitronectin; non-essential roles for the highly-expressed alphavbeta3 and alphavbeta5 integrins.* J Neuroinflammation, 2011. **8**: p. 157.

359. Milner, R., *Microglial expression of alphavbeta3 and alphavbeta5 integrins is regulated by cytokines and the extracellular matrix: beta5 integrin null microglia show no defects in adhesion or MMP-9 expression on vitronectin.* Glia, 2009. **57**(7): p. 714-23.

360. Witting, A., et al., *Phagocytic clearance of apoptotic neurons by Microglia/Brain macrophages in vitro: involvement of lectin-, integrin-, and phosphatidylserine-mediated recognition.* J Neurochem, 2000. **75**(3): p. 1060-70.

361. Milner, R. and I.L. Campbell, *Cytokines regulate microglial adhesion to laminin and astrocyte extracellular matrix via protein kinase C-dependent activation of the alpha6beta1 integrin.* J Neurosci, 2002. **22**(5): p. 1562-72.

362. Chamak, B. and M. Mallat, *Fibronectin and laminin regulate the in vitro differentiation of microglial cells.* Neuroscience, 1991. **45**(3): p. 513-27.

363. Kurpius, D., E.P. Nolley, and M.E. Dailey, *Purines induce directed migration and rapid homing of microglia to injured pyramidal neurons in developing hippocampus.* Glia, 2007. **55**(8): p. 873-84.

364. Gyoneva, S., A.G. Orr, and S.F. Traynelis, *Differential regulation of microglial motility by ATP/ADP and adenosine.* Parkinsonism Relat Disord, 2009. **15 Suppl 3**: p. S195-9.

365. Orr, A.G., et al., *Adenosine A(2A) receptor mediates microglial process retraction.* Nat Neurosci, 2009. **12**(7): p. 872-8.

366. Eyo, U.B., et al., *Modulation of microglial process convergence toward neuronal dendrites by extracellular calcium.* J Neurosci, 2015. **35**(6): p. 2417-22.

367. Gu, N., et al., *Microglial P2Y12 receptors regulate microglial activation and surveillance during neuropathic pain.* Brain Behav Immun, 2016. **55**: p. 82-92.

368. Noda, M., et al., *Calcium influx through reversed NCX controls migration of microglia.* Adv Exp Med Biol, 2013. **961**: p. 289-94.

369. Sunkaria, A., et al., *Migration and Phagocytic Ability of Activated Microglia During Post-natal Development is Mediated by Calcium-Dependent Purinergic Signalling.* Mol Neurobiol, 2016. **53**(2): p. 944-54.

370. Nasu-Tada, K., S. Koizumi, and K. Inoue, *Involvement of beta1 integrin in microglial chemotaxis and proliferation on fibronectin: different regulations by ADP through PKA.* Glia, 2005. **52**(2): p. 98-107.

371. Ohsawa, K. and S. Kohsaka, *Dynamic motility of microglia: purinergic modulation of microglial movement in the normal and pathological brain.* Glia, 2011. **59**(12): p. 1793-9.

372. Ohsawa, K., et al., *P2Y12 receptor-mediated integrin-beta1 activation regulates microglial process extension induced by ATP.* Glia, 2010. **58**(7): p. 790-801.

373. Kim, C., et al., *beta1-integrin-dependent migration of microglia in response to neuron-released alpha-synuclein.* Exp Mol Med, 2014. **46**: p. e91.

374. Yao, H., et al., *Nonmuscle myosin light-chain kinase mediates microglial migration induced by HIV Tat: involvement of beta1 integrins.* FASEB J, 2013. **27**(4): p. 1532-48.

375. Ullrich, O., et al., *Regulation of microglial expression of integrins by poly(ADP-ribose) polymerase-1.* Nat Cell Biol, 2001. **3**(12): p. 1035-42.

376. Kurpius, D., et al., *Early activation, motility, and homing of neonatal microglia to injured neurons does not require protein synthesis.* Glia, 2006. **54**(1): p. 58-70.

377. Persson, A.K., et al., *Contribution of sodium channels to lamellipodial protrusion and Rac1 and ERK1/2 activation in ATP-stimulated microglia.* Glia, 2014. **62**(12): p. 2080-95.

378. Harl, B., et al., *Chloride channel blockers suppress formation of engulfment pseudopodia in microglial cells.* Cell Physiol Biochem, 2013. **31**(2-3): p. 319-37.

379. Zierler, S., et al., *Chloride influx provokes lamellipodium formation in microglial cells.* Cell Physiol Biochem, 2008. **21**(1-3): p. 55-62.

380. Schwab, A., *Function and spatial distribution of ion channels and transporters in cell migration.* Am J Physiol Renal Physiol, 2001. **280**(5): p. F739-47.

381. Hines, D.J., et al., *Microglia processes block the spread of damage in the brain and require functional chloride channels.* Glia, 2009. **57**(15): p. 1610-8.

382. Swiatkowski, P., et al., *Activation of microglial P2Y12 receptor is required for outward potassium currents in response to neuronal injury.* Neuroscience, 2016. **318**: p. 22-33.

383. Lim, H.M., et al., *UDP-Induced Phagocytosis and ATP-Stimulated Chemotactic Migration Are Impaired in STIM1-/- Microglia In Vitro and In Vivo.* Mediators Inflamm, 2017. **2017**: p. 8158514.

384. Echeverry, S., M.J. Rodriguez, and Y.P. Torres, *Transient Receptor Potential Channels in Microglia: Roles in Physiology and Disease.* Neurotox Res, 2016.

385. Fan, Y., L. Xie, and C.Y. Chung, *Signaling Pathways Controlling Microglia Chemotaxis.* Mol Cells, 2017. **40**(3): p. 163-168.

386. Vincent, C., T.A. Siddiqui, and L.C. Schlichter, *Podosomes in migrating microglia: components and matrix degradation.* J Neuroinflammation, 2012. **9**: p. 190.

387. Siddiqui, T.A., et al., *Regulation of podosome formation, microglial migration and invasion by Ca(2+)-signaling molecules expressed in podosomes.* J Neuroinflammation, 2012. **9**: p. 250.

388. Ohsawa, K., et al., *Involvement of P2X4 and P2Y12 receptors in ATP-induced microglial chemotaxis.* Glia, 2007. **55**(6): p. 604-16.

389. Irino, Y., et al., *Akt activation is involved in P2Y12 receptor-mediated chemotaxis of microglia.* J Neurosci Res, 2008. **86**(7): p. 1511-9.

390. Lee, S.H., et al., *Role of iPLA(2) in the regulation of Src trafficking and microglia chemotaxis.* Traffic, 2011. **12**(7): p. 878-89.

391. Miller, A.M. and N. Stella, *Microglial cell migration stimulated by ATP and C5a involve distinct molecular mechanisms: quantification of migration by a novel near-infrared method.* Glia, 2009. **57**(8): p. 875-83.

392. Ifuku, M., et al., *TLR2 controls random motility, while TLR7 regulates chemotaxis of microglial cells via distinct pathways.* Brain Behav Immun, 2016. **58**: p. 338-347.

393. Ito, S., et al., *Induction of matrix metalloproteinases (MMP3, MMP12 and MMP13) expression in the microglia by amyloid-beta stimulation via the PI3K/Akt pathway.* Exp Gerontol, 2007. **42**(6): p. 532-7.

394. Lee, S.H., et al., *beta-arrestin 2-dependent activation of ERK1/2 is required for ADP-induced paxillin phosphorylation at Ser(83) and microglia chemotaxis.* Glia, 2012. **60**(9): p. 1366-77.

395. Lee, S.H., et al., *Regulation of Integrin alpha6 Recycling by Calcium-independent Phospholipase A2 (iPLA2) to Promote Microglia Chemotaxis on Laminin.* J Biol Chem, 2016. **291**(45): p. 23645-23653.

396. Lee, S. and C.Y. Chung, *Role of VASP phosphorylation for the regulation of microglia chemotaxis via the regulation of focal adhesion formation/maturation.* Mol Cell Neurosci, 2009. **42**(4): p. 382-90.

397. Frade, J.M. and Y.A. Barde, *Microglia-derived nerve growth factor causes cell death in the developing retina.* Neuron, 1998. **20**(1): p. 35-41.

398. Streit, W.J., *Microglia and macrophages in the developing CNS.* Neurotoxicology, 2001. **22**(5): p. 619-24.

399. Vilhardt, F., *Microglia: phagocyte and glia cell.* Int J Biochem Cell Biol, 2005. **37**(1): p. 17-21.

400. Antony, J.M., et al., *Endogenous microglia regulate development of embryonic cortical precursor cells.* J Neurosci Res, 2011.

401. Caviness, V.S., Jr., T. Takahashi, and R.S. Nowakowski, *Numbers, time and neocortical neuronogenesis: a general developmental and evolutionary model.* Trends Neurosci, 1995. **18**(9): p. 379-83.

402. Rezaie, P., *Microglia in the Human Nervous System during Development.* Neuroembryology, 2003. **2003;2**: p. 18-31.

403. Jung, S., et al., *Analysis of fractalkine receptor CX(3)CR1 function by targeted deletion and green fluorescent protein reporter gene insertion.* Mol Cell Biol, 2000. **20**(11): p. 4106-14.

404. Ito, D., et al., *Microglia-specific localisation of a novel calcium binding protein, Iba1.* Brain Res Mol Brain Res, 1998. **57**(1): p. 1-9.

405. Esiri, M.M. and J.O. McGee, *Monoclonal antibody to macrophages (EMB/11) labels macrophages and microglial cells in human brain.* J Clin Pathol, 1986. **39**(6): p. 615-21.

406. Andjelkovic, A.V., et al., *Macrophages/microglial cells in human central nervous system during development: an immunohistochemical study.* Brain Res, 1998. **814**(1-2): p. 13-25.

407. Venkatesan, C., et al., *Chronic upregulation of activated microglia immunoreactive for galectin-3/Mac-2 and nerve growth factor following diffuse axonal injury.* J Neuroinflammation, 2010. **7**: p. 32.

408. Lalancette-Hebert, M., et al., *Selective ablation of proliferating microglial cells exacerbates ischemic injury in the brain.* J Neurosci, 2007. **27**(10): p. 2596-605.

409. Reichert, F. and S. Rotshenker, *Galectin-3/MAC-2 in experimental allergic encephalomyelitis.* Exp Neurol, 1999. **160**(2): p. 508-14.

410. Walther, M., et al., *Galectin-3 is upregulated in microglial cells in response to ischemic brain lesions, but not to facial nerve axotomy.* J Neurosci Res, 2000. **61**(4): p. 430-5.

411. Avignone, E., et al., *Status epilepticus induces a particular microglial activation state characterized by enhanced purinergic signaling.* J Neurosci, 2008. **28**(37): p. 9133-44.

412. Block, M.L., L. Zecca, and J.S. Hong, *Microglia-mediated neurotoxicity: uncovering the molecular mechanisms.* Nat Rev Neurosci, 2007. **8**(1): p. 57-69.

413. Scholzen, T. and J. Gerdes, *The Ki-67 protein: from the known and the unknown.* J Cell Physiol, 2000. **182**(3): p. 311-22.

414. Cheong, J.W., et al., *Induction of apoptosis by apicidin, a histone deacetylase inhibitor, via the activation of mitochondria-dependent caspase cascades in human Bcr-Abl-positive leukemia cells.* Clin Cancer Res, 2003. **9**(13): p. 5018-27.

415. Meijering, E., O. Dzyubachyk, and I. Smal, *Methods for cell and particle tracking.* Methods Enzymol, 2012. **504**: p. 183-200.

416. Tan, S.S., et al., *Separate progenitors for radial and tangential cell dispersion during development of the cerebral neocortex.* Neuron, 1998. **21**(2): p. 295-304.

417. Anderson, S.A., et al., *Interneuron migration from basal forebrain to neocortex: dependence on Dlx genes.* Science, 1997. **278**(5337): p. 474-6.

418. Anderson, S.A., et al., *Distinct cortical migrations from the medial and lateral ganglionic eminences.* Development, 2001. **128**(3): p. 353-63.

419. Ransohoff, R.M. and A.E. Cardona, *The myeloid cells of the central nervous system parenchyma.* Nature, 2010. **468**(7321): p. 253-62.

420. Bystron, I., C. Blakemore, and P. Rakic, *Development of the human cerebral cortex: Boulder Committee revisited.* Nat Rev Neurosci, 2008. **9**(2): p. 110-22.

421. Cina, C., et al., *Expression of connexins in embryonic mouse neocortical development.* J Comp Neurol, 2007. **504**(3): p. 298-313.

422. Rakic, P., *A small step for the cell, a giant leap for mankind: a hypothesis of neocortical expansion during evolution.* Trends Neurosci, 1995. **18**(9): p. 383-8.

423. Haydar, T.F., et al., *Differential modulation of proliferation in the neocortical ventricular and subventricular zones.* J Neurosci, 2000. **20**(15): p. 5764-74.

424. Kurz, H., *Physiology of angiogenesis.* J Neurooncol, 2000. **50**(1-2): p. 17-35.

425. Kamiryo, T., et al., *Development of the rat meninx: experimental study using bromodeoxyuridine.* Anat Rec, 1990. **227**(2): p. 207-10.

426. Sturrock, R.R., *A morphological study of the development of the mouse choroid plexus.* J Anat, 1979. **129**(Pt 4): p. 777-93.

427. Johansson, P.A., et al., *Blood-CSF barrier function in the rat embryo.* Eur J Neurosci, 2006. **24**(1): p. 65-76.

428. Furuta, Y., D.W. Piston, and B.L. Hogan, *Bone morphogenetic proteins (BMPs) as regulators of dorsal forebrain development.* Development, 1997. **124**(11): p. 2203-12.

429. Currle, D.S., et al., *Direct and indirect roles of CNS dorsal midline cells in choroid plexus epithelia formation.* Development, 2005. **132**(15): p. 3549-59.

430. von Frowein, J., A. Wizenmann, and M. Gotz, *The transcription factors Emx1 and Emx2 suppress choroid plexus development and promote neuroepithelial cell fate.* Dev Biol, 2006. **296**(1): p. 239-52.

431. Monier, A., et al., *Distribution and differentiation of microglia in the human encephalon during the first two trimesters of gestation.* J Comp Neurol, 2006. **499**(4): p. 565-82.

432. Santos, A.M., et al., *Embryonic and postnatal development of microglial cells in the mouse retina.* J Comp Neurol, 2008. **506**(2): p. 224-39.

433. Walton, N.M., et al., *Microglia instruct subventricular zone neurogenesis.* Glia, 2006. **54**(8): p. 815-25.

434. Peri, F. and C. Nusslein-Volhard, *Live imaging of neuronal degradation by microglia reveals a role for v0-ATPase a1 in phagosomal fusion in vivo.* Cell, 2008. **133**(5): p. 916-27.

435. Svahn, A.J., et al., *Development of ramified microglia from early macrophages in the zebrafish optic tectum.* Dev Neurobiol, 2012.

436. Raivich, G., *Like cops on the beat: the active role of resting microglia.* Trends Neurosci, 2005. **28**(11): p. 571-3.

437. Casano, A.M. and F. Peri, *Microglia: multitasking specialists of the brain.* Dev Cell, 2015. **32**(4): p. 469-77.

438. Romberger, D.J., *Fibronectin.* Int J Biochem Cell Biol, 1997. **29**(7): p. 939-43.

439. Stewart, G.R. and A.L. Pearlman, *Fibronectin-like immunoreactivity in the developing cerebral cortex.* J Neurosci, 1987. **7**(10): p. 3325-33.

440. De Gasperi, R., M.A. Gama Sosa, and G.A. Elder, *Presenilin-1 regulates the constitutive turnover of the fibronectin matrix in endothelial cells.* BMC Biochem, 2012. **13**: p. 28.

441. Kasahara, Y., R. Koyama, and Y. Ikegaya, *Depth and time-dependent heterogeneity of microglia in mouse hippocampal slice cultures.* Neurosci Res, 2016. **111**: p. 64-9.

442. Petersen, M.A. and M.E. Dailey, *Diverse microglial motility behaviors during clearance of dead cells in hippocampal slices.* Glia, 2004. **46**(2): p. 195-206.

443. Li, C., et al., *RhoA determines lineage fate of mesenchymal stem cells by modulating CTGF-VEGF complex in extracellular matrix.* Nat Commun, 2016. **7**: p. 11455.

444. Graupera, M., et al., *Angiogenesis selectively requires the p110alpha isoform of PI3K to control endothelial cell migration.* Nature, 2008. **453**(7195): p. 662-6.

445. Grinberg, Y.Y., J.G. Milton, and R.P. Kraig, *Spreading depression sends microglia on Levy flights.* PLoS One, 2011. **6**(4): p. e19294.

446. Cukierman, E., et al., *Taking cell-matrix adhesions to the third dimension.* Science, 2001. **294**(5547): p. 1708-12.

447. Legate, K.R., et al., *Integrin adhesion and force coupling are independently regulated by localized PtdIns(4,5)2 synthesis.* EMBO J, 2011. **30**(22): p. 4539-53.

448. Eyo, U.B., et al., *Neuronal hyperactivity recruits microglial processes via neuronal NMDA receptors and microglial P2Y12 receptors after status epilepticus.* J Neurosci, 2014. **34**(32): p. 10528-40.

449. Schiefer, J., et al., *Microglial motility in the rat facial nucleus following peripheral axotomy.* J Neurocytol, 1999. **28**(6): p. 439-53.

450. Gorelik, R. and A. Gautreau, *The Arp2/3 inhibitory protein arpin induces cell turning by pausing cell migration.* Cytoskeleton (Hoboken), 2015. **72**(7): p. 362-71.

451. Smolders, S., et al., *Maternal immune activation evoked by polyinosinic:polycytidylic acid does not evoke microglial cell activation in the embryo.* Front Cell Neurosci, 2015. **9**: p. 301.

452. Maecker, H.T. and J. Trotter, *Flow cytometry controls, instrument setup, and the determination of positivity.* Cytometry A, 2006. **69**(9): p. 1037-42.

453. Madadizadeh, F., M. Ezati Asar, and M. Hosseini, *Common Statistical Mistakes in Descriptive Statistics Reports of Normal and Non-Normal Variables in Biomedical Sciences Research.* Iran J Public Health, 2015. **44**(11): p. 1557-8.

454. Zhang, F., et al., *Microglial migration and interactions with dendrimer nanoparticles are altered in the presence of neuroinflammation.* J Neuroinflammation, 2016. **13**(1): p. 65.

455. Greig, L.C., et al., *Molecular logic of neocortical projection neuron specification, development and diversity.* Nat Rev Neurosci, 2013. **14**(11): p. 755-69.

456. Dudvarski Stankovic, N., et al., *Microglia-blood vessel interactions: a double-edged sword in brain pathologies.* Acta Neuropathol, 2016. **131**(3): p. 347-63.

457. Svahn, A.J., et al., *Development of ramified microglia from early macrophages in the zebrafish optic tectum.* Dev Neurobiol, 2013. **73**(1): p. 60-71.

458. Maheshwari, G., et al., *Cell adhesion and motility depend on nanoscale RGD clustering.* J Cell Sci, 2000. **113 (Pt 10)**: p. 1677-86.

459. Le Saux, G., et al., *Spacing of integrin ligands influences signal transduction in endothelial cells.* Biophys J, 2011. **101**(4): p. 764-73.

460. Blandin, A.F., et al., *Glioma cell dispersion is driven by alpha5 integrin-mediated cell-matrix and cell-cell interactions.* Cancer Lett, 2016. **376**(2): p. 328-38.

461. Sieger, D., et al., *Long-range Ca2+ waves transmit brain-damage signals to microglia.* Dev Cell, 2012. **22**(6): p. 1138-48.

462. Finlay, B.L. and R.B. Darlington, *Linked regularities in the development and evolution of mammalian brains.* Science, 1995. **268**(5217): p. 1578-84.

463. Sauvageot, C.M. and C.D. Stiles, *Molecular mechanisms controlling cortical gliogenesis.* Curr Opin Neurobiol, 2002. **12**(3): p. 244-9.

464. Rezaie, P., N.J. Cairns, and D.K. Male, *Expression of adhesion molecules on human fetal cerebral vessels: relationship to microglial colonisation during development.* Brain Res Dev Brain Res, 1997. **104**(1-2): p. 175-89.

465. Stettler, E.M. and D.S. Galileo, *Radial glia produce and align the ligand fibronectin during neuronal migration in the developing chick brain.* J Comp Neurol, 2004. **468**(3): p. 441-51.

466. Moroi, M., et al., *Involvement of activated integrin alpha2beta1 in the firm adhesion of platelets onto a surface of immobilized collagen under flow conditions.* Thromb Haemost, 2000. **83**(5): p. 769-76.

467. Toyjanova, J., et al., *Matrix confinement plays a pivotal role in regulating neutrophil-generated tractions, speed, and integrin utilization.* J Biol Chem, 2015. **290**(6): p. 3752-63.

468. Costa, P., et al., *Integrin-specific control of focal adhesion kinase and RhoA regulates membrane protrusion and invasion.* PLoS One, 2013. **8**(9): p. e74659.

469. Zhao, H., et al., *Role of integrin switch and transforming growth factor Beta 3 in hypoxia-induced invasion inhibition of human extravillous trophoblast cells.* Biol Reprod, 2012. **87**(2): p. 47.

470. Pankov, R. and K.M. Yamada, *Fibronectin at a glance.* J Cell Sci, 2002. **115**(Pt 20): p. 3861-3.

471. ffrench-Constant, C., *Alternative splicing of fibronectin--many different proteins but few different functions.* Exp Cell Res, 1995. **221**(2): p. 261-71.

472. Ffrench-Constant, C., et al., *Reappearance of an embryonic pattern of fibronectin splicing during wound healing in the adult rat.* J Cell Biol, 1989. **109**(2): p. 903-14.

473. Xia, P. and L.A. Culp, *Adhesion activity in fibronectin's alternatively spliced domain EDa (EIIIA): complementarity to plasma fibronectin functions.* Exp Cell Res, 1995. **217**(2): p. 517-27.

474. Chen, W. and L.A. Culp, *Adhesion mediated by fibronectin's alternatively spliced EDb (EIIIB) and its neighboring type III repeats.* Exp Cell Res, 1996. **223**(1): p. 9-19.

475. Peters, J.H. and R.O. Hynes, *Fibronectin isoform distribution in the mouse. I. The alternatively spliced EIIIB, EIIIA, and V segments show widespread codistribution in the developing mouse embryo.* Cell Adhes Commun, 1996. **4**(2): p. 103-25.

476. Frantz, C., K.M. Stewart, and V.M. Weaver, *The extracellular matrix at a glance.* J Cell Sci, 2010. **123**(Pt 24): p. 4195-200.

477. Morla, A., Z. Zhang, and E. Ruoslahti, *Superfibronectin is a functionally distinct form of fibronectin.* Nature, 1994. **367**(6459): p. 193-6.

478. Lock, J.G., B. Wehrle-Haller, and S. Stromblad, *Cell-matrix adhesion complexes: master control machinery of cell migration.* Semin Cancer Biol, 2008. **18**(1): p. 65-76.

479. Dufour, S., et al., *Attachment, spreading and locomotion of avian neural crest cells are mediated by multiple adhesion sites on fibronectin molecules.* EMBO J, 1988. **7**(9): p. 2661-71.

480. Miyake, K., et al., *Requirement for VLA-4 and VLA-5 integrins in lymphoma cells binding to and migration beneath stromal cells in culture.* J Cell Biol, 1992. **119**(3): p. 653-62.

481. Julich, D., et al., *Cross-Scale Integrin Regulation Organizes ECM and Tissue Topology.* Dev Cell, 2015. **34**(1): p. 33-44.

482. Yuryev, M., et al., *In vivo Calcium Imaging of Evoked Calcium Waves in the Embryonic Cortex.* Front Cell Neurosci, 2015. **9**: p. 500.

483. Yokota, Y., et al., *Radial glial dependent and independent dynamics of interneuronal migration in the developing cerebral cortex.* PLoS One, 2007. **2**(8): p. e794.

484. Yoshida, N., et al., *Decrease in expression of alpha 5 beta 1 integrin during neuronal differentiation of cortical progenitor cells.* Exp Cell Res, 2003. **287**(2): p. 262-71.

485. Avila, A., et al., *Glycine receptor alpha2 subunit activation promotes cortical interneuron migration.* Cell Rep, 2013. **4**(4): p. 738-50.

486. Carbonell, W.S., et al., *Migration of perilesional microglia after focal brain injury and modulation by CC chemokine receptor 5: an in situ time-lapse confocal imaging study.* J Neurosci, 2005. **25**(30): p. 7040-7.

487. Smolders, S.M., et al., *Age-specific function of alpha5beta1 integrin in microglial migration during early colonization of the developing mouse cortex.* Glia, 2017.

488. Liapi, A., et al., *Stromal-derived factor 1 signalling regulates radial and tangential migration in the developing cerebral cortex.* Dev Neurosci, 2008. **30**(1-3): p. 117-31.

489. Li, M. and R.M. Ransohoff, *Multiple roles of chemokine CXCL12 in the central nervous system: a migration from immunology to neurobiology.* Prog Neurobiol, 2008. **84**(2): p. 116-31.

490. Zhu, Y., et al., *Chemokine Signaling Controls Integrity of Radial Glial Scaffold in Developing Spinal Cord and Consequential Proper Position of Boundary Cap Cells.* J Neurosci, 2015. **35**(24): p. 9211-24.

491. Yang, Z., et al., *Activation of integrin beta1 mediates the increased malignant potential of ovarian cancer cells exerted by inflammatory cytokines.* Anticancer Agents Med Chem, 2014. **14**(7): p. 955-62.

492. Yu, Y., et al., *Stromal cell-derived factor-1 (SDF-1)/CXCR4 axis enhances cellular invasion in ovarian carcinoma cells via integrin beta1 and beta3 expressions.* Oncol Res, 2013. **21**(4): p. 217-25.

493. Kiss, D.L., L.C. Windus, and V.M. Avery, *Chemokine receptor expression on integrin-mediated stellate projections of prostate cancer cells in 3D culture.* Cytokine, 2013. **64**(1): p. 122-30.

494. Huang, Y.C., et al., *Stromal cell-derived factor-1 enhances motility and integrin up-regulation through CXCR4, ERK and NF-kappaB-dependent pathway in human lung cancer cells.* Biochem Pharmacol, 2007. **74**(12): p. 1702-12.

495. Teicher, B.A. and S.P. Fricker, *CXCL12 (SDF-1)/CXCR4 pathway in cancer.* Clin Cancer Res, 2010. **16**(11): p. 2927-31.

496. Rot, A. and U.H. von Andrian, *Chemokines in innate and adaptive host defense: basic chemokinese grammar for immune cells.* Annu Rev Immunol, 2004. **22**: p. 891-928.

497. Lu, D.Y., et al., *SDF-1alpha up-regulates interleukin-6 through CXCR4, PI3K/Akt, ERK, and NF-kappaB-dependent pathway in microglia.* Eur J Pharmacol, 2009. **613**(1-3): p. 146-54.

498. Peled, A., et al., *The chemokine SDF-1 activates the integrins LFA-1, VLA-4, and VLA-5 on immature human CD34(+) cells: role in transendothelial/stromal migration and engraftment of NOD/SCID mice.* Blood, 2000. **95**(11): p. 3289-96.

499. Petty, J.M., et al., *Crosstalk between CXCR4/stromal derived factor-1 and VLA-4/VCAM-1 pathways regulates neutrophil retention in the bone marrow.* J Immunol, 2009. **182**(1): p. 604-12.

500. Legate, K.R., S.A. Wickstrom, and R. Fassler, *Genetic and cell biological analysis of integrin outside-in signaling.* Genes Dev, 2009. **23**(4): p. 397-418.

501. Cantley, L.C., *The phosphoinositide 3-kinase pathway.* Science, 2002. **296**(5573): p. 1655-7.

502. Mendoza, M.C., E.E. Er, and J. Blenis, *The Ras-ERK and PI3K-mTOR pathways: cross-talk and compensation.* Trends Biochem Sci, 2011. **36**(6): p. 320-8.

503. Tanabe, S., et al., *Functional expression of the CXC-chemokine receptor-4/fusin on mouse microglial cells and astrocytes.* J Immunol, 1997. **159**(2): p. 905-11.

504. Lipfert, J., et al., *CXCR4 and CXCR7 form a functional receptor unit for SDF-1/CXCL12 in primary rodent microglia.* Neuropathol Appl Neurobiol, 2013. **39**(6): p. 667-80.

505. Bernhagen, J., et al., *MIF is a noncognate ligand of CXC chemokine receptors in inflammatory and atherogenic cell recruitment.* Nat Med, 2007. **13**(5): p. 587-96.

506. Yoshida, D., R. Nomura, and A. Teramoto, *Signalling pathway mediated by CXCR7, an alternative chemokine receptor for stromal-cell derived factor-1alpha, in AtT20 mouse adrenocorticotrophic hormone-secreting pituitary adenoma cells.* J Neuroendocrinol, 2009. **21**(5): p. 481-8.

507. Schonemeier, B., et al., *Regional and cellular localization of the CXCl12/SDF-1 chemokine receptor CXCR7 in the developing and adult rat brain.* J Comp Neurol, 2008. **510**(2): p. 207-20.

508. Ohtani, Y., et al., *Expression of stromal cell-derived factor-1 and CXCR4 chemokine receptor mRNAs in cultured rat glial and neuronal cells.* Neurosci Lett, 1998. **249**(2-3): p. 163-6.

509. Slusarczyk, J., et al., *Prenatal stress is a vulnerability factor for altered morphology and biological activity of microglia cells.* Front Cell Neurosci, 2015. **9**: p. 82.

510. Rezaie, P., et al., *Expression of beta-chemokines and chemokine receptors in human fetal astrocyte and microglial co-cultures: potential role of chemokines in the developing CNS.* Glia, 2002. **37**(1): p. 64-75.

511. Jones, J.L. and R.A. Walker, *Integrins: a role as cell signalling molecules.* Mol Pathol, 1999. **52**(4): p. 208-13.

512. Constantin, G., et al., *Chemokines trigger immediate beta2 integrin affinity and mobility changes: differential regulation and roles in lymphocyte arrest under flow.* Immunity, 2000. **13**(6): p. 759-69.

513. Kokovay, E., et al., *Adult SVZ lineage cells home to and leave the vascular niche via differential responses to SDF1/CXCR4 signaling.* Cell Stem Cell, 2010. **7**(2): p. 163-73.

514. Dalmau, I., et al., *Development of microglia in the prenatal rat hippocampus.* J Comp Neurol, 1997. **377**(1): p. 70-84.

515. Jimenez, C., et al., *Role of the PI3K regulatory subunit in the control of actin organization and cell migration.* J Cell Biol, 2000. **151**(2): p. 249-62.

516. Dumstrei, K., R. Mennecke, and E. Raz, *Signaling pathways controlling primordial germ cell migration in zebrafish.* J Cell Sci, 2004. **117**(Pt 20): p. 4787-95.

517. Heit, B., et al., *PI3K accelerates, but is not required for, neutrophil chemotaxis to fMLP.* J Cell Sci, 2008. **121**(Pt 2): p. 205-14.

518. Schneble, N., et al., *Phosphoinositide 3-kinase gamma ties chemoattractant- and adrenergic control of microglial motility.* Mol Cell Neurosci, 2017. **78**: p. 1-8.

519. Meller, J., et al., *Integrin-Kindlin3 requirements for microglial motility in vivo are distinct from those for macrophages.* JCI Insight, 2017. **2**(11).

520. Bohlen, C.J., et al., *Diverse Requirements for Microglial Survival, Specification, and Function Revealed by Defined-Medium Cultures.* Neuron, 2017. **94**(4): p. 759-773 e8.

521. Gosselin, D., et al., *An environment-dependent transcriptional network specifies human microglia identity.* Science, 2017. **356**(6344).

522. McGrath, K.E., et al., *Embryonic expression and function of the chemokine SDF-1 and its receptor, CXCR4.* Dev Biol, 1999. **213**(2): p. 442-56.

523. Lysko, D.E., M. Putt, and J.A. Golden, *SDF1 regulates leading process branching and speed of migrating interneurons.* J Neurosci, 2011. **31**(5): p. 1739-45.

524. Bezzi, P., et al., *CXCR4-activated astrocyte glutamate release via TNFalpha: amplification by microglia triggers neurotoxicity.* Nat Neurosci, 2001. **4**(7): p. 702-10.

525. Brown, A.S., *Epidemiologic studies of exposure to prenatal infection and risk of schizophrenia and autism.* Dev Neurobiol, 2012. **72**(10): p. 1272-6.

526. Patterson, P.H., *Immune involvement in schizophrenia and autism: etiology, pathology and animal models.* Behav Brain Res, 2009. **204**(2): p. 313-21.

527. Fortier, M.E., G.N. Luheshi, and P. Boksa, *Effects of prenatal infection on prepulse inhibition in the rat depend on the nature of the infectious agent and the stage of pregnancy.* Behav Brain Res, 2007. **181**(2): p. 270-7.

528. Lowe, G.C., G.N. Luheshi, and S. Williams, *Maternal infection and fever during late gestation are associated with altered synaptic transmission in the hippocampus of juvenile offspring rats.* Am J Physiol Regul Integr Comp Physiol, 2008. **295**(5): p. R1563-71.

529. Harvey, L. and P. Boksa, *A stereological comparison of GAD67 and reelin expression in the hippocampal stratum oriens of offspring from two mouse models of maternal inflammation during pregnancy.* Neuropharmacology, 2012. **62**(4): p. 1767-76.

530. Giovanoli, S., et al., *Stress in puberty unmasks latent neuropathological consequences of prenatal immune activation in mice.* Science, 2013. **339**(6123): p. 1095-9.

531. Samuelsson, A.M., et al., *Prenatal exposure to interleukin-6 results in inflammatory neurodegeneration in hippocampus with NMDA/GABA(A) dysregulation and impaired spatial learning.* Am J Physiol Regul Integr Comp Physiol, 2006. **290**(5): p. R1345-56.

532. Meyer, U., et al., *Adult behavioral and pharmacological dysfunctions following disruption of the fetal brain balance between pro-inflammatory and IL-10-mediated anti-inflammatory signaling.* Mol Psychiatry, 2008. **13**(2): p. 208-21.

533. Sedel, F., et al., *Macrophage-derived tumor necrosis factor alpha, an early developmental signal for motoneuron death.* J Neurosci, 2004. **24**(9): p. 2236-46.

534. Tremblay, M.E., R.L. Lowery, and A.K. Majewska, *Microglial interactions with synapses are modulated by visual experience.* PLoS Biol, 2010. **8**(11): p. e1000527.

535. Aarum, J., et al., *Migration and differentiation of neural precursor cells can be directed by microglia.* Proc Natl Acad Sci U S A, 2003. **100**(26): p. 15983-8.

536. Jonakait, G.M., et al., *Microglial regulation of cholinergic differentiation in the basal forebrain.* Dev Neurobiol, 2011. **72**(6): p. 857-64.

537. Krady, J.K., et al., *Ciliary neurotrophic factor and interleukin-6 differentially activate microglia.* J Neurosci Res, 2008. **86**(7): p. 1538-47.

538. Streit, W.J., et al., *Comparative evaluation of cytokine profiles and reactive gliosis supports a critical role for interleukin-6 in neuron-glia signaling during regeneration.* J Neurosci Res, 2000. **61**(1): p. 10-20.

539. Lacroix, S., et al., *Delivery of hyper-interleukin-6 to the injured spinal cord increases neutrophil and macrophage infiltration and inhibits axonal growth.* J Comp Neurol, 2002. **454**(3): p. 213-28.

540. Lee, K.M., S.M. Jeon, and H.J. Cho, *Interleukin-6 induces microglial CX3CR1 expression in the spinal cord after peripheral nerve injury through the activation of p38 MAPK.* Eur J Pain, 2010. **14**(7): p. 682 e1-12.

541. Shi, L., et al., *Activation of the maternal immune system alters cerebellar development in the offspring.* Brain Behav Immun, 2009. **23**(1): p. 116-23.

542. Wierzba-Bobrowicz, T., et al., *Quantitative analysis of activated microglia, ramified and damage of processes in the frontal and temporal lobes of chronic schizophrenics.* Folia Neuropathol, 2005. **43**(2): p. 81-9.

543. Monji, A., et al., *Neuroinflammation in schizophrenia especially focused on the role of microglia.* Prog Neuropsychopharmacol Biol Psychiatry, 2013. **42**: p. 115-21.

544. Juckel, G., et al., *Microglial activation in a neuroinflammational animal model of schizophrenia--a pilot study.* Schizophr Res, 2011. **131**(1-3): p. 96-100.

545. Ratnayake, U., et al., *Behaviour and hippocampus-specific changes in spiny mouse neonates after treatment of the mother with the viral-mimetic Poly I:C at mid-pregnancy.* Brain Behav Immun, 2012. **26**(8): p. 1288-99.

546. Dumic, J., S. Dabelic, and M. Flogel, *Galectin-3: an open-ended story.* Biochim Biophys Acta, 2006. **1760**(4): p. 616-35.

547. Kohmura, Y., et al., *Lipopolysaccharide (LPS)-induced intra-uterine fetal death (IUFD) in mice is principally due to maternal cause but not fetal sensitivity to LPS.* Microbiol Immunol, 2000. **44**(11): p. 897-904.

548. Dahlgren, J., et al., *Interleukin-6 in the maternal circulation reaches the rat fetus in mid-gestation.* Pediatr Res, 2006. **60**(2): p. 147-51.

549. Ashdown, H., et al., *The role of cytokines in mediating effects of prenatal infection on the fetus: implications for schizophrenia.* Mol Psychiatry, 2006. **11**(1): p. 47-55.

550. Brown, A.S.P., P.H., *The Origins of Schizophrenia.*2011: Columbia University Press. 448.

551. Cai, Z., et al., *Cytokine induction in fetal rat brains and brain injury in neonatal rats after maternal lipopolysaccharide administration.* Pediatr Res, 2000. **47**(1): p. 64-72.

552. Pratt, L., et al., *Maternal inflammation promotes fetal microglial activation and increased cholinergic expression in the fetal basal forebrain: role of interleukin-6.* Pediatr Res, 2013.

553. Manitz, M.P., et al., *The role of microglia during life span in neuropsychiatric disease - an animal study.* Schizophr Res, 2012.

554. Li, W.Y., Y.C. Chang, and L.J. Lee, *Prenatal infection affects the neuronal architecture and cognitive function in adult mice.* Dev Neurosci, 2014. **36**(5): p. 359-70.

555. Zhu, F., et al., *Minocycline alleviates behavioral deficits and inhibits microglial activation in the offspring of pregnant mice after administration of polyriboinosinic-polyribocytidilic acid.* Psychiatry Res, 2014. **219**(3): p. 680-6.

556. Hsiao, E.Y., et al., *Modeling an autism risk factor in mice leads to permanent immune dysregulation.* Proc Natl Acad Sci U S A, 2012. **109**(31): p. 12776-81.

557. Willi, R., et al., *Altered GSK3beta signaling in an infection-based mouse model of developmental neuropsychiatric disease.* Neuropharmacology, 2013. **73**: p. 56-65.

558. Krstic, D., et al., *Systemic immune challenges trigger and drive Alzheimer-like neuropathology in mice.* J Neuroinflammation, 2012. **9**: p. 151.

559. Pineda, E., et al., *Maternal immune activation promotes hippocampal kindling epileptogenesis in mice.* Ann Neurol, 2013. **74**(1): p. 11-9.

560. Mallard, C., et al., *White matter injury following systemic endotoxemia or asphyxia in the fetal sheep.* Neurochem Res, 2003. **28**(2): p. 215-23.

561. Kuypers, E., et al., *Effects of intra-amniotic lipopolysaccharide and maternal betamethasone on brain inflammation in fetal sheep.* PLoS One, 2013. **8**(12): p. e81644.

562. Le Belle, J.E., et al., *Maternal inflammation contributes to brain overgrowth and autism-associated behaviors through altered redox signaling in stem and progenitor cells.* Stem Cell Reports, 2014. **3**(5): p. 725-34.

563. Jonakait, G.M., *The effects of maternal inflammation on neuronal development: possible mechanisms.* Int J Dev Neurosci, 2007. **25**(7): p. 415-25.

564. Hsiao, E.Y. and P.H. Patterson, *Activation of the maternal immune system induces endocrine changes in the placenta via IL-6.* Brain Behav Immun, 2011. **25**(4): p. 604-15.

565. Girard, S., et al., *IL-1 receptor antagonist protects against placental and neurodevelopmental defects induced by maternal inflammation.* J Immunol, 2010. **184**(7): p. 3997-4005.

566. Gayle, D.A., et al., *Maternal LPS induces cytokines in the amniotic fluid and corticotropin releasing hormone in the fetal rat brain.* Am J Physiol Regul Integr Comp Physiol, 2004. **286**(6): p. R1024-9.

567. Richetto, J., et al., *Prenatal Immune Activation Induces Maturation-Dependent Alterations in the Prefrontal GABAergic Transcriptome.* Schizophr Bull, 2013.

568. Holloway, T., et al., *Prenatal stress induces schizophrenia-like alterations of serotonin 2A and metabotropic glutamate 2 receptors in the adult offspring: role of maternal immune system.* J Neurosci, 2013. **33**(3): p. 1088-98.

569. Lipina, T.V., et al., *Maternal immune activation during gestation interacts with Disc1 point mutation to exacerbate schizophrenia-related behaviors in mice.* J Neurosci, 2013. **33**(18): p. 7654-66.

570. Korzhevskii, D.E.K., O.V. , *Brain Microglia and Microglial Markers.* Neuroscience and Behavioral Physiology, 2016. **46**(3): p. 284-290.

571. Muffat, J., et al., *Efficient derivation of microglia-like cells from human pluripotent stem cells.* Nat Med, 2016.

572. Hong, S., L. Dissing-Olesen, and B. Stevens, *New insights on the role of microglia in synaptic pruning in health and disease.* Curr Opin Neurobiol, 2016. **36**: p. 128-34.

573. Viswanathan, G.M., et al., *Optimizing the success of random searches.* Nature, 1999. **401**(6756): p. 911-4.

574. Salter, M.W. and S. Beggs, *Sublime microglia: expanding roles for the guardians of the CNS.* Cell, 2014. **158**(1): p. 15-24.

575. van den Ameele, J., et al., *Thinking out of the dish: what to learn about cortical development using pluripotent stem cells.* Trends Neurosci, 2014. **37**(6): p. 334-42.

576. Lively, S. and L.C. Schlichter, *The microglial activation state regulates migration and roles of matrix-dissolving enzymes for invasion.* J Neuroinflammation, 2013. **10**: p. 75.

577. De Simone, R., et al., *TGF-beta and LPS modulate ADP-induced migration of microglial cells through P2Y1 and P2Y12 receptor expression.* J Neurochem, 2010. **115**(2): p. 450-9.

578. Luhmann, H.J., et al., *Spontaneous Neuronal Activity in Developing Neocortical Networks: From Single Cells to Large-Scale Interactions.* Front Neural Circuits, 2016. **10**: p. 40.

579. Bitzenhofer, S.H., et al., *Layer-specific optogenetic activation of pyramidal neurons causes beta-gamma entrainment of neonatal networks.* Nat Commun, 2017. **8**: p. 14563.

580. Miller, M.J., et al., *Autonomous T cell trafficking examined in vivo with intravital two-photon microscopy.* Proc Natl Acad Sci U S A, 2003. **100**(5): p. 2604-9.

581. Devenport, D. and N.H. Brown, *Morphogenesis in the absence of integrins: mutation of both Drosophila beta subunits prevents midgut migration.* Development, 2004. **131**(21): p. 5405-15.

582. Klapproth, S., et al., *Minimal amounts of kindlin-3 suffice for basal platelet and leukocyte functions in mice.* Blood, 2015. **126**(24): p. 2592-600.

583. Xu, W., H. Baribault, and E.D. Adamson, *Vinculin knockout results in heart and brain defects during embryonic development.* Development, 1998. **125**(2): p. 327-37.

584. Marella, M. and J. Chabry, *Neurons and astrocytes respond to prion infection by inducing microglia recruitment.* J Neurosci, 2004. **24**(3): p. 620-7.

585. Skaliora, I., et al., *Differential patterns of semaphorin expression in the developing rat brain.* Eur J Neurosci, 1998. **10**(4): p. 1215-29.

586. Takamatsu, H., T. Okuno, and A. Kumanogoh, *Regulation of immune cell responses by semaphorins and their receptors.* Cell Mol Immunol, 2010. **7**(2): p. 83-8.

587. Andrews, W.D., M. Barber, and J.G. Parnavelas, *Slit-Robo interactions during cortical development.* J Anat, 2007. **211**(2): p. 188-98.

588. Liu, X., et al., *Slit2 regulates the dispersal of oligodendrocyte precursor cells via Fyn/RhoA signaling.* J Biol Chem, 2012. **287**(21): p. 17503-16.

589. Allendoerfer, K.L. and C.J. Shatz, *The subplate, a transient neocortical structure: its role in the development of connections between thalamus and cortex.* Annu Rev Neurosci, 1994. **17**: p. 185-218.

590. Sierra, A., et al., *Janus-faced microglia: beneficial and detrimental consequences of microglial phagocytosis.* Front Cell Neurosci, 2013. **7**: p. 6.

591. Scheppke, L., et al., *Notch promotes vascular maturation by inducing integrin-mediated smooth muscle cell adhesion to the endothelial basement membrane.* Blood, 2012. **119**(9): p. 2149-58.

592. Collins, C. and W.J. Nelson, *Running with neighbors: coordinating cell migration and cell-cell adhesion.* Curr Opin Cell Biol, 2015. **36**: p. 62-70.

593. da Fonseca, A.C., et al., *The impact of microglial activation on blood-brain barrier in brain diseases.* Front Cell Neurosci, 2014. **8**: p. 362.

594. Van den Bossche, J., et al., *Regulation and function of the E-cadherin/catenin complex in cells of the monocyte-macrophage lineage and DCs.* Blood, 2012. **119**(7): p. 1623-33.

595. Meng, W. and M. Takeichi, *Adherens junction: molecular architecture and regulation.* Cold Spring Harb Perspect Biol, 2009. **1**(6): p. a002899.

596. Tham, T.N., et al., *Developmental pattern of expression of the alpha chemokine stromal cell-derived factor 1 in the rat central nervous system.* Eur J Neurosci, 2001. **13**(5): p. 845-56.

597. Kolodziej, A., et al., *Tonic activation of CXC chemokine receptor 4 in immature granule cells supports neurogenesis in the adult dentate gyrus.* J Neurosci, 2008. **28**(17): p. 4488-500.

598. del rio Hortega P. Microglia. In: Penfield W, A.E., *Cytology and Cellular Pathology of the Nervous System.* New York: Hoeber, 1932: p. 481-534.

599. Chen, S., et al., *CNS Macrophages Control Neurovascular Development via CD95L.* Cell Rep, 2017. **19**(7): p. 1378-1393.

600. Yin, J., et al., *Up-regulated basigin-2 in microglia induced by hypoxia promotes retinal angiogenesis.* J Cell Mol Med, 2017.

601. Biswas, S., et al., *Laminin-Dependent Interaction between Astrocytes and Microglia: A Role in Retinal Angiogenesis.* Am J Pathol, 2017. **187**(9): p. 2112-2127.

602. Mizoguchi, Y. and A. Monji, *Microglial Intracellular Ca2+ Signaling in Synaptic Development and its Alterations in Neurodevelopmental Disorders.* Front Cell Neurosci, 2017. **11**: p. 69.

603. Edmonson, C.A., M.N. Ziats, and O.M. Rennert, *A Non-inflammatory Role for Microglia in Autism Spectrum Disorders.* Front Neurol, 2016. **7**: p. 9.

604. Askew, K. and D. Gomez-Nicola, *A story of birth and death: Insights into the formation and dynamics of the microglial population.* Brain Behav Immun, 2017.

605. Eggen, B.J., et al., *Microglial phenotype and adaptation.* J Neuroimmune Pharmacol, 2013. **8**(4): p. 807-23.

606. Giovanoli, S., et al., *Preventive effects of minocycline in a neurodevelopmental two-hit model with relevance to schizophrenia.* Transl Psychiatry, 2016. **6**: p. e772.

607. Barron, H., S. Hafizi, and R. Mizrahi, *Towards an Integrated View of Early Molecular Changes Underlying Vulnerability to Social Stress in Psychosis.* Mod Trends Pharmacopsychiatry, 2017. **31**: p. 96-106.

608. Harry, G.J. and A.D. Kraft, *Microglia in the developing brain: A potential target with lifetime effects.* Neurotoxicology, 2012. **33**(2): p. 191-206.

609. Delpech, J.C., et al., *Early life stress perturbs the maturation of microglia in the developing hippocampus.* Brain Behav Immun, 2016. **57**: p. 79-93.

610. Kaminska, B., M. Mota, and M. Pizzi, *Signal transduction and epigenetic mechanisms in the control of microglia activation during neuroinflammation.* Biochim Biophys Acta, 2016. **1862**(3): p. 339-51.

611. Mattei, D., et al., *Maternal immune activation results in complex microglial transcriptome signature in the adult offspring that is reversed by minocycline treatment.* Transl Psychiatry, 2017. **7**(5): p. e1120.

612. Delpech, J.C., et al., *Microglia in neuronal plasticity: Influence of stress.* Neuropharmacology, 2015. **96**(Pt A): p. 19-28.

613. Takatsuru, Y., et al., *Early-life stress increases the motility of microglia in adulthood.* J Physiol Sci, 2015. **65**(2): p. 187-94.

614. Gumusoglu, S.B., et al., *The role of IL-6 in neurodevelopment after prenatal stress.* Brain Behav Immun, 2017.

615. Johnson, F.K. and A. Kaffman, *Early life stress perturbs the function of microglia in the developing rodent brain: new insights and future challenges.* Brain Behav Immun, 2017.

616. Fan, L.W. and Y. Pang, *Dysregulation of neurogenesis by neuroinflammation: key differences in neurodevelopmental and neurological disorders.* Neural Regen Res, 2017. **12**(3): p. 366-371.

617. Antonson, A.M., et al., *Maternal viral infection during pregnancy elicits anti-social behavior in neonatal piglet offspring independent of postnatal microglial cell activation.* Brain Behav Immun, 2017. **59**: p. 300-312.

618. Mattei, D., et al., *Minocycline rescues decrease in neurogenesis, increase in microglia cytokines and deficits in sensorimotor gating in an animal model of schizophrenia.* Brain Behav Immun, 2014. **38**: p. 175-84.

619. Van den Eynde, K., et al., *Hypolocomotive behaviour associated with increased microglia in a prenatal immune activation model with relevance to schizophrenia.* Behav Brain Res, 2014. **258**: p. 179-86.

620. Turano, A., J.H. Lawrence, and J.M. Schwarz, *Activation of neonatal microglia can be influenced by other neural cells.* Neurosci Lett, 2017. **657**: p. 32-37.

621. Bernstein, H.G., Y. Piontkewitz, and G. Keilhoff, *Commentary: Maternal immune activation evoked by polyinosinic: polycytidylic acid does not evoke microglial cell activation in the embryo.* Front Cell Neurosci, 2016. **10**: p. 41.

622. Yamamuro, K., et al., *Potential primary roles of glial cells in the mechanisms of psychiatric disorders.* Front Cell Neurosci, 2015. **9**: p. 154.

623. Clarke, L.E. and B.A. Barres, *Emerging roles of astrocytes in neural circuit development.* Nat Rev Neurosci, 2013. **14**(5): p. 311-21.

624. de Souza, D.F., et al., *Changes in Astroglial Markers in a Maternal Immune Activation Model of Schizophrenia in Wistar Rats are Dependent on Sex.* Front Cell Neurosci, 2015. **9**: p. 489.

625. Elsayed, M. and P.J. Magistretti, *A New Outlook on Mental Illnesses: Glial Involvement Beyond the Glue.* Front Cell Neurosci, 2015. **9**: p. 468.

626. Gottlieb, A., I. Keydar, and H.T. Epstein, *Rodent brain growth stages: an analytical review.* Biol Neonate, 1977. **32**(3-4): p. 166-76.

627. Clancy, B., et al., *Extrapolating brain development from experimental species to humans.* Neurotoxicology, 2007. **28**(5): p. 931-7.

628. Smith, A.M. and M. Dragunow, *The human side of microglia.* Trends Neurosci, 2014. **37**(3): p. 125-35.

629. Mildner, A., et al., *P2Y12 receptor is expressed on human microglia under physiological conditions throughout development and is sensitive to neuroinflammatory diseases.* Glia, 2017. **65**(2): p. 375-387.

630. Galatro, T.F., et al., *Transcriptomic analysis of purified human cortical microglia reveals age-associated changes.* Nat Neurosci, 2017. **20**(8): p. 1162-1171.

631. Burns, T.C., et al., *Mouse models rarely mimic the transcriptome of human neurodegenerative diseases: A systematic bioinformatics-based critique of preclinical models.* Eur J Pharmacol, 2015. **759**: p. 101-17.

632. Masuch, A., et al., *Microglia replenished OHSC: A culture system to study in vivo like adult microglia.* Glia, 2016. **64**(8): p. 1285-97.

633. Yamada, K.M., R. Pankov, and E. Cukierman, *Dimensions and dynamics in integrin function.* Braz J Med Biol Res, 2003. **36**(8): p. 959-66.

Résumé

Les microglies sont des cellules hématogène mais prennent place dans le système nerveux central (SNC) au cours du développement embryonnaire pour constituer la population résidente des cellules immunitaires. Elles sont les médiateurs crucials du bon développement et de l'entretien des réseaux de neurones dans le SNC. De nombreux aspects de la physiologie microgliale et les mécanismes qui sous-tendent leurs fonctions au cours du développement embryonnaire du cerveau sont encore largement méconnues. Cette thèse de doctorat porte sur la migration des cellules microgliales au cours du développement embryonnaire du cortex et elle débouche sur trois grandes conclusions. (1) Les cellules microgliales embryonnaires in situ sont très dynamiques et adaptent leur phénotype à leur environnement local. (2) La vitesse de migration des microglies ex vivo dépend des intégrines beta1 qui exercent des fonctions à la fois inhibitrices et promotrices sur la migration selon l'âge embryonnaire. (3) Les microglies jouent probablement un rôle dans l'étiologie des troubles du développement neurologique, mais il faudrait que les futures recherches se concentrent sur le dysfonctionnement des microglies plutôt que sur leur activation immunitaire classique

Mots clés: matrice extracellulaire; integrines; migration cellulaire; inflammation maternelle; développement; souris

Nederlandse samenvatting

Microglia onstaan in het bloed maar reizen naar het centrale zenuwstelsel (CZS) tijdens de embryonale ontwikkeling om daar de residente populatie van immuuncellen te vormen. Microglia spelen een cruciale rol in de ontwikkeling en in het onderhoud van neuronale netwerken in het CZS. Vele aspecten van de fysiologie van microglia en de mechanismen waarmee ze hun taken uitvoeren tijdens embryonale hersenontwikkeling blijven echter onopgehelderd. Deze doctoraatsdissertatie focust op de migratie van microglia tijdens de ontwikkeling van de embryonale hersencortex. Uit dit werk kunnen drie grote conclusies getrokken worden. (1) *In situ* embryonale microglia zijn erg dynamische cellen die hun fenotype aanpassen aan de lokale omgeving waarin ze zich bevinden. (2) De snelheid waarmee microglia *ex vivo* migreren is afhankelijk van β1 integrines, dewelke zowel migratiefaciliterende als -inhiberende functies hebben die varieren naar gelang de ontwikkelingsleeftijd. (3) Microglia spelen hoogstwaarschijnlijk een rol in het ontstaan van neuroontwikkelingsstoornissen, maar verder onderzoek zoekt beter in de richting van defecten in de ontwikkelingsgerelateerde functies van microglia dan naar klassieke immuunactivatie.

Sleutelwoorden: extracellulaire matrix; integrines; cellulaire migratie; maternale inflammatie; ontwikkeling; muizen

English summary

Microglial migration and adhesion molecules during embryonic brain development

Abstract:

Microglia are blood-borne cells but take up residence in the central nervous system (CNS) during embryonic development to constitute the resident pool of immune cells. They are crucial mediators of the healthy development and maintenance of neural networks in the CNS. Many aspects of the physiology of microglia and the mechanisms underpinning their tasks during embryonic brain development are still unresolved. This doctoral dissertation focuses on migration of microglial cells during embryonic cortical development. All together, this dissertation brings forwards three major conclusions. (1) In situ embryonic microglia are highly dynamic cells that adapt their phenotype to their local environment. (2) Microglial migration speed ex vivo is dependent on β1 integrins that exert both migration promoting and inhibiting functions which are age-specifically regulated. (3) Microglia likely play a role in the etiology of neurodevelopmental disorders, but further research should focus on microglia dysfunction rather than classical microglial immune activation.

Keywords: extracellular matrix; integrins; cellular migration; maternal inflammation; development, mice

Curriculum Vitae

Sophie Marie-Thérèse Smolders was born on 22nd of November 1988 in Sint-Truiden, Belgium. In 2006, she graduated from GO! atheneum Sint-Truiden, in Sciences-Mathematics. In 2011, she obtained a Master's degree at Hasselt University/transnational University Limburg in Biomedical Sciences, option Clinical Molecular Sciences with great distinction. Sophie conducted her Master dissertation at BIOMED in the lab of Physiology. In the same year and lab, she started as a PhD student and teaching assistant under promotorship of Prof. dr. Bert Brône. There she continued to unravel the process of microglial migration in the embryonic mouse brain and started to teach "Cell Physiology" to first year bachelor students in Biomedical Sciences and Medicine under supervision of Prof. dr. Bert Brône and Prof. dr. Jean-Michel Rigo. She was actively involved in the organization and practical reshapement of this course and supervised several bachelor and master students in the lab. During the period of her PhD Sophie followed numerous courses and workshops, including project and time management, scientific writing and presenting, professional education and teaching, career development and coaching for growth, and together with two fellow PhD students and Prof. dr. Marcel Ameloot she organized the second µFiBR symposium. In 2014, Sophie started a joint degree with Université Pierre et Marie Curie, Paris, France under supervision of dr. Pascal Legendre. The results obtained during the course of this PhD were partially published in international peer reviewed journals and were presented at several (inter)national conferences.

Published manuscripts

Silke Smolders*, Sofie Kessels*, **Sophie MT Smolders**, Florent Poulhes, Olivier Zelphati, Cedric Sapet and Bert Brône. Magnetofection is superior to other chemical transfection methods in a microglial cell line. Journal of Neuroscience methods. *Accepted.* (5-year IF 2.43) * equally contributing.

Sophie MT Smolders, Nina Swinnen, Sofie Kessels, Kaline Arnauts, Silke Smolders, Barbara Le Bras, Jean-Michel Rigo, Pascal Legendre°, Bert Brone°. Age-specific function of α5β1 integrin in microglial migration during early colonization of the developing mouse cortex. GLIA. 2017. (5-year IF 5.41) ° equally contributing

Rik Paesen, **Sophie Smolders**, Jose Manolo de Hoyos Vega, Bert O Eijnde, Dominique Hansen, Marcel Ameloot. Fully automated muscle quality assessment by Gabor filtering of second harmonic generation images. J Biomed Opt, 2016. 21(2): p. 26003. (5-Year IF 2.93)

Rik Paesen, **Sophie Smolders**, Inez Wens, Kristof Notelaers, Jose Manolo de Hoyos Vega, Virginie Bito, Bert O Eijnde, Dominque Hansen, Marcel Ameloot. On the interpretation of second harmonic generation intensity profiles of striated muscle. J Biomed Opt. 2015 Aug;20(8):86010. (5-Year IF 2.93)

Silke Smolders*, **Sophie MT Smolders***, Nina Swinnen, Annette Gärtner, Jean-Michel Rigo°, Pascal Legendre°, Bert Brône°. Maternal immune activation evoked by polyinosinic:polycytidylic acid does not evoke microglial cell activation in the embryo. Front Cell Neurosci. 2015 Aug 5;9:301. (5-year IF 4.10) *° equally contributing.

Nina Swinnen, **Sophie Smolders** , Ariel Avila, Kristof Notelaers, Rik Paesen, Marcel Ameloot, Bert Brône, Pascal Legendre*, Jean-Michel Rigo*. Complex invasion pattern of the cerebral cortex by microglial cells during development of the mouse embryo. GLIA. 2013;61(2):150-63. (5-year IF 5.41). * equally contributing.

Manuscripts in preparation

Silke Smolders, **Sophie MT Smolders**, Tina Notter, Urs Meyer, Bert Brône. Controversies and prospects for microglial alterations following maternal immune activation as a model for neurodevelopmental disorders. Brain, behaviour and immunity. *In preparation*

Sophie MT Smolders, Tim Vangansewinkel, Sven Hendrix, Bert Brône. Injury and repair mirroring development: a changing central nervous system microenvironment instructs microglial phenotype. Acta Neuropathologica. *In preparation*

Oral presentations

S. MT Smolders, N. Swinnen, K. Arnauts, S. Smolders, B. Le Bras, JM. Rigo, P. Legendre, B. Brone. Age-specific function of α5β1 integrin in microglial migration during early colonization of the developing mouse cortex.

- *Euron PhD Workshop & BSCDB Spring Meeting on Microglia in development and disease, May 4-5; 2017; UHasselt, Hasselt, Belgium*
- *Gordon Research Seminars: Fibronectin, Integrins & Related Molecules, January 28 -29; 2017; Ventura, California, United States of America*

S. Smolders, N. Swinnen, B. Brône, JM. Rigo. Migration of microglia in the embryonic neocortex.

- *Euron PhD days: EURON and THEME joint PhD meeting, September 22-23; 2011; Bad Honnef, Germany*

Selected poster presentations

S. MT Smolders, N. Swinnen, S. Kessels, K. Arnauts, S. Smolders, B. Le Bras, JM. Rigo, P. Legendre, B. Brone. Age-specific function of α5β1 integrin in microglial migration during early colonization of the developing mouse cortex.

- *XIII European Meeting on Glial Cells in Health and Disease, July 8-11; 2017; Edinburgh, United Kingdom*
- *Euron PhD Workshop & BSCDB Spring Meeting on Microglia in development and disease, May 4-5; 2017; UHasselt, Hasselt, Belgium*
- *Microglia Meeting 2017: From Biology to Pathology, April 20-21; 2017; UMCG, Groningen, The Netherlands*
- *Gordon Research Conference: Fibronectin, Integrins & Related Molecules, January 29 - February 3; 2017; Ventura, California, United States of America*
- *BSCDB autumn meeting 2016: Cell Adhesion and Communication. October 13-14; 2016; Ghent, Belgium*

S. Smolders, A. Avila, N. Swinnen, T. Struys, I. Lambrichts, M. Ameloot, N. Hellings, J.-M. Rigo, B. Brône. Migration of microglia in the embryonic neocorex: cellular and molecular interactions.

- *11th Congress of the Belgian Society for Neuroscience. May 22; 2015; Mons, Belgium*
- *The immune-brain axis: from molecules to behavior. March 12-13; 2015; Diepenbeek, Belgium*
- *Belgian Society of Physiology and Pharmacology: Autumn meeting 2014. October 20; Brussels, Belgium*
- *EMBL Conference Microglia: Guardians of the Brain. March 26-29; 2014; Heidelberg, Germany*
- *XI European Meeting on Glial Cells in Health and Disease, July 3-6; 2013; Berlin, Germany*

S. Smolders, N. Swinnen, B. Brône, JM. Rigo. Migration of microglia in the embryonic neocortex.

- *16th Euron PhD meeting, September 27-28; 2012; Maastricht, The Netherlands*
- *Belgian Society for Cell and Developmental Biology: Spring meeting 2012: Cell Adhesion and Cell Polarity in Development and Disease. April 27-28; 2012; Ghent, Belgium*
- *8th FENS Forum of Neuroscience, July 14-18; 2012; Barcelona, Spain*
- *Belgian Society of Physiology and Pharmacology: Spring meeting 2012. March 16; 2012; Brussels, Belgium*
- *Cytokines and Cell trafficking in Immunological Disorders. February 9; 2012; Diepenbeek, Belgium*
- *IUAP meeting, December 16; 2011; Ghent, Belgium*

Awards

3rd Award Oral presentation "Migration of microglia in the embryonic neocortex" *Euron PhD days: EURON and THEME joint PhD meeting, September 22-23; 2011; Bad Honnef, Germany*

Bursaries

- FWO Travel Grant for International Mobility and BSCDB Travel Grant to participate in the Gordon Research Seminars & Conference on Fibronectin and related molecules in Ventura, California, USA, 2017
- Several FWO Travel Grants for International Mobility and Boehringer Ingelheim Fonds Travel Grant to perform research in the lab of dr. Legendre in the light of a joint degree at UPMC, Paris, France from 2014 until 2017

- Internation Mobility Travel Grant by Hasselt University to attend an EMBL course on Advanced Fluorescence Techniques in Heidelberg, Germany, 2015
- Boehringer Ingelheim Fonds Travel Grant to attend a VIB Summer School on Advanced Light Microscopy, Ghent, Belgium, 2015
- BSN Travel Grant to attend the 8th FENS Forum in Barcelona, Spain, 2012

Dankwoord - Acknowledgments

Dit is het dan. De laatste zinnen die ik op papier zet voor mijn doctoraat. Save the best for last. Elk doctoraat kent ups en downs, het mijne was niet anders. De momenten van vreugde - toch diegene die met de experimenten te maken hadden - waren relatief dun gezaaid, de frustraties en traantjes waren talrijker aanwezig (ik heb de drie keer wel gehaald Quirine en Nina ;-)). Nu ik alles zo samen zie, geven de herinneringen aan de afgelopen zes jaren en dit boekje me veel voldoening en een zekere fierheid. Ik heb het gehaald. Het is dankzij mijn familie, vrienden, ex- en huidige collega's - er zijn er in zes jaar wel een aantal gekomen en gegaan - dat ik ben blijven doorzetten en deze tekst nu kan schrijven. Ik heb hieronder geprobeerd om iedereen met wie ik heb samengewerkt te bedanken in een soort chronologische volgorde per thema. Mijn excuses voor de lengte, maar zes tot acht jaren mensen en herinneringen brengen wat tekst met zich mee…

Lots of gratitude go to my promoters and co-promotor Bert Brône, Pascal Legendre and Jean-Michel Rigo. Thank you for letting me work on the microglial cells and for your guidance and trust throughout the years. Thank you to my UHasselt doctoral committee members Marcel Ameloot, Ivo Lambrichts and Niels Hellings for following my project progress and for giving valuable scientific input both for my research and for my thesis manuscript. I am also grateful to my UPMC and external jury members Isabelle Dusart, Michel Mallat, Etienne Audinat and Charles ffrench-Constant for their interest in my work and for critically evaluating the manuscript. Thank you for your valuable constructive comments in order to improve my work.

Fysiologie op Biomed was mijn tweede thuis (allé, figuurlijk want ik heb wel meerdere "thuizen"). Stuk voor stuk schatten van collega's en van bazen, ja dat mag gezegd worden Bert en Jean-Michel. **Bert**, ik werd jouw eerste doctoraatstudent. En meteen eentje van Sint-Truiden, dat kon al niet stuk (kuch kuch). Ik moet wel zeggen dat jij de "grotere" Truineaar bent van ons twee, en dat mag je ook figuurlijk nemen. Ik heb me ongelooflijk gelukkig mogen prijzen met jou als PI. Wat hebben we samen gelachen tijdens verscheidene bierdegustaties (bijvoorbeeld met Peter Ponsaerts in Gent), badminton-matchkes, skiën in Landgraaf, zuidwaarts wandelen in Berlijn op zoek naar eten (toen was ik wel minder happy: hongerige Sophie is lastige Sophie), de labretreats, Biomeddagen en BBQ's. Ook tijdens de vele sciencemomenten waren jouw grapjes een welgekomen afleiding. Ik kon je geduld, begrip en spontaniteit altijd erg appreciëren. Ondanks je chaotische gedachten en wilde ideeën die vaak de nodige stress met zich meebrachten voor mij, werkte je enthousiasme aanstekelijk en dat heeft me er vaak bovenop geholpen. Ook al had je dat misschien zelden door. Dankjewel voor de vrijheid die je me gaf (wat niet altijd makkelijk was voor iemand zoals ik), je oprechtheid en de vele kansen om actief mee te werken aan het onderwijs.

Jean-Michel, heel eventjes mijn promotor, dan mijn co-promotor, aan jou heb ik erg veel te danken. Jij hebt mij heel veel kansen gegeven, als juniorstudent, als seniorstudent, als doctoraatstudent (o.a. de opstart van de bidiplomering met Parijs) en als assistent met het implementeren van een aangescherpte onderwijsaanpak. Je bent erg begaan met de ontwikkeling en het geluk van je collega's en wat ben je snel met antwoorden op e-mails ondanks je agenda die zit volgestouwd met 101 afspraken op 1 dag. Er kan altijd wel een knipoogsmiley vanaf en je geeft met plezier advies over de aanschaf van de laatste nieuwe Apple snufjes, maar ook over hoe deze

te negeren ten voordele van de work-life balance ;-). Een echte duizendpoot ben je, in alle drukte ook nog even Arabisch leren…wie doet het je na ☺. Bedankt voor je steun, je vertrouwen en je hulp met het Frans.

Pascal, my "Parisian" promotor, thank you for accepting me as a member of your DSCO research team and for always being so welcoming, also when you were stuck with me in your own small office. One day you took revenge when you locked me up inside your office upon going for lunch so I was the one who got stuck. I learned so much from you: spinal cord isolations (yes you really taught me those yourself should your colleagues not believe it!), scientific criticism, writing, and a small portion of scientific French. I think you secretly must have laughed a lot with my language errors (did you never hear about the "la culotte" story?). I enjoyed the many celebrations and funny chats we had during the last months in Paris in the corridor near the lab, with real champagne (thanks to you) and the inevitable pile of sweets (mostly thanks to the female part of the group). Rumor has it you are a chocolate addict. Luckily <*les cloches belges*> brought you some chocolate from time to time :-P. You as well put trust in me and invested lots of time in discussing my project and the corrections for the papers. Thank you for all of that.

Nina, pretty ballerina, het is eigenlijk mede dankzij jou dat ik begonnen ben aan een doctoraat binnen de Fysiologiegroep. Jij hebt mij ingewijd in de wereld van de microglia, en samen gingen we op zoek naar de eigenschappen van deze intrigerende en soms ook wel frusterende groene microglia cellen tijdens gezonde embryonale ontwikkeling en na maternale inflammatie. Het beviel me erg. Ik bleef geboeid en ben uiteindelijk op een zijproject "migratie van microglia" van jouw grote project terecht gekomen. Dat "zijproject" bleek toch niet zo "zij" te zijn :-D. We hebben heel wat gelijkenissen. Beiden hebben we een allergie voor rommel en vuil (jij nog meer dan ik) en als er boze mails gestuurd werden of pogingen tot gezamenlijk opruimen was jij de katalysator, ik was dat later toen jij weg was (of Nathalie Geurts ;)). We delen ook een liefde voor nagels: jij lakt ze mooi, ik bijt de mijne meestal af en moet ze dan lakken om te voorkomen dat ik geen nagels meer overhoud. Verder zijn we fan van welnessavondjes met moddermaskers en van mode. Je hebt altijd een hele nuchtere en eerlijke kijk op de zaken, maar bent toch begripvol en laat je niet zomaar beïnvloeden. Dankjewel voor je engagement, ook toen we nog in je vrije tijd van je vroegen om microglia te tellen (het meest vervelende karweitje ever! en Silke is het vast en zeker met me eens), voor wat je met de MIA paper hebt gedaan, voor je onvoorwaardelijke steun en vertrouwen, voor alle keren dat je me hebt kunnen kalmeren de afgelopen 8 jaren (en dat zijn er wel een hoop geweest), voor je gastvrijheid en je trouwe vriendschap.

Val, gij zijt het grootste patéke wat ik ooit ben tegengekomen. Het levende voorbeeld van beauty with brains …én met twee kindjes! Wat heb ik me geamuseerd op de bureau samen met u! We hebben lief en leed gedeeld, muziek, VISA-kaarten, kledij en fruit (zoals granaatappels, met de nodige spetters tot gevolg, ik denk dat er nog spatten hangen op de muur waarlangs jij gezeten hebt :-P maar die zullen intussen gemaskeerd zijn door de spatten die Silke met hare havermout en koffie heeft veroorzaakt ;-). Jij hield wel je proteïnerepen en ik mijn sandwichekes met choco (die hebben uiteindelijk toch geweken voor de gezondere salades). Jij staat gelijk aan efficiëntie, recht voor de raap en neemt geen blad voor je mond, wat nogal eens kon botsten ;-). Het verbaast me nog steeds wat jij allemaal klaar krijgt: een hele menu op tafel toveren voor 4 personen op 45

min tijd, ritjes in de meest fancy auto's op circuits en op congres, even naar Zwitserland verhuizen en daar je doctoraat afmaken, eigenhandig verbouwen en tegels plaatsen met een halve duim,… . Ik ben dan heel blij dat alles uiteindelijk op zijn pootjes is terecht gekomen voor je, inclusief de vele huisdiertjes groot en klein die nu bij je vertoeven, en ik duim voor de volgende stappen. Dankjewel voor al je eerlijkheid, vertrouwen, goede raad en gastvrijheid, waar dan ook ter wereld en je vriendschap vanaf de eerste moment dat we de bureau deelden.

Kathleen, ondanks dat we samen gestudeerd hebben, zijn we op Biomed pas meer in contact gekomen met elkaar. Jij zat daar - ocharme - tussen al die Biofysica mannen, maar geen erg, jij kon wel tegen een stootje. Al snel bleek dat wij, samen met Nina een liefde hadden om dingen te organiseren en zo hebben we voor opvolging gezorgd van het eerste µFiBR symposium. We hebben dat goed gedaan onder ons drietjes onder leiding van Marcel en dankzij jou hadden we een officiële outfit voor het organiserend comité. Je bent een getalenteerde duizendpoot: doctoreren, zingen, dansen, viool spelen, haken, breien, knutselen, events organiseren. Niet te geloven hoe je het allemaal klaar krijgt. Altijd toon je interesse en sta je klaar om te helpen. Vaak hebben we bij elkaar kunnen ventileren over de mislukte experimenten en de nachtelijke metingen op de confocale, maar ik heb me evenzeer ook ziek gelachen met je droge maar toch sappige manier van verhalen vertellen. Dankjewel voor je steun en voor mij regelmatig een hart onder de riem te steken toen ik in Parijs zat.

Kristof, Rik en **Ben**, de anciens en ex-Biofysica leden, en **Nick** en **Eli** de huidge Biofysica anciens. Dankjulliewel om me telkens verder te helpen als ik kwam aankloppen met de melding "ik krijg geen scherp beeld" of "ik krijg de gasfles niet open" of "de scanhead maakt een vreemd geluid" of "de MaiTai geeft geen output" en ga zo maar door. Kristof, dankuwel om me zo vaak verder te helpen met ImageJ en voor de interesse in mijn project. Je was altijd bereid te luisteren en dacht altijd mee naar een oplossing. Ik kijk er al naar uit om opnieuw collega's te worden! Rik, met jou heb ik veel samengewerkt en dat was altijd even aangenaam. We hebben samen gepubliceerd, studenten begeleid en dat was een hele verrijking voor mij. Bedankt om altijd klaar te staan en om geïnteresseerd te zijn in hoe het met me ging en met mijn project.

Pia & Ariel, you guys were amazing. Both very different, but so talented, hard working and nice colleagues. Ariel, I could not think of one think you didn't know anything about. We owe you lots of credit for setting up the time-lapse imaging in the lab. It is thanks to you that Nina and I could enjoy a swifter start with our migration experiments. Even later on when you were already in Canada, you were still answering my questions about imaging and objectives. Pia, my sweet Pia, I instantly smile when I think of you waving to say hello in the corridors of Biomed. You were always friendly and joyful, I have never seen you down nor angry. And for sure it hasn't been an easy path for you and Ariel. I am happy we could collaborate on a project and that we remained in contact over the years. Thank you both for your friendship.

De ancien Fysiologieladies **Inge, Kathérine** en **Ann:** bedankt om mij als een lid te beschouwen van Fysiologie toen ik nog student was. Jullie hebben me meermaals goede raad gegeven, tot op heden. Jullie zijn stuk voor stuk ZO lieve en oprechte dames, altijd in voor een leuke babbel. Buikdans was dan niet zo een succes (althans niet voor mij), tennis ging al wat beter en samen

met **Sofie N** hebben we toch een aantal leuke herinneringen kunnen opbouwen aan tennismatchkes tegen de immunologen (Niels en Jerome) en morfoloog (Tim VG). Sofie N, jij bent uiteindelijk het onderwijsteam van Fysiologie kort komen versterken en wat was dat fijn. We hebben veel samengewerkt, gelachen en studentenergernissen gedeeld ;-). **Elke, Marjolein**, met jullie heb ik ook hele leuke momenten beleefd. Al hebben we niet veel samengewerkt op Biomed, de etentjes, make-up en welnessproducten demo's bij mijn thuis konden jullie wel pruimen en het was altijd heel aangenaam om jullie erbij te hebben. Hopelijk zien we elkaar nog eens. Dankjullie allemaal voor de leuke sfeer op Biomed en de gezellige momenten daarbuiten.

Windelief, wat ben jij een brok energie. Het was altijd een plezier jou tegen te komen in de gangen of wanneer je binnensprong op de bureau. Ik zag je zelden slecht gezind, en als dat zo was, was je daar altijd heel open over. Je weet van aanpakken, kan supergoed koken en dus uiteraard kwam ik graag van je kookkunsten proeven (o.a. bij het Wiemesmeer). Daarnaast hebben we samen wel een deel restaurantjes geëvalueerd ;-). De avondjes stappen met jou waren altijd superleuk. Jouw dierenliefde is ongekend en moet vaak lachen als ik aan (onze) dierenverhalen denk. Zo kwam ik thuis met een jong en pluizig vrouwtjeskonijntje van bij jou, om bij mijn gecastreerd mannetje te zetten…en bleek dat later ook gewoon een mannetje te zijn. Ook met de Jan-van-gent vergelijking met Jerome (door Jerome zelf) heb ik me ziek gelachen, zó jij ☺. Dankjewel om de gangen op te fleuren, voor je steun en voor de vele gezellige avondjes.

Kaline, aan jou heb ik heel veel te danken. Zonder jou experimenteel werk was er maar een kleine Chapter 4 in dit boekje. Je bent je seniorstage bij mij komen doen en hebt eigenhandig de transwell en adhesie assays geoptimaliseerd, inclusief de analyse daarvan. Nog vele andere zaken heb je gedaan die niet in dit boekje staan. Je hebt erg goed je plan getrokken, want dit was een project waar je alleen op hebt gewerkt. Nooit was iets teveel, ook al deden we voor de 24ste keer flow cytometrie om de activatiestatus van het β1 integrine te detecteren, je gaf niet op. Dankjewel voor je harde werk en grote inzet tijdens je stage en voor de gezellige momenten aan de FACS, de confocale en tijdens het uit eten als we samen laat gewerkt of geredeneerd hadden over de resultaten. Heel veel succes met je doctoraat in Leuven!

Quirinetje/Quirinemien/Q-tie. Jij bent echt een ongelooflijke madam én mama. Het hart op de tong. Wat heb ik me snel thuisgevoeld op Biomed dankzij jou. Je bracht leven in de brouwerij (lees: fysiologiegang) en bent altijd zo een beetje een lijm geweest binnen Biomed. Je hebt altijd een luisterend oor, goede raad, weet altijd wel wat spannends te vertellen en jij hield me meestal up to date over de laatste nieuwtjes binnen Biomed want ik wist en weet nog steeds nooit van iets. Ik kon echt met alles terecht bij jou. Ik denk dat we de afgelopen jaren heel wat gezaagd hebben tegen elkaar en het feit dat we dat konden heeft ons beiden goed gedaan (ook al denk jij dat jij teveel zaagde!!). Ik kan me zo al enkele momenten voor de geest halen waar we naar elkaar gebeld hebben in volle paniek :-D. Dankjewel om er altijd te zijn voor mij, ondanks alle drukte en ondanks de vele moeilijke momenten die je zelf hebt gekend. Je bent buiten een supercollega, ook een goede vriendin geworden. Ik ben heel blij voor u dat je eindelijk rust hebt en je nu volledig kan gaan voor wat je met hart en ziel doet: onderwijs. Je verdient het dubbel en dik. Ook dankjewel voor de fijne samenwerking tijdens "De cel als organisme" wat later "Celcommunicatie" werd, heb het altijd jammer gevonden dat je later je eigen opleidingsonderdelen kreeg en niet meer

meedraaide in het onze. Verder verdien je ook een hele grote dankuwel om een groot stuk van de inleiding in dit boekje grondig na te lezen en nuttige suggesties te geven, dat apprecieerde ik heel erg. Quirine, Biomed's Supermama, ik kijk al uit naar je volgende kunstige creaties, je hebt talent!

Silke … mijne mede-SSer, microglia- en doctoraatsklankbord. Je zou nog liever hebben dat ik gewoon "danku" schrijf hier zodat ik minder stress zou hebben en mijn thesis op tijd zou kunnen uploaden. Zo onbaatzuchtig jij, zolang iemand anders maar gelukkig is. Wat moet ik hier toch maar schrijven hier, er is zoveel te zeggen. Ook al lijken we voor vele mensen zusjes en voelt dat soms ook zo, we zijn toch merkbaar verschillend op een aantal vlakken ;-). Ik had initieel een beetje schrik dat er veel zou veranderen toen Val langs me wegging en er iemand nieuw in de plaats zou komen, maar die schrik was geheel onterecht. De rommel, papiertjes, vuile havermoutborden en bestek, en de muziek (bij u wel wat stiller ;-)) bleven gewoon bestaan :-P. Nu, die chaos nam ik er graag bij, want wat ben jij een supercollega, -vriendin en -mens gebleken. Jij verdraagt zoooveel. Oh god wat heb ik tegen je gezaagd en je blééf geïnteresseerd mijn "aflopen-gelijk-ne-wekker" en grommelbuien maar aanhoren. Engelengeduld heb je op vlak van mensen. Niets was je ooit teveel en je kwam altijd opgewekt - er zaten soms wel kleine variaties in je niveau van opgewektheid - de bureau binnen. Wat mis ik je "Goeiemorgend Phietje, hoe gaat ie?!" met je handtas, sporttas, zak met eten en autosleutels en portefeuille allemaal in je handen. Als jij er was, was er leven en wat ging de tijd snel als we samen op de bureau waren. Samen hebben we microglia onderzocht, de o-zo-fijne tellingen gedaan, geredeneerd, gediscusieerd, onzelf gefrustreerd, gepresenteerd, gepubliceerd en noem maar op. Je hebt véél tegenslag gekend in je doctoraat, jij was precies de pechmagneet voor heel fysiologie. Ik hoop dat het tij nu voor je gekeerd is, ik ben zo fier op jou (nu, ben wel minder enthousiast over de lat die je zo hoog hebt gelegd voor mij :s ;-)). Dankjewel lieve Silke om er altijd te zijn voor me zowel voor werkgerelateerde als niet werkgerelateerde zaken.

Sofie K, de nieuwe (inmiddels niet meer zó nieuw ☺) versterking van het microglia- én het fysiologie onderwijsteam. Wat ben ik blij dat jij er bent geweest tijdens mijn doctoraat want jij, samen met Elisia, hebben ervoor gezorgd dat er western blot in de integrine paper staat, wat toch een redelijke must was. Je bent altijd zo rustig en ik weet als ik iets aan u vraag, dat het goed komt. Ik sta vaak versteld wat je allemaal gedaan krijgt en hebt gekregen het afgelopen jaar (het was een vréselijk druk eerste jaar voor jou) en dat gaat precies maar allemaal zo, ik hoor je nooit klagen. Je leert erg snel en hebt veel maturiteit. Daarnaast ben je altijd even vriendelijk, begaan met iedereen en staat altijd klaar om te helpen. Je bent een echte aanwinst voor het team. Samen met **Jolien** zal je nog wel wat microglia-avontuurtjes beleven ;-). Veel succes met jouw 6 jaren, Jolien, jij met je 4 jaren die je zonet gestart bent. Komt allemaal goed!

Verder wil ik graag een grote dankjewel uiten naar alle andere supercoole leden van het Fysiologie/Cardiologie team **Jacobine**, **Jirka, Giovanni, Joris, Lize, Jens, Dorien, Maxim, Virginie en Ruth** (temporarily a member of physiology). You all made my time here so much more fun. Thank you all for your valuable input during the labmeetings, your enthusiasm and your kind words. During the lab retreats or outside of work, I learned to know many of you better and I have laughed a lot with your jokes, pranks and dry humor. Lize en Dorien, de vaste waarden binnen het fysiologie onderwijsteam. We hebben samen veel gewerkt aan het onderwijs, ons

geamuseerd tijdens het lesgeven, maar ook erna want er was altijd wel vanalles te vertellen over wat we hadden meegemaakt in de lessen. Jacobine heeft ook verschillende jaren actief meegedraaid in de practica en in Thema 1, dankjewel voor je inzet en je mailtjes om te polsen hoe het me ging. Lize, de jogmomenten over de middag, samen fietsen (al gebeurde dat langs mijne kant niet zoveel ☺), de babbels over en het mogen verorberen van lekker eten (dankuwel Jaume) werden heel erg geapprecieerd, alsook het vele werk wat je stak in organiseren met de lab retreat samen met Silke, Sofie, Jens en Petra (vette pluim voor jullie allen by the way!). Dorien, jij stond ook altijd klaar om te helpen. Ook toen ik last minute kwam aankloppen voor qPCR, niets was teveel om me alles uit te helpen en me te helpen met primerontwikkeling. Ook voor celfysiologie heb je (extra) veel op je genomen, altijd was alles goed geregeld. Net zoals je thesis die eigenlijk al af is, wat ben je toch goed voorbereid, daar kunnen velen een puntje aan zuigen ;-). Many thanks to all of you for the super nice collaborations, the support over all these years and for the nice chats in good and bad times. For those who still have to finish their PhD, best of luck!

Jo, Rosette en Petra, jullie drietjes zijn een gevestigde waarde binnen fysiologie. Jullie staan altijd paraat. Jo dankjewel voor de BV-2 celkweek en voor het verzorgen van mijn muisjes in de quarantaine ruimte. Hier en daar wat plagerijen, gezellige babbels en veel tips heb ik van je gekregen voor onze reizen in Spanje, dankjewel voor je vertrouwen. Rosette, wat was ik blij toen je meer uren kreeg bij ons. Jij hebt me heel veel geholpen het laatste jaar en we hebben vele gezellige momenten gehad samen in de isolatieruimte. Niets is je ooit teveel, je leert graag en snel nieuwe dingen bij en blijft altijd rustig, begripvol en vriendelijk (wat heel fijn was voor mij, want ik joeg me meestal op). Dankjewel voor je harde inzet en voor je interesse en steun buiten het werk om. Petra, jij bent paté nummer twee ;-). Jij brengt zoveel leven in de brouwerij, o.a. met je lach die je het verdiep onder of boven je nog hoort, staat altijd voor iedereen klaar en bent altijd op de hoogte van alle (sappige) nieuwtjes. Al hebben we niet echt veel "samengewerkt in het lab", ik heb me rotgeamuseerd met u, meestal ging het dan om ludieke zaken zoals ideeën uitwerken voor grappige powerpoints, karaoke en dansen, lab retreat activiteiten. Jij was ook altijd begaan met ieder zijn geluk, dankjewel om naar me te luisteren en me verschillende harten onder de riem te steken.

Monara, Juliette and **Maria** (visiting PhD student from Granada) thank you for being so awesome colleagues and friends, so glad we were all together in the same lab in Paris. You made my days so much brighter when I was there…and my pants so much smaller (after all *<cafés gourmands>)*. I enjoyed our times together at lunch, for a coffee, for the after work dinners and make-up sessions. Monara, I even had the pleasure to welcome you in Hasselt and to do crossfit together! You are a strong woman in many ways. Thank you both for all your support, your comforting words and the feeling that we were in this together. Also many thanks to the other members of the DSCO group **Barbara, Christine, Jean-Marie, Hervé, Antony, Hervé le petit** (thank you for proof reading my French summary)**, Gonz, Dong dong, Quong, Silvia and the whole team of François Tronche**. You made me feel at home by sharing with me your offices, going out for lunch together, doing or discussing research together (ISH-Barbara!), the funny conversations and your interest in my work.

Stefanie, we hebben samen gestudeerd en groepswerkjes gemaakt met Dorien H en Birgit**.** We hebben dat later doorgetrokken naar diner & dance en dan naar gezellige avondjes uit eten, drinken en bijbabbelen. Ik was erg blij toen je ons op Biomed bent komen vervoegen. Je zal je me misschien moeilijk geloven, maar jij bent een van de rustigste personen die ik ken en hebt altijd een erg kalmerend effect op mij. Zo lief en frivool als je bent, zo hard moet ik lachen als ik zie dat je je opjaagt en iets (of iemand :-D) om zeep wil helpen. Jij kan zo droog uit de hoek komen, ik amuseer me altijd bij je. Dankjewel om regelmatig bij me binnen te springen voor een babbel over het onderzoek, de vakantie, trouw of je huis en voor je steun tijdens het schrijven van dit boekje. Jouw bezoekjes op en buiten het werk waren altijd een welgekomen afleiding.

Hannelore, want ben jij een straffe madam zeg. Een echte publiceermachine en wetenschapster in hart en nieren. Altijd tip top inorde, geconcentreerd, iedereen helpen, veel te veel onderwijs geven (en ook nog avondonderwijs hieromtrent volgen!), allemaal naast je full time onderzoek. Ik snap niet hoe je het allemaal combineert. We hebben ook ongeveer samen het schrijfproces doorgemaakt, en voor mij was dat alleszins een grote steun. Je hebt me hééél vaak een hart onder de riem gestoken, bleef me zelfs aanmoedigen toen ik in Parijs zat, leidde me naar de verschillende doelen in het schrijven van mijn thesis met een zelfgemaakte M&M kalender (hoe origineel ☺!) en dat heeft goed gewerkt (misschien een tip voor iedereen die iets van mij gedaan wil krijgen: gebruik eten als lokmiddel. PS dat werkt ook zo met **Bert** :-P). Bedankt voor de vele bezoekjes en de fijne babbels over wat te doen na ons doctoraat, de experimenten, onderzoeksfrustraties, trouwen en verdedigen en voor je grote steun het afgelopen jaar.

Tim VG, jou ken ik ook al lang en gelukkig ben je er nog steeds (tegen mijn originele verwachtingen in). We zaten regelmatig samen aan de bureau in de kelder toen we stage liepen. Jij één jaartje verder dan mij. We hadden enkele gemeenschappelijke interessepunten: sport (meerbepaald badminton en tennis), ijsjes en extracellulaire matrix met de bijbehorende antilichamen ;-). Wat heb ik me ziek gelachen met de stommiteiten (en ja dat waren er een aantal) die we aan elkaar uitwisselden "moet ge nu weer weten wat ik gedaan heb" en met uwe droge humor. Dankuwel voor de fijne sportmomenten, voor de vele oprechte hoe-gaat-het-met-u-Sophie-s, voor je luisterend oor wanneer ik dipjes had maar ook wanneer het goed ging. Je bent echt een goede wetenschapper, altijd bereid om te helpen en neemt je taken erg serieus. Daarmee ben ik ook heel blij om samen met u aan een review te kunnen schrijven. Nu rest je enkel nog de eindspurt in te zetten voor het behalen van je doctoraat. Heel veel succes hiermee!

Een hele grote dankuwel gaat uit naar alle technische en administratieve ondersteuning die iedereen en dus ook ik krijgt/heb gekregen op Biomed. Ik wil in het bijzonder **Joke**, **Paul** & wijlen **Wilfried**, **Yennick** en **Melissa** bedanken voor alle goede zorgen van de dieren, het reilen en zeilen van het animalium en de vele gezellige babbels daarbuiten. Dankuwel **Kim P** en **iedereen van het ATP** die telkens zorgden voor superleuke Biomeddagen en BBQ's, wat houd ik hier onvergetelijke herinneringen aan over. **Katrien W** en **Christel**, wij hebben ook veel samengewerkt (alle, ik stond meestal aan jullie deur met vragen over de cryostaat, microscoop en FACS), dankjullie wel voor jullie hulp en de fijne babbels. **Tom, Ivo** en **Marc**, de EM experts, dankjullie wel voor al de tijd die jullie gespendeerd hebben aan staalverwerking en inspectie. Jammer genoeg wouden die microglia zich niet laten zien. Desalniettemin heel erg bedankt voor jullie torenhoge inzet. **Regine**,

dankjewel voor de piccobello afwas, het poetsen van de labo's en de koffiemachines. Het was altijd fijn als ik je tegenkwam in de gangen om een snelle babbel te slaan, je was altijd even opgewekt. **Véronique** en **Rani,** jullie zijn zowat de ondersteunde ruggengraat van heel Biomed. Het is paniek als jullie er niet zijn. Dankjulliewel voor het dagelijkse reilen en zeilen op Biomed, voor het doorsturen van emails naar heel Biomed, voor de hulp met printen en Gmail aangelegenheden en specifiek Véronique voor alle administratieve ondersteuning tijdens de eindfase van mijn doctoraat. Dankjewel om je geduld niet te verliezen met mij. En oh ja, Véronique, danku voor mij niet 1x een blauwe plek te bezorgen bij de talkrijke bloednames. Danku aan alle ex- en huidige Biomed collega's die mijn tijd hier en op congres onvergetelijk gemaakt hebben.

Ook de steun van vrienden en familie heeft bijgedragen, en niet het minste, aan het behalen van mijn doctoraat. **Birgit,** mijn schat, mijn bestie, en maid of honor ;-). Jij bent er altijd voor me geweest, al van kinds af aan. We zijn eigenlijk altijd samen door het leven gegaan, het was pas na onze studies op 't unief dat onze wegen letterlijk wat meer begonnen te scheiden maar niet figuurlijk. We hebben lief (letterlijk, haha ☺) en leed gedeeld. Zalig al die keren dat mijn kaken en buik pijn doen en dat de tranen over ons gezicht rollen van het lachen. We hoefden elkaar soms maar aan te kijken en we zijn vertrokken. Ik kan zoooovele grappige en leuke momenten bedenken die we gedeeld hebben: slakken uit de vijver vissen, sneeuwschool, koningrijk, Platja d'Aro en MJA Mallorca (oh god), onze 18-jarige feestjes, samen op kot, de vele filmavondjes met Buggles en Ben & Jerry's, de verjaardags- en nieuwjaarsfeestjes, gezellig tafelen, welnessavondjes, trouwjurk kiezen, enz. Ik denk dat we het komende jaar nog veel van die anekdotes zullen bespreken ;-). Dankjewel voor je onvoorwaardelijke vriendschap en steun de afgelopen bijbenadering 22 jaar, het is een zaligheid jou als beste vriendin, en als deel van mijn familie te hebben.

Verder wil ook graag mijn vriendinnen die ik over heb gehouden aan de tennis op 't Demerstrand, **Anouschka** en **Gwen**, heel erg bedanken voor de aangename sportafleiding, de gezellige etentjes en ontbijtjes en de luisterende oortjes voor mijn doctoraatsfrustraties. Dankuwel **Nathalie**, ex-collega en crossfit coach. Toen je nog op Biomed werkte als postdoc hebben we vaak fijn gebabbeld over eten, sport, voeding, onderwijs en je gaf graag goede raad, die ik graag opvolgde. Menig maal heb je me voorgesteld om eens te komen proberen op de crossfit en ik ben bezweken. De crossfit sleept me nog steeds doorheen mijn doctoraat. Het is een geweldige manier om al mijn frustraties kwijt te kunnen. Jij en Pieter hebben iets prachtigs opgebouwd, dikke proficiat. Bij deze ook dankuwel aan al mijn crossfitbuddies die steeds vragen hoe het met mij en met mijn boekje gaat. Jullie maken alle momenten van doodgaan toch een beetje aangenamer.

Yves, mijn kleine maar toch oudere broer, **Virginie, Bompa Wilfried, Marraine**, wijlen **Bompa Freyke** en wijlen **Nenen,** mijn schoonouders **Marina** en **Luc** en schoonzus **Jolien,** dankjulliewel voor de fijne momenten van afleiding, de etentjes, tripjes en jullie jarenlange steun en interesse in hoe het met me ging "op school ☺". Bompa Wilfried, jij wist me keer op keer te verbazen met je kennis over macrofagen en de hersenen, je hebt zelfs mijne integrine paper proefgelezen en ik ben blij dat je bijdrage vereeuwigd staat in de wetenschappelijke literatuur.

En HIER **moetieke**, hier is het stukje waar je naar opzoek bent. Je was het al aan het zoeken in mijn draft versie maar tevergeefs, ongeduldige curieuze neus (hihi, van wie zou ik dat toch geërfd hebben?)! **Mama** (moetieke)**, Papa** (Smollieke)**, Dickske en Lieve**, mijn vier ouders. Wat moet ik hier toch maar schrijven. Woorden komen te kort, papier kom ik te kort en voor de moment ontbreekt me ook een zakdoek. Jullie vier hebben mij altijd onvoorwaardelijk gesteund in welk opzicht dan ook. Zonder jullie had ik hier niet gestaan (afgezien van het feit dat mama en papa een biologische vereiste waren om mij ter wereld te brengen). Ik kan niet beschrijven hoe dankbaar ik jullie ben en hoe gelukkig ik ben met jullie als mijn ouders. We hebben allemaal zo een sterke band met elkaar, ook al hebben jullie me weinig gezien de afgelopen tijd of hoorden jullie me weinig, weet dat ik vaak aan jullie dacht. Jullie luisterende oortjes en bemoedigende woorden, de vele keren dat ik met mijn pootjes onder tafel mocht schuiven en zelfs niet hoefde op te ruimen, jullie bezoekjes in Parijs, de crèmekes van Dickske en de Vidékes van Lieve, de vele wijntjes, de dikke knuffels, de keren samen shoppen (o.a. voor een trouwjurk), en noem maar op: al deze momenten waren een immens plezier voor mij. Dankjulliewel om er voor me te zijn in lichte en in donkere dagen.

Jeroen, dankzij jou ben ik blijven doorzetten. Jij hebt meegedoctoreerd met mij. Ook al heb je hier nooit voor gekozen. Geen enkele keer heb je gezucht als ik weer eens laat of in het weekend moest werken. Je hebt superveel geduld en begrip voor me getoond. Ik was de persoon die zat te zuchten en jij was gewoon weer fier op mij. Misschien was je ook gewoon blij dat je even van me verlost was en kon kijken op tv wat je wou, maar toch ben ik daar niet van overtuigd gezien de beperkte tijd die we samen hadden en hebben. Met meedoctoreren refereer ik niet enkel naar de volle emotionele lading die je kreeg te verwerken telkens er iets mislukte in het lab, of wanneer ik het niet meer zag zitten, of wanneer ik gestrest was voor presentaties, of wanneer de analyses nergens op uitdraaiden, enz. Je hebt ook macro's in Excel voor me geschreven, mee met me in het lab gestaan, al was het dan om mijn time-lapse experimenten mee op te ruimen en tipjesdoosjes te vullen. Zelfs kooien van de muizen heb je me helpen uitkuisen in de kerstvakantie! Je was altijd even geïnteresseerd, je wou weten waar alles voor diende. Ik heb meer foto's van jou in het lab dan van mezelf. Dankjewel om altijd klaar te staan om me op te vangen (dag en nacht), al ging het vaak over de telefoon en was je zelf overladen met werk. Dankjewel om mijn gefrustreerde ik te verdragen, ik geloof oprecht dat je met mij hebt afgezien. Dankjewel om zo hard in me te geloven, terwijl ik dat zelf amper deed, en me te blijven overtuigen. Dat moet een erg vermoeiend karweitje geweest zijn. Dankjewel om me zo vaak blij te maken met kleine dingetjes. Het laatste jaar is er veel van onze kostbare quality time opgeofferd geweest en ik beloof dat ik na vandaag weer beter voor jou ga zorgen. En in mei komend jaar, wordt die belofte vereeuwigd. Ik kan al niet wachten (ik heb natuurlijk ook al lang genoeg gewacht *kuch kuch* ;-))! Dankjewel dat jij mijn allesje wil zijn voor altijd ☺.

"Love only grows by sharing.
You can only have more for yourself by giving it away to others."

Brian Tracy